

Nanotech France 2019

NanoMaterials for Energy & Environment

NanoMatEn 2019 – NanoMetrology 2019

Joint International Conferences and Exhibition

26 – 28 June 2019

Palais des Congrès d'Issy

Issy-Les-Moulineaux, Paris, France

Book of Abstracts

Organizer



SETCOR
Conferences & Exhibitions

Nanotech / Biotech Plenary session I

Geometry, construction and modelling for carbon nanotori

Pakhapoom Sarapat¹, James M. Hill², Duangkamon Baowa³

¹Department of Mathematics, Faculty of Science, Bangkok 10400 Thailand

²School of Information Technology & Mathematical Sciences, University of South Australia,
Mawson Lakes, SA, Australia

³Centre of Excellence in Mathematics, CHE, Si Ayutthaya Rd., Bangkok 10400 Thailand

Abstract

After the discovery of circular formations of single walled carbon nanotubes called fullerene crop circles, their structure has become one of the most researched amongst carbon nanoparticles due to their particular interesting physical properties. Several experiments and simulations have been conducted to understand these intriguing objects, including their formation and their hidden characteristics. It is scientifically conceivable that these crop circles, nowadays referred to as carbon nanotori, can be formed by bending carbon nanotubes into ring shaped structures or by connecting several sections of carbon nanotubes. Toroidal carbon nanotubes are likely to have many applications, especially in electricity and magnetism. In this talk, we discuss their geometry, construction and modelling and some of the existing known analytical expressions, as obtained from the Lennard-Jones potential and the continuum approximation, for their interaction energies with other nanoparticles are summarised.

Keywords: Carbon nanotori, Nanotechnology, Interaction energy, Lennard-Jones potential, Continuum approximation.

Multidimensionality of plasmonic colors. Application to image multiplexing

Nipun Sharma¹, Marie Vangheluwe², Alice Vermeulin², Nathalie Destouches¹

1. HID Global CID, 92150 Suresnes, France

¹ Univ Lyon, UJM-Saint-Etienne, CNRS, Institut d Optique Graduate School, Laboratoire Hubert Curien UMR 5516, F-42023, Saint-Etienne, France. Email: nathalie.destouches@univ-st-etienne.fr

² HID Global CID, 92150 Suresnes, France

Abstract:

Printing multiplexed color images that can be observed independently under white light in specific observation conditions is of great interest for applications to security, data storage or design. Few articles have recently demonstrated that dichroic plasmonic colors could be used to produce polarization sensitive dual-image multiplexing [1,2]. The concept can be generalized and extended to at least three-fold image multiplexing using both reflection and transmission configurations. Here, a method is proposed to implement image multiplexing with anisotropic metallic nanoparticles that can be produced with different technologies. The demonstration is illustrated using a laser scanning process, which is cost-effective, rapid and flexible [3]. The nanocomposite film is initially nearly color-less with metallic precursors in the form of ions, atoms and small nanoparticles (1-2 nm). A femtosecond laser grows and shapes metallic nanoparticles at the same time it tunes the size distribution and the spatial distribution of these nanoparticles in the film. The laser process results in the generation of plasmonic nanostructured pixels where the film birefringence and dichroism can be controlled to produce unprecedented color gamuts that satisfy conditions for three-fold image multiplexing. Each nanostructured area is characterized by a set of colors exhibited in each selected mode. We further explain the conditions that the color gamuts in the three modes must fulfil to produce three-fold image multiplexing and how such conditions can be satisfied with plasmonic colors. Three-fold image multiplexing (Figure 1a) is shown using different color combinations. Such laser processing is also applied to print dual multiplexed color images with more freedom in the choice of colors (Figure 1b). This methodology could be implemented with other technologies like electron beam lithography

with a larger freedom on the choice of colors, along with a higher spatial resolution, at however higher processing cost and time.

Keywords: metallic nanoparticles, TiO₂, thin films, laser process, dichroism.

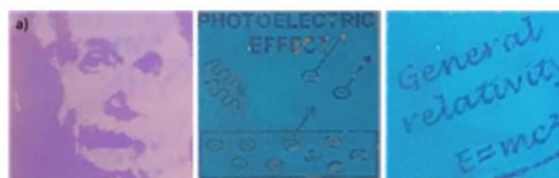


Figure 1: Three-fold image multiplexing: the first image is observed in reflection, the next two ones in transmission between two polarizers; the sample is rotated in its plane to get the second and the third images.

References:

1. E. Heydari, et al. *Adv. Funct. Mater.*, 2017, 27, 1–6.
2. X. M. Goh, et al. *Nat. Commun.*, 2014, 5, 5361.
3. Z. Liu, et al. *ACS Nano*, 2017, 11, 5031–5040.

Nanotech - Session I.A: Nanomaterials Fabrication / Synthesis

Scalable Synthesis of Catalytic Nanoparticles by Atomic Layer Deposition

Xinhua Liang

Missouri University of Science and Technology, Department of Chemical and Biochemical Engineering, Rolla, USA

Abstract:

Heterogeneous catalysts normally consist of small metal particles dispersed on a high surface area porous support. Traditional methods, such as wet-chemical processing, can produce metal particle catalysts as small as several nanometers, but these methods cannot precisely control the size of the catalytic nanoparticles and disperse them homogeneously within the porous substrates. In addition, heterogeneous catalysts cannot selectively convert specific molecules in the reactant mixture to catalyze only desired reactions. Novel approaches are required to synthesize stable metal nanoparticles catalysts with tightly controlled sizes to further advance the knowledge of their unique size-dependent catalytic behavior. Recently, atomic layer deposition (ALD) has been used to prepare highly dispersed, highly active metal nanoparticles. In this presentation, I will introduce some examples of nanostructured catalysts prepared by ALD, such as Ni nanoparticles, Pt-Co bimetallic nanoparticles, and CeO₂ doped TiO₂ nanoparticles.

Keywords: atomic layer deposition (ALD), highly dispersed, bimetallic nanoparticles, scalable synthesis, fluidized bed reactor

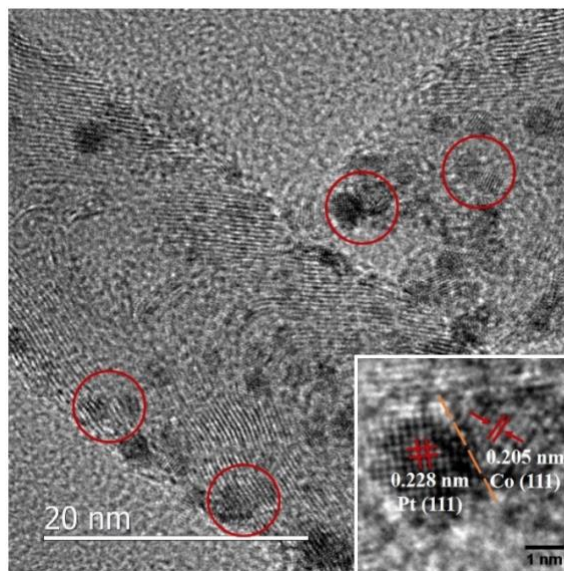


Figure 1: Figure illustrating highly dispersed Pt-Co bimetallic nanoparticles deposited on MWCNTs by ALD.

References:

1. Jiang, C., Shang, Z., Liang, X. (2015), Chemoselective transfer hydrogenation of nitroarenes catalyzed by highly dispersed, supported nickel nanoparticles, *ACS Catalysis*, 5 (8), 4814-4818.
2. Shang, Z., Liang, X. (2017), "Core-Shell" nanostructured supported size-selective catalysts with high catalytic activity, *Nano Letters*, 17 (1), 104-109.
3. Wang, X., He, Y., Liu, Y., Park, J., Liang, X. (2018), Atomic layer deposited Pt-Co bimetallic catalysts for selective hydrogenation of α , β -unsaturated aldehydes to unsaturated alcohols, *Journal of Catalysis*, 366, 61-69.

SELF-SHAPING AND SELF-ASSEMBLY OF NANOMATERIALS BY EVAPORATIVE PROCESSES

Dr. Marco Faustini

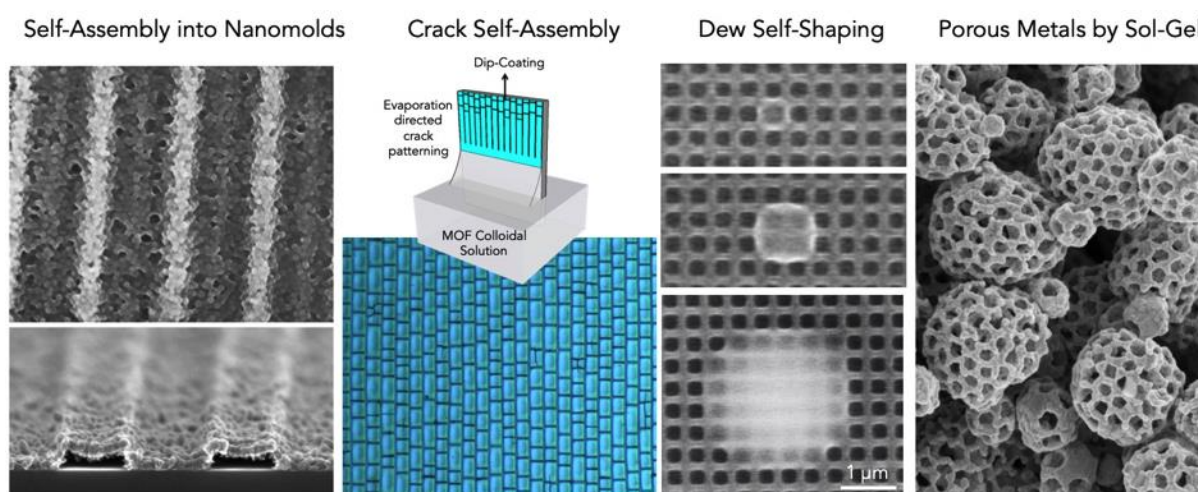
Sorbonne Université, CNRS, Collège de France, 4, Place Jussieu, Paris, France
<https://www.lcmcp.cnrs.fr/sites/marco-faustini/>, marco.faustini@upmc.fr

Abstract

In this talk, I will describe our initiative in shaping inorganic and hybrid nanomaterials (inorganic and hybrid colloids, gels and Metal-Organic Frameworks) at multiple scales¹ by evaporative approaches. The goal is to rationally combine the original properties of the functional nanomaterials (composition, confinement, high porosity, sorption selectivity, capillary condensation...)² and of the periodic structures (light and liquid confinement, guiding...) to achieve new multifunctional platforms for fundamental studies and applications in electrocatalysis, dew engineering and sensing.

Several original strategies will be described: (i) confined colloidal self-assembly into nanomolds,³ (ii) crack self-assembly of

colloidal gels⁴ and (iii) dew self-shaping and manipulation on hybrid surfaces.⁵ Examples of application of these systems will be presented. Sensing platforms (1D, 2D photonic crystals, graded materials, diffraction gratings) based on several nanoporous materials were developed for the easy-detection of toxic compounds by using a simple and accessible tool such as the camera of a smart phone.^{3,4,6} Unusual wetting at the nanoscale and self-shaping of femtoliter dew droplets on sol-gel hybrid surfaces will be also described.⁵ At last, an « unexplored » sol-gel chemistry of noble metals (e.g. Iridium based materials) is proposed to fabricate hollow and ultraporous catalytic films for Oxygen Evolution Reactions in PEM electrolyzers.⁷



Reference:

1. M. Faustini; L. Nicole; E. Ruiz-Hitzky; C. Sanchez, *Advanced Functional Materials*, 28, 1704158, 2018
2. R. Li; M. Boudot; C. Boissière; D. Grosso; M. Faustini, *ACS Applied Materials & Interfaces*, 9, 14093-14102, 2017
3. O. Dalstein; D. R. Ceratti; C. Boissière; D. Grosso; A. Cattoni; M. Faustini, *Advanced Functional Materials*, 26, 81-90, 2016
4. O. Dalstein; C. Sicard; O. Sel; H. Perrot; C. Serre; C. Boissière; M. Faustini, *Angewandte Chemie International Edition*, 56, 14011-14015, 2017
5. M. Faustini; A. Cattoni; J. Peron; C. Boissière; P. Ebrard; A. Malchère; P. Steyer; D. Grosso, *ACS Nano*, 12, 3243-3252, 2018
6. M. Boudot; A. Cattoni; D. Grosso; M. Faustini, *Journal of Sol-Gel Science and Technology*, 1-10, 2016.
7. M. Faustini, M. Giraud, D. Jones, J. Rozière, M. T. R. Porter, M. Bahri, O. Ersen, C. Sanchez, C. Tard, J. Peron, *Advanced Energy Materials*, 2019

Fabrication of two-layer nanocomposite WC/a-C coatings by a combination of pulsed arc evaporation and electro-spark deposition in vacuum

Dmitry V. Shtansky,* Konstantin A. Kuptsov, Aleksander N. Sheveyko, Daria A. Sidorenko

National University of Science and Technology "MISIS", Leninsky prospect 4, Moscow 119049, Russia

Abstract:

New cost-efficient technology combining pulsed arc evaporation (PAE) and electro-spark deposition (ESD) in vacuum was developed and implemented to coat Ti with two-layer WC/a-C coating in a single technological run using the same WC-6%Co electrode. A thick bottom ESD layer (70-90 μm thick) was composed of β -Ti ($\sim 70\%$), β -(W,Ti) C_{1-x} and a small amount of α -Ti. A thin upper PAE layer had two sublayers (3.2 and 1.6 μm thick) sequentially deposited in an Ar and C_2H_4 atmosphere. Both sublayers had a nanocomposite, nearly amorphous structure, in which small disordered β -WC $_{1-x}$ crystallites were dispersed in a-C matrix. The two-layer PAE/ESD coating demonstrated a superior tribological performance when compared with its single layer counterparts: both low wear rate ($1.4 \times 10^{-7} \text{ mm}^3/\text{Nm}$) and coefficient of friction (0.15-0.18) were documented. This was provided by a combination of high toughness and thickness of the ESD layer (which prevented the substrate from plastic deformation) and low friction coefficient of the top PAE layer (due to its nearly amorphous WC/a-C structure with a large amount of graphitized carbon acting as a solid lubricant). At the same time, it was attributed to tailored mechanical properties of the coating system whose hardness gradually increased from 3.6 GPa (Ti substrate) to 7 GPa (bottom of the ESD layer), then to 13 GPa (top of the ESD layer), and finally to 20-21 GPa (PAE coating). *In-situ* mechanical TEM tests demonstrated that the PAE/ESD interface withstood stresses as high as 560 MPa without failure, thereby indicating high adhesion strength between the layers.

Keywords: WC/a-C coatings, pulsed arc evaporation, electro-spark deposition, friction and wear, in-situ mechanical test.

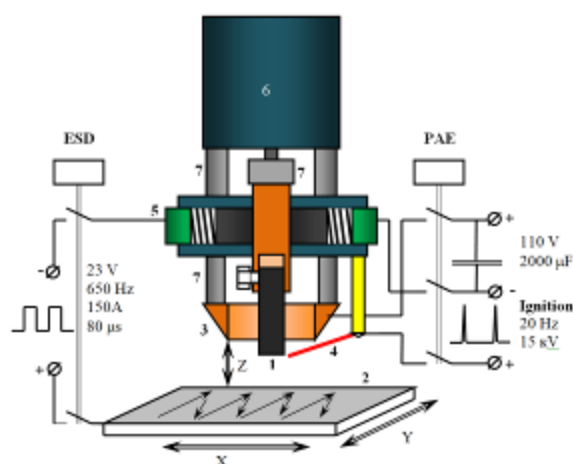


Figure 1: Scheme of rotating deposition module mounted on a 3-axis computer numerical control unit. 1 – WC-Co electrode, 2 – substrate, 3 – circular anode, 4 – ignition electrode, 5 – brush assembly, 6 – electric motor, 7 – insulating ceramics.

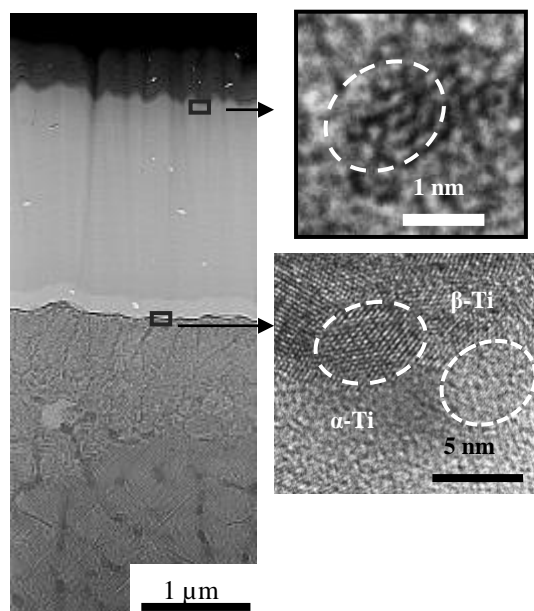


Figure 2: TEM micrographs of two-layer PAE/ESD coating.

Facile Synthesis of Lead Iodide Nanostructures by Chemical, Hydrothermal, and Microwave Techniques and their Characterizations: A Comparative Study

S. AlFaify^{1*}, Mohd. Shkir¹, I.S. Yahiya^{1,2}, V Ganesh¹, Bakhtiar Ul Haq^{1,3}

¹Advanced Functional Materials & Optoelectronics Laboratory (AFMOL), Department of Physics, Faculty of Sciences, King Khalid University, P.O. Box 9004, Abha, Saudi Arabia.

²Nano-Science & Semiconductor Labs, Department of Physics, Faculty of Education, Ain Shams University, Roxy, 11757 Cairo, Egypt.

³Department of Physics, Faculty of Science, Universiti Teknologi Malaysia, UTM, Skudai, 81310 Johor, Malaysia.

Abstract:

Lead iodide (PbI₂) nanostructures have been synthesized by chemical, Hydrothermal, and Microwave irradiation techniques. SEM analysis indicated the formation of aligned nanocrystals and nanorods of an average diameter between 110 nm to 400 nm. The powder X-ray diffraction and FT-Raman spectroscopic analysis confirm the formation of a 2H-PbI₂ polytypic predominantly. These studies also show that there is no extra phase due to any kind of impurity in the synthesized nanostructures. The optical energy band gap of nanostructures prepared by chemical, hydrothermal, and microwave irradiation methods were found to be 2.283, 2.493, 2.542 eV, respectively, as obtained from UV-VIS absorption measurements and 2.345, 2.356, 2.375 eV, respectively, as calculated from diffuse reflectance data. These values show a clear increase in the band gap due to the confinement effects in the prepared nanostructures. Photoluminescence spectra were recorded at a fixed excitation wavelength and show a clear blue shift in the emission peaks which is due to the recombination of free excitons with the band to band type transitions and to quantum confinement effects. Furthermore, the dielectric study has been performed and a good enhancement in the dielectric constant has been observed due to the small size of the fabricated nanostructures in comparison to the bulk material. For a fundamental understanding of the PbI₂ nanostructures, band structure calculations have been carried out utilizing the full potential linearized augmented-plus-local-orbital (FP-L(APW+lo)) method based on the density functional theory. Apparently, the PbI₂ nanostructures have promising potentials for

optoelectronic applications and as precursors in modern perovskite solar cells.

Keywords: PbI₂, Nanostructure, Hydrothermal, Microwave, SEM, X-ray diffraction, FT-Raman spectroscopic analysis, Optical & Dielectric & Photoluminescence properties, Optoelectronic & Perovskite solar cell applications.



Figure 1: SEM micrographs of PbI₂ nanostructures prepared by co-precipitation (A₁-A₄), hydrothermal (B₁-B₂), and microwave irradiation (C₁-C₂) techniques.

References:

1. Zhu, X., Wei, Z., Jin, Y. & Xiang, A. Growth and characterization of a PbI₂ single crystal used for gamma ray detectors. *Crystal Research and Technology* **42**, 456–459 (2007).
2. Xiao, R., Hou, Y., Fu, Y., Peng, X., Wang, Q., Gonzalez, E., & Yu, D. (2016). Photocurrent mapping in single-crystal methylammonium lead iodide perovskite nanostructures. *Nano letters*, 16(12), 7710-7717.

Nanostructured inks based on gold nanoparticles and polyelectrolytes

N. Bridonneau,^{1,3} S. Zrig,^{2,3} F. Carn^{1,3}

¹ Université de Paris, Laboratoire Matière et Systèmes Complexes, Paris, France

² Université de Paris, Laboratoire Interfaces Traitements Organisation et DYnamique des Systèmes, Paris, France

³ Université de Paris, Labex “Science and Engineering for Advanced Materials”, Paris, France

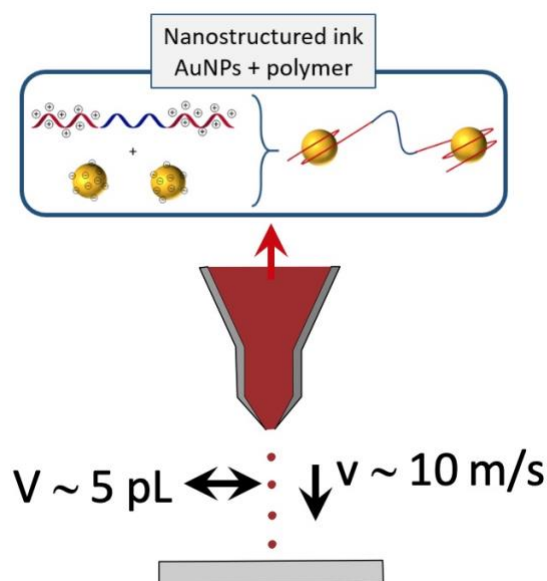
Abstract:

Evaporating colloidal suspension leads to the formation of a variety of solid patterns, ranging from the concentric rings of a dried coffee drop to the uniform deposits of solid pigments left after paint drying. In the last decade, several groups have shown that evaporating suspensions of plasmonic nanoparticles is an efficient way toward the elaboration of nanostructured functional devices such as for instance gauge sensors,¹ substrate for Surface-Enhanced Raman Spectroscopy (SERS)² or diagnostic tools³. In spite of these achievements, the final deposited nanostructures are rather big ($\sim \mu\text{m}$) compared to the size of the nanoparticles, restricted to a limited number of 2D patterns, and the interparticle distance is poorly controlled, hindering the development of applications.

To increase the structural control at the nanometric scale, we developed a new method to self-assemble gold nanoparticles in bulk (3D) before deposition on model surfaces with controlled roughness and charge density. The nanostructuring relies on electrostatic interaction between negatively charged surfactants stabilizing the gold particles and ammonium functions of a polylysine-polyethyleneglycol copolymer designed on purpose.

This presentation will first present the different structures (SAXS and cryo-TEM) obtained in bulk by complexation between nanoparticles and polymers (polyelectrolytes or grafted polymers). Then, the correlation will be established between these 3D structures and the 2D patterns obtained after droplet deposition and drying as a function of the surface characteristics (sign of surface charge and charge density) and the speed of droplet deposition (μ -pipette or inkjet printer). These results will be compared to those obtained with reference individual nanoparticles.

Keywords: nanoparticle, gold, coffee ring, complexation, ink-jet printing



Scheme 1: Deposition of nanostructured inks using the inkjet printing technique

References:

1. C. Farcau, N. M. Sangeetha, H. Moreira, B. Viallet, J. Grisolia, D. Ciuculescu-Pradines, and L. Rossier, *ACS Nano*, 5, 7137 (2011).
2. R. Chen, L. Zhang, X. Li, L. Ong, Y. Gaung Soe, N. Sinsua, S. L. Gras, R. F. Tabor, X. Wang and W. Shen, *ACS Sens.*, 2, 1060 (2017).
3. S. Devineau, M. Anyfantakis, L. Marichal, L. Kiger, M. Morel, S. Rudiuk and D. Baigl, *J. Am. Chem. Soc.*, 138, 11623 (2016).

Substrate Dependent Molecular Doping of Supported Graphene by Charge Transfer Process

A. Armano^{1,3}, G. Buscarino^{1,2}, M. Cannas¹, F. M. Gelardi¹, F. Giannazzo⁴, E. Schilirò⁴, R. Lo Nigro⁴, and S. Agnello^{1,2,4,*}

¹ Università degli Studi di Palermo, Dipartimento di Fisica e Chimica, Palermo, Italia

² Università degli Studi di Palermo, ATeN Center, Palermo, Italia

³ Università degli Studi di Catania, Dipartimento di Fisica e Astronomia, Catania, Italia

⁴ Consiglio Nazionale delle Ricerche—Istituto per la Microelettronica e Microsistemi, Catania, Italia

Abstract:

Graphene (Gr) is one of the most promising carbon based nanomaterials for various applications in microelectronic. In fact, thanks to its two-dimensional structure, the Gr is featured by excellent properties which make it a good candidate in the development of many nanoscale devices: radio-frequency transistors, barristors, vertical THz transistors, nanocomposites, and solar cells, for both rigid or flexible systems. However, the feasibility of these applications requires an accurate control of Gr charge carrier properties, such as density and charge sign. Soft thermal treatments in molecular oxygen atmosphere have proved to be a profitable way to pursue these aims, preserving the quality of Gr [1-5]. By this technique, the oxygen diffusion in the interstitial space between graphene and substrate, allows to induce a stable p-type doping in Gr, through the charge balancing in a oxygen reduction reaction (Figure 1). Herein, we report the study on the dependence of this doping process on the use of various oxides (SiO₂, Al₂O₃, and HfO₂) as support for Gr made by chemical vapor deposition. In particular, the different efficiency, and dynamics of the doping process are highlighted. By using Raman spectroscopy (Figure 2), a threshold temperature for doping is revealed, as well as a different kinetics. These features are related to the peculiar water affinity of substrate surface, which determines different number of reaction sites, and thus different maximum available doping. Moreover, the temperature distribution of the oxygen reaction sites is revealed, and related to the doping kinetics. Therefore, we conducted a systematic study of doping dependence on the features of the grafene-substrate interstitial space. In particular, by opportune chemical treatments, we modulated both its dimension (changing the Gr-substrate distance), and the hydrophilicity of the surface.

Keywords: graphene, carbon-based nanomaterial, 2D nanomaterial, doping, charge transfer, thermal treatment, Raman spectroscopy, surface water affinity, oxygen reduction.

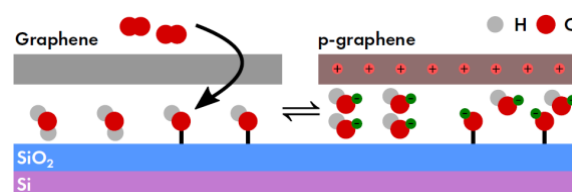


Figure 1: Depiction of Gr doping through O₂ reduction process in which electrons are provided by Gr.

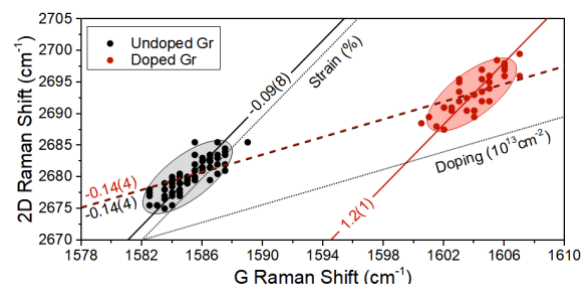


Figure 2: Doped (red) and undoped (black) Gr compared by G and 2D Raman band correlation

References:

1. Armano et al., (2019) Graphene-SiO₂ interaction from composites to doping, *Phys. Status Solidi A* In press.
2. Armano et al., (2018) Monolayer graphene doping and strain dynamics induced by thermal treatments in controlled atmosphere *Carbon* 127, 270-279.
3. A. Piazza et al., (2016). Substrate and atmosphere influence on oxygen p-doped graphene *Carbon* 107, 696-704.
4. A. Piazza et al., (2016) Effect of air on oxygen p-doped graphene on SiO₂, *Phys. Status Solidi A* 213 (9) 2341-2344.
5. A. Piazza et al., (2015) Graphene p-type doping and stability by thermal treatments in molecular oxygen controlled atmosphere, *J. Phys. Chem. C* 119 (39) 22718-22723.

High Planarity Nitrogen-doped Graphene Synthesis from Imidazole Ring Materials using Solution Plasma Process

Y. Muta¹, N. Saito^{1,2,3,*}

¹Department of Chemical Systems Engineering, Nagoya University

²Institutes for Innovation for Future Society

³Conjoint Research Laboratory in Nagoya University, Shinshu University

*Corresponding author e-mail: hiro@sp.materials.nagoya-u.ac.jp

Abstract:

Nitrogen-doped graphene is one of the new material that expected for use as oxygen reduction reaction catalyst, conductive thin film, and so on. Our research group has been studying about nitrogen-doped-graphene bottom up synthesis using solution plasma process (SPP). However, the conventional graphene synthesized from 6-members ring material (pyridine, es.) had low planarity and crystallinity. In these days, we successfully prepare nitrogen-doped graphene with high planarity and crystallinity from 5-members ring material. However, the 6-members ring synthesis from 5-members ring mechanism is unclear. So it must be revealed for next step study like as increasing synthesis rate, and so on. In this research, we aimed to elucidate the initial formation reactions from 5-members ring molecule.

Imidazole was selected as reactant. All the molecular structures were optimized using an ab-initio MO calculation program: the Gaussian 09. To estimate the primary path, the transition state of the reaction was determined by an intrinsic reaction coordinates (IRC) calculation. Moreover, the reaction was discussed from the viewpoint of the variation of standard modes.

From the result of the IRC and the vibration calculation, the reaction proceeds with the trend of some steps. The structure change is shown in Figure 1. The intermolecular C-C bonding rotate 90 degrees and then 5-members ring dimer structure will be transformed to 6-members ring structure. The modes involved in the transition state showed the following changes. At first, the expansion between the imidazole becomes unstable. And next, C-N connection in the imidazole will start to expand. After that, the C-C connection between the imidazole will rotate.

It was suggested that the reaction proceeds by starting expansion and contraction because of the balance of π -conjugated state around C-N connection collapses by obtaining a charge of N in imidazole.

In this study, it suggested that a compound having an imidazole ring is suitable as a synthesis source of high planarity nitrogen-doped graphene using solution plasma.

Keywords: solution plasma process (SPP), nitrogen-doped-graphene, ab-initio MO calculation

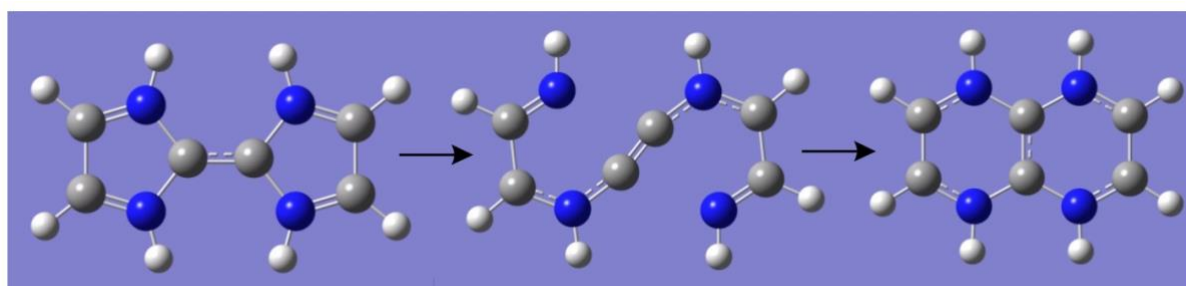


Figure 1: Imidazole 5 to 6 members ring transformation reaction

A Novel Amino-rich Carbon Synthesis through Liquid Phase Plasma for Efficient Heavy Metal Ions Capture

M. Tipplook,¹ N. Saito,^{1,2,3,4*}

¹Department of Chemical Systems Engineering, Graduate School of Engineering, Nagoya University

²Center for Energy and Environmental Science, Shinshu University

³Japan Science and Technology Corporation (JST), Open Innovation Platform with Enterprises, Research Institute and Academia (OPERA)

⁴Japan Science and Technology Corporation (JST), Strategic International Collaborative Research Program (SICORP)

Abstract:

Amino-modified carbons (NH₂-C) are promising as an adsorbent for the removal of several pollutants such as heavy metal ions due to their cost-effectiveness, high surface area, and powerful complex formation with the heavy metal ions. However, it is still a great challenge to develop NH₂-C with high amino group loading for enhance the adsorption capacity.

In this study, a one-step synthesis of NH₂-C through discharge plasma in mixed solution of carbon and amino precursors was investigated. It was presented as a new synthesis route to loading high amino-groups on the carbon adsorbent. Results showed that the characteristics of the NH₂-C such as amino group incorporation, morphology, microstructure, and porosity could be conveniently adjusted by the amino precursor content. The maximum adsorption capacity was observed to be 145.84, 127.59, 109.72, and 94.93 mg·g⁻¹ for Cu²⁺, Pb²⁺, Zn²⁺, and Cd²⁺, respectively. These values were remarkably higher than that of NH₂-SWCNT, NH₂-MWCNT, NH₂-activated carbon, NH₂-graphene, NH₂-graphite synthesized by a conventional process. The adsorption mechanism was controlled by the electrons sharing between amino group and heavy metal ions. Besides, the NH₂-C was regenerated and found to be applicable for reuse in five consecutive adsorption/desorption cycles without significant loss in adsorption capacity, making it a great potential material towards water purification.

Keywords: solution plasma process, amino modified carbon, adsorbent, heavy metal ions, waste water treatment, adsorption.

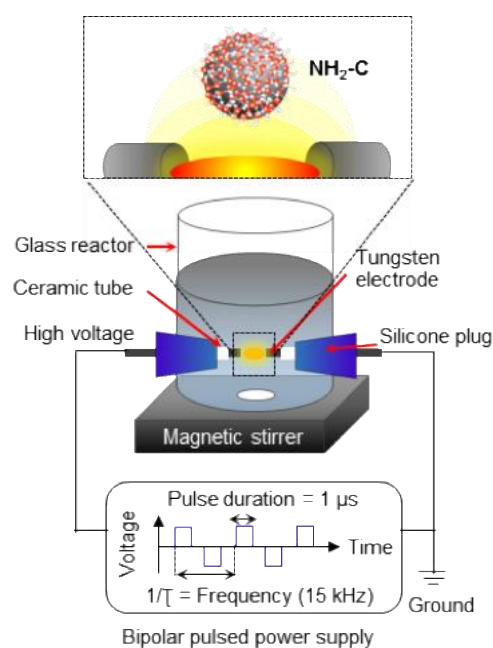


Figure 1: Schematic illustration of the solution plasma process setup for the synthesis of the NH₂-C.

References:

1. Saito N., Bratescu M. A., Hashimi K. (2018), Solution plasma: A new reaction field for nanomaterials synthesis, *Jpn. J. Appl. Phys.*, 57, 0102A4.

Unidirectional coupling of surface plasmonic waves on silver surfaces with asymmetric nanogroove fabricated with glancing angle deposition technique

Chong-Cin Hou, Ti-Li Lin, Hung-Chih Kan

¹Department of Physics, National Chun Chen University, Chiayi, Taiwan ROC

Abstract:

We report on our results of the excitation of surface plasmonic waves with asymmetric nanogrooves on Ag films fabricated with electron beam lithography and glancing angle deposition technique. We patterned the Poly(methyl methacrylate) (PMMA) film with nanogrooves of various widths on an indium tin oxide (ITO) coated glass substrate. The silver film was deposited on the sample surface with a glancing incident angle. This leads to the asymmetry of the groove structure on the Ag film (Fig. 1). By focusing a laser beam of 532 nm wavelength on the groove we were able to excite surface plasmonic waves on the Ag/air interface and characterized the intensity of the surface plasmonic waves with nearfield scanning optical microscopy (NSOM). We found that the asymmetry in the intensities of the surface plasmonic waves excited on both sides of the groove depends strongly on the width of the groove as well as the thickness of the underlying PMMA film. Unidirectional coupling of the surface plasmonic waves propagating on either side of the grooves on the Ag/air interface can be achieved with proper choice of the groove width as well as PMMA film thickness. We simulated the interaction between the incident light and the groove structures with the finite difference time domain method, and analyze the intensity of the surface plasmonic wave intensities on the Ag/air interface. The results of our simulation show excellent agreement with the measurements. Furthermore, our simulation also indicates the unidirectional coupling of surface plasmonic waves with individual asymmetric grooves are also automatically broad band in nature.

Keywords: Surface plasmonic waves, unidirectional coupling, nanogroove, nearfield scanning optical microscopy, finite difference time domain method, FDTD.

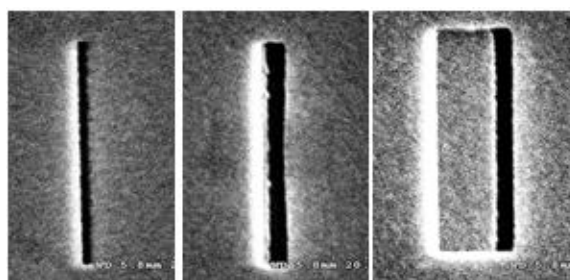


Figure. 1 The SEM image of the top view of the asymmetric nanoslit structure fabricated with glancing angle incidence deposition method.

Magneto-Electrodeposition of CoFe_2O_4 and Granular Co-Cu Nanowire Arrays

N. Labchir^{1,2*}, A. Hannour², D. Vincent¹, A. Ihlal², M. Sajieddine³

¹Laboratory of Hubert Curien, univ-Lyon, University of Jean Monnet, UMR CNRS, 42000 Saint-Etienne, France

²Laboratory of Materials and Renewable Energies, Faculty of Sciences Agadir, BP 8106, Cité Dakhla, 80000 Agadir, Morocco.

³Laboratory of Physics of Materials, University of Sultan Moulay Slimane, FST, BP 523, 23000 Béni Mellal, Morocco.

Abstract:

In telecommunications systems, many studies have been undertaken to integrate non reciprocal passive components. A self-biased magnetic nanocomposite based on nanowire arrays of cobalt ferrite CoFe_2O_4 and cobalt-copper Co-Cu nanoparticles was elaborated by magneto-electrodeposition technique into nanoporous alumina membranes.

CoFe_2O_4 and granular Co-Cu nanowire arrays were electrochemically prepared in nanoporous alumina membranes in the presence of external applied magnetic field. We demonstrate that the application of a magnetic field MF during the synthesis of nanowires can control their chemical and physical properties. XRD studies have shown the presence of a polycrystalline appearance for electrodeposited nanowires. The morphology and the chemical composition of CoFe_2O_4 and Co-Cu nanowires were studied by scanning electron microscope and energy dispersive X-ray spectrometry (SEM / EDXS), the results showed that the wire diameter vary between 200 and 350 nm and that the magnetic field changes the elemental percentages of iron, cobalt and copper inside the membrane pores. The AFM images show that the magneto-electrodeposited samples have a higher surface roughness. SQUID studies indicate that the nanowires electrodeposited by the application of a magnetic field have a coercive field H_c of 1300 and 700 Oe, and a squareness ratio M/M_s of 0.31 and 0.37 for CoFe_2O_4 and Co-Cu nanowires, respectively.

As a consequence, the as-prepared nanocomposites are a promising candidates for the future coplanar microwave circulators operating without external magnetic field. To work towards the integration and miniaturization of circulators, nanotechnology can offer interesting solutions.

Keywords: electrodeposition, nanowires, cobalt ferrite, cobalt-copper, alumina membrane, magnetic field.

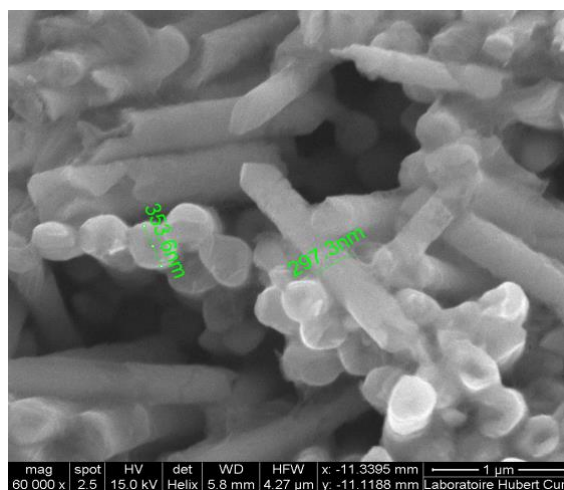


Figure 1: SEM image for CoFe_2O_4 nanowires electrodeposited in AAO membrane.

References:

1. Hannour et al., Journal of Magnetism and Magnetic Materials 353, 29 – 33,(2014).
2. A. Tchangoulia et al., EPJ Web of Conferences 75, 06001 (2014).
3. A. Tchangoulia, Ph.D. Thesis, University of Jean Monnet, Saint-Etienne France, 2014.

Surface functionalization of single crystal Molybdenum Disulfide: role of surface defectivity

A. Ghiami,^{1,3,*} M. Timpel,² M. V. Nardi,² R. Verucchi,¹

¹ Institute of Materials for Electronic and Magnetism, IMEM-CNR, Trento Division, Via alla Cascata 56/C, Povo, 38100 Trento, Italy

² Department of Industrial Engineering, University of Trento, Via Sommarive 9, 38123 Trento, Italy

³ School of Materials Science and Technology, Department of Chemistry, University of Parma, Parco Area delle Scienze 17/A, 43124 Parma, Italy

Abstract:

Possibility of cleaving Transition Metal Dichalcogenides (TMDCs) unveiled a broad prospect in a variety of application spanning electronics, optoelectronics, sensors, piezoelectric etc. thanks to its paramount features concluding, high charge carrier mobility and on/off ratio, direct band gap in the form of monolayer, as well as high chemical stability and many others.

Attaching molecules of different functionality on 2D-TMDCs like MoS₂ would even increase their capability, making them a potential candidate for a wider range of applications.

Perfect lattice of MoS₂ found to be chemically inert, reduces the possibility of formation of a reliable bond with molecules. Pristine MoS₂, regardless of the way it has been produced, contains different types of defects. Among those, sulfur vacancies are the most abundant one, found to be chemically reactive and available for anchoring group of molecules like thiols.

In this work, we study the influence of surface defectivity rate on functionalization efficiency of MoS₂. We have prepared samples with two different defectivity rate by annealing single crystal MoS₂ in vacuum at 300 and 500 °C. Functionalization was achieved through dipping the samples in ethanol containing 1 mM Mercaptoundecyl phosphonic acid (MUPA) molecule for 24 hours. To study the influence of thermal treatment and chemical functionalization on interface electronic properties and the nature of interaction between molecule and MoS₂ substrate, we have applied a variety of characterization techniques concluding, x-ray/ultraviolet photoelectron spectroscopy (XPS/UPS), μ -Raman and ATR-FTIR analysis. Based on our findings, thermal treatment introduces sulfur defects which its amount increases by increasing the annealing temperature. On the other hand, functionalization

occurs filling the sulfur vacancies by thiol anchoring group of the MUPA. Also, it has been found that, functionalization degree of the sample annealed at 500 °C, increased three times relative to its untreated counterpart, which is a clear evidence of the influence of surface defectivity on functionalization degree.

Keywords: MoS₂, thermal treatment, sulfur vacancies, thiol functionalization.

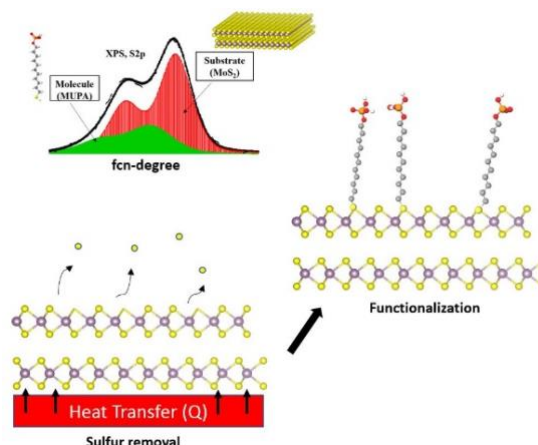


Figure 1: Annealing the sample creates sulfur vacancy, that are filled by MUPA molecules through wet-chemical functionalization. The functionalization degree is based on S2p core level by XPS analysis.

References:

1. Ding, Q.; Czech, K. J.; Zhao, Y.; Zhai, J.; Hamers, R. J.; Wright, J. C.; Jin, S. Basal-Plane Ligand Functionalization on Semiconducting 2H-MoS₂ Monolayers. *ACS Appl. Mater. Interfaces* 2017, 9, 12734–12742.
2. Nan, H.; Wang, Z.; Wang, W.; Liang, Z.; Lu, Y.; Chen, Q.; He, D.; Tan, P.; Miao, F.; Wang, X.; et al. Strong Photoluminescence Enhancement of MoS₂ through Defect Engineering and Oxygen Bonding. *ACS Nano* 2014, 8, 5738–5745.

Electric Field Induced Template-Less Ultrafast Micro/Nano Patterning of Polymer Thin Film

P. Roy¹, P. S. G. Pattader^{1,2}

¹ Centre for Nanotechnology, Indian Institute of Technology Guwahati, Assam 781039, India

² Department of Chemical Engineering, Indian Institute of Technology Guwahati, Assam 781039, India

Abstract:

Electric field induced instability at the polymer/air or polymer/polymer interface has been extensively studied over the decades due to its potential application in soft lithography. So far patterning of a polymer thin film in a well-organised fashion following this method requires templated electrode and is a time consuming and costly affair. We propose a simple ultra fast technique which gives rise to the templateless patterning of thin viscoelastic polymer film without any sophisticated equipment. We used polymer – anisotropic liquid crystal bilayer system with highly dissimilar dielectric permittivity to induce ultrafast destabilization of the interface. As an experimental model system, we report Poly dimethyl siloxane (PDMS) – 5CB bilayer sandwiched between two transparent Indium Tin Oxide (ITO) coated glass electrodes in a parallel plate capacitor arrangement (Figure 1a). Up on application of the electric field, micro/nano wells are formed randomly with local hexagonal closed pack arrangement with specific lengthscale (Figure 1b). This process of instability is kinetically faster (almost instantaneously) than that of the PDMS-Air bilayer system. As the time scale of the destabilization of the interface is merely of the order of few seconds and anisotropic 5CB being a dielectric material that exhibits electrowetting phenomenon, the motion of 5CB-PDMS-Air contact line can be used to align the microstructure formed at the interface of the PDMS-5CB (Figure 1c). We propose a methodology for fast micro/nano scale ‘e-writing’ based on the above principle. We also demonstrated that well-arranged one-dimensional array of microwells fabricated in this manner can be used as pixelated light reflectors when filled with LC and can be switched ‘off’ and ‘on’ in presence or absence of solvent vapor respectively.

Keywords: Electric field, Instability, Dynamic contact line, Liquid crystal, Micro-nano patterning.

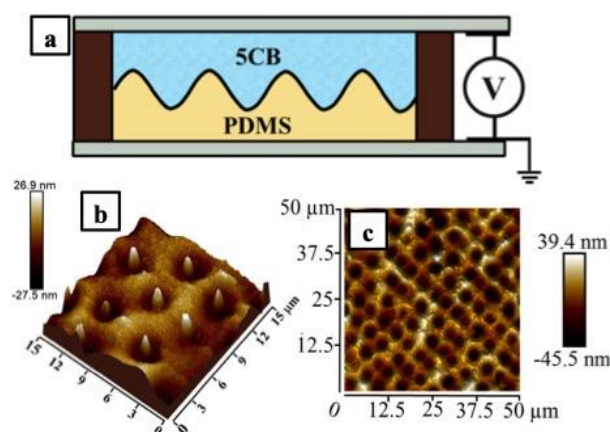


Figure 1: a) Schematic of the experimental set up for the electric field induced patterning of polymer thin film. b) AFM image of the hexagonal close-packed microstructure at the polymer surface. c) Electric field and dynamic contact line (EF-DCL) induced 1D alignment of microwells in PDMS.

Acknowledgment:

PSGP acknowledges DST SERB, Grant no. ECR/2015/000447 and MeitY - grant no. 5(9)/2012-NANO for financial assistance.

References:

1. Schaffer, E., Thurn-albrecht, T., Russell, T. P., Ullrich, S. (2000), Electrically Induced Structure Formation and Pattern Transfer, *Nature*, 403, 874–877.
2. Pattader, P. S. G., Banerjee, I., Sharma, A., Bandyopadhyay, D. (2011), Multiscale Pattern Generation in Viscoelastic Polymer Films by Spatiotemporal Modulation of Electric Field and Control of Rheology, *Adv. Funct. Mater.*, 21, 324–335.

Silver/Collagen Composite Coating on Porous Titanium Oxide by Electrochemical Deposition

S.F. Ou,^{1,*} X.H. Huang,^{1,2}

¹ National Kaohsiung University of Science and Technology, Kaohsiung, Taiwan

Abstract:

Endosseous implants have been shown to be an excellent method for replacing natural teeth. However, inflammation around the implant due to bacterial adhesion and its subsequent colonization at the implant site is considered a major cause for implant failures [1]. Silver nanoparticles have become increasingly popular in biomedical applications due to its ability to destroy pathogens in superior potency at lower concentrations as compared to when bulk silver quantities are applied [2]. Electrochemical deposition is a high efficient process for coating silver on Ti implants. However, the deposited silver exhibited a dendritic structure and cannot disperse uniformly on Ti implant, as shown in Figure.1(a) and (c).

This study aimed to reduce the size of the deposited silver particles and improve the uniformity of the silver on Ti surface by adding collagen into the electrolyte. A porous oxide was formed on Ti by micro-arc oxidation following by electrochemical deposition of silver in silver and collagen containing solution. The effects of electrochemical-deposition voltage, duration and collagen concentration on the composition of the coating were investigated.

Results indicated that a long deposition duration and high voltage resulted in high amounts of silver on the titanium oxide surface. In addition, silver grew into a dendritic structure under long deposition duration. Addition of collagen into electrolyte is beneficial to uniformly disperse the deposited silver particles by inhibited the silver deposition rate. However, high collagen concentration and the long deposition duration caused silver particles to agglomerate. The agglomerates comprised silver and collagen identified by x-ray diffraction spectroscopy and Fourier-transform infrared spectrometer, respectively. The deposited silver particles not only covered the surface of the oxide layer but also existed in the pores inside the oxide layer observed by cross-sectional transmission electron microscopy. The silver/collagen coating

exhibited improved anti-microbial activity toward gram-negative *Escherichia coli* than Ti owing to the antibacterial effects of the silver nanoparticles. The novel composite silver/collagen coatings can potentially be used in orthopedic and dental implants to simultaneously improve osseointegration and prevent post-surgical infection.

Keywords: Endosseous implants, silver nanoparticle, collagen, antibacterial.

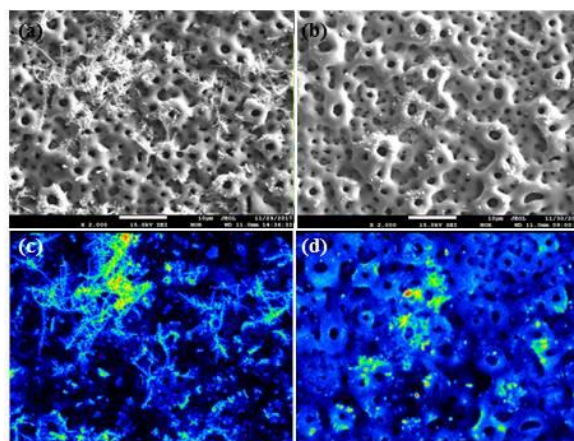


Figure 1 Surface morphology of (a) silver coating and (b) silver/collagen coating on Ti. (c) and (d) is silver element distribution image of (a) and (b), respectively.

References:

1. Costerton, J.W., Stewart, P.S., Greeberg, E.P. (1999), Bacterial biofilms: a common cause of persistent infections. *Sci.*, 284(5418), 1318-22.
2. Yang, F., Ren, Z., Chai, Q., Cui, G., Jiang, L., Chen, H., Feng, Z., Chen, X., Ji, J., Zhou, L., Wang, W., Zheng, S. (2016), A novel biliary stent coated with silver nanoparticles prolongs the unobstructed period and survival via anti-bacterial activity, *Sci. Rep.*, 6, 21714.

Nanotech - Session I.B: Nanomaterials Synthesis / Properties

Polymer nanocomposites based on 2D fillers: A challenge?

P. A. R. Muñoz¹, C. L. C. Rodriguez¹, M. C. C. dos Santos¹, G. S. Medeiros¹, G. J. M. Pinto¹, R. J. E. Andrade¹, G. J. M. Fechine*¹

¹ MackGraphe - Graphene and Nanomaterials Research Center, Mackenzie Presbyterian University, São Paulo, Brazil

Abstract:

The most important advantage of two-dimensional (2D) particles as fillers is their large surface area that enhances the interface with the polymer. This peculiarity leads to significant improvements in different properties of the polymer matrix with the insertion of very low content of particles, which may not reach 1% by mass¹. In the case of 2D particles, the high dispersion degree in the polymeric matrix by using melt mixing process might turn in a challenge due to the need for tuning the processing conditions for the singular shape of 2D particles. Two new strategies were used to insert pre-exfoliated 2D material into the polymer matrix, liquid-phase feeding (LPF), and solid-solid deposition (SSD) (Figure 1)². Graphene (Gr), graphene oxide (GO), hBN and MoS₂ were already used as 2D material and several polymers (PS, PCL, PLA, HDPE, LDPE, PET and PBAT) were used as matrices. The strategy was chosen based on melting behavior of each polymer. All 2D materials were obtained by liquid exfoliation techniques and previously characterized by several techniques (Raman, AFM, TGA and XRD). The polymer nanocomposites were characterized by using traditional techniques (tensile mechanical test, molecular weight, rheological measurements and transmission electron microscopy). Moreover, a technique beyond micro and nanoscale was also used allowing the evaluation of the nanocomposite morphology for millimeter samples size (X-ray Microtomography). The results show that both methods could be suitable as large-scale manufacturing, and the process parameters must be optimized to obtain a low level of agglomerates (Figure 2). The methodologies described here show indications that can be extendable to all thermoplastic polymers and 2D materials providing nanocomposites with suitable morphology to obtain singular properties and triggering the start of the manufacturing process on a large scale.

Keywords: 2D material, polymer nanocomposite, manufacturing, characterization.

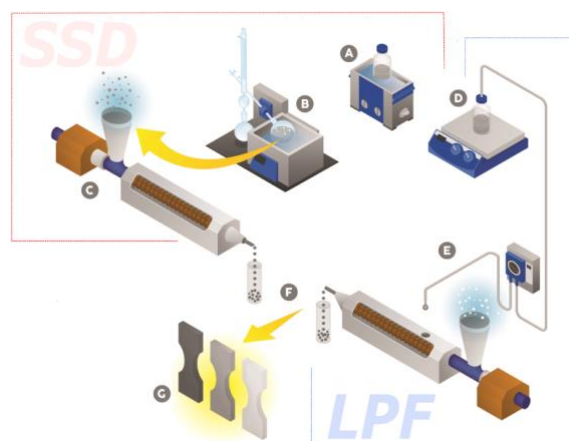
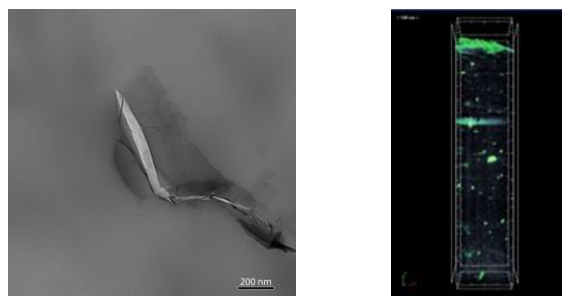


Figure 1: Schematic of SSD and LPF methods, developed for 2D/polymer composite processing at a high production rate².



(a)

(b)

Figure 2: TEM image of PCL/GO (a) and X-ray Microtomography of PS/GO (b).

References:

- 1 J. R. Potts, D. R. Dreyer, C. W. Bielawski and R. S. Ruoff, Graphene-based polymer nanocomposites, *Polymer (Guildf)*, 2011, **52**, 5–25.
- 2 P. A. R. Muñoz, C. F. P. de Oliveira, L. G. Amurin, C. L. C. Rodriguez, D. A. Nagaoka, M. I. B. Tavares, S. H. Domingues, R. J. E. Andrade and G. J. M. Fechine, Novel improvement in processing of polymer nanocomposite based on 2D materials as fillers, *Express Polym. Lett.*, 2018, **12**, 930–945.

Construction of Functional Conical Nanopores in view of sensing applications

N. Arroyo,^{1,*} F. Picaud,¹

¹Laboratoire de Nanomédecine, Imagerie et Thérapeutiques, Université de Bourgogne-Franche-Comté, Besançon, France

Abstract:

Alzheimer is a distressing disease, which comes from an accumulation of protein aggregates such as amyloid fibrils. It inflicts a lot of pressure on both the patient and his family since no treatment exists for now. Amyloids and how they aggregate themselves seem to be a marker for the predisposition of Alzheimer¹. However, there is presently no dedicated equipment able to follow or analyze, in real time, the amyloid fibril formation. Single nanopore detection technology is considered as one of the major breakthroughs in the field of nanotechnology over the last decades². Indeed, the “Oxford Nanopore” company is able now to propose biological nanopores able to sequence DNA molecules³ with high performances. Unlike the biological ones, solid-state nanopores present advantages such as robustness and a diameter modulability ranging from a few to hundred of nm. This makes them good candidates for detecting objects from short DNA strands to nanoparticles⁴. However several factors should be overcome to detect small proteins such as amyloid fibril. We can cite for instance the unspecific adsorption of proteins in the nanopore, the nanopore lifetime, or the free energy barrier to enter or escape the nanopore. Here, we aim to use functionalized nanopores to measure the state of aggregation and allow an early medical supervision of the patient. The nanopore surface coverage by PEG molecules will help amyloids or other structures to enter and diffuse inside the nanopore. The measurement of the electrical intensity going through this nanopore could thus be the ideal way to quantify these amyloid translocations. By studying the intensity variation observed when a molecule structure translocates through the structure, it seems possible to have a better knowledge of what kinds of amyloid can be found in a patient blood sample. We develop in this study, numerical simulations on functionalized conical nanopores to take advantage of the ionic current rectification

effect. We present early work of nanofluidics obtained by molecular dynamics simulation on these nanocones. For this, we compare the behaviour of water molecules and of different ions under the presence or the absence of PEG functions on the nanopore surface. These preliminary results with only solvent molecules will allow us to determine the best geometrical functionalized nanopore to analyze the amyloid fibrils translocation inside the nanocone.

Keywords: functionalization, conical nanopore, molecular dynamics simulation, electrical detection.

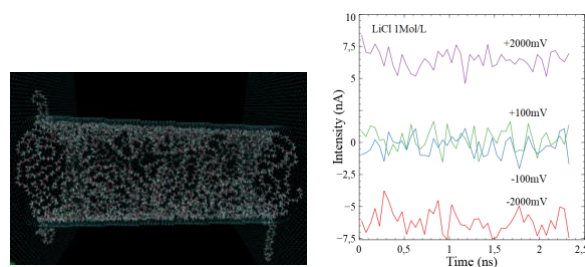


Figure 1: Left : side view of the conical nanopore functionalized by PEG molecules. Right : ionic currents through the nanopore caused by Li^+ and Cl^- diffusion under different electrical fields

References:

1. Chiti, F.; Dobson, C. M. *Annu Rev Biochem* **2006**, 75, 333(b) Knowles, T. P. J.; Vendruscolo, M.; Dobson, C. M. *Nat Rev Mol Cell Bio* **2014**, 15, 384.
2. Lepoitevin, M.; Ma, T.; Bechelany, M.; Janot, J. M.; Balme, S. *Advances in Colloid and Interface Science* **2017**(b) Wanunu, M. *Phys Life Rev* **2012**, 9, 125.
3. Deamer, D.; Akeson, M.; Branton, D. *Nat Biotechnol* **2016**, 34, 518.
4. Balme, S.; Coulon, P.-E.; Lepoitevin, M.; Charlot, B.; Yandrapalli, N.; Favard, C.; Muriaux, D.; Bechelany, M.; Janot, J. M. *Langmuir* **2016**, 32, 8916.

Marrying Spin Crossover and Graphene Field Effect Transistors for Novel Sensing Devices

E.P. van Geest¹, S.A. Bonnet¹ and G. F. Schneider¹

¹Leiden University, Faculty of Science, Leiden Institute of Chemistry, Einsteinweg 55, 2333CC Leiden, The Netherlands

Abstract:

Spin crossover materials, which are well-known molecular materials, have pronounced switching behavior that can be induced by environmental factors.¹ Combined with graphene in the form of a gated graphene field effect transistor,² we aim to combine these materials to produce new structures that are useful in biosensing, for instance as a breath analyzer to identify small molecules.

By careful design of the hybrid structures, graphene field effect transistors were fabricated that could electrically detect spin switches in the spin crossover material, while they were physically and electrically separated from each other (see figure 1). Further on, we produced thin films of the spin crossover materials which were used in device fabrication to perform biosensing through electrical detection of induced spin switches in presence of a variety of volatile organic compounds. To follow up on this work, we want to extend the set of analytes with biologically relevant molecules using our unique device as a sensing platform.

Keywords:

Graphene field effect transistor, spin crossover, contactless sensing, molecular material engineering

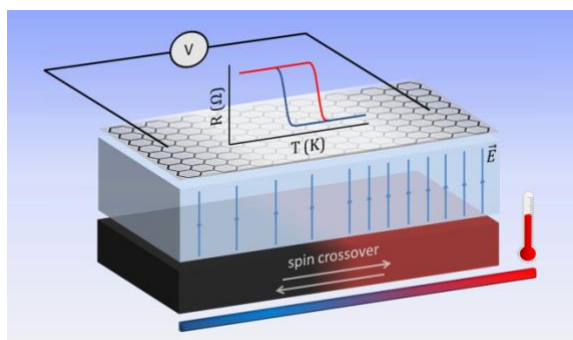


Figure 1: Schematic representation of a graphene field effect transistor (GFET) constructed on a SCO microcrystal, separated by a dielectric spacer. Spin transitions are

monitored remotely by changes in the electronic properties of graphene, induced by variations in the electrostatic potential of the crystal.

References:

1. P. Gütlich, A. B. Gaspar, Y. Garcia, Spin state switching in iron coordination compounds. *Beilstein J. Org. Chem.* **9**, 342-391 (2013).
2. W. Fu, L. Jiang, E. P. van Geest, L. M. C. Lima, G. F. Schneider, Sensing at the Surface of Graphene Field-Effect Transistors. *Adv. Mater.* **29**, 1603610 (2017).

Investigation of N-doped Carbon Dots Synthesized by Solution Plasma for Detection of Nitro Aromatic Molecules

Kyusung Kim^{1,3} and Nagahiro Saito^{1,2,3,4*}

¹Department of Chemical Systems Engineering, Graduate School of Engineering, Nagoya University, Nagoya, Japan

²Conjoint Research Laboratory in Nagoya University, Shinshu University

³Japan Science and Technology Corporation (JST), Open Innovation Platform with Enterprises, Research Institute and Academia (OPERA),

⁴Japan Science and Technology Corporation (JST), Strategic International Collaborative Research Program (SICORP)

Abstract:

Carbon dots (CDs) are one of the new research areas on carbon nanomaterial, which are represented by carbon nanotubes (CNTs) and graphene. The CDs have the unique optical property due to quantum confinement effect by their particle size. Using the fluorescence property, the CDs can be utilized many kinds of applications such as bio imaging, photocatalysts and ion/molecule detection. Many researchers have focused on the doping of hetero atom in the CDs because the concentration and type of hetero atom are dominant factors to control the intensity and color of fluorescence. Solution plasma (SP) is an unconventional synthesis process for highly hetero-atom doped carbon materials at room temperature. A polymerization of cyclic organic monomer by electron transfer at interface of the plasma / liquid and their low synthesis temperature allow to existence of the hetero atoms in the carbon frameworks. In this study, nitrogen doped carbon dots (NCDs) were synthesized by solution plasma and nitro group molecules detection by NCDs was investigated. The NCDs were synthesized using pyridine and water mixture by the SP. The NCDs emitted a strong blue fluorescence (420nm) light under UV light at 350 nm. The nitrogen concentration of NCDs increased up to 16 at. %, as a result, the quantum yield of NCDs increased to 43 %, simultaneously. The fluorescence property can be changed by Förster resonance energy transfer (FRET) between NCDs and specific molecule. In order to reveal molecule detection property of NCDs, various kinds of nitro aromatic compounds were used. Especially, the rapid decreasing of intensity of fluorescence (about 4%) was observed by even 1ppb of 4-nitrophenol (Figure 1).

Keywords: Solution plasma, carbon dots, fluorescence, molecule detection

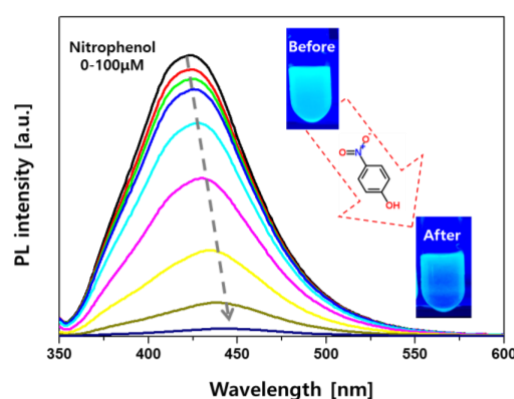


Figure 1: Fluorescence change of NCDs with different concentration of 4-nitrophenol

References:

- Hui, D., Shang, B.Y., Ji, S.W., Huan, M.X., (2016) Full-Color Light-Emitting Carbon Dots with a Surface-State-Controlled Luminescence Mechanism, *ACS Nano*, 10, 484-491.
- Morishita, T., Ueno, T., Panomsuwan, G., Yoshida, A., Bratescu, M.A., Saito, N. (2016), Fastest formation route of nanocarbons in solution plasma process, *Sci. Rep.*, 6, 36880.

On the Study of Omni-phobicity of Doubly Reentrant 3D Structures by Using Two-photon Polymerization

H.Y. Ni,¹ P.Y.Chen,² P.Y.Chen,² C.S. Wu,¹ H.T. Hsu,¹ C.C. Fu,¹

¹ National Tsing Hua University, Institute of NanoEngineering and MicroSystems, Hsinchu, Taiwan

² National Tsing Hua University, Department of Materials Science and Engineering, Hsinchu, Taiwan

Abstract:

Recently, scientists found that the mushroom-like nanostructures on the springtail cuticle show anti-penetrating [1]. This special pattern is composed of mushroom-like nanostructure, which can be classified as “doubly reentrant structure” because of the negative curvature on the overhanging part. Such structures have been demonstrated to be effective in preventing liquid penetration. When the liquid contacts to the array of doubly reentrant structures, it would wet the top surface first and start to penetrate. The penetration of liquid would stop when the contact frontier reaches the bottom of the overhangs, where the surface tension point upward. Theoretically, all kinds of liquids can be blocked at this point if there is no other external force. While it is difficult in nanofabrication of the doubly reentrant nanostructures. There were only a few groups successfully fabricate such structure and achieve superhydrophobic properties without further surface chemical modification [2, 3]. Despite using etching process and gray-tone lithography, however, these processes were too complex, not high flexibility and with the high cost.

In this study, we utilized two-photon polymerization (TPP) platform developed by ourselves. It can manufacture 3D arbitrary nanostructures with sub-micron resolution. In TPP, when a near-infrared femtosecond laser is focused into the UV-curable photoresist, two-photon absorption would take place in a focused spot with high photon density. Through this mask-less lithography process, we can fabricate the structure easily, fast and have high flexibility. Figure 1 shows the SEM and FIB images of the doubly reentrant structure. The water contact angle of photoresist is about 33° when it is smooth. However, the angle increases from 33° to more than 150° on the structured surfaces. This result indicates that without any further chemical modification the structures make the surface become superhydrophobicity

even if it is intrinsic hydrophilic material (Figure 2).

Keywords: two-photon polymerization, omni-phobicity, superhydrophobic, nanofabrication.

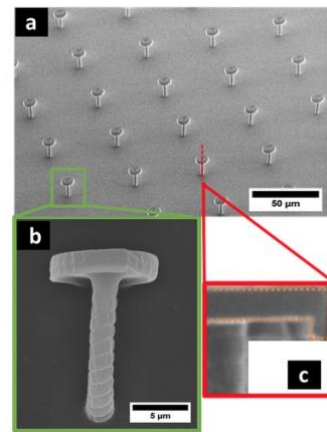


Figure 1: SEM images of the doubly reentrant structure.

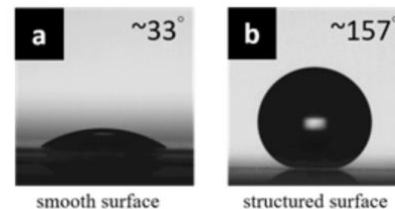


Figure 2: The contact angle of (a) smooth surface and (b) structured surface of the same material

References:

1. R. Helbig, J. Nickerl, C. Neinhuis, and C. Werner. (2011), Smart Skin Patterns Protect Springtails, *Plos One*, 25105.
2. T. Y. Liu and C. J. Kim. (2014), Turning a Surface Superrepellent Even to Completely Wetting Liquids, *Science*, 1096-1100.
3. M. S. Lee, P. H. Wu, W. S. Hsu, and Ieee. (2017), Fabrication of a Transparent Structured Superomniphobic Surface Using a Multiple Partial Expose Method, in *30th IEEE International Conference on MEMS* 1314-1317.

Preparation and characterization of PVA nanocomposites with bio-functionalized NDs

T. Remiš,^{1,*} T. Kovářík,¹ J. Kadlec,¹ P. Bělský,¹ R. Medlín,¹

¹ University Of West Bohemia, New Technologies - Research Centre, Pilsen, Czech Republic

Abstract:

Poly (vinyl alcohol) (PVA) has a long and successful history of applications in the biomedical and pharmaceutical area. At the forefront of multidisciplinary research in nanomedicine, carbon nanomaterials have demonstrated unprecedented potential for a variety of regenerative medicine applications. Nanodiamonds (NDs) are a unique class of carbon nanoparticles that are gaining increasing attention to their biocompatibility, highly functional surfaces, optical properties and intriguing physical properties. In this work, we have developed advanced PVA and NDs based nanocomposite membrane in a single step using a solution-casting method from an aqueous medium and achieved high dispersibility of NDs in the PVA matrix. The resulting nanocomposites have excellent properties derived from NDs and PVA. It has been found that thermal and mechanical properties increase dramatically with increasing NDs content, suggesting a strong chemical interaction between NDs and PVA. We assume that NDs will be a suitable nano-filler for PVA membranes. This work examines properties of PVA matrix reinforced with NDs particles and their potential application in biomedical field.

Keywords: nanodiamonds, nanocomposite, membrane, poly(vinyl alcohol), TGA, DMA, DSC, SAXS/WAXS, SEM

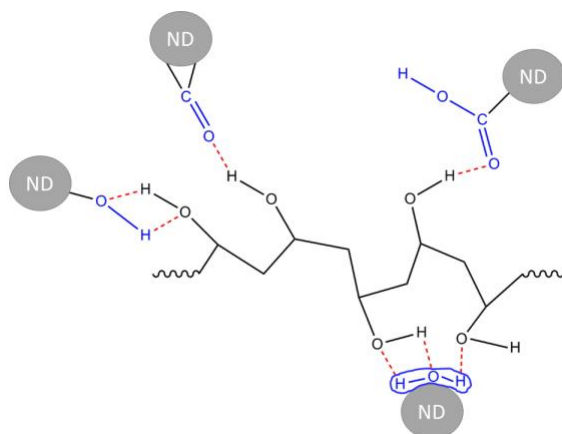


Figure 1: Schematic illustration of the interaction between PVA and NDs particles.

References:

1. Morimune, S., Kotera, M., Nishino, T., Goto, K., Hata, K. (2011). Poly (vinyl alcohol) nanocomposites with nanodiamond. *Macromolecules*, 44(11), 4415-4421.

Effects of He ion irradiation on silicon carbide nanowhiskers

E. Aradi*, J. Lewis-Fell, G. Greaves, S.E. Donnelly and J.A. Hinks

^aSchool of Computing and Engineering, University of Huddersfield, Queensgate, Huddersfield, HD1 3DH, United Kingdom.

Abstract:

Silicon carbide (SiC) is currently intended to be used as structural confinement material in some nuclear fusion and Generation IV fission reactor projects. This because it possesses remarkable high temperature strength, chemical inertness and small neutron capture cross section that make it promising for applications in advanced nuclear systems such as DEMO fusion reactor [1]. In these environments SiC will be exposed to high level of irradiation, high temperatures and accumulation of helium gas bubbles from radioactive decay. Nanoporous materials have been shown to possess high radiation tolerance due to their large free surface that acts as a unsaturable sink for radiation induced damage [2]. Using in-situ transmission electron microscopy studies, we investigate the response of SiC nanowhiskers (NWs) as a model system for nanoporous SiC to radiation damage, and compared to thin foils which represented bulk SiC, with an aim of revealing its radiation tolerance in nuclear environment. The SiC samples were irradiated with 6 keV He at temperatures between 100 and 1273 K and doses up to 50 dpa. At temperatures below 250 K, the NWs amorphised at almost 10 times the dose which the foils amorphized. At temperatures between 250 K and 500 K, the NWs remained crystalline and no He bubble nucleation occurs up to the doses studied. Between 773 and 1273 K, He bubble nucleation occurs with the bubble density increasing with increasing dose. In contrast to single crystalline samples at 1273 K, no He platelets or bubble discs were observed in the NWs with increasing dose indicating a high radiation tolerance. Radiation induced segregation and precipitation was also observed to occur in the NW samples for high temperature irradiation.

Keywords: silicon carbide; irradiation; nanoporous; nanowhiskers; radiation damage, amorphisation, He bubbles; radiation tolerance.

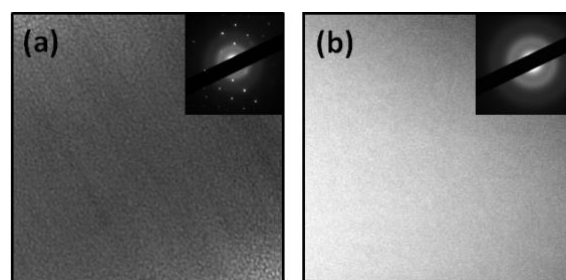


Figure 1: Bright field transmission electron microscopy images for (a) SiC NW and (b) SiC foils irradiated with 6 keV He to 10 dpa and at room temperature. The insets show the selected area diffraction patterns for the respective samples showing the NW being partially amorphous while the foil was completely amorphous.

References:

1. R. . Harrison, S. Ebert, J. . Hinks, and S. . Donnelly, "Damage microstructure evolution of helium ion irradiated SiC under fusion relevant temperatures," *J. Eur. Ceram. Soc.*, no. December 2017, p. 24, 2018.
2. E. M. Bringa *et al.*, "Are nanoporous materials radiation resistant?," *Nano Lett.*, vol. 12, no. 7, pp. 3351–3355, 2012.

Similarities and differences of fractional end charges in graphene zigzag ribbon and polyacetylene

S.-R Eric Yang

Physics Department, Korea University, Seoul, Korea

Abstract:

In polyacetylene and graphene nanoribbons a soliton with a fractional charge exists as a domain wall connecting two different phases. In polyacetylene a fermion mass potential in the Dirac equation produces an excitation gap, and a twist in this scalar potential produces a zero energy soliton. Similarly, in gapful graphene nanoribbons a distortion in the chiral gauge field can produce a solitonic domain wall between two neighboring zigzag edges with different chiralities [1]. The existence of a soliton in polyacetylene can lead to formation fractional charges on the opposite ends of polyacetylene. However, the situation is different in graphene nanoribbons since antiferromagnetic coupling between the opposite zigzag edges gives rise to integer boundary charges [2].

We show that presence of disorder in graphene nanoribbons partly mitigates the effect of antiferromagnetic coupling between the opposite zigzag edges. As a consequence of this, midgap states can have fractional charges on the opposite zigzag edges in the weak disorder regime [3]. The probability density of such a state is shown in Fig.1. The measurement of the differential conductance in atomically precise graphene zigzag nanoribbons [4] using a scanning tunneling microscopy may provide rich information on the distribution of edge charges.

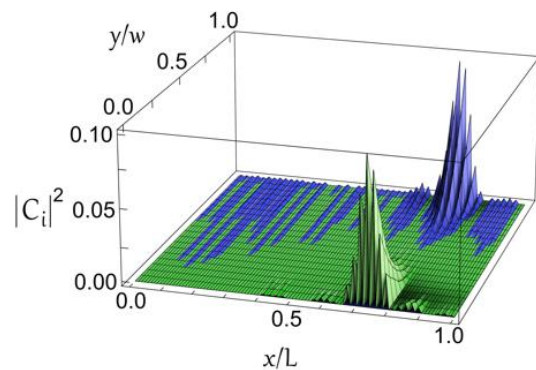


Figure 1 A midgap state with fractional charges of $1/2$ residing on the opposite zigzag edges. Plot displays the probability density of the midgap state as a function of coordinate (x,y) .

References:

1. Y. H. Jeong, S.C. Kim and S.-R. Eric Yang, Topological gap states of semiconducting armchair graphene ribbons, *Phys. Rev. B* **91**, 205441 (2015).
2. Y. H. Jeong and S.-R. Eric Yang, Topological end and Zak phase states of rectangular armchair ribbon, *Annals of Physics* **385**, 688 (2017).
3. Y. H. Jeong, S.-R. Eric Yang, and M. C. Cha, Fractional edge charges of interacting disordered graphene zigzag nanoribbon (submitted).
4. J. Cai , P. Ruffieux, R. Jaafar , M. Bieri , T. Braun , S. Blankenburg , M. Muoth , A. P. Seitsonen, M. Saleh, X. Feng , K. Mullen and R. Fasel, *Nature* **466**, 470 (2010); P. Ruffieux, S. Wang , B. Yang , C. Sanchez-Sanchez , J. Liu, T. Dienel, L. Talirz , P. Shinde, C. A. Pignedoli, D. Passerone, T. Dumslaff , X. Feng, K. Mullen and G. Fasel R, *Nature* **531**, 489 (2016).

The Influence of Graphene Oxide on the Epitaxial Integration of PLD-grown SrTiO₃ with Si(001) substrate

Z. Jovanović^{1,2,*}, U. Gabor¹, E. Tchernychova³, M. Podlogar⁴, D. Suvorov¹, M. Spreitzer^{1,*}

¹ Advanced Materials Department, Jožef Stefan Institute, Ljubljana, Slovenia

² Laboratory of Physics, Vinča Institute of Nuclear Sciences, Belgrade, Serbia

³ National Institute of Chemistry, Ljubljana, Slovenia

⁴ Department for nanostructured materials, Jožef Stefan Institute, Ljubljana, Slovenia

* Corresponding authors. Email addresses: zoran.jovanovic@ijs.si, matjaz.spreitzer@ijs.si

Abstract:

Epitaxial integration of oxides with semiconductor substrates is often limited by the lattice mismatch between the two material systems and their dissimilar chemical properties. However, in case of 2D materials the strict requirements of traditional epitaxy can be mediated by the weak van der Waals interactions. As a result, a 2D material, such as graphene, can allow remote epitaxial registry with a substrate at long distances [1] or act as a template by itself [2].

In the present work, we have investigated the potential of graphene oxide (GO) as epitaxy-enabling agent for the pulsed-laser deposition (PLD) growth of strontium titanate (STO) on Si(001) substrate. We have determined that GO can direct the growth of STO to a smooth, compact and pinhole-free layer, with single out-of-plane orientation. Furthermore, our results show that directing growth of STO on GO is less demanding in terms of interface control and vacuum conditions, which are important advantages for development of large area PLD processes.

Keywords: pulsed-laser deposition, silicon, graphene oxide, strontium titanate, epitaxy, oxide electronics.

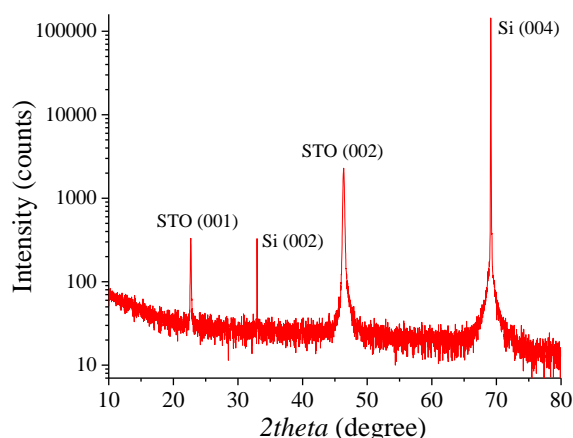


Figure 1: X-ray diffractogram of SrTiO₃ PLD-grown on graphene oxide-mediated Si (001) surface.

References:

1. Kim, Y., S.S. Cruz, K. Lee, B.O. Alawode, C. Choi, Y. Song, J.M. Johnson, C. Heidelberger, et al.; *Remote epitaxy through graphene enables two-dimensional material-based layer transfer*; *Nature* **544** (2017) 340.
2. Shi, Y., W. Zhou, A.-Y. Lu, W. Fang, Y.-H. Lee, A.L. Hsu, S.M. Kim, K.K. Kim, et al.; *van der Waals Epitaxy of MoS₂ Layers Using Graphene As Growth Templates*; *Nano Lett.* **12** (2012) 2784-91.

Electric Conductivity in Silicone-Carbon Black nanocomposites : percolation and Variable range hopping on a fractal

R. NEFFATI,^{1*} J. M. C. Brokken-Zijp²

¹ King Khalid University, Department of Physics, PO. Box 9032, Abha 61413, KSA

² The Dutch Polymer Institute, Technical University of Eindhoven, PO. Box 513, 5600 MB Eindhoven, The Netherlands

Abstract:

DC conductivity, of silicone-Carbon Black (CB) nanocomposites is measured when changing various experimental parameters and correlated to the fractal morphology of CB network (Figure 1a). The influence of filler volume fraction, temperature and electric field strength, are discussed using percolation and variable range hopping on a fractal as theoretical background. One also investigates effects of curing rate and CB content on both surface's morphology and conductivity (figure 1b).

The fractal aspect of CB network is studied by optical microscopy (OM) as well as Small angle X rays scattering (SAXS). Electric conductivity is measured using four points setup. AFM and STM are used to study respectively surface morphology and conductivity.

Low percolation threshold $\phi_c = 0,15\%$ and scaling exponent $\mu \sim 2,6$ of conductivity with CB volume fraction. The later exponent is correlated to the measured fractal dimension $d_f = 2,4$. Conduction at low temperature proceeds by mean of variable range hopping on the CB fractal network with a Mott's exponent $m = 0,65$ and temperature $T_0 = 64$ K. Non-Ohmic conductivity curves at different temperatures could be superposed into a unique master curve and the onset field of non-linearity Scales with temperature with a typical exponent $x_T \sim 1,2$. At low curing rate, capillary forces have time to bring down all CB particles from the surface into the bulk whereas at fast curing rate the roughness and conductivity of the surface remain high.

Keywords: DC electric conductivity, nanocomposites, percolation, Variable range hopping, non ohmic conduction, surface morphology, surface conductivity

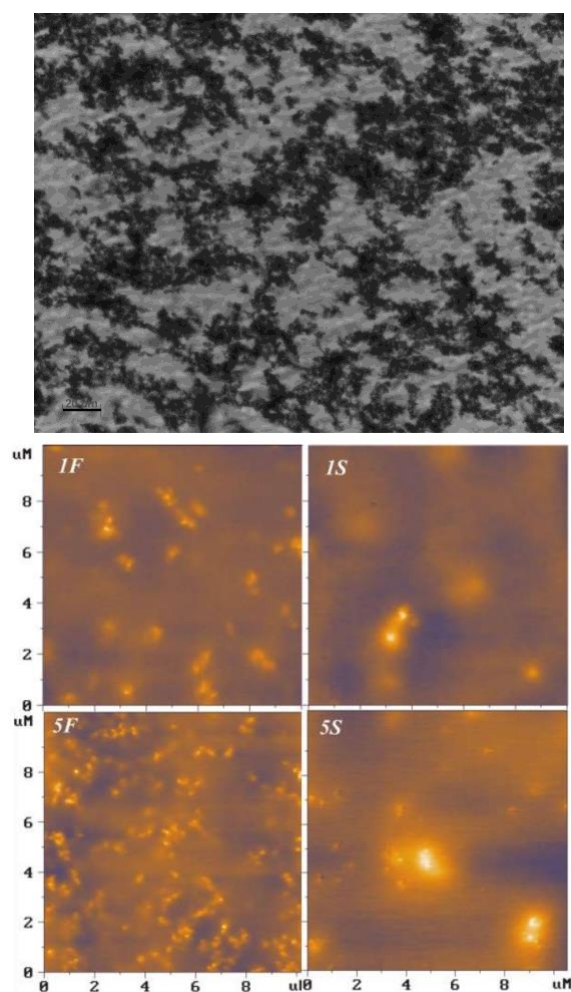


Figure 1: (a) Optical Microscope picture (X40) of 1wt% cured silicone-printex XE2 revealing the fractal Carbon Black network. (b) AFM picture of silicone-printex XE2 with different Carbon black content and different curing rate (1F) 1wt% without inhibitor. (5F) 5wt% without inhibitor (1S) 1wt% with 0,5 wt% inhibitor (5S) 5wt% with 0,5 wt% inhibitor. Color scale is 0-60nm from dark to clear.

References:

1. R. NEFFATI et al Macromol. Rapid Commun. 2003, 24, 113–117.
2. R. NEFFATI, et al. to be publish

Exploring the densification behavior of iron powder admixed with nanopowder and nanographite

Swathi K. Manchili*, Johan Wendel, Eduard Hryha, Lars Nyborg

Department of Industrial and Materials Science, Chalmers University of Technology,
Gothenburg 41956, Sweden

Abstract:

Improving the density of the press and sinter powder metallurgy components has constantly been pursued since it opens up the possibilities for their adaption into new and demanding application areas. Of the different ways to improve the sinter density, addition of nanopowder to the conventional micrometer sized metal powder is considered to be an effective solution. Nanopowder, owing to its high surface-to-volume ratio activates the sintering process at lower temperatures. Therefore, blending nanopowder to typically used micron-sized powder can contribute to a higher sinter density. Additionally, it can be hypothesized that the melting point could be reduced when the particle size is reduced to nanometer levels. Furthermore, the presence of nanographite can also influence the sintering process by acting as a dispersed reducing agent and aiding the process of sintering.

This study addresses the application of different kinds of nanoscale constituents as additives to conventional micron-sized iron powder. The powder blend is subjected to press and sinter route. The sintering phenomenon and also the influence exerted by the nanoscale additives is studied.

Keywords: sintering, dilatometry, electron microscopy, press and sintering, nanopowder, nanographite

Investigation of Vertically-Aligned Multi-Walled Carbon Nanotubes Bundles Mutual Coupling

L.Beccacece^{1,2*}, S. Xavier¹, C.Tripon-Canseliet², Y. Oussar³

¹Thales Research and Technology, Palaiseau, France

²Sorbonne Université – Faculté des Sciences - CNRS, Paris, France

³ESPCI Paris –PSL - CNRS, Paris, France

Abstract:

Despite vertically-aligned singlewall (SW) or multiwall (MW) CNTs technology have been theoretically studied by the international scientific community (e.g. [1], [2]) for antennas application, experimental demonstration of monopoles or dipoles based on this technology have not been performed yet. On the other hand, for thermal management and interconnexions, vias fabrication [3], [4] with vertically aligned MWCNT (VAMWCNTs) bundles settles at a good level of mastering. In this paper, we investigate, for the first time fabrication and characterization of coplanar waveguide (CPW) based RF-devices integrating two large VAMWCNTs bundles grown with thermally enhanced chemical vapor deposition (TECVD) process at 700°C, to analyse microwave signal coupling between them. The device we present consists in a CPW line characterized by a length of 600µm, a signal trace width of 120µm, integrating a gap of 20µm at the center of the signal line and VAMWCNTs bundles with a diameter of 100µm and a length of 730µm. The fabricated device is depicted in Fig. 1.

After S-parameters measurements operated between 100MHz and 25GHz with a Rhode & Shwarz ZVA50 network analyzer we found that thanks to the mutual coupling between the bundles we can enhance the signal transfer, as shown in Fig. 2. In the overall frequency band we see an average increase of 5% in the transmission coefficient, brought by the VAMWCNTs bundles.

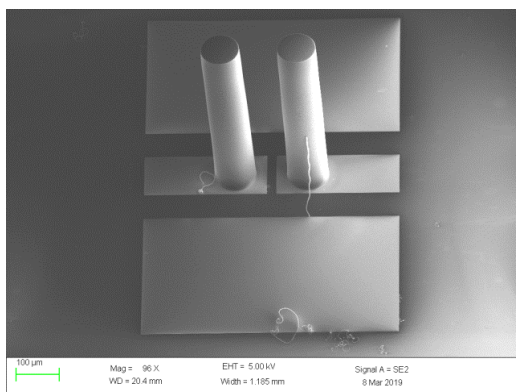


Figure 1: CPW-based device integrating VAMWCNTs bundles.

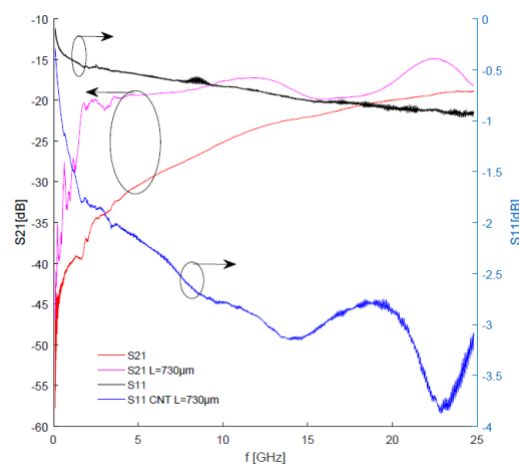


Figure 2: Return Loss and Insertion Loss comparison for the CPW-only and for the CPW integrating the two bundles.

Keywords: Carbon nanotubes, CNTs, MWCNTs, CNTs bundle, RF-device, mutual coupling, CPW

References:

1. N. Fichtner et al. "Investigations on CNT antennas", *Advances in Radio Science*, Vol. 6, pp. 209–211, May 2008.,
2. S.A. Maksimenko, G.Ya. Slepian, A.M. Nemilentsau, M.V. Shuba, "Carbon nanotube antenna: Far-field, near-field and thermal-noise properties", *Physica E: Low Dimensional Systems and Nanostructures*, Vol. 40, pp. 2360–2364, May 2008.
3. Mizuhisa Nihei et al, "Low-resistance Multi-walled Carbon Nanotube Vias with Parallel Channel Conduction of Inner Shells", *Proceedings of the IEEE 2005 International Interconnect Technology Conference*, 2005.
4. Nicolo' Chiodarelli et al, "Measuring the electrical resistivity and contact resistance of vertical carbon nanotube bundles for application as interconnects", *Nanotechnology* 22, 2011.

Unprecedented 1D Double Wires and 2D Mobile grids: Co/Bipyridine coordination networks at the solid/liquid interface

X. Sun ^{1*}, X. Yao ¹, F. Lafalet ¹, G. Lemerrier ², J. C. Lacroix ¹

¹ Université Paris Diderot, Sorbonne Paris Cité, ITODYS, UMR 7086 CNRS, Paris, France

² Université Reims Champagne-Ardenne, Institut Chimie Moléculaire Reims, Reims, France.

Abstract:

Series of molecules with bipyridine terminal unit bearing a central bridge (bpy-X-bpy) can adapt a cis-to-trans isomerization which can generate various self-assembled architectures and have been successfully observed by Scanning Tunneling Microscopy (STM) at the solid/liquid interface ^{1, 2}. Introduction of Co²⁺ ions on these assemblies generates an in situ chemical reaction between the terminal bipyridine groups from the ditopic ligands and Co²⁺ ions. Large monodomains of 1D double wires are formed by Co²⁺/ligand coordination, with polymer lengths of more than 150 nm. The polymers are organized in parallel 8 nm apart, the voids between two wires being occupied by solvent molecules. Non-linear two dimensional (2D) grids, showing high surface mobility, co-exist with the wires. The wires are formed from linear chain motifs where each cobalt center is bonded to two bipyridines. 2D grids are generated from a bifurcation motif where one cobalt bonds to three bipyridines. Surface reconstruction of the grids and of the 1D wires were observed under the STM tip. Analysis of these movements strongly indicates surface reaction at the solid liquid environments ³.

Keywords: STM, isomerization, coordination, ligands, Cobalt, pyridine, solid liquid interface

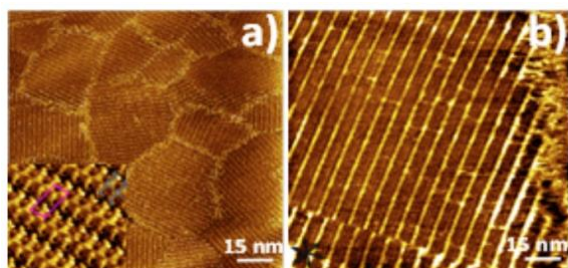


Figure 1: STM images showing the evolution from bpy-X-bpy self-assemblies to Co-bipyridine coordination polymers.

References:

1. **X. Sun**, D. Frath, F. Lafalet, J. C. Lacroix (2018) "Supramolecular Networks and Wires Dominated by Intermolecular BiEDOT Interactions", *J. Phys. Chem. C* 122, 22760–22766.
2. **X. Sun**, F. Lafalet, G. Lemerrier, F. Maurel, J. C. Lacroix, (2017) "Molecular Isomerization and Multiscale Phase Transitions of a Ditopic Ligand on a Surface", *J. Phys. Chem. C* 121, 20925–20930.
3. **X. Sun**, X. L. Yao, D. Frath, F. Lafalet, G. Lemerrier, J. C. Lacroix, (2019) "Unprecedented 1D Double Wires and 2D Mobile grids: Co/Bipyridine coordination networks at the solid/liquid interface" *To be submitted*

Effect of carbon nanotubes and seawater ageing on interlaminar fracture toughness of glass fiber/epoxy composites

C. Rubio-González*, J.A. Rodríguez-González

Centro de Ingeniería y Desarrollo Industrial, Av. Pie de la Cuesta #702, Col. Desarrollo San Pablo, C.P. 76125, Querétaro, Qro., Mexico.

Abstract:

The ability of carbon nanotubes to improve mechanical properties of fiber reinforced composites has made them an excellent candidate as nanofillers for the design and fabrication of composite structures. However, when composite structures are exposed to seawater ageing, their interlaminar interfaces can be adversely affected due to hydrolysis, plasticization and matrix swelling, causing delamination when they are subjected to impact and fracture loading conditions. Thus, research on the interlaminar fracture toughness of composite laminates modified with carbon nanotubes is needed to prevent delamination failure of composite structures especially when they are under environmental degradation like seawater ageing. In this regard, the present work investigates the influence of carbon nanotubes and seawater ageing on the mode I and mode II interlaminar fracture toughness of based-prepreg glass fiber/epoxy composite laminates. To this aim, double cantilever beam and end notched flexure tests were conducted to evaluate the mode I and mode II interlaminar fracture toughness of the glass fiber/carbon nanotubes/epoxy composite laminates with and without seawater ageing. The first part of the investigation reports the moisture absorption content of composite laminates exposed to seawater ageing for 4512 h at ~70 °C. Then, the outcomes of the interlaminar fracture tests are presented in terms of the resistance curve of the specimens with and without carbon nanotubes. Experimental results showed the positive effect of carbon nanotubes on the mode I and mode II interlaminar fracture toughness of composite laminates compared to the neat glass fiber/epoxy laminate. It was also found that seawater ageing promotes a moderately increase in the interlaminar fracture toughness of composite laminates due to matrix plasticization. These results were explained in terms of the damage mechanisms and

morphology observed at the fracture surfaces of tested specimens by scanning electron microscopy.

Keywords: Carbon nanotubes, interlaminar fracture toughness, seawater ageing, damage mechanism.

**NanoMetrology
Session I.C:
Nanomaterials
characterization /
Modelling**

From the Atomic Structure to the Optoelectronic Properties Studies of 1D and 2D Nanostructures via TEM

R. Arenal^{1,2,3,*}

¹Laboratorio Microscopias Avanzadas, INA, U. Zaragoza, 50018 Zaragoza – Spain

²Fundacion ARAID, 50018 Zaragoza – Spain

³Instituto de Ciencias de Materiales de Aragon, CSIC-U. Zaragoza, 50009 Zaragoza – Spain

Abstract:

The recent advances in transmission electron microscopes (TEM) bring access to electron probes of one angstrom within energy resolutions of <100 meV even working at low acceleration voltages (40-80 kV) [1-2]. These performances offer new possibilities for probing the optical, dielectric and electronic properties of nanomaterials with unprecedented spatial information, as well as for studying the atomic configuration of nanostructures [1-15]. In this contribution, I will present a selection of recent works involving all these matters. These works will concern the study of the atomic structure & configuration of 1D and 2D atomically thin nanostructures (including nanotubes & graphene/graphene-like materials, nanodiamonds in pristine and hybrid forms) as well as the opto-electronic properties studies carried out via EELS measurements [2-15]. These works will illustrate the excellent capabilities offered by the use of a Cs probe-corrected (S)TEM, combined with the use of a monochromator, to study these properties within a very good spatial resolution. In summary, these studies elucidate critical questions concerning the local chemistry and the structure of these materials. This detailed knowledge is essential for better understanding the outstanding properties of such nano-structures.

Keywords: 1D-2D nanomaterials, transmission electron microscopy, plasmonic nanostructures, HR(S)TEM, EELS, electron tomography.

References:

1. “Advanced Transmission Electron Microscopy: Applications to Nanomaterials”, Eds. L. Francis, A. Mayoral and R. Arenal. Springer (2015).
2. M. Serra, R. Arenal, R. Tenne, *Nanoscale* 11, 8073-8090 (2019).
3. R. Arenal, L. Henrard, L. Roiban, et al., *J. Phys. Chem. C* 118, 25643–25650 (2014).
4. P. Torruella, R. Arenal, F. de la Peña, et al., *Nano Lett.* (2016).
5. R. Canton-Vitoria, Y. Ahmed, M. Pelaez-Fernandez, R. Arenal, C. Bittencourt, C.P. Ewels, N. Tagmatarchis, *NPJ 2D Materials and Applications* (2017).
6. H.Y. Feng, F. Luo, R. Arenal, F. Garcia, G. Armelles, A. Cebollada, *Nanoscale* 9, 37 (2017).
7. L. Lajaunie, C. Padannaud, C. Martin, P. Puech, C. Hu, M.J. Biggs, R. Arenal, *Carbon* 112, 149-161 (2017).
8. L. Liu, U. Diaz, R. Arenal, G. Agostini, P. Concepcion, A. Corma, *Nature Materials* 16 (2017).
9. L. Liu, D. Zakharov, R. Arenal, et al., *Nat Comm.*, (2018).
10. L. Lajaunie, G. Radovsky, R. Tenne, R. Arenal, *Inorganic Chemistry* (2018).
11. L. Lajaunie, A. Ramasubramaniam, L. Panchakarla, R. Arenal, *Appl. Phys. Lett.* 113, 031102 (2018).
12. R. Arenal, *Microscopy and Microanalysis* 23 (S1), 2274-2275 (2017).
13. L. Vallan, R. Canton-Vitoria, H. Gobeze, Y. Jang, R. Arenal, A. Benito, W. Maser, F. D'Souza, N. Tagmatarchis, *J. Amer. Chem. Soc.*, 140, 13488-13496 (2018).
14. R. Arenal, et al. to be submitted.
15. Research supported by the Spanish MINECO (MAT2016-79776-P, AEI/FEDER, EU), Government of Aragon through project DGA E13_17R (FEDER, EU) and European Union H2020 programs ETN project “Enabling Excellence” (642742), “Graphene Flagship” (785219), “ESTEEM3” (823717) and Flag-ERA GATES (JTC 2017).

Atomic Scale Imaging and Spectroscopy: insight into single atom behaviour and collective electron motion in 1D and 2D materials

U. Bangert^{1*}, E. O'Connell¹, K. Moore¹, E. Courtney¹, E. T. Adegoke¹, M. Conroy¹, Q. Ramasse², D. Kepatsoglou², H. Hofsäss³, J. Amani³, S.-S. Tu⁴, B. Kardynal⁴

¹Dept of Physics, School of Sciences & Bernal Institute, University of Limerick, Limerick, Ireland

²SuperSTEM Laboratory, STFC Daresbury Campus, Daresbury WA4 4AD, United Kingdom

³II. Physikalisches Institut, Georg-August-Universität Göttingen, Friedrich-Hund-PLatz 1, 37077 Göttingen, Germany

⁴Peter Grünberg Institut 9, Forschungszentrum Jülich, 52425 Jülich, Germany

Abstract:

In this talk the characterisation of properties of 1-D and 2-D nano-materials via transmission electron microscopy on a highly spatially and energy resolved scale will be presented, covering observations on carbon nanotubes and graphene, as well as on 2-D TMDCs which are currently attaining great interest. It will also touch on a more recent and increasingly investigated, different class of 2-Ds, namely Domain Walls in ferro-electrics.

Single atom behaviour in 1-Ds and 2-Ds, including the determination of sites and dynamics of individual foreign atoms/vacancies/ad-atoms/electric dipoles will be revealed via high angle annular dark-field (HAADF) scanning transmission electron microscopy. Moreover, first observations of the behaviour of atoms introduced via ion-beam implantation in order to controllably functionalise 2-D and, generally, nano-materials, will be shown. One of the aims of ion implantation in combination with atomic-scale assessment of the implanted material is the proof of concept for the fabrication of nano-devices, e.g., single photon emitters, employing 2-Ds.

The talk will furthermore follow the development and application of methods for atomic-scale bandstructure characterisation, revealing, a.o., the local electronic structure and energetics connected with defect states and, especially, with collective electron (plasmon) excitations. The use of electron energy loss spectroscopy (EELS) in the low loss regime, in order to determine bandstructure and, in particular, plasmon energies, localisation and enhancement in specific nano-structured environments, will be demonstrated.

Keywords: 1-D and 2-D materials, atomic scale transmission electron microscopy and

spectroscopy, ion implantation, sites/constellations/ dynamics of individual atoms and defects, electronic structure, plasmons, nano-devices.

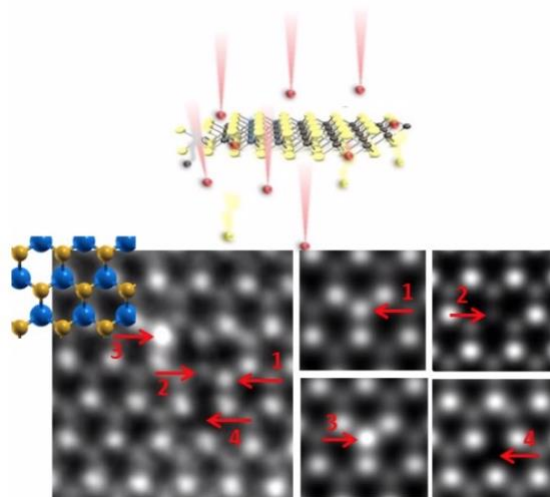


Figure 1: Shown on the left is an atomic resolution HAADF image of 2-D MoS₂ (with overlaid model structure representing Mo as blue and S as yellow balls), ion-implanted with Se. The red arrows point towards a Se atom substituting S (1), substituting Mo (2), attached as ad-atom (3), and a S di-vacancy (4). On the right are four image simulations with Dr Probe, of the respective atom constellations in the left image.

All experimental results are supported by image and EELS simulations and modelling, which in turn are backed up by DFT calculations of the nano-material's bandstructure, supporting the observation of the sites of atoms, their dynamics and energetics,.

The talk will also touch on what the future will bring in terms of observing materials behaviour on the nano/atomic scale under environmental conditions (in liquids and gases, under heating and biasing), via in-situ TEM.

Dynamic Contact Behaviours between Crystalline Nanoparticles

W. F. Sun,^{1,*} P. W. Chen,¹

¹ State Key Laboratory of Explosion Science and Technology, Beijing Institute of Technology, Beijing, P. R. China, 100081

Abstract:

Contact behaviours at the ultrascale nanoscale are sensitively dependent on the atomic arrangement and play an important role in engineering the mechanical, thermal or electrical conductivity properties of nanodevices. However, the effect of surface steps common in crystalline nanoparticles on the high-speed nanoscale contact behaviours has been rarely touched upon. In this work, high speed contact behaviours between diamond nanospheres including contact force, contact radius and mean contact stress have been studied using fully atomistic molecular dynamics simulations. This work could strengthen the capability of solving the problems experienced in practical applications where high-speed nanoparticle collisions are involved, such as magnetron sputtering, energetic nanoparticle's explosion.

Keywords: contact mechanics, Hertz model, diamond, nanoparticles, high-speed, molecular dynamic simulation.

References:

1. Sun, W. F., (2013), The dynamic effect on mechanical contacts between nanoparticles, *Nanoscale*, 5, 12658-12669.

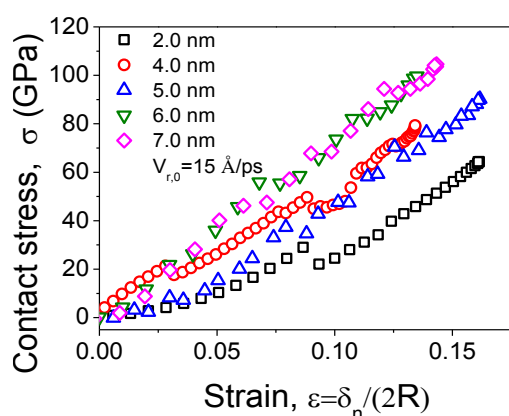


Figure 1: Mean contact stress as a function of nanoparticle's strain obtained from the high speed head-on normal impact between crystalline diamond nanospheres of various particle diameter ranging from 2.0 to 7.0 nm. The initial relative impact velocity is 1500 m/s. This work aims to explore the effect of surface steps common in crystalline nanoparticles on the dynamic mechanical response.

Seeing Small: Understanding Catalyst Nanoparticles in Fuel Cells by Advanced Electron Microscopy

Paulo J. Ferreira,^{1,2,3*}

¹University of Texas at Austin, Materials Science and Engineering Program, Austin, TX, USA

²IST, University of Lisbon, Department of Mechanical Engineering, Lisbon, Portugal

³International Iberian Nanotechnology Laboratory, Braga, Portugal

Abstract:

A thorough knowledge of the atomic structure and composition of catalyst nanoparticles is paramount to the development of advanced materials for proton exchange membrane fuel cells (PEMFC), one of the most promising energy conversion devices for automotive and stationary applications. Pt and Pt-based alloys nanoparticles (NPs) are currently used as the catalyst to promote the kinetics of the hydrogen oxidation and oxygen reduction reactions in the anode and cathode of the fuel cell, respectively. Yet, the durability of the catalysts remains the main issue for their commercialization.

In this talk, the focus is to understand the behavior of Pt and Pt-alloy NPs during the various stages of fuel cell cycling. For this purpose a set-up was developed to simulate the effect of voltage cycling on the cathode side of the fuel cell. In this set up, catalyst NPs supported on carbon nanotubes and amorphous carbon were deposited on a gold TEM grid attached to a gold plate, which is used as a working electrode in a three electrode electrochemical cell [1,2]. The NPs were then observed by advanced transmission electron microscopy, before and after cycling. The experiments show particle migration in conjunction with carbon corrosion during the initial cycles, whereas the appearance of single atoms and atomic clusters on the surface of the carbon support appear after additional voltage cycling as a result of surface dissolution of NPs. For the case of alloyed NPs, the experiments show a heterogeneous deposition of Pt on the NPs.

Keywords: Catalysts, Nanoparticles, Proton Exchange Membrane Fuel Cells, Aberration-corrected TEM/STEM, Tomography, Identical Location TEM.

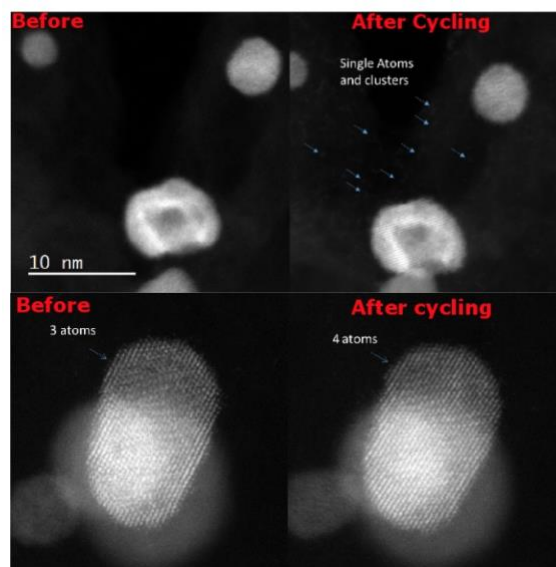


Figure 1: Appearance of single atoms and atomic clusters on the carbon support after voltage cycling, b) Deposition of a single atom on the surface of a nanoparticle.

References:

1. S. Rasouli, D. Myers, N. Kariuki, K. Higashida, N. Nakashima, P. Ferreira (2018), On the Electrochemical Degradation of Pt-Ni Nanocatalysts: An Identical Location Aberration-Corrected STEM Study, *Nano Letters*, 19 (1), pp. 46-53, (2018)
2. Somaye Rasouli, Deborah Myers, Kenji Higashida, Naotoshi Nakashima, Peter Crozier, Paulo Ferreira, (2019), Electrochemical Evolution of Pt Nanoparticles on CNTs and Amorphous Carbon Observed by Identical-Location Aberration-Corrected TEM, (submitted)

Modelling Graphene Wrinkles Formation on Metal Substrate in CVD

N. Thamwattana,^{1*} B. Cox,² T. Dyer,³

¹ University of Newcastle, School of Mathematical and Physical Sciences, Newcastle, Australia

² University of Adelaide, School of Mathematical Sciences, Adelaide, Australia

³ University of Wollongong, School of Mathematics and Applied Statistics, Wollongong, Australia

Abstract:

Chemical vapour deposition (CVD) is a popular technique for producing high-quality graphene sheets on a substrate. However, the cooling process causes the graphene sheet to undergo a strain-induced, out-of-plane buckling resulting in graphene wrinkles. These wrinkles often lead to undesirable effects on the properties of the graphene sheet. In this talk, we construct a mathematical model to understand the conformations of these wrinkles. Initially an arch-shaped wrinkle is modelled this is then generalised to incorporate graphene self-adhesion through van der Waals interactions across the wrinkle sides. Variational techniques are utilised to determine the lowest-energy conformation for both models. We find these models predict lowest-energy structures similar to those seen in experiments.

Keywords: graphene, chemical vapour deposition, wrinkles, calculus of variations, van der Waals interactions.

Characterization of nano-TiO₂ in commercial sunscreens via Inverse Supercritical Fluid Extraction and Miniaturized Asymmetrical Flow Field-Flow Fractionation

G. Heinzmann^{1,*}, F. Meier¹, D. Müller², S. Cattaneo², T. de Vries³, M. Portugal-Cohen⁴, L. Calzolari⁵, T. Klein¹

¹ Postnova Analytics GmbH, Landsberg, Germany

² Centre Suisse d'Electronique et de Microtechnique (CSEM), Landquart, Switzerland

³ FeyeCon Carbon Dioxide Technologies, Weesp, The Netherlands

⁴ Ahava Dead Sea Laboratories Ltd, Holon, Israel

⁵ Joint Research Center, European Commission, Ispra, Italy

E-Mail: info@postnova.com

Abstract:

Ambiguous media coverage about the pros and cons of “nano-enhanced” consumer products in recent years has significantly propelled the discussion about their safety. With this ongoing discussion, regulatory authorities such as the European Commission launched several regulations dealing with the declaration of products, which contain nanomaterial ingredients. One is the “European Regulation EC No 1223/2009 of 30 November 2009 on cosmetic products, in which it is stated that “all ingredients present in the form of nanomaterials shall be clearly indicated in the list of ingredients. [...] by the word ‘nano’ in brackets” [1]. However, until now, there is still a clear lack of analytical methodologies, which can provide a straightforward and reliable testing procedure for such products.

We present here a novel approach to reliably assess the nanoparticulate content of commercially available sunscreens. This approach encompasses a mild and environmentally friendly removal of water and lipophilic sunscreen ingredients via inverse supercritical fluid extraction (inverse SFE) followed by the determination of the size distribution as well as the elemental composition of the nanoparticulate content via miniaturized Asymmetrical Flow Field-Flow Fractionation [2] hyphenated with UV, Multi-Angle Light Scattering and Inductively-coupled Plasma Mass Spectrometry detection (mAF4-UV-MALS-ICP-MS) [3,4].

This setup enables a straightforward and clear distinction of “non-nano sunscreens” from “nano sunscreens” with high confidence under environmentally friendly conditions and has the potential to be the testing procedure of choice,

when it comes to the verification of the “nano-labelling” of commercially available cosmetic products.

Keywords: Field-flow fractionation, nano, titanium dioxide, cosmetics, sample preparation, inverse supercritical fluid extraction.

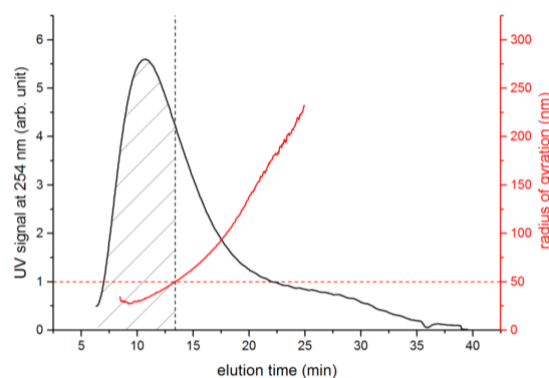


Figure 1: Size distribution of titanium dioxide nanoparticles in a commercial sunscreen after inverse SFE treatment and mAF4-UV-MALS analysis (reproduced with permission from 4.).

References:

1. European Regulation EC No 1223/2009 of **30 November 2009** on cosmetic products.
2. Müller D., Cattaneo S., Meier F. et al., *Frontiers in Chemistry*, **2015**, 3.
3. Müller D., Cattaneo S., Meier F. et al., *Journal of Chromatography A*, **2016**, 1440, 31-36.
4. Müller D., Cattaneo S., Meier F. et al., *Analytical Chemistry*, **2018**, 90(5), 3189-3195.

Support by the European Commission 7th Framework Programme (project SMART-NANO, NMP4-SE-2012-280779) is gratefully acknowledged.

Impedance Standards for Scanning Microwave Microscopy

T. Le Quang, D. Vasyukov, J. Hoffmann, A. Buchter, M. Zeier
Federal Institute of Metrology METAS, Bern, Switzerland

Abstract:

The scanning microwave microscopy (SMM) is a still rather new member of the family of scanning probe techniques. It has attracted attention due to its ability to characterize various electrical properties of samples, like dopant density, sheet conductance and dielectric properties. The basic working principle is to send a microwave signal to the scanning tip, where it is reflected depending on the sample underneath. The material parameters at the tip-sample contact determine the measured reflection coefficient, S_{11} , in amplitude and phase. As demonstrated recently in a report of SMM measurements on n-doped GaAs films [1], authors are able to extract quantitatively carrier densities of unknown GaAs samples after calibrating their SMM using S_{11} measured on three samples with known dopant density. The method is based on the same principle as the short-open-load (SOL) algorithm used for the one-port calibration of vector network analyzers. The same three-term error model can be applied to the SMM [2].

Here, we present SMM measurements performed on gold micron-scale structures fabricated on a free SiN membrane. To check the SOL equivalent method, we produce four similar structures (see Fig.1 as an example) having different nominal sizes to obtain various capacitances between 1-10 fF as confirmed by our Comsol simulations. Among these four samples, we choose randomly three devices as known samples to calibrate our SMM and the impedance of the remaining unknown device is calculated and compared to its nominal value (red diamonds in Fig.2) obtained from our simulations. As illustrated in Fig.2, a good agreement between nominal values of impedance and those obtained using the SOL equivalent method and either raw experimental S_{11} (blue crosses) or S_{11} acquired from simulations (black circles). While all (experimental and simulated) data plotted in Fig.2 are only obtained at 9.41 GHz, Comsol simulations suggest that this conclusion remains

valid in the whole frequency range between 1-50 GHz.

Keywords: Scanning microwave microscopy, scanning probe microscopy, microwave, impedance standards, calibration algorithm, electrical properties, semiconductors.

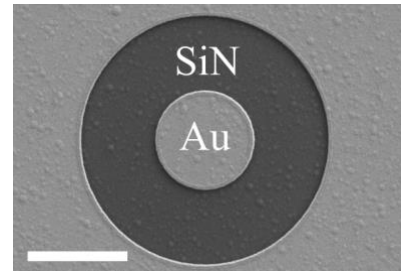


Figure 1: Scanning electron microscopic image of one capacitor. Gray and black regions are the deposited gold film and the exposed SiN membrane respectively. The scale bar is 4 μm .

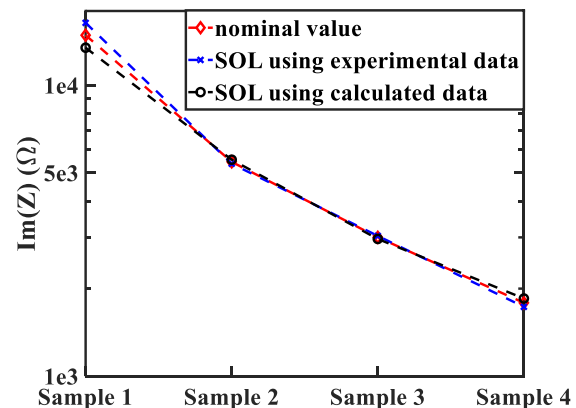


Figure 2: Comparison between nominal values of impedance (red diamonds) and those obtained by applying the SOL equivalent method to experimental S_{11} (blue crosses) and to values acquired from Comsol simulation (black circles). Here, the used frequency is 9.41 GHz.

References:

1. Arne Buchter, *et al.* (2018), Scanning microwave microscopy applied to semiconducting GaAs structures, *Rev. Sci. Instrum.*, 89, 023704.
2. J. Hoffmann, *et al.* (2018), A Calibration Algorithm for Nearfield Scanning Microwave Microscopes, *IEEE-NANO*, 2012.

Quantitative Nanomechanical Measurements of Carbon Nanotube-Metal Interfaces

C. Yi,¹ F. Gou,¹ C. Dmuchowski,² X. Chen,³ C. Ke,^{1,2*}

¹ State University of New York at Binghamton, Department of Mechanical Engineering, Binghamton, USA

² State University of New York at Binghamton, Materials Science and Engineering Program, Binghamton, USA

³ Xi'an Jiaotong University, School of Mechanical Engineering, Xi'an, China

Abstract:

The envisioned lightweight, high strength and enhanced durability characteristics of nanofiber-reinforced metal-matrix nanocomposites (MMNC) are attractive to a number of industries such as the aerospace, automotive and chemical industries. Carbon nanotubes (CNTs) are a type of light and strong material and hold promise as reinforcing fibers for disruptive MMNC technology. The load transfer on CNT-metal interfaces plays a critical role in achieving the enhanced bulk mechanical properties of CNT-reinforced MMNC. However, the interfacial load transfer characteristics of CNT-metal interfaces remain not well understood, which is in part due to the technical challenges associated with the small sizes of these nanostructures and nano interfaces. We report quantitative nanomechanical measurements of the mechanical strengths of the respective interfaces formed by individual double-walled CNTs with aluminum (Al) and titanium (Ti). The nanotube-metal interfacial strength is characterised by using *in situ* scanning electron microscopy nanomechanical single-nanotube pull-out techniques, as illustrated in Figure 1. The nanomechanical measurements reveal a shear-lag effect in the load transfer characteristics of the CNT-metal interfaces. CNT is found to possess a much stronger binding affinity with Ti as compared with Al. The study also reveals that thermal annealing has a profound impact on the CNT-metal interfacial strength. The research findings are useful to better understand the reinforcing mechanism of nanotubes and ultimately contribute to the optimal design and performance of nanotube-reinforced MMNC.

Keywords: interfacial strength, carbon nanotubes, metal matrix nanocomposites, thermal annealing, nanomechanical testing.

Figure 1: Figure illustrating the *in situ* scanning electron microscopy nanomechanical single-

nanotube pull-out testing scheme that is employed to measure the mechanical strength of the nanotube-metal interface. The tested interface is formed inside a sandwiched metal/nanotube/metal composite. A pre-calibrated atomic force microscopy cantilever that is mounted to a 3D nanomanipulator stage acts as a force sensor.

References:

1. Yi, C., Chen, X., Gou, F., Dmuchowski, C.M., Sharma, A., Park, C., Ke, C. (2017) Direct Measurements of the Mechanical Strength of Carbon Nanotube - Aluminum Interfaces, *Carbon*, 125, 93-102.
2. Yi, C., Bagchi, S., Dmuchowski, C.M., Gou, F., Chen, X., Park, C., Chew, H.B., Ke, C. (2018) Direct Nanomechanical Characterization of Carbon Nanotube - Titanium Interfaces, *Carbon*, 132, 548-555.

Nanomechanical Properties of embedded silica beads: nanoindentation versus PFT-QNM

R. Coq Germanicus¹, D. Mercier², F. Mickaël³, P. Descamps⁴, Ph. Leclère⁵

¹ CRISMAT, CNRS UMR6508, ENSICAEN, Normandie Université, 14050 Caen, France.

² CRM Group, Liège Belgium.

³ BRUKER, Nano Surfaces, 7 rue de la Croix Martre, 91120 Palaiseau, France.

⁴ IRSEEM, ESIGELEC, Normandie Université, Uniroouen 76000 Rouen, France.

⁵ CIRMAP, Service de Chimie des Matériaux Nouveaux, Université de Mons, Belgique.

Abstract:

Nanomechanical properties are key parameters to understand the macroscopic behavior and mechanical strain partitioning of materials. Nowadays different techniques based on the interaction between a specific probe and the studied sample have been developed to obtain the mechanical properties. The widely used is the classical depth-sensing instrumented nanoindentation where the curve force-displacement is recorded when a vertical rigid indenter penetrates the material. More recently the Peak Force Tapping Quantitative Nanomechanical Mapping (PFT-QNM)^[1,2], based on an Atomic Force Microscopy (AFM), provides local mechanical properties with a force control of the applied force on the cantilever combined with the spatial resolution of the AFM. In this mode, the probe is intermittently in contact with the sample during a short period. The maximum applied force to the cantilever is controlled to limit sample deformation to few nanometers. This mode achieves to the quantitative nano-mechanical properties such, deformation, adhesion and the contact modulus^[3]. In this study, we propose to analyze and compare the mechanical properties of silica beads embedded in an epoxy resin using instrumented nanoindentation tests and PFT-QNM measurements (Figure 1.a). Used as packaging for microelectronic devices, this composite material (Figure 1.b) is investigated to reach mechanical, thermic and electrical properties required to protect high integrated device^[4]. The aim main is take advantage of this two complementary probe-sample techniques for obtaining

nanomechanical properties of a material with a relative high Young's modulus of 72 GPa determined by nanoindentation and the DMT (Derjagin, Muller, Toropov) model used for the PFT-QNM (Figure 1.c.d).

Keywords: Silica, nanomechanical, nanoindentation, AFM, PFT-QNM, Young's modulus, hardness

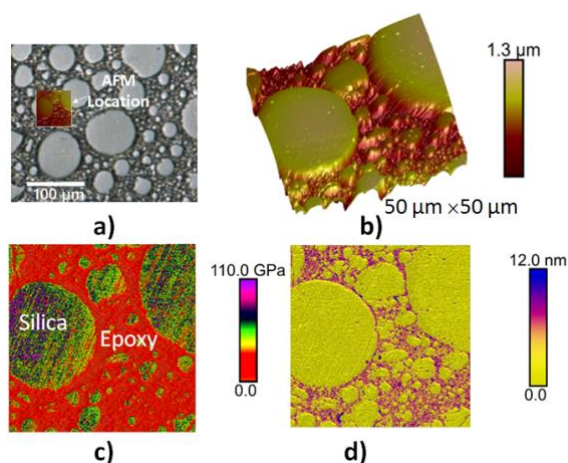


Figure 1: a) Optical view of the silica beads embedded in the epoxy matrix b) AFM topography, c) Contact modulus mapping and d) Deformation signal related to the mechanical hardness.

References:

1. M. E. Dokukin, I. Sokolov, *Langmuir* 2012,
2. O. Arnould, D. Siniscalco, A. Bourmaud, A. Le Duigou, C. Baley, *Industrial Crops and Products* 2017, 97, 224.
3. L. Morales-Rivas, A. González-Orive, C. Garcia-Mateo, A. Hernández-Creus, F. G. Caballero, L. Vázquez, *Scientific Reports* 2015, 5, 17164.
4. S. Komori, Y. Sakamoto, in *Materials for Advanced Packaging*, Springer, Boston, MA, 2009, pp. 339–363.

Spectroscopic studies of the stability of size-selected polyynes synthesized by Pulsed Laser Ablation in water

Sonia Peggiani^{1,*}, Anna Facibeni¹, Alberto Milani¹, Andrea Lucotti², Valeria Russo¹, Andrea Li Bassi¹ and Carlo S. Casari¹

¹Micro- and Nanostructured Materials Laboratory, Department of Energy, Politecnico di Milano, via Ponzio 34/3, 20133 Milano, Italy

²Department of Chemistry, Materials, and Chemical Engineering “Giulio Natta”, Politecnico di Milano, Via L. Mancinelli 7, 20133 Milano, Italy

Abstract:

Recent years have seen a growing interest in carbyne, the ideal infinite linear chain based on sp-hybridized carbon atoms. Real finite chains of alternated single and triple bonds are called polyynes, promising functional nanostructures which can be used for the development of advanced materials and devices for energy and electronic applications [1,2].

In this work, we investigated size-selected polyynes synthesized by pulsed laser ablation (PLA) in water focusing on their stability in time at different conditions.

PLA is a versatile and effective technique that allows the production of nanostructures. In particular, it is known that ablation of graphite or carbon-based particles suspended in solvent allows the formation of a series of hydrogen-capped polyynes of different length. The laser pulse absorbed by the target forms a plasma plume of the ablated material. The plume expands and cools down generating a cavitation bubble. The liquid rapidly quenches the bubble and favors the aggregation in nanostructures.

An open issue is the stability of these linear carbon chains, in fact they tend to rearrange and cross-link forming sp² bonds. In order to find simple and scalable way to stabilize polyynes by PLA in water we performed spectroscopic studies of mixture and size-selected polyynes by UV-Vis and surface-enhanced Raman spectroscopy (SERS) where Ag colloids are used as SERS-active medium. The ablation of a graphite target was performed by a Nd:YAG nanosecond pulsed laser at 532 nm in different volumes of water (100 ml, 50 ml, 10 ml, 2 ml) and the synthesized hydrogen-capped polyynes have been studied both as a mixture and as size-selected chains (C_nH₂: n=4-16) separated by high-performance liquid chromatography (HPLC).

Our mixture of hydrogen-capped polyynes shows a strong decrease in the intensity of the

peaks in the SERS and UV-Vis spectra already after 1 day, in accordance with literature. However, we have studied two stabilization strategies, the size-selected polyynes and the dried mixture of polyynes with Ag colloid, and we have observed in both cases stability at least after 2 months (see Figure 1). Finally, to find new conditions of stability of polyynes in view of developing novel nanomaterials we investigate the effects of the change of the ablation conditions such as temperature, influence of pH and addition of metallic salts to water.

Keywords: polyynes, pulsed laser ablation in water, PLA, stability, UV-Vis spectra, SERS spectra, HPLC, Ag colloids

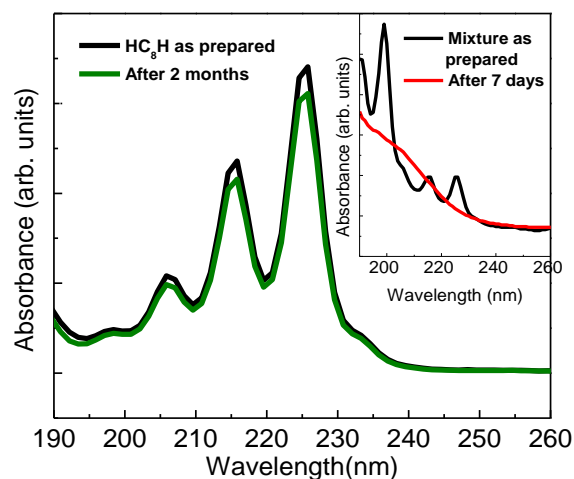


Figure 1: UV-Vis spectrum of size-selected polyynes (C₈) as prepared and after 2 months; in the inset, UV-Vis spectrum of the mixture of polyynes as prepared and after 7 days.

References

1. C.Casari et al., *Nanoscale*, 8, 8, 4414-4435, 2016.
2. C.Casari et al., *MRS Communications*, 8, 2, 207-219, 2018.

Development and application of a multifunctional nanoindenter: coupling to electrical measurements and integration in-situ in a Scanning Electron Microscope

S. Comby-Dassonneville¹, F. Volpi¹, C. Boujrouf¹, G. Beutier¹, G. Parry¹, M. Braccini¹, S. Iruela¹, A. Antoni-Zdziobek¹, Y. Champion¹, F. Charlot², R. Martin², F. Roussel-Dherbey², L. Maniguet², D. Pellerin³, M. Verdier¹

¹ Univ. Grenoble Alpes, CNRS, Grenoble INP, SIMaP, 38000 Grenoble, France

² Univ. Grenoble Alpes, Grenoble INP, CMTC, 38000 Grenoble, France

³ Scientec / CSInstruments, 91940 Les Ulis, France

Abstract:

Nanoindentation is a well-known characterisation technique dedicated to local mechanical testing of materials at small scales. In the past decades, numerous efforts have been made to expand the capabilities of nanoindentation technique [1]: real-time electron imaging, coupling with multifunctional characterisation tools, high temperature measurements,...

The present submission reports the development of a home-made multifunctional characterisation device based on a commercial nanoindentation head. This device combines mechanical to electrical characterisations, and can be integrated in-situ in a Scanning Electron Microscope (SEM) :

- Electrical characterisations cover both resistive and capacitive measurements.
- In-situ SEM integration allows precise positioning of nanoindentation tests (precision better than 100nm) as well as the positioning of electrically-coupled indentation maps.

Selected applications will be shown:

- Dielectric permittivity determination under mechanical load: an experimental procedure and a data-processing method have been set up to quantitatively extract the dielectric permittivity of insulating films from capacitive-nanoindentation (Fig.1). The procedure eliminates the effect of the stray capacitance which usually disturbs local capacitance measurements by AFM.
- Leakage current through insulators under mechanical load: Insulating films are known to degrade when subjected to mechanical stresses. This phenomenon is critical for industrial applications (microelectronics, electrotechnics,...). The present device allows the real-time monitoring of this insulation degradation. Leakage mechanisms

with or without mechanical load will be discussed.

- Multifunctional property mapping: The combined mapping of mechanical and electrical properties is also possible. An illustration will be shown on a multiphase alloy developed for its compromise between high tensile strength and high electrical conductivity.

A multifunctional characterisation tool will be presented, as well as selected applications. Prospects are numerous : capacitive-nanoindentation can fill a gap between quantitative characterisations at macro-scales and relative characterisations at nanoscale; leakage measurements under mechanical loads should help the understanding of oxide degradations; SEM-integration opens to multifunctional property mapping;...

Keywords: Multifunctional local characterisations; Nanoindentation; In-situ SEM; Dielectric permittivity; Leakage current.

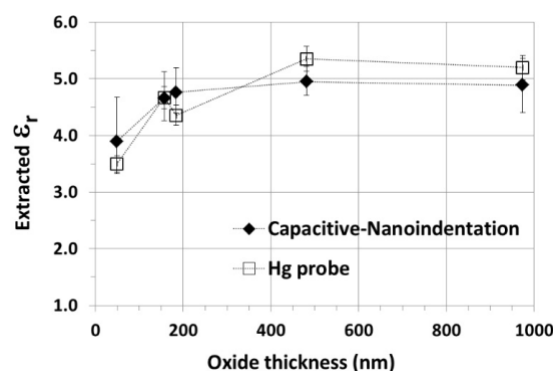


Figure 1: Local measurements of dielectric permittivity on different silica films (compared to macroscopic Hg-probe measurements).

References:

1. H. Nili, K. Kalantar-Zadeh, M. Bhaskaran, S. Sriram, In situ nanoindentation: Probing nanoscale multifunctionality, Prog Mater Sci. 58 (2013).

Synthesis, Characterization and Thermal Conductivity Modeling of Nanofluids for Advanced Heat Transfer Applications

M.M. Ghosh,* and Sujoy Das

Department of Metallurgical and Materials Engineering, National Institute of Technology,
Durgapur - 713 209, India

Abstract: In this work an easy method for synthesizing silver (Ag) nanoparticles through chemical route in an aqueous medium under atmospheric condition at ambient temperature has been developed. The synthesized nanoparticles have been characterized with different techniques, such as, X-ray diffraction, Fourier transform infrared spectroscopy, field emission scanning electron microscopy, energy dispersive X-ray spectroscopy, high resolution transmission electron microscopy, UV-visible spectroscopy and dynamic light scattering measurements. Experimental observations have revealed the absence of any metal oxide layer around the nanoparticles which are found to remain stable under ambient conditions. The nanofluids have been prepared by dispersing the nanoparticles in water medium. The thermal conductivity of the nanofluids with different volume fraction loading of Ag nanoparticles has been measured by transient hot wire method and the results have shown an increasing trend of enhancement in thermal conductivity with nanoparticles concentration within low volume fraction loading range.

A multiscale model comprising of molecular dynamics (MD) simulations coupled with Brownian dynamics and associated microconvection simulation has been developed focusing on the interfacial heat conduction from a heat source to a nanofluid for estimating the enhancement in thermal conductivity of the nanofluid. The prediction of the model agrees well with experimental data and hence, the model can be used for thermal design of the nanofluid.

Keywords: Ag nanoparticles, Nanofluids, Thermal Conductivity, Stability, Multiscale Modeling.

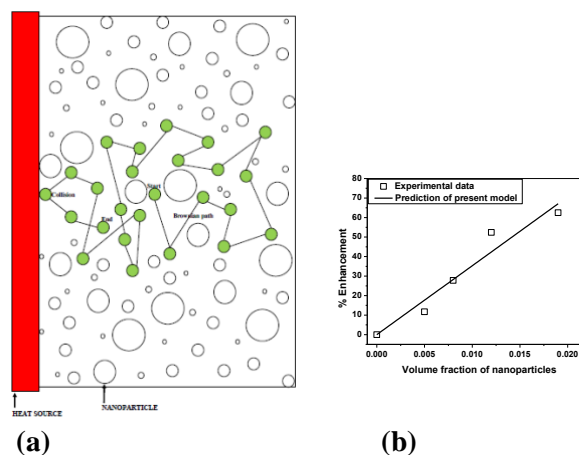


Figure 1: (a) Schematic representation of a sample nanofluid considered in the present multiscale model, (b) Enhancement in thermal conductivity estimated on the basis of present multiscale model and also experimentally obtained values for water based Ag nanofluid, with varying volume fraction loading of nanoparticles.

References:

1. Das, S., Bandyopadhyay, K. and Ghosh, M.M. (2018) A Study on Thermal Conductivity and Stability of Nanofluids Containing Chemically Synthesized Nanoparticles for Advanced Thermal Applications, *J. Mater. Eng. Perform.*, 27, 3994-4004.
2. Das, S., Rai, R.K. and Ghosh, M.M. (2013) **A Model of Heat Transfer in Nanofluids Using MD-Stochastic Simulation**, In: Proceedings of the International Conference on Precision, Meso, Micro and Nano Engineering (COPEN 8: 2013), held at Calicut, India during Dec. 13-15, 2013.

* Corresponding/presenting author. Ph. no.: +919434788182, email: madanmohan.ghosh@mme.nitdgp.ac.in

**Nanotech
Session I.D:
Nanomaterials properties**

Detection and characterization of nanoparticles via stimuli-induced heating

C. Geers,^{1*} L. Steinmetz,¹ A. Milosevic,¹ M. Bonmarin,³ B. Rothen-Rutishauser,¹ A. Petri-Fink,^{1,2}

¹ University of Fribourg, Adolphe Merkle Institute, Fribourg, Switzerland

² University of Fribourg, Chemistry Department, Fribourg, Switzerland

³ University of Cincinnati, College of Engineering and Applied Science, Cincinnati, USA

Abstract

A large variety of methods exists to analyze engineered nanoparticles (NPs) in liquid or solid complex environments, however, depending on the environment the methods suffer from limitations in complexity of sample preparation, NP specifications or data analysis requiring specific expertise.

For instance, fluorescent microscopy, e.g. requires fluorescent NPs or labelling with fluorescent dyes, which can, however, change the properties and behavior of NPs [1]. Other methods used to detect and quantify NPs or analyze their size, size distribution, and colloidal state in complex environments like dark-field hyperspectral imaging, electron microscopy, dynamic light scattering or inductively coupled plasma mass or optical emission spectrometry (ICP-MS/ICP-OES), require complex and time-consuming sample preparation, are lacking spatial information, only analyze a small portion of the sample, or chemically digest the NPs for their quantification.

A number of NPs have the ability to produce heat upon external stimulation (e.g. magnetic NPs upon stimulation by an alternating magnetic field) [2], plasmonic NPs (e.g. gold (Au) NPs, silver (Ag) NPs) by absorbing and scattering light [3], or upon other mechanisms (e.g. carbon nanotubes) [4].

In this talk I will present a new technique based on lock-in-thermography (LIT) to measure and quantify the heat produced by NPs upon light stimulation. This heat can be recorded with an infrared camera and is processed by a specially developed LIT algorithm to yield 2D-images for detection of NPs and analysis of their properties (e.g. aggregation, dissolution). The advantage of this set-up is the fast and accurate detection of NPs in a variety of matrices, without requiring complicated sample preparation and a large analysis area.

Keywords: nanoparticle analysis, nanoparticle detection, aggregation, dissolution, detection,

nanoparticle heating, stimuli responsive nanoparticles, cell association, biological environments, infrared imaging.

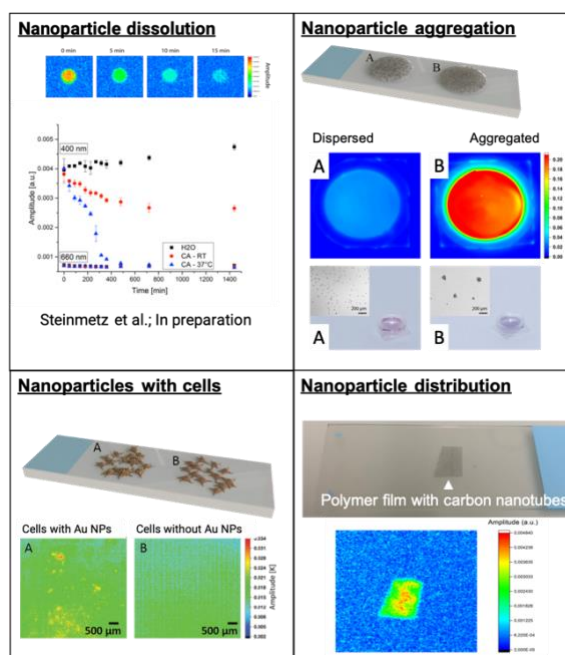


Figure 1: Figure illustrating the different possibilities of analyzing nanoparticles with LIT. The advantages are the rapidity of the measurements, the large analysis area (3.5 cm²) and the detection and analysis of nanoparticles in solid and liquid environments without complicated sample preparation.

References:

1. L. Rodriguez-Lorenzo, K. Fytianos, F. Blank, C. Von Garnier, B. Rothen-Rutishauser, and A. Petri-Fink, *Small*, 10, 1341 (2014)
2. C. A. Monnier, M. Lattuada, D. Burnand, F. Crippa, J. C. Martinez-Garcia, A. M. Hirt, B. Rothen-Rutishauser, M. Bonmarin, A. Petri-Fink, *Nanoscale*, 8, 27 (2016)
3. K. Jiang, D. A. Smith, A. Pinchuk, *J. Phys. Chem. C*, 117 27073 (2013)
4. R. Singh, S. V Torti, *Adv. Drug Deliv. Rev.*, 65 2045 (2013)

Comparison of the oxygen barrier properties of nano ZnO coated PET and PHBHHx packaging films via ultrasonic spray coating

M. Abbas,^{1*} M. Buntinx,¹ W. Deferme,^{2,3} N. Reddy,¹ R. Peeters,¹

¹Hasselt University, IMO-IMOMEC, Packaging Technology Center, Wetenschapspark 27, B-3590 Diepenbeek, Belgium

²Hasselt University, IMO-IMOMEC, Functional Materials Engineering Group, Wetenschapspark 1, B-3590 Diepenbeek, Belgium

³IMEC vzw–Division IMOMEC, Wetenschapspark 1, B-3590 Diepenbeek, Belgium

Abstract

Synthetic polymers are widely used due to their low cost¹ and high performance. On the other hand, these synthetic polymers have a negative impact on the environment because most of them are non-biodegradable and they can not be decomposed by microorganisms or bacteria. Bioplastics are more environmentally friendly due to their biobased origins and/or biodegradability². However, their barrier properties are not optimal for food packaging applications. In the past, nanoparticles (NPs) of zinc oxide (ZnO), titanium dioxide (TiO₂) and aluminum oxide (Al₂O₃) have been used in matrices of various bio(polymers) through different processing methods such as extrusion blow moulding³, solvent casting⁴ etc., to optimize the barrier properties. Wet chemical deposition, physical vapor deposition and chemical vapor deposition are the prominent deposition techniques of these nanoparticles. In this research, ultrasonic spray coating – a wet chemical technique – has been adopted to deposit ZnO NPs on commercial poly(ethylene terephthalate) PET and self-made poly(3-hydroxybutyrate-co-3-hydroxyhexanoate) PHBHHx films. In order to achieve a uniform coated layer, several experiments were performed to optimize the ink concentration and operating parameters of the spray coating method. An ink with 2.5 wt.% ZnO NPs was prepared in 1 wt.% polyvinyl alcohol (PVA), isopropanol (IPA) and de-ionized (DI) water. Optimized parameters of spray coating process were following: pump flow rate (0.1 ml/min), path speed (10 mm/sec), generator power (2.5 watts), nozzle to substrate distance (75 mm), hot plate temperature (30 °C) and amount of coated layers (50x). The scanning electron microscope (SEM) results demonstrate a uniformly deposited ZnO NPs layer on PET film (Fig. 1) and its barrier properties e.g. oxygen transmission rates (OTR) results show a decreasing trend for a coated PET film as compared to a neat PET film. For PHBHHx packaging film, a non-uniform coated layer of

ZnO NPs was observed in SEM results (Fig. 2), due to poor adhesion of ZnO NPs on its surface. Therefore, a non significant decreasing trend is observed for OTR results of a ZnO NPs coated PHBHHx film.

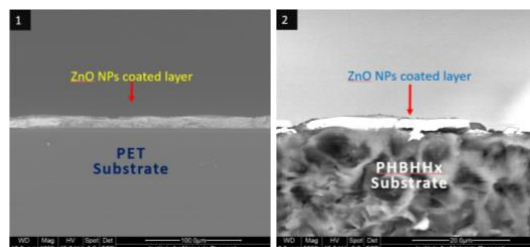


Fig. 1: SEM cross-sectional image of a 50-layer ZnO NPs coated PET film

Fig. 2: SEM cross-sectional image of a 50-layer ZnO NPs coated PHBHHx film

Keywords: Poly(ethylene terephthalate) (PET), Poly(3-hydroxybutyrate-co-3-hydroxyhexanoate) PHBHHx, ultrasonic spray coating, oxygen transmission rate.

References:

1. <https://www.nap.edu/read/2307/chapter/5>
2. <https://www.european-bioplastics.org/bioplastics/>
3. Jasim Ahmed, Yasir Ali Arfat, Hassan Al-Attar, Rafael Auras, Mohammad Ejaz, “Rheological, structural, ultraviolet protection and oxygen barrier properties of linear low-density polyethylene films reinforced with zinc oxide (ZnO) nanoparticles”, *Food packaging and shelf life*, vol. 13, pp. 20-26, 2017.
4. Yasir Ali Arfat, Jasim Ahmed, Abdulsalam Al Hazza, Harsha Jacob, Antony Joseph, “Comparative effects of untreated and 3-methacryloxypropyltrimethoxysilane treated ZnO nanoparticle reinforcement on properties of polylactide-based nanocomposite films”, *International Journal of Biological Macromolecules* 101 (2017) 1041–1050

Resistivity of Nanometer Thick Manganite Films Under Elastic Strain

G.A.Ovsyannikov^{1*}, T.A. Shaikhulov¹, V.A.Shakhunov¹, A.A. Klimov¹, V.L. Preobrazhensky², N. Tiercelin³, P.Pernod³

¹ Kotelnikov Institute of Radio Engineering and Electronics, RAS, Moscow, 125009, Russia

² Prokhorov General Physics Institute RAS, Moscow, 119991, Russia

³ Univ. Lille, CNRS, Centrale Lille, ISEN, Univ. Valenciennes, UMR 8520 - IEMN, F-59000 Lille, France

Abstract:

A complex study of the electron transport and magnetic characteristics of epitaxial manganite films $\text{La}_{0.7}\text{Ba}_{0.3}\text{MnO}_3$ (LBMO) was carried out under conditions of the crystal structure tension caused by a mismatch between the parameters of the LBMO crystal and the substrate. The epitaxial thin films with the thickness 40-100 nm were grown by Pulsed Laser Deposition at $T=700\text{-}800\text{C}$ in pure oxygen pressure 0.3-1 mbar. The substrates (110)NGO, (001)STO, (001)LAO, (001) LSAT and ferroelectric crystals (011) PMN-PT were used. By comparison of the lattice parameter of LBMO targets with substrate's one the lattice mismatches were derived [1,2]. A nonmonotonic temperature dependence of the resistance of a LBMO film deposited on ferroelectric crystals PMN-PT was observed. This feature is typical for manganites and indicating the presence of ferromagnetism in the system. Ferroelectric crystal PMN-PT was used as an active substrate for application of elastic stress to the manganite films. The strong anisotropy of resistive parameter was observed. Figure 1 shows the dependence of the resistance of the LBMO film on the electric field strength applied normally to the substrate. The resistance was measured in two directions parallel to [001] and [011] axes of the substrate. Hysteretic dependence of the resistance of the LBMO film on the piezoelectric strain of the substrates was detected. The strongest variation of the resistance of the film is observed in the same area of the electric field as variation of the mechanical deformation of the substrate [3]. It is shown that the stable resistive states arise as a result of asymmetric inplane deformations of the films.

Keywords: epitaxial manganite film, lattice mismatch, piezoelectric deformation, resistive states.

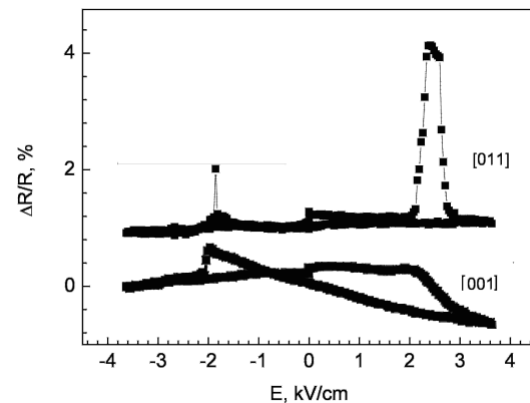


Figure 1: The dependence of the resistance of the LBMO film on the electric field strength applied to the substrate (011)PMN-PT. Measurements are made in two directions parallel to [100] and [011] axes of the PMN-PT substrate.

References:

1. Millis A.J., Darling T., Migliori A. (1998) Quantifying strain dependence in "colossal" magnetoresistance manganites *J. Appl. Phys.* 83, 1588-1591.
2. Ovsyannikov G. A., Petrzhik A. M., Borisenko I. V., Klimov A. A., Ignatov Yu. A., Demidov V. V., Nikitov S. A. (2009) Magnetotransport Characteristics of Strained $\text{La}_{0.7}\text{Sr}_{0.3}\text{MnO}_3$ Epitaxial Manganite Films *J. Exp. Theor. Phys.* 108, 48-55.
3. Ovsyannikov G.A., Shaikhulov T.A., Shakhunov V.A., Mathurin T., Tiercelin N., Pernod P., Preobrazhensky V.L. (2019) Resistivity of manganite thin film under strain. *J. of Superconductivity and Novel Magnetism in press.*

Au_{NPs}-supported magnetite nanoparticles: a composite material for catalysis and energy storage

B. Ballarin¹, M.C. Cassani¹, I. Ragazzini¹, C. Parise¹, D. Nanni¹, N. Sangiorgi², D. Rinaldi^{3*}, L. Montalto³, P. Mengucci³

¹Dipartimento di Chimica Industriale "Toso Montanari", Università di Bologna, Via Risorgimento 4, I-40136, Bologna, Italy; barbara.ballarin@unibo.it

²CNR-ISTEC, Via Via Granarolo, 64 – I-48018 Faenza (RA) Italy

³Dept. SIMAU, Università Politecnica delle Marche, via Brecce Bianche, I-60131 Ancona, Italy; d.rinaldi@univpm.it

Abstract:

Magnetic nanomaterials have been intensively explored for various technological applications in these last years. Fe₃O₄NPs are one of the most widely used magnetic nanomaterials, which has inherent high surface to volume ratio and magnetic property^[1]. As well as the pristine form, they can be used as different nanocomposites materials including Fe₃O₄@Au_{NPs}, Fe₃O₄@Pt_{NPs}, and Fe₃O₄@carbon dots. The combination of different nanoscale functionalities is capable of endowing the substrate with enhanced properties giving great application potentials in different fields (i.e. catalysis, environmental remediation, sensors, energy devices, etc.)^{[2][3]}. In this work a convenient method for the preparation of Au_{NPs} supported magnetite nanoparticles (Fe₃O₄@Yne-Au or Fe₃O₄-Au) was presented. Fe₃O₄NPs, obtained by co-precipitation of iron sulphate salts^[4] in alkaline media (i.e. NH₃) were used modified with a propynylcarbamate moiety (or pristine) and then reacted with an aqueous solution of chloroauric acid as the only reactant, without any need of additional reducing and/or stabilizing agents^{[5][6]}. These systems have been used for the preparation of electrodes for pseudocapacitors assembly obtained by electrodeposition. Composite materials based on Fe₃O₄@Yne-Au (or Fe₃O₄-Au) and polyaniline (PANI) have been grown up on graphite foil by cycling the potential in a 0.5 M H₂SO₄ + 0.1 M LiClO₄ solution. The film characterization by SEM and EDS as well as the charge-discharge test (C/D) and impedance test (EIS) will be presented.

Keywords: Magnetite, Au nanoparticles, Conducting polymers, Pseudocapacitor, Electrodeposition.

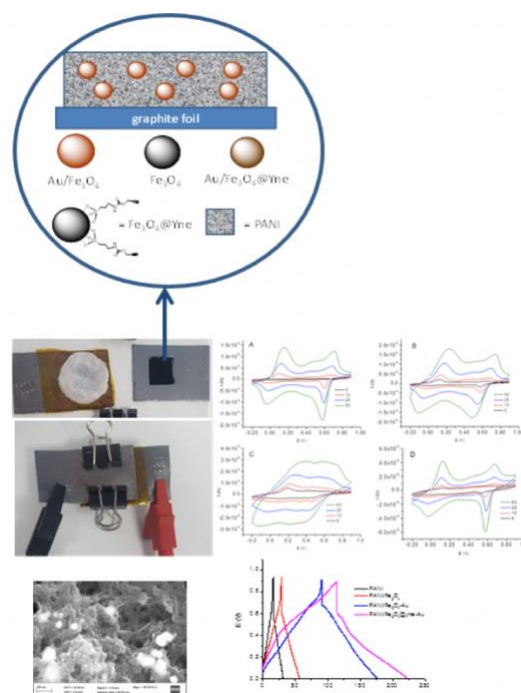


Figure 1: Figure illustrating the composite film used in this work and the pseudocapacitor preparation.

References:

1. H. Lu, *et al.* (2007), *Angew. Chemie - Int. Ed.*, 46, 1222.
2. P. Miao, *et al.*, (2017) *ACS Appl. Mater. Interfaces*, 9, 3940.
3. E. M. de Moura *et al.*, (2015) *RSC Adv.*, 2015, 5, 15035.
4. R. B. N. Baig *et al.*, (2012) *Chem. Commun.*, 48, 6220.
5. B. Ballarin *et al.*, (2017) *ACS Sustain. Chem. Eng.*, 5, 4746.
6. B. Ballarin *et al.*, (2019) *Ceramics International*. 45, 449.

Electromagnetic Shielding Effectiveness and Dissipation of Electrostatic Discharge of PC/ABS Filled with Nano Carbon Black

W. Sriseubsai,^{1*} A. Tippayakraisorn,¹

¹ Industrial Engineering Department, Faculty of Engineering,
King Mongkut's Institute of Technology Ladkrabang, Ladkrabang, Bangkok, Thailand.

Abstract:

Objective of this research was to study the electromagnetic shielding effectiveness (SE) and dissipation of electrostatic discharge (ESD) of polymer blends between polycarbonate (PC) and acrylonitrile-butadiene-styrene (ABS) filled with carbon black powder (CBp) and carbon black masterbatch (CBm). The mixtures of PC/ABS/CB composites were prepared for the injection molding to make the specimens with thickness of 4 mm. The D-optimal mixture design which was the constrained mixture designs was applied with this experiment (Figure 1). The experiments were performed with limitation of carbon black which could not exceeding 17 percent by weight due to the melt flow rate of mixture. The EMI SE was measured between the frequency ranges of 800 to 3,000 MHz according to the MIL-STD-285. The result showed that the trend of the SE values increases with increasing amount of the filler. The particle sizes had little effect on the SE values due to the mixing method. Carbon black powder which smaller particle sizes is not dispersed well in the plastic matrix. The SE values of PC/ABS/CBp is close with the SE values of PC/ABS that filled with carbon black masterbatch. The results of the performance testing for shielding electromagnetic waves showed that there were limitations of these composited material applications because the electromagnetic shielding effectiveness was not high enough when compared to metal materials. The surface resistivity of the PC/ABS/CB composites was determined according to the ASTM D257 for studying and dissipation the effects of electrostatic discharge (ESD). It was found that the surface resistivity of the plastic with no additives was 10^{12} Ω /square. When the amount of fillers was increased, the trend of surface resistivity of plastic composites decreased to the range of 10^6 - 10^{11} Ω /square, which was suitable for the application in the dissipation of electrostatic discharge which require materials

with a surface resistivity in the range 10^4 to 10^{11} Ω /square. This plastic composite can be used in the electronic packaging.

Keywords: PC/ABS; carbon black, electromagnetic shielding effectiveness, dissipation of electrostatic discharge

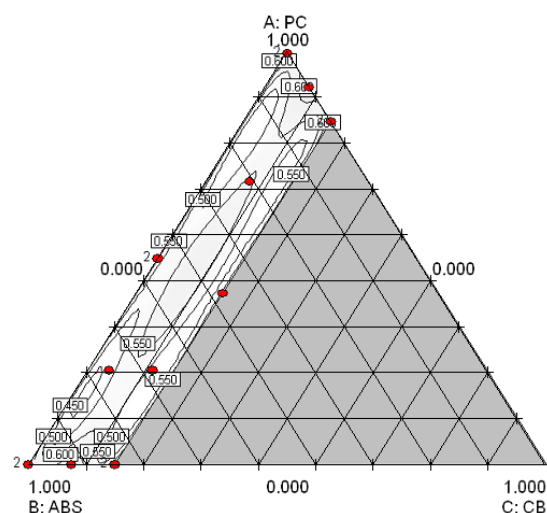


Figure 1: Mixture Design.

References:

1. Chi-Yuan Huang and Tey-Wen Chiou.(1998), The Effect of reprocessing on The EMI Shielding Effectiveness of Conductive Fibre Reinforced ABS Composites. *European Polymer Journal*. 34(1), 37-43.
2. Dang, Baokang; Chen, Yipeng; Yang, Ning; and et al.(2018), Effect of carbon fiber addition on the electromagnetic shielding properties of carbon fiber/polyacrylamide/wood based fiberboards, *Nanotechnology.*, 29(19).

Role of Defects in the Sensing Mechanism of Single-Wall Carbon Nanotube Field-Effect Transistors

A. Hankins, M. Paranjape

Georgetown University, Department of Physics, Washington D.C., USA

Abstract:

In nanotechnology, understanding the effect of interfaces and defects becomes critically important in determining a material's properties and device performance. It is well known that one-dimensional and two-dimensional materials exhibit excellent physical, electrical, thermal, and optical properties, making them highly desirable for a wide array of applications. However, their low dimensionality also means their performance can be susceptible to defects in the material and the interfaces they form with other device components. Carbon nanotubes are often used in sensing applications, typically, in a field-effect transistor configuration (CNTFET). The interface between the contact electrode metal and the nanotube forms a Schottky barrier, which has an important role in establishing both transistor and sensor characteristics. Modifications to this interface by the environment can modulate the barrier and produce a change in device characteristics. Transistor operation may also be modified by the presence of defects in the carbon nanotube structure. The role of defects and the interplay between the Schottky barrier and the defects present in the carbon nanotube represent critical areas of interest for CNTFET based sensors. Therefore, the purpose of this study is to explore how defects in single-walled carbon nanotubes can affect the sensing mechanism of CNTFET devices. Gas exposure measurements were performed on near pristine (low defect) nanotube devices and compared with induced, highly-defective nanotube devices. By utilizing selective passivation to isolate structural components that contribute to the sensing mechanism, results show that the presence of defects, and their relative densities, has a critical role in gas sensing performance. With only nanotube sidewall gas interaction, the response shows contrary behavior depending on low or high defect densities. The presence of these defects, or worse, inaccurately assuming their absence in as-grown nanotubes, likely explains why several research groups still continue to

debate the gas sensing mechanism. These results represent an important step toward understanding the effect of both interfaces and defects for carbon nanotube sensor development and adds a critical piece of understanding necessary for the development of future nanoscale sensors.

Keywords: carbon nanotubes, field-effect transistor, defects, Schottky barriers, sensing, selective passivation

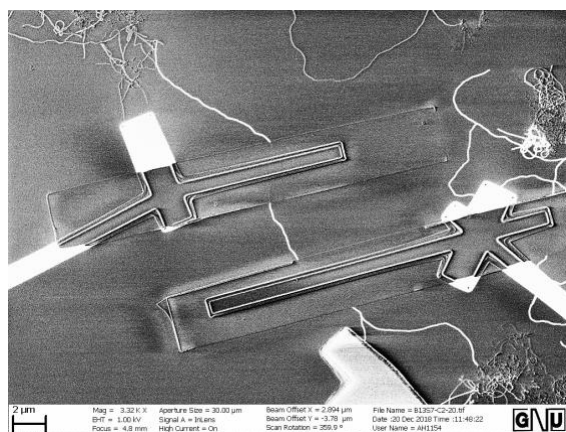


Figure 1: Figure depicting selectively passivated CNTFET device used for exploring the effect of defects in carbon nanotube structure on transistor characteristics. Individual single-walled carbon nanotubes are fabricated into field-effect transistors. The electrodes and interface region are passivated using aluminum oxide, isolating these regions from gas molecules thereby separating the sensor response due to the interface from that of the nanotube channel.

References:

1. J. Zheng, A. Boyd, A. Tselev, M. Paranjape and P. Barbara, "Mechanism of NO₂ detection in carbon nanotube field effect transistor chemical sensors," *Applied Physics Letters*, vol. 88, pp. 123112-1-3, 2006.
2. P. G. Collins, "Defects and Disorder in Carbon Nanotubes," in *Oxford Handbook of Nanoscience and Technology: Frontiers and Advances*, Oxford, Oxford University Press, 2009.

YF₃:Yb³⁺, Er³⁺ luminophore as a potential new sensor of high pressure and high temperature

S. Goderski,^{1,*} P. Woźny,¹ M. Runowski,¹ V. Lavín,² S. Lis¹

¹ Adam Mickiewicz University in Poznań, Faculty of Chemistry, Poznań, Poland

² Universidad de La Laguna, Departamento de Física, San Cristóbal de La Laguna, Spain

Abstract

In recent years the measurements of the high pressure and temperature using luminescence properties of nano- and microcrystalline luminophors started to be intensively investigated. Such materials allows contactless sensing of pressure/temperature in applications where it is hard or impossible to utilize commonly used sensors, such as: high pressure chambers, temperature sensing of small elements, biosensing, etc. Part of such luminescent materials are inorganic nano- and microcrystalline luminophores doped with lanthanide(III) or (II) ions, such as: Sm²⁺, Er³⁺, Tm³⁺, Eu³⁺, Nd³⁺, Pr³⁺, Ho³⁺. They have good luminescence properties, narrow emission bands resulting from 4f-4f electron transitions, very good chemical and physical stability, resistance to photobleaching, thermalized levels, small broadening of emission bands with the temperature. Temperature or pressure can be determined by relating its value with luminescence parameters: luminescence intensity ratio, band ratio, lifetimes, peak centroid position, full width at half maximum.

New contactless sensors can be applied for development of new materials in high pressures/temperatures, simulations of geological processes, temperature measurements of small objects (e.g.: cells, nanowires).

In this work we would like to show you the preparation method and spectroscopic characterization of the YF₃:Yb³⁺, Er³⁺ luminophore excited with IR light. We determined the possibility of using this material as a sensor for both temperature and pressure up to 478 K and 8 GPa, respectively. We also checked if it is possible to determine both parameters at the same time. Sample was additionally characterized with techniques, such as: XPRD, SEM, EDS.

Keywords: upconversion, contactless sensing, high pressure, high temperature, luminescence, yttrium fluoride YF₃, lanthanide.

The work was supported by grant no. POWR.03.02.00-00-I023/17 co-financed by the European Union through the European Social Fund under the Operational Program Knowledge Education Development.

References:

1. Runowski, M., Marciniak, J., Grzyb, T., Przybylska, D., Shyichuck, A., Barszcz, B., Katrusiak, A., Lis, S. (2017) Lifetime nanomanometry – high-pressure luminescence of up-converting lanthanide nanocrystals – SrF₂:Yb³⁺, Er³⁺, *Nanoscale*, 9, 16030-16037.
2. Runowski, M., Woźny, P., Stopikowska, N., Guo, Q., Lis, S. (2019) Optical Pressure Sensor Based on the Emission and Excitation Band Width (fwhm) and Luminescence Shift of Ce³⁺-Doped Fluorapatite—High-Pressure Sensing, *ACS Appl. Mater. Interfaces*, 11(4), 4131-4138.
3. Runowski, M., Shyichuck, A., Tyminiński, A., Grzyb, T., Lavín, V., Lis, S. (2018) Multifunctional Optical Sensors for Nanomanometry and Nanothermometry: High-Pressure and High-Temperature Upconversion Luminescence of Lanthanide-Doped Phosphates—LaPO₄/YPO₄:Yb³⁺-Tm³⁺, *ACS Appl. Mater. Interfaces*, 10(20), 17269–17279.
4. Brites, D. S. C., Balabhadra, S., Carlos, L. D. (2018) Lanthanide-Based Thermometers: At the Cutting-Edge of Luminescence Thermometry, *Adv. Optical Mater.*, 1801239-1801269.

Multifunctional nanomodifiers of cellulose fibers based on core/shell type structure doped with chosen Ln³⁺ ions

M. Skwierczyńska,^{1*} M. Runowski,¹ S. Goderski,¹ P. Kulpiński,² S. Lis,¹

¹ Adam Mickiewicz University in Poznan, Faculty of Chemistry, Department of Rare Earths, Poland

² Technical University of Lodz, Department of Man-Made Fibers, Poland

Abstract:

Cellulose based composites have recently attracted increasing attention. A perfect example of these composites are the cellulose fibers modified with the use of special modifiers or fillers. The presence of modifier particles inside or on the surface of the fiber ensures their unique properties. So far many different types of modified fibers have been obtained, e.g. antibacterial, catalytic, conductive, magnetic, photoluminescent, thermochromic and so on. However, the preparation of cellulose fibers exhibiting more than one additional functionality is still a challenge.

We report a way of preparation of luminescent-magnetic cellulose fibers. The fibers owe their properties to the introduction of modifier nanoparticles (NP). The modifier NPs were composed of core/shell type nanostructures, having a magnetic core covered by an inner silica shell and an external luminescent shell, consisted of rare earth fluorides doped with Tb³⁺ and Eu³⁺ ions. The response to the applied external magnetic field and the bright multicolour luminescence is guaranteed by the magnetite (Fe₃O₄) core and the external shell, respectively. The fibers were produced by a dry-wet spinning method, with the use of N-methylmorpholine-N-oxide (NMMO) as a direct solvent of cellulose. The synthesis of the modifier NPs involves the deposition of lanthanides-doped fluorides on the magnetic core/shell surface. Magnetic, spectroscopic, structural, morphological and surface properties of synthesized products were investigated.

These types of luminescent-magnetic fibers are excellent material for textile and documents protection, because they are almost impossible to counterfeit, and at the same time their authenticity can easily be proven using UV light or a magnetometer.

The work was supported by grant no. POWR.03.02.00-00-I026/16 co-financed by the European Union through the European Social Fund under the Operational Program Knowledge Education and by Polish National

Science Centre (grant number 2016/21/B/ST5/00110).

Keywords: Luminescence; Magnetism; Lanthanide(III) ions; Multifunctional cellulose microfibers; Core/shell nanomaterials;

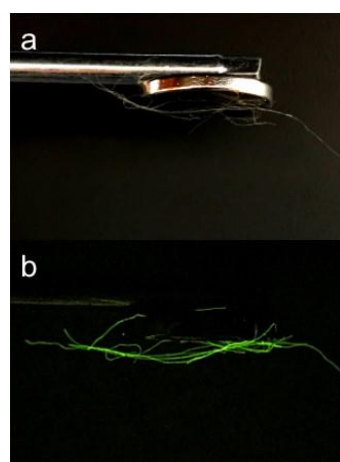


Figure 1: Photographs of luminescent-magnetic fibers captured by a neodymium magnet, taken in day-light (a) and under UV-light, $\lambda_{ex} = 254$ nm (b).

References:

1. Kulpiński, P., Erdman, A., Grzyb T., Lis, S., Luminescent cellulose fibers modified with cerium fluoride doped with terbium particles (2016), *Polym. Compos.*, 37, 153–160.
2. Skwierczyńska, M., Runowski, M., Goderski, S., Szczytko, J., Rybusiński, J., Kulpiński, P., Lis, S. Luminescent-Magnetic Cellulose Fibers, Modified with Lanthanide-Doped Core/Shell Nanostructures (2018) *ACS Omega*, 3, 10383–10390.
3. Skwierczyńska, M., Runowski, M., Kulpiński, P., Lis, S. Modification of cellulose fibers with inorganic luminescent nanoparticles based on lanthanide(III) ions (2019) *Carbohydr. Polym.*, 206, 742–748.

Mechanical Behaviors of $Ti_3C_2T_x$ Paper

K. Liao,^{1,*} S. H. Luo,¹

¹ Khalifa University of Science and Technology, Department of Aerospace Engineering, Abu Dhabi, United Arab Emirates

Abstract

Two-dimensional (2D) materials are generally referred to thin-layered materials consisting of a single or a few layers of atoms. A typical example is graphene, a single layer of carbon atoms arranged in hexagonal lattice. Since the successful isolation of graphene more than a decade ago, there has been a new wave of research to explore other 2D materials, such as phosphorene, Mxenes, transition metal dichalcogenides, and borophene, to name just a few. These materials are attractive for their potentially diverse applications in electronics, photonics, sensing, and energy devices due to the unique properties of thin-layered materials in terms of electrostatic efficiency, mechanical strength, tunable electronic structure, optical transparency, and sensor sensitivity.

MXenes consist of few atoms thick layers of transition metal carbides, nitrides, or carbonitrides. These conductive, layered materials with tunable surface terminations have been shown to be promising for energy storage applications, composites, photo catalysis, water purification, and gas sensors. In this work, we report the characterization of mechanical behavior of $Ti_3C_2T_x$ (MXene) papers.

Free-standing and flexible $Ti_3C_2T_x$ papers were fabricated by vacuum-assisted filtration of given volume of $Ti_3C_2T_x$ solution via filtration membrane. The concentration of $Ti_3C_2T_x$ was about 4 mg/ml, and the thickness of the $Ti_3C_2T_x$ paper varied from 5 μm to 40 μm . X-ray diffraction (XRD) patterns was obtained by benchtop XRD system. A field-emission scanning electron microscope was used to obtain high-magnification of cross-section area of $Ti_3C_2T_x$ paper. A typical image of Mxene paper is shown in Fig. 1.

The thickness and size distribution of $Ti_3C_2T_x$ flakes was obtained by the statistical analysis of more than 200 $Ti_3C_2T_x$ flake samples, using an atomic force microscope. Thermogravimetric analysis (TGA) of a strip of $Ti_3C_2T_x$ paper (about 5 mg) was performed. Mechanical tests of $Ti_3C_2T_x$ paper was performed on a dynamic mechanical analyzer. For quasi-static tensile,

cyclic tensile, and creep test of $Ti_3C_2T_x$ strips, strain-controlled, force-controlled, and creep mode were used respectively, with preload of 0.01N. A typical stress-strain curve is shown in Fig. 2. The results of mechanical characterization (tensile, cyclic, and creep) of Mxene papers will be discussed in some detail the presentation.

Keywords: Two-dimensional materials, *Mxene*, Mechanical behavior.

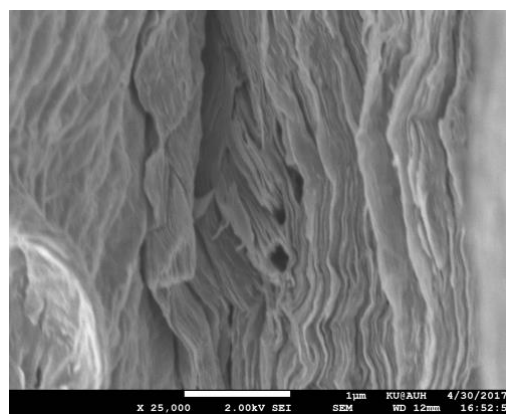


Fig. 1 – microscopic image of the cross-section of a Mxene paper.

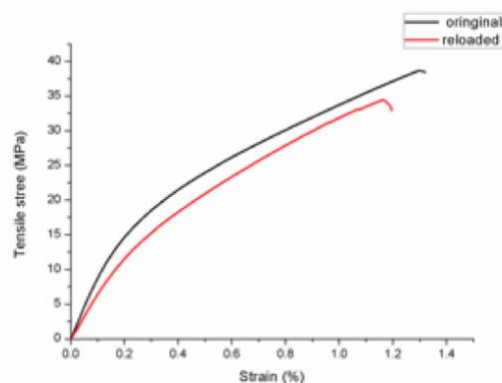


Fig. 2 – A typical stress-strain curve of Mxene paper under tensile load.

Mechanical properties and dislocation nucleation in nanoparticles with blunt edges

Jonathan Amodeo¹, Khalid Lizoul²

¹Université de Lyon, INSA-Lyon, MATEIS UMR5510 CNRS, 69632 Villeurbanne, France
Email : jonathan.amodeo@insa-lyon.fr

²Université de Lyon, Université Jean Monnet, LASPI EA-3059, 42023 Saint-Etienne, France
Email: khalid.lizoul@gmail.com

Abstract

While generally renowned for their functional properties, nanoparticles (NPs) also exhibit particularly fascinating mechanical properties such as a size-dependent elastic regime as well as increased yield strength and ductility. In addition to SEM and *in situ* TEM tests, atomistic simulations are extensively used to complement experimental approaches and successfully provide theoretical evidences of elementary plasticity mechanisms in nano-objects. Nevertheless, samples designed for MD nanomechanical simulations are regularly model-shaped. Indeed, virtual NPs and nanowires (NWs) exhibit faceted flat surfaces bounded by sharp edges and vertices whilst nanospheres are generally perfectly (and symmetrically) shaped, contrary to their more random experimental counterparts. What are the consequences of such shape simplifications?

Attempting to confront this fundamental question, we propose here to investigate the mechanical response and the elementary plasticity processes of blunt NPs under compression compared to their originally perfectly cubic and sharp shape using a large set of MD simulations.

The L1₂ Ni₃Al crystalline structure is used as it provides a wide selection of dislocation-based processes but results still apply to other crystalline structures.

While the lack of size-effect in originally cubic-shaped NPs is confirmed, a strong shape-effect is noticed i.e. smoothing corners and edges leads to strengthening.

Furthermore, while the plastic deformation of nano-objects is generally attributed to dislocation-based processes happening from the surface of the sample, here we

show that homogeneous dislocation nucleation also occurs in blunt NPs giving a certain range of sizes, in a similar manner to nanoindentation.

The nucleation of partial dislocation in partial slip systems with higher Schmid factors is also confirmed as well as their contribution to deformation twinning.

A similar set of simulations applied to Si NPs will also be presented.

This study emphasizes how much the design of virtual samples is crucial to model nano-objects mechanical properties using MD and provides new insights on potential incipient plasticity features at the nano-scale.

Effective properties of nanoparticle clusters in resonant regimes

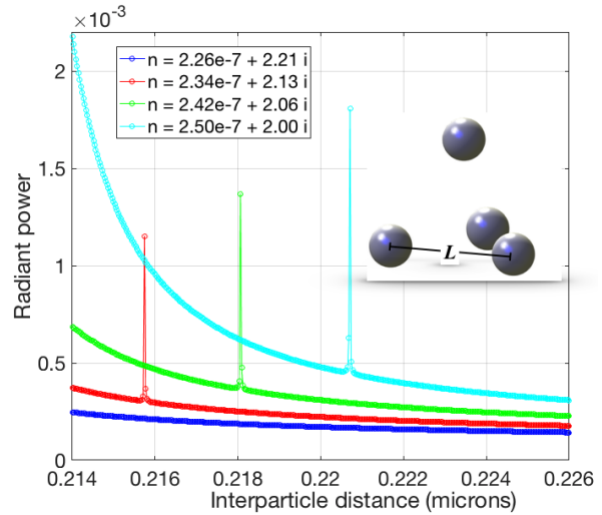
C. Blanchard *, D. De Sousa Meneses

CNRS, CEMHTI UPR3079, Univ. Orléans, F-45071 Orléans, France

Abstract:

The general framework of this contribution concerns the optical properties of clusters made up of particles that are small compared to the wavelength of the incoming light. One way to study this problem is to employ a multipole approach whose chief foundation is to split the field arriving at each particle into two sources: (i) the external incident field which must be expanded in terms of vectors harmonics and (ii) the scattered fields of all the other particles after having rewritten them in terms of vector harmonics about the origin of the current particle. Note that the former initiates the scattering process while the latter is usually obtained by using the addition theorems. If the retained number of orders N in the expansion is not sufficient, the calculated fields may result inaccurate and even totally wrong. Obviously N must not be less than that necessary when computing an individual particle. At first glance, it might be tempting to claim that the expansion needs a decreasing quantity of multipoles as the particles get smaller. However, the surface-to-surface distances between the particles is another crucial parameter and it is known that the required N to reach convergence increases when the scatterers get closer [1]. While this last statement is somewhat intuitive, a more surprising result lies in that N must be dramatically extended for very small particles when the refractive index n has a large imaginary part [2].

In this contribution, we consider clusters in which the constitutive particles are randomly distributed. The fraction volume is sufficient to allow the particles to be close to one another. We are therefore in the case previously mentioned where the number of orders in the expansion can be rather large. However, here, the emphasis is put on particles with a real part of n that almost vanishes. We show that if the imaginary part of n is taken inside a certain range of values, sharp resonances appear. For the sake of illustration, we calculated in Fig. 1 the radiant power for a simple system of 4 particles, arranged in a



tetrahedron, in terms of their surface-to-surface distance L . The calculation is done for different n

Figure 1: Scattering of 4 particles in terms of the separation distance.

while the ratio particles' radius to wavelength is $R/\lambda = 0.01$.

We will show that the optical response of a cluster comprising several hundreds of particles is seriously altered in the regime where these resonances arise, i.e., in the band ranging from the transverse optical to the longitudinal optical frequencies (ω_{TO} and ω_{LO}). Accordingly, the effective refractive index n_{eff} of the material notably diverges from the values predicted by the effective medium theory such as Maxwell-Garnett for instance. Our main objective is to quantify this deviation after having proposed a technique allowing the retrieval of n_{eff} and having looked into the nature of the resonances.

Keywords: Scattering properties of nanoparticles, effective medium theories.

References:

1. Claro, F. (1984) Theory of resonant modes in particular matter, *Phys. Rev. B.*, 30, 4989-4999.
2. Mackowski, D.W. (1994), Calculation of total cross sections of multiple-sphere clusters, *J. Opt. Soc. Am. A*, 11, 2851-2861.

Cavitation Growth Dynamics of Pinned Surface Nanobubbles

D. Dockar,^{1,*} M. K. Borg,¹ J. M. Reese,¹

¹ University of Edinburgh, Institute of Multiscale Thermofluids, Edinburgh, EH9 3JL, UK

Abstract:

Cavitation is a complex fluid phenomenon where a bubble can spontaneously form in a liquid in response to a local drop in pressure. Accumulated generation and subsequent collapse of these cavitating bubbles can have very destructive effects on engineering surfaces and have long been a problem in turbomachinery. However, being able to control and target these collapsing bubbles at the micro to nanoscale could have promising applications, such as for surface cleaning, waste-water treatment, and cancer treatment and diagnosis.

Many classical analyses of cavitation, such as the Blake threshold and Rayleigh-Plesset equation, assume sphericity of the nucleating bubble¹. However, approaching the nanoscale, bubbles can be found existing stably on hydrophobic substrates. These surface nanobubbles have spherical cap shapes and grow with a constant contact radius (CCR) due to pinning of the contact line². These two key details mean that the classical models often fail to capture the behaviour of surface nanobubble cavitation.

In this work we use high fidelity Molecular Dynamics (MD) to investigate the cavitation dynamics of surface nanobubbles in response to different environmental pressures. We demonstrate that the threshold for unstable cavitation growth can be many MPa lower for surface nanobubbles, compared to the classical prediction for spherical bubbles, We describe a new model that can predict the corrected threshold for surface nanobubbles³. We also find that the dynamics of surface nanobubble oscillations differ from current models, in particular an increased resonant frequency, and we offer possible explanations for these effects.

Keywords: cavitation, surface nanobubbles, molecular dynamics, nanofluids, contact line, pinning, stability, interfacial flow

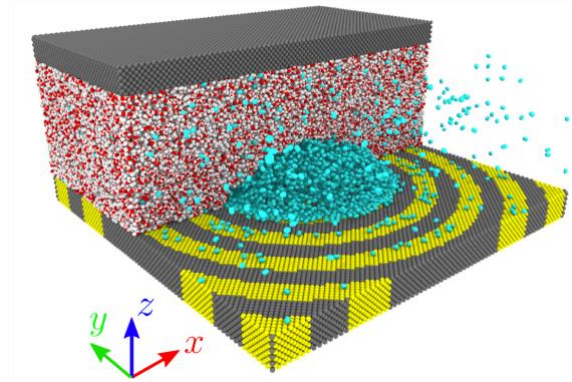


Figure 1: Molecular dynamics simulation of surface nanobubble cavitation growth. Pressure is controlled by vertical displacement of the top channel wall. The patterned lower channel wall provides contact line pinning.

References:

1. Brennen, C. E. (2013), *Cavitation and Bubble Dynamics*; Cambridge University Press.
2. Lohse, D., Zhang, X. (2015), Surface Nanobubbles and Nanodroplets. *Rev. Mod. Phys.*, 87, 981–1035.
3. Dockar, D., Borg, M. K., Reese, J. M. (2019), Mechanical Stability of Surface Nanobubbles. *Langmuir*.

Optical properties of the polyvinyl chloride / graphene oxide composites

M. Baibarac,^{1*} M. Stroe,¹ L. Stangescu,¹ M. Daescu,¹ E. Matei,¹ L. C. Cotet,² L. Baia,³

¹National Institute of Materials Physics, Department of Optical Processes in Nanostructure Materials, Magurele - Bucharest, Romania

²Babes-Bolyai University, Faculty of Chemistry and Chemical Engineering, Department of Chemical Engineering, Cluj-Napoca, Romania

³Babes-Bolyai University, Faculty of Physics, Cluj-Napoca, Romania

Abstract:

A new synthesis method is proposed for the obtaining of composites based on polyvinyl chloride (PVC) and graphene oxide (GO). In contrast with the previous protocols [1], which were reported to result in membranes, we prepare PVC spheres by the interaction of the commercial PVC grains with hexyl ethyl cellulose (HEC) and lauroyl peroxide (LPO) at the temperature of 60°C. The addition of GO sheets dispersed in dimethylformamide (DMF) at above synthesis mixture leads to the composites of the type the PVC spheres coated with the GO sheets, having a graphene concentration equal to 0.5, 1, 2, 3, 4 and 5 wt.%. Using Raman scattering, IR spectroscopy, photoluminescence (PL) and scanning electron microscopy (SEM), new optical properties of the PVC spheres covered with the GO sheets are reported. According to the SEM investigations, this method allows to transform the PVC grains with the size between 75 µm - 227 µm into spheres with sizes varying from 0.7 µm to 3.5 µm, when the GO concentration in the PVC/GO composite mass increases from 0.5 to 5 wt.%. As increasing the GO concentration in the PVC/GO composite mass, the main changes in Raman and IR spectra of these materials consist in: i) the change of the ratio between the relative intensities of the Raman lines situated in the spectral ranges 600-750 and 2850-3000 cm⁻¹, assigned to the vibrational modes of stretching C-Cl and asymmetrical stretching CH₃, from 0.39 to 1.63; ii) the gradual increase in the intensity of the D and G Raman bands of the GO sheets; and iii) the ratio between the absorbances of IR bands localized in the spectral ranges 600-750 and 2750-3250 cm⁻¹ is changed from 1.28 to 0.36, when the GO concentration is equal to 0 and 5 wt.%, respectively. These

changes indicate the appearance of several repeating units of the type ClCH=CH-, CH₂=CCl- and/or -CH=CCl- as a result of the partial dehydrogenation of the macromolecular chains. A consequence of this process is the generation of new C-OH bonds onto the GO sheets surface. A PL band with the maximum at 325 nm is reported in the case of the PVC spheres. In this context, a PVC PL quenching process is demonstrated to be induced by the increase of the GO sheets concentration in the PVC/GO composite weight. An application of this composite will be as flame-retardant material for interior finishing, the transport and clothing industry as well as construction products

Keywords: graphene, macromolecular compound, composites, Raman scattering, IR spectroscopy, photoluminescence.

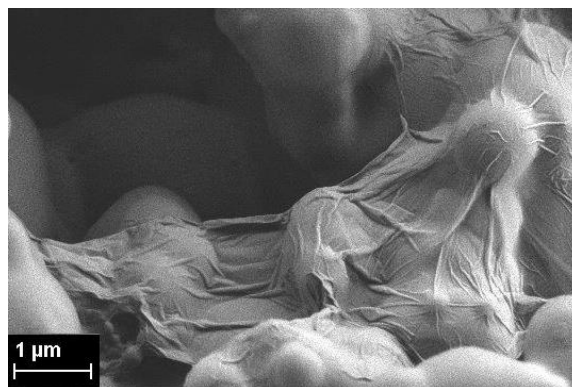


Figure 1: SEM images of the PVC spheres covered with the GO sheets.

References:

1. Zhao, Y., Lu, J., Liu, X., Wang, Y., Lin, J., Peng, N., Li, J., Zhao, F. (2016) Performance enhancement of polyvinyl chloride ultrafiltration membrane modified with graphene oxide, *J. Colloid. Interface Sci.* 480, 1-8.

Nanotech / Biotech Joint Plenary session II

Paradigms for the Interaction of Nanoscale Objects with Living Organisms:

Kenneth Dawson

Centre For BioNano Interactions (CBNI), School of Chemistry and Chemical Biology, University
College Dublin, Belfield, Dublin 4, Ireland, www.cbni.eu
e-mail: Kenneth.A.Dawson@cbni.ucd.ie

Abstract

Man-made nanostructures are of the size and nature that they gain access to new biological (intracellular and other) compartments, and there are potentially endogenous energy dependent mechanisms to lead them there. We summarise the foundations and progress to date in this arena. In particular we clarify the range of nanoscale (surface, shape etc) control parameters that may determine the biological outcomes. These considerations suggest an enduring potential to target substances to specific locations, for benefit of therapeutics, and the progress to date is summarized.

In the (typical) absence of exquisite control of the nanoscale structures (and thereby processes) *in vivo*, nanoscale materials are (guided by biomolecular coronas derived from the biological environment) incorporated and ultimately processed within endogenous intra-, trans- and cellular trafficking and processing pathways. There they may persist for extended periods of weeks, months (or longer) potentially either leading to persistent dysregulation of signaling and other biological processes, or slow degradative production of secondary (and other downstream) metabolites not commonly observed in other situations. The absence of much in depth understanding of the long term effects represents the most obvious risk in the arena.

It is clear that new future dimensions are opening up at the nanoscale, involving convergent outcomes between the nanoscale structures, gene editing, and other forms of biological intervention. These areas are in their infancy, but one can already see many of the key issues for the future.

As a community, and a society, our management of these arenas was dedicated, and sincere and quite effective, but we confronted new questions and issues, without the tools early on to deal with them. What we

learned from responsible management of 'risk' issues (in the larger sense) may be useful for future generations of risk managers in other arenas.

Safety testing of manufactured nanomaterials

Peter Kearns ¹ and Mar Gonzalez ¹

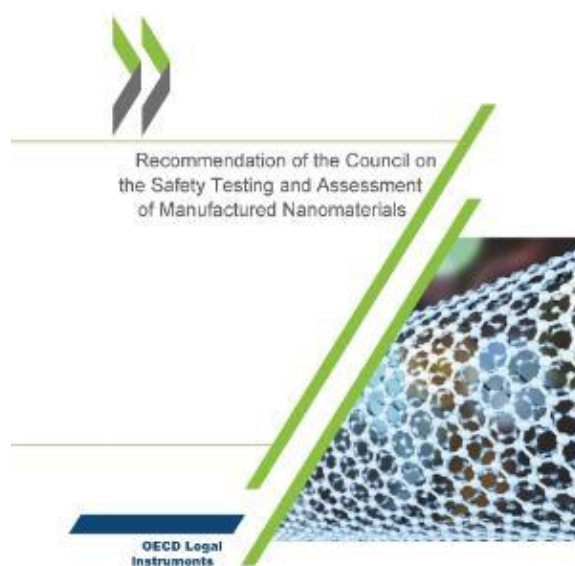
¹ Organisation for Economic Co-operation and Development; Environment, Health and Safety Division; Paris, France

Abstract:

This presentation will introduce OECD's programme of work on the safety of manufactured materials, which was established in 2006. OECD is an intergovernmental organisation. The programme of work is managed by the Working Party on Manufactured (WPMN), which includes representatives from OECD governments together with some non-member governments, other international organisations, industry, NGOs and academia. The programme works towards globally science-based approaches to the regulatory safety testing of nanomaterials. A major achievement of the programme has been the OECD Recommendation on the safety testing and assessment of manufactured nanomaterials, which was adopted by the OECD Council in September 2013. The OECD Council is the governing body of OECD represented at ambassadorial level. This Recommendation is an OECD legal instrument, which guides the work of OECD's WPMN. This presentation will go on to describe the main features of the Recommendation. It will also note the various regulatory tools for testing and assessment, which have been adopted under the auspices of the Recommendation. This will include an overview of the efforts to adapt existing Test Guidelines, or adopt new Test Guidelines, relevant to nanomaterials. It will also consider tools related to exposure assessment. A report will also be noted, which was adopted by the OECD Council in May 2019. It covers the implementation of the Recommendation in OECD member countries, (including the EU), as well as other adherents to this legal instrument. The presentation will focus on how the Recommendation has assisted, and continues to assist, in the adaptation of regulatory framework to nanomaterials.

Keywords: OECD, nanomaterials, science-based safety assessment, test guidelines, hazard identification, risk assessment, legal

instruments, exposure assessment, physical-chemical properties.



References:

1. OECD/LEGAL/0400, Recommendation of the OECD Council on the Safety Testing and Assessment of Manufactured Nanomaterials.
2. C(2019)55/REV1, Report on the Implementation of the Recommendation of the OECD Council on the Implementation of the Recommendation of the Council on the Safety Testing and Assessment of Manufactured Nanomaterials

Growth inhibition of Staphylococcus Aureus (Staph) and Escherichia coli (E. coli) by a combined treatment of ZnO nanoparticles and femtosecond laser light

Crysthal Alvarez¹, Alma Hernandez¹, Natanael Cuando² and Guillermo Aguilar^{1,*}

¹University of California Riverside, Department of Mechanical Engineering, Riverside, USA

²Universidad de Guanajuato, Salamanca Guanajuato, México

Abstract:

Recently, efforts have been made to create a transparent ceramic cranial implant comprised of nanocrystalline yttria-stabilized zirconia (nc-YSZ) that will provide optical access to the brain. This has been referred to as Window to the Brain (WttB) in the literature [1]. WttB (Figure 1) will allow the use of laser and photonic treatments and diagnostics in areas with difficult optical access in the brain. For example, the WttB platform would allow for non-invasive antibacterial treatments based on laser light. This is important as conventional antibiotics are prevented to reach the brain tissue due to the blood brain barrier. Moreover, infection is still one of the frequent cranial implant complications [2-3]. To address potential infections in the WttB platform, we have studied the antibacterial effect of commercial Zinc Oxide (ZnO) nanoparticles and femtosecond laser light on bacterial solutions of Staphylococcus aureus (*S. aureus*) and Escherichia coli (*E. coli*). Infrared (1030nm) laser light was used to enhance the antibacterial effect of ZnO nanoparticles by irradiating bacterial solutions with low power ultrashort laser pulses (890mW, 230fs). In our previous study [4], we concluded that the effect of the combination of ZnO nanoparticles and femtosecond laser treatment had the highest growing inhibition on Escherichia coli (*E. coli*) than each alone. *E. coli* is one of the most common studied bacteria, however, *S. aureus* is the most common bacterium found in cranial implant infections. In this study, we will present the combined effect of these killing methods and a comparison between the two bacteria strains and to independent and sole treatments of ZnO and femtosecond laser light.

Keywords: Transparent nanocrystalline yttria stabilized-zirconia, Window to the Brain, Antibacterial treatments, Staphylococcus aureus, Escherichia coli, zinc oxide.

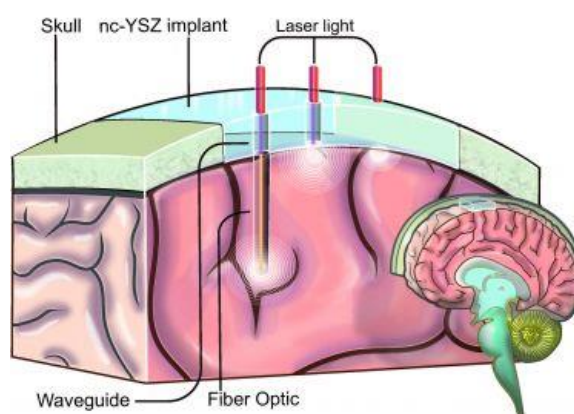


Figure 1: Conceptual schematic of the Window to the Brain (WttB)

References:

1. Y. Damestani, C.L. Reynolds, J. Szu, M.S. Hsu, Y. Kodera, D.K. Binder, B.H. Park, J.E. Garay, M.P. Rao, and G. Aguilar (2013) Transparent nanocrystalline yttria-stabilized-zirconia calvarium prosthesis, *Nanomedicine: Nanotechnology, Biology, and Medicine*, 9, 1135-1138.
2. Joby Jaber, Kenneth Gambrell, Paul Tiwana, Chris Madden and Rick Finn, (2013), Long-Term Clinical Outcome Analysis of Poly-Methyl-Methacrylate Cranioplasty for Large Skull Defects, *J. of Oral and Maxillofacial Surgery*, 71, e81-e88.
3. Yasaman Damestani et al (2016), Evaluation of laser bacterial anti-fouling of transparent nanocrystalline yttria-stabilized-zirconia cranial implant, *Lasers in Surgery and Medicine*, 48, 782-789.
4. Alvarez, C., et al. (2018), Antibacterial studies of ZnO nanoparticle coatings on nanocrystalline YSZ irradiated with femtosecond laser light, *Optical Imaging, Therapeutics, and Advanced Technology in Head and Neck Surgery and Otolaryngology*, V. 10469. International Society for Optics and Photonics.

Strategies of biological similarity to ensure safe use of conventional + novel nanomaterials

W. Wohlleben^{1*}

¹ BASF SE, Dept. Material Physics and Dept. Experimental Toxicology, Ludwigshafen, Germany

Abstract:

Nanomaterials are commercialized in a various grades that are optimised in composition, size, shape, coating for specific applications. As the scope of the different reporting and registration schemes in EU countries, in the USA and Canada includes nanoforms of widespread materials, the need arises to evaluate if the different grades can be grouped for risk assessment purposes. Additionally, there is necessity to ensure the safe use of innovative nanomaterials early during R&D, ideally by read-across without animal testing.

The project nanoGRAVUR (BMBF, 2015-2018) developed a framework for grouping of nanomaterials. Different groups may result for each of the three distinct perspectives of Occupational, Consumer and Environmental safety. Each is assessed by a risk matrix that integrates hazard and exposure indicators. The indicators are harmonised between the three perspectives and are based:

- tier 1 on intrinsic physical-chemical properties (what they are) or GHS classification of the non-nano form (human tox, ecotox, physical hazards);
- tier 2 on extrinsic physical-chemical properties, release from nano-enabled products, in-vitro assays with cells (where they go; what they do);
- tier 3 on case-specific testing, potentially in-vivo studies to substantiate the similarity within groups or application-specific exposure testing

The methods developed by nanoGRAVUR fill several gaps highlighted in the ProSafe reviews, and are useful to implement both the ECHA concept of nanoforms as well as the EPA concept of discrete forms.

Case studies include families of Fe₂O₃, SiO₂, CeO₂, organic pigment, ZnO, Cu, TiO₂ (nano)forms. Benchmark nanomaterials and benchmark nano-enabled products are essential to achieve reproducible groupings across different labs with slightly differing equipment (e.g. for dustiness, sanding, dispersion stability,

reactivity). Benchmark materials span the dynamic range of each property (often about three to five orders of magnitude), and thus help to assess the relevance of any dissimilarity between different nanoforms. For all properties investigated, we derive decadic bands as appropriate level of biological relevance, and compare which properties are most susceptible to different (nano)forms.

The methods and case studies are currently further developed in the GRACIOUS H2020 project, which adds the perspective of read-across and introduces purpose-specific requirements for the level of certainty and similarity.

Keywords: grouping, similarity, dissolution, reactivity, transformation, dispersion stability

References:

1. Wigger, Henning, Wendel Wohlleben, and Bernd Nowack. **2018**. 'Redefining environmental nanomaterial flows: Consequences of the regulatory nanomaterial definition on the results of environmental exposure models', *Environmental Science: Nano*, 5: 1372-85.
2. Koltermann-Jüly, Johanna, Johannes G. Keller, Antje Vennemann, Kai Werle, Philipp Müller, Lan Ma-Hock, Robert Landsiedel, Martin Wiemann, and Wendel Wohlleben. **2018**. 'Abiotic dissolution rates of 24 (nano)forms of 6 substances compared to macrophage-assisted dissolution and in vivo pulmonary clearance: Grouping by biodissolution and transformation', *NanoImpact*, 12: 29-41.
3. Amorim, Mónica J. B., et al. **2018**. 'Environmental Impacts by Fragments Released from Nanoenabled Products: A Multiassay, Multimaterial Exploration by the SUN Approach', *Environmental Science & Technology*, 52: 1514-24.

Nanocrystals for Medicinal Applications

L. Mondragón,¹ E. Casals,^{2,3} L. Russo,¹ A. García-Sanz,² J. Piella,¹ I. Abasolo,⁴ N. Bastús,¹ V. Puntès^{1,2,5}

¹ Institut Català de Nanociència i Nanotecnologia (ICN2), Bellaterra, Spain

² Vall d'Hebron Institute of Research (VHIR), Barcelona, Spain

³ School of Biotechnology and Health sciences, Wuyi University, Jiangmen, 529020, China

⁴ CIBBIM-Nanomedicine, Vall d'Hebron Institute of Research (VHIR), Universitat Autònoma de Barcelona (UAB), Networking Research Centre on Bioengineering, Biomaterials and Nanomedicine (CIBER-BBN), Barcelona, Spain

⁵ Institut Català de Recerca i Estudis Avançats, (ICREA), Barcelona, Spain

Abstract:

Last decade has seen a flourishing in the study of the properties of inorganic nanoparticles for medical applications. Nanoparticles display properties that are strongly determined by both morphology and environment and in the physico-chemical context where they are immersed, therefore allowing to monitor and manipulate biological states. Inorganic nanoparticles behave as "artificial atoms", since their high density of electronic states -which controls many physical properties- can be extensively and easily tuned by adjusting composition, size and shape and used in biological environments. Indeed, nanotechnology's ability to shape matter on the scale of molecules is opening the door to a new generation of diagnostics, imaging agents, and drugs for detecting and treating disease at its earliest stages. But perhaps more important, it is enabling researchers to combine a series of advances, creating thus nanosized particles that may contain drugs designed to kill tumours together with targeting compounds designed to home-in on malignancies, and imaging agents designed to light up even the earliest stage of cancers. In fact, a description of cancer in molecular terms seems increasingly likely to improve the ways in which human cancers are detected, classified, monitored, and (especially) treated, and for that, nanoparticles, which are small and therefore allows addressing molecular structures in a unique manner, may be especially useful for those tasks.

One of the most fascinating effects of loading or conjugating a nanoparticle and a drug, is how the biodistribution of that drug is altered. By associating the drug to the NP, its physicochemical fate is modified, and, indeed, it is the properties of the NP and the conjugate what determines the fate (pharmacokinetics and biodistribution) of the carried drug. Thus,

nanocarriers can strongly contribute to modifications in pharmacokinetics and biodistribution, by driving the drug through different pathways, depending on the physicochemical properties of the nanocarrier (e.g., size and surface charge), which is especially appealing in the case of very toxic drugs.¹ The fate of the drug and the vehicle will also strongly depend on the portal of entry, either injected (intravenously, intramuscularly, peritoneal), via the gastrointestinal track, via the respiratory system or through the skin.

It is also necessary to investigate the aspects related to the unstable nature of NPs and their biotransformations. In fact, while there is an increasing body of evidence that pristine manufactured NPs can enter and affect organisms when dosed under standard exposure scenarios, this evidence often lacks proper exposure assessment in terms of rates of change between NP states during their exposure time. The underlying strategy is an analogue of the integration of kinetic (what does the body do to the drug) and dynamic (what does the drug do to the body) concepts in pharmacology, where the most exquisite knowledge of the interactions between substances and the organism, down to the genotypic variation, with a clear control of intended and side effects exists.

Keywords: Inorganic nanoparticles, drug delivery, biodistribution, pharmacodynamics, pharmacokinetics.

References:

1. Ruenraroengsak P et al. (2010) Nanosystem drug targeting: Facing up to complex realities. *Journal of Controlled Release* 141: 265–276; Vasir JK et al. (2005) Nanosystems in drug targeting: Opportunities and challenges. *Current Nanoscience* 1: 47–64.

Nanotech / Biotech
Session II.A:
Nanotechnology for life
science

Single-molecule Protein Analysis Using Nanopores

Xiaohua Huang*, Wenxu Zhang and Sylvia Liang

Department of Bioengineering, and Materials Science and Engineering Program,
University of California at San Diego, La Jolla, California, USA 92093-0412

Abstract:

Existing technologies for protein analysis remain very limited, or even primitive as compared to genomic technologies. Unlike DNA which can be easily amplified and sequenced, proteins cannot be amplified. Therefore, sensitive and quantitative protein analysis requires a technology that is capable of direct single-molecule measurements. In theory, the nanopore technology has such a capability. The seminal idea of using protein nanopores for direct sequencing of biopolymers such as DNA and protein was conceived by George Church and David Deamer almost three decades ago¹. Today, direct single-molecule sequencing of long DNA molecules using nanopores has become a reality^{2, 3}. On the other hand, protein analysis or sequencing using nanopores is still relatively unexplored due to some technical limitations, in particular the inability to consistently translocate unfolded proteins through nanopores, and the difficulty in the engineering of the required nanopores and electronic amplifiers.

Here we will present our work on a nanopore method for direct single-molecule analysis of proteins. We will discuss the basic theory on protein identification using ionic current blockage profiles of fully denatured proteins and whole proteome databases. We will also present some preliminary experimental results on the acquisition of current blockage profiles using solid-state nanopores and the computational algorithms for direct single-molecule protein identification.

Keywords: single-molecule protein analysis, nanopore, electrophoretic transport, nanofabrication, neural network, signature fingerprinting, proteome database, neural network, machine learning.

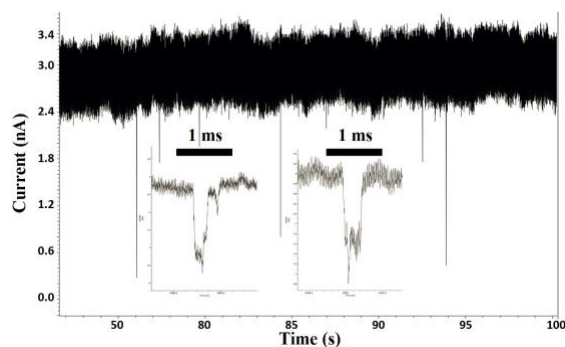


Figure 1: Unfolding and imparting charge to proteins for electrophoretic transport through nanopores. Shown is the current blockage profile of the translocation of unfolded bovine serum albumin through a silicon nitride nanopore with a diameter of ~ 3 nm and a thickness of 10 nm. Two events are enlarged and shown in the insets.

References:

1. Church, G.M., Deamer, D., Branton, D., Balderalli, R. & Kasianowicz, J., Characterization of individual polymer molecules based on monomer-interface interactions. US Patent No. 5,795,782 (1998).
2. Branton, D. et al., The potential and challenges of nanopore sequencing. *Nat Biotechnol* **26**, 1146-1153 (2008).
3. Deamer, D., Akeson, M. & Branton, D., Three decades of nanopore sequencing. *Nat Biotechnol* **34**, 518-524 (2016).

Future of nanoparticles research in mosquito control with lasers and consciousness

Soam Prakash

Quantum Biology labs, Faculty of Science, Dayalbagh Educational Institute, Dayalbagh Agra India
282 005

Abstract

Nanoparticles research for mosquito control* has grown extensively in last 20 yrs and different nanoparticles of different geometry have been synthesized extensively for controlling vectors of many diseases such as Malaria, Dengue, Zika, Chikungunya, Filariasis. Controlling of vectors at all places of different climatic and geographical regions warrant cutting edge technology. The synthesis of different geometries could be achieved by integrating different wave length, phases, colors, frequencies, intensities, The desired results are obtained by skilling specific characteristics like Laser, consciousness.(Soni and Prakash,2011,12,13,14,15,16 and Yadav and Prakash,2018,Parisha and Prakash 2018,etc). We have experimented extensively on control of mosquitoes larvae in our laboratories by adapting various advanced technologies using EM,X-RDs, AFMs with synthesized nanoparticles and found significantly that not only human consciousness interferes but even laser beams when integrated do can significantly modify the geometry of nanoparticles viz, AuNPs, AgNPS, ZnNPS and even some bimetallic nanoparticles like AU-AGNPs. This indicates a grand future design in experimentation for not only controlling mosquitoes of different countries and climatic regions and different species but can enhance the synthesis and control over manufacturing of Nanoparticles research. This scenario** shall be discussed during the presentation.

References

1. **Shweeta Yadav and Soam Prakash.2018. Effect of Laser on the synthesis of Gold Nanoparticles with Reference to Geometry,vol-7,No-4 ,Advances in Nanoparticles ;2018.
2. *Namita Soni and Soam Prakash,2013, Possible mosquito controlby Silver Nanoparticles synthesisby Soil fungus (Aspergillus niger 2587), vol2, No-2May2013

New surfactants in wet ball milling and an innovative embedding of Nanocrystals into a granulate matrix

Dr. Matthias Rischer

Director Drug Delivery & Innovation Projects, Losan Pharma GmbH, Germany

Abstract: The Nanocrystal Technology by wet ball milling is getting more and more interest and importance for experts in formulation screening, tox study and clinical trial sample supply for low soluble API's with a problem in bioavailability. The reason is a fast set-up and scale-up of the manufacturing process, the easy application of the liquid Nanocrystal formulations in such studies and the available downprocessing possibilities to come to the final dosage form (capsules, tablets, stickpacks). Losan Pharma has invented in a cooperation a new and fast screening system for nanomilling which has meanwhile reached commercialisation (Zentrimix 380R® from Hettich Labs, Germany). In order to widen the application of the Nanocrystal system new surfactants with improved toxic and hemolytic properties in comparison to the reference sodium dodecyl sulfate (SDS) have been used with a potent model drug substance to evaluate their potential as stabilisers in the Nanocrystal suspensions. As SDS is very limited in use due to its toxicity especially for tox studies or parenteral applications new surfactants need to be developed to improve this situation. In addition a new downprocessing approach is presented to embed the obtained Nanocrystal suspensions via a extrusion like process into a granulate (with the possibility of a continuous granulation) and a comparison has been made to the conventional fluid bed spray drying process which has been implemented before.

Keywords: Screening methods, DoE, wet ball milling, nanocrystal suspensions, granulation, dissolution, oversaturation

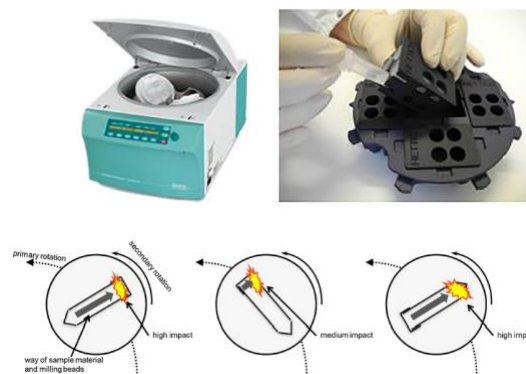


Figure 1: Figure illustrating the efficient and predictive nanomilling screening equipment with a short description of its function

References:

1. Hagedorn et. al. Int. J. Pharm. 530 (2017), 79-88

Feasibility of Ultraaccurate Nanopore DNA Sequencing

Wenxu Zhang* and Xiaohua Huang

Department of Bioengineering, Program in Materials Science and Engineering,
University of California, San Diego, La Jolla, California, USA 92093-0412

Abstract:

Three decades later after its conception¹, nanopore DNA sequencing has become a reality^{2, 3}. The nanopore technology being commercialized by Oxford Nanopore Technologies Inc. offers unprecedented long reads, high speed and throughput, the capability to identify modified bases, portability and low initial equipment cost. Raw sequencing accuracy has improved dramatically and sequencing cost is also dropping very rapidly over the past two years. It is becoming a competitive and go-to technology for sequencing, in particular for *de novo* genome sequencing and assembly. However, its tremendous potential and widespread adoption have been hindered by the relatively low consensus accuracy that can be achieved due to systematic sequencing errors. Most errors are primarily deletions and insertions because of the difficulty in precise decoding of homopolymers, which is perhaps one of the greatest obstacles remaining.

We will present our work on the physics of nanopore DNA sequencing, and its limitations and theoretical potential using computational modeling. First, based on experimental sequencing data, we constructed a physical model for nanopore DNA sequencing. We simulated nanopore DNA sequencing using computational modeling and finite element methods. We developed the algorithms and neural network-based machine learning for sequencing decoding. We also explored the nanopore architecture required for detecting the transition events during the nucleotide-tonucleotide translocation for counting of homopolymers. Our work indicated the feasibility of detecting such events for highly accurate sequencing of homopolymers. We will present our results on the maximal potential and limitations of the current generation of nanopore sequencing technologies, and the exciting perspective of ultraaccurate long-read DNA

sequencing using nanopore technologies in the near future.

Keywords: Nanopore, DNA sequencing, homopolymers, neural network, machine learning, computational modeling, simulations, finite element methods.

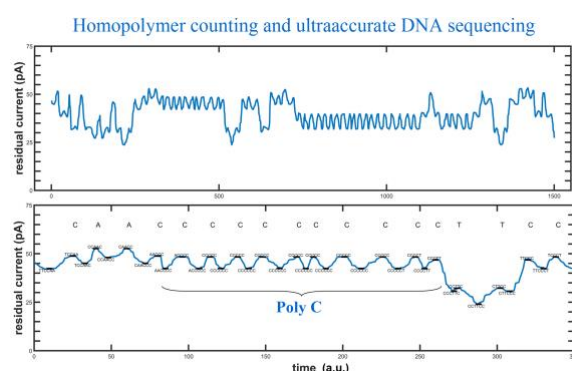


Figure 1: Resolution of homopolymers and ultraaccurate DNA sequencing. Shown on the top panel is the simulated current blockage profile of the translocation of a DNA sequence. The bottom panel shows a portion of the decoded sequence that contains a 11-base long poly C stretch.

References:

1. Church, G.M., Deamer, D., Branton, D., Balderalli, R. & Kasianowicz, J., Characterization of individual polymer molecules based on monomer-interface interactions. US Patent No. 5,795,782 (1998).
2. Branton, D. et al., The potential and challenges of nanopore sequencing. *Nat Biotechnol* **26**, 1146-1153 (2008).
3. Deamer, D., Akeson, M. & Branton, D., Three decades of nanopore sequencing. *Nat Biotechnol* **34**, 518-524 (2016).

The mechanical properties of electrospun fibrinogen, blended fibrinogen:PCL and fibrinogen:collagen nanofibers

M. Guthold,^{1,*} C. C. Helms², S. R. Baker³, J. Sigley¹, E. Voyles¹, S. Banerjee¹, J. Sharpe¹, Z. Zhang¹, J. Diaz-Silveira¹, K. Bonin¹

¹ Wake Forest University, Department of Physics, Winston-Salem, NC 27109, USA

² University of Richmond, Department of Physics, Richmond, VA 23173, USA

³ University of Leeds, Leeds Institute of Cardiovascular & Metabolic Medicine, Leeds, LS2 9NL, United Kingdom

Abstract:

Background. Fibrinogen, collagen and poly- ϵ -caprolactone (PCL) are suitable, non-immunogenic and widely available materials to form cell scaffolds for biomedical and tissue engineering applications. Fibrinogen forms the provisional matrix in wound healing, collagen is a key protein of the extracellular matrix, and PCL is an approved biocompatible and biodegradable polyester. Cells are sensitive to the biochemical, structural and mechanical properties of the substrates they are grown on. Having a suite of different, mechanically well-characterized, biocompatible materials would accelerate progress in tissue engineering.

Objective. Create nanofibers that have similar dimensions to the fibers of the extracellular matrix, and determine their mechanical properties.

Methods. Fibers with diameters on the order of hundred nanometers were electrospun from fibrinogen, collagen and PCL, and blended fibrinogen:collagen and fibrinogen:PCL. The mechanical properties of these fibers were tested with an atomic force microscopy (AFM)-based technique.

Results. Fibers spun from different materials displayed a wide range of mechanical properties, providing a range of options for different bioengineering applications. Highlights include: Pure fibrinogen and collagen fibers mimic the properties of their natural counterparts (fibrin and collagen fibers); electrospun fibrinogen fibers are significantly softer, more extensible and more elastic than electrospun collagen fibers. PCL fibers show similar properties as fibrinogen fibers. Blended fibrinogen:collagen fibers are more extensible than either fibrinogen or collagen fibers. PCL blended fibers show large, plastic (permanent) deformations and extreme strain softening.

Conclusions. Significant progress has been made in creating a library of nanofibers, made from biocompatible materials fibrinogen, collagen and PCL, and determining their mechanical properties.

Keywords: nanofibers, fibrin fibers, electrospun fibers, fibrinogen, collagen, polycaprolactone AFM lateral force measurements, mechanical characterization

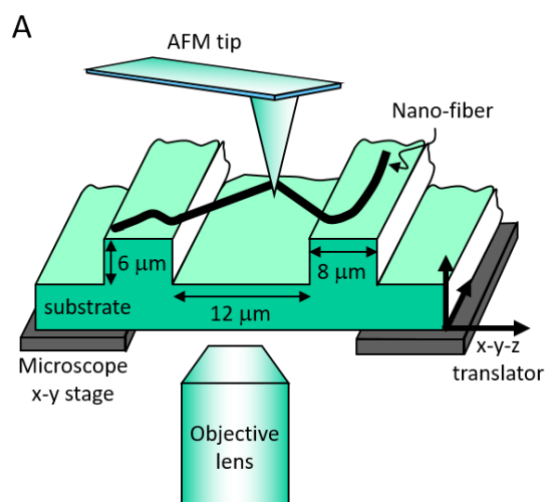


Figure 1. Combined AFM/optical microscope set-up to determine the mechanical properties of nanofibers.

Charged polysaccharide multilayers as protein-repellent coatings for medical implant materials

Matej Bračič¹, Tamilselvan Mohan¹, Rupert Kargl^{1,2}, Karin Stana-Kleinschek^{1,2}

¹ Laboratory for Characterization and Processing of Polymers (LCPP), Faculty of Mechanical Engineering, University of Maribor, Maribor, Slovenia.

² Institute for Chemistry and Technology of Materials (ICTM), Graz University of Technology, Stremayrgasse 9, 8010 Graz, Austria.

Abstract:

The biofilm formation triggered by uncontrolled protein adsorption, on small-diameter vascular graft implants is one of the leading cause of infections during implantation. Herein, we report of polysaccharide based nano-coatings as protein-repellent coatings to tackle this challenge. A simple layer-by-layer strategy to functionalize surfaces of poly(caprolactone) (PCL) with antifouling multilayers manufactured from the positively charged aminocellulose and the negatively charged cellulose sulphate was employed successfully. The multilayers formed coatings of up-to 20 $\mu\text{g}/\text{cm}^2$. The zwitterionic nature of the coatings has shown to repel bovine serum albumin (BSA), γ -globulin, and fibrinogen proteins, as shown by means of a quartz crystal microbalance.

Given the multiple functionalities and different physiochemical properties of polysaccharide-based multilayer coatings, this system showed to be easily extended to various material surfaces, thereby broadening its potential applicability also in microfluidics, diagnostic biosensors and others.

Keywords: aminocellulose, cellulose sulphate, polysaccharide multilayers, protein-repellent, quartz crystal microbalance

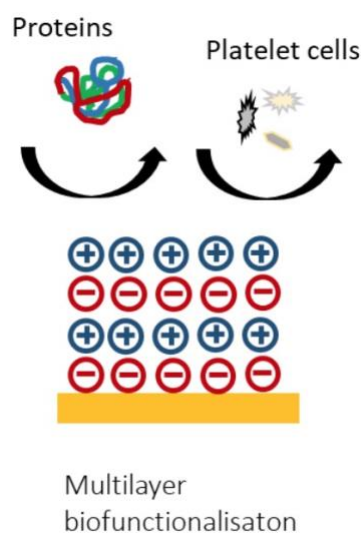


Figure 1: A scheme of protein-repellent charged-polysaccharide multilayers on a PCL surface.

References:

1. K. A. Rocco, M. W. Maxfield, C. A. Best, E. W. Dean and C. K. Breuer, In vivo applications of electrospun tissue-engineered vascular grafts: a review, *Tissue Engineering Part B*, 2014, 20, 628-640.

Acknowledgement:

This work was financed by the Slovenian research agency: Project Z2-9216.

Graphene-Based Coatings for Inhibiting Bacterial Growth in Hospital Environment

I. Bellagamba,^{1,4} H.C. Bidsorkhi,^{1,4} E. Bruni,^{2,4} D. Cavallini,^{1,4} M. Saccucci,³ A. Polimeni,³ D. Uccelletti,^{2,4} M.S. Sarto,^{1,4}

¹Sapienza University of Rome, Department of Astronautic, Electrical and Energetic Engineering, Rome, Italy

²Sapienza University of Rome, Department of Biology and Biotechnology C. Darwin, Rome, Italy

³Sapienza University of Rome, Department of Oral and Maxillofacial Sciences, Rome, Italy

⁴Sapienza University of Rome, Research Center for Nanotech Applied to Engineering (CNIS), Rome, Italy

Abstract:

The proliferation of antibiotic-resistant bacteria represents a considerable problem that affect hospital environments. This increases the occurrence of major infections for patients during their hospitalization. One of the possible ways of pathogen infections is the direct contact of the patient's body with high-touch surfaces and instruments. In this context, the use of nanomaterials for bactericidal surface treatments [1] may represent an innovative solution. Recent scientific breakthroughs have demonstrated that graphene-based nanomaterials show great antimicrobial properties [2, 3], without exerting relevant cytotoxic effect on human cell lines [4, 5]. In this work, three different graphene-based coatings have been evaluated for inhibiting bacterial growth on surfaces. In particular, we assessed the bacterial growth inhibition due to graphene nanoplatelets (GNPs, Fig.1a), zinc-oxide nanorods (Fig.1b) sprayed on GNPs coatings (ZnO-GNP) and zinc-oxide-decorated GNPs (ZNGs, Fig.1c), on either metallic (Fig.1d), plastic or polymer-texture substrates. The suspensions have been applied by the spray deposition method. The main antimicrobial mechanism of these nanostructures is based on membrane punctuation. This mechanical damage is a characteristic behavior of GNPs, ZnO-NRs and, in particular, of ZNGs [1, 3]. The antimicrobial activity of the coatings has been evaluated on Gram-positive (*Staphylococcus aureus*) and Gram-negative (*Pseudomonas aeruginosa*) bacteria, which are the main pathogens associated with nosocomial infections. Results obtained from the colony forming units count (CFU) method show that all the coatings have a good antibacterial behaviour. As an example, we report (Fig.1e) the survival curve of *S. aureus* after the different coating deposition on metallic surface.

Keywords: graphene-based coatings, bactericidal properties, bacterial inhibition, graphene nanoplatelets, zinc-oxide nanorods.

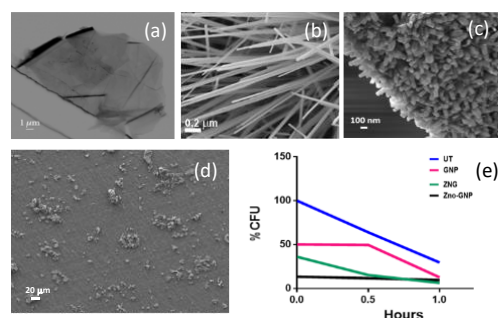


Figure 1: SEM imaging of (a) graphene nanoplatelets (GNPs), (b) zinc-oxide nanorods (ZnO-NRs), (c) zinc-oxide-decorated GNPs (ZNGs), (d) ZNG-coating on metallic substrate and (e) survival curve of *S. aureus* deposited on metallic nosocomial surface treated with the nanostructures.

Acknowledgement: the study has been financed by INAIL under grant NANODISP.

References:

1. Saccucci, M., Bruni, E., Uccelletti, D., Bregnocchi, A., Sarto, M.S., Bossù, M., Di Carlo, G., Polimeni, A., (2018) Surface disinfections: Present and future, *Journal of Nanomaterials*, 8950143.
2. Zanni, E., Bruni, E., Chandraiaghari, C.R., De Bellis, G., Santangelo, M.G., Leone, M., Bregnocchi, A., Mancini, P., Sarto, M.S., Uccelletti, D., (2017) Evaluation of the antibacterial power and biocompatibility of zinc oxide nanorods decorated graphene nanoplatelets: New perspectives for antibiodeteriorative approaches, *Journal of Nanobiotechnology*, 15(1),57.
3. Bregnocchi, A., Zanni, E., Uccelletti, D., Marra, F., Cavallini, D., De Angelis, F., De Bellis, G., Bossù, M., Ierardo, G., Polimeni, A., Sarto, M.S. (2017) Graphene-based dental adhesive with anti-biofilm activity, *Journal of Nanobiotechnology*, 15(1),89.
4. Zanni, E., De Palma, S., Chandraiaghari, C.R., De Bellis, G., Cialfi, S., Talora, C., Palleschi, C., Sarto, M.S., Uccelletti, D., Mancini, P. (2016) In vitro toxicity studies of zinc oxide nano- and microrods on mammalian cells: A comparative analysis, *Materials Letters*, 179, pp. 90-94
5. Ficociello, G., De Caris, M.G., Trillò, G., Cavallini, D., Sarto, M.S., Uccelletti, D., Mancini, P. (2018) Anti-candidal activity and in vitro cytotoxicity assessment of graphene nanoplatelets decorated with zinc oxide nanorods, *Nanomaterials*, 8(10),752.

Interaction of Telomeric DNA i-motif with Carbon Nanotubes. A Molecular Dynamics Analysis of the Structure and Stability

T. Panczyk,^{1,*} P. Wolski,¹ P. Wojton¹

¹ Jerzy Haber Institute of Catalysis and Surface Chemistry
Polish Academy of Sciences, Krakow, Poland

Abstract:

Non canonical DNA structures like i-motifs and G-quadruplexes play important role as regulatory elements for replication and transcription processes and in the development of cancer. Their appearance and stabilization in response to presence of some ligands is an important topic in the design of novel anticancer drugs. It was found [1] that carboxylated carbon nanotubes are unique ligand which can selectively stabilize i-motifs at neutral pH.

This work deals with the analysis of the protonated and deprotonated states of the natural sequence d[(CCCTAA)₃CCCTAA] of the telomeric DNA forming the intercalated i-motif. The i-motif is analyzed as an isolated structure or paired with the complementary sequence d[TTAGGG(TTAGGG)₃] which, in turn, forms the G-quadruplex structure.

We found that hydrogen bonds exist in the case of protonated i-motif and this form is thermodynamically the most stable. The hydrogen bonds, however, vanish in the case of unprotonated i-motif and we found that i-motif in such a case deteriorates spontaneously towards hairpin or random coil structures. [2] Thus, the isolated i-motif at the neutral pH is thermodynamically an unstable structure. A different situation appears when the i-motif exists together with the complementary G-quadruplex. Then, the overall structure becomes very stable no matter which pH conditions are considered. At acidic pH the stability of the overall structure is obvious due to appearance of hydrogen bonds within the Hoogsteen pairs in the i-motif. However, at the neutral pH these hydrogen bonds vanish. Nevertheless, we found that the i-motif is still preserved and only some weakening of the structure is observed.

Analysis of the interaction of the i-motif with functionalized carbon nanotubes leads to the conclusion that adsorption does not significantly affect the stability of the i-motif structure. I-motif binds strongly to the nanotube surface and

move on the surface quite freely with preferential occupation of the nanotube tips. The protonation state affects the structure of the adsorbed i-motif: unprotonated state tend to deteriorate and wrap the nanotube surface while the protonated one keeps its stiff structure intact. Thus, the conclusion is that the observed stabilization of the i-motif by carboxylated nanotubes is mainly due to local reduction of pH and transition of the i-motif from the deprotonated to the protonated state. (This work was supported by Polish National Science Centre, grant 2017/27/B/ST4/00108)

Keywords: telomere, DNA, i-motif, carbon nanotube, molecular dynamics

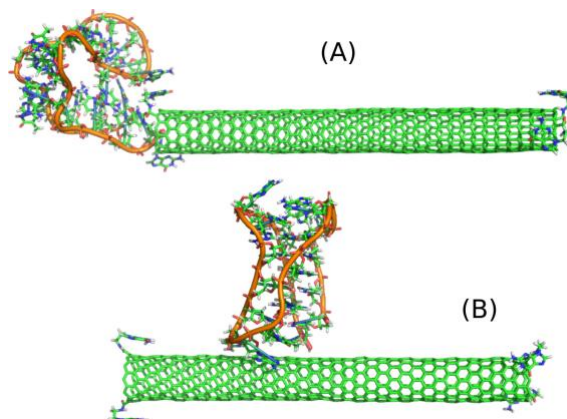


Figure 1: Figure illustrating the structure of the i-motif – carbon nanotube constructs. (A) unprotonated i-motif; (B) protonated i-motif

References:

1. Chen, Y.; Qu, K.; Zhao, C.; Wu, L.; Ren, J.; Wang, J.; Qu, X. (2012) Insights into the Biomedical Effects of Carboxylated Single-Wall Carbon Nanotubes on Telomerase and Telomeres., *Nat. Commun.* 3, 1074..
2. P. Wolski, K. Nieszporek, T. Panczyk (2019), G-quadruplex and i-motif Structures within the Telomeric DNA Duplex. A Molecular Dynamics Analysis of Protonation States as Factors Affecting their Stability, *J. Phys. Chem. B.*, 123, 468–479.

Nanotech / Biotech
Session II.B:
Nanotechnology for drug
and gene delivery

Incorporation in Titanate nanotubes as a way to improve compression properties of active pharmaceutical ingredients

B. Sipos¹, K. Pintye-Hódi¹, G. Regdon Jr.¹, Z. Kónya^{2,3}, M. Viana^{4,*}, T. Sovány¹

¹Institute of Pharmaceutical Technology and Regulatory Affairs, University of Szeged, H-6720 Szeged, Hungary

²Department of Applied and Environmental Chemistry, University of Szeged, H-6720 Szeged, Hungary

³Reaction Kinetics and Surface Chemistry Research Group, Hungarian Academy of Sciences-University of Szeged, H-6720 Szeged, Hungary

⁴Department of Pharmaceutical Technology, Faculty of Pharmacy, University of Limoges, PEIRENE EA 7500, 87000 Limoges, France

Abstract:

Titanate nanotubes (TNTs) are biocompatible nanomaterials with a particular tubular shape and good physicochemical stability that make them interesting for pharmaceutical applications. Indeed TNTs can be filled with active pharmaceutical ingredients (APIs) and may serve as drug carriers for therapeutic use.

Based on the fact that tablet is still the most frequently pharmaceutical form developed by industry, tableting ability of TNT-API composites was investigated.

Compressibility of i) pure TNTs, ii) 4 different API (diltiazem hydrochloride DiltHCl, diclofenac sodium DicNa, atenolol ATN and hydrochlorothiazide HCT) and iii) TNTs loaded with the API was studied using a powder functionality test based on energetic analysis of compression and rupture cycles [1]. The equipment (Lloyd 6000R uniaxial press) provided tablets of the samples without any excipient, and therefore allowed thorough investigation of the behavior of the components. The 50-250 MPa compaction range was explored. Physicochemical characterisation of the composites was also performed using SEM, FT-IR and DSC-TG [2].

Results indicated that, compared to pure API, TNT-API composites presented improved compressibility due to better flowability and particle rearrangement and improved plasticity. Although this positive effect was clear for the 4 types of API, differences were observed, depending on the efficacy of API incorporation. Indeed flowability improvement was high for DiltHCl and DicNa that were shown to completely fill the TNTs, while it was less pronounced for ATN and DicNa that were only partly incorporated in TNTs. Reduced elasticity

was observed in all cases, even when API was not fully incorporated (case of the strongly elastic ATN).

Post compressional properties such as compaction ratio and tensile strength, confirm the improved compression ability of all TNT-API : higher densification and mechanical strength were obtained over the entire compression range investigated.

In conclusion, TNTs are promising carrier materials, providing important technological benefits in the field of direct tablet compression. TNTs improve the flowability of the incorporated API, decrease elastic recovery and enlarge the compression range. The presence of TNTs enhance the compactibility of the 4 API tested, even when incorporation is incomplete. This observation proves that the processability of TNTs is extremely good, which makes this excipient a promising carrier nanomaterial.

Keywords: Titanate nanotubes, direct tableting, compressibility, composites, diltiazem hydrochloride, diclofenac sodium, atenolol, hydrochlorothiazide

References:

1. Viana, M., Ribet, J., Rodriguez, F., Chulia, D. (2005) Powder Functionality Test: A Methodology for Rheological and Mechanical Characterization. *Pharm. Dev. Technol.*, 10, 327–338,
2. Sipos, B., Pintye-Hódi, K., Kónya, Z., Kelemen, A., Regdon Jr., G., Sovány, T. (2017) Physicochemical characterisation and investigation of the bonding mechanisms of API-titanate nanotube composites as new drug carrier systems, *Int. J. Pharm.* 518, 119–129.

Nanoinks for photothermally responsive inkjet-printed patterns: from hyperthermia and drug release to encrypted writing

P. Pallavicini,^{1,*} L. De Vita,¹ M. Borzenkov,² G. Chirico,² P. Ihalainen,³ J. Sarfraz³

¹ University of Pavia, Department of Chemistry, Pavia, Italy

² University Milano Bicocca, Department of Physics “G. Occhialini”, Milano, Italy

³ Åbo Akademi University, Center for Functional Materials, Turku, Finland

Abstract:

Gold nanostars (GNS) and nanoparticles of inorganic materials (eg CuS) display intense LSPR absorptions in the Near IR that once photoexcited relax thermally. Accurate tuning of the coatings of such NP allow to dissolve them in solvent mixtures suitable for inkjet printers and to obtain 2D printed patterns on flat bulk surfaces. GNS can be inkjet printed on a paper substrate, observing a significant photothermal effect ($\Delta T \cong 20$ °C) when patterns are under NIR excitation (800nm) even with low laser intensity ($I \cong 0.2$ W/cm²). Model molecules can be grafted on the exposed surface of GNS in the printed patterns and released thanks to heating by NIR irradiation, as an example of smart devices for localized thermal treatment combined with temperature-triggered drug release.¹ Similar results can be obtained with the less expensive CuS by exciting inkjet printed patterns at 800 nm, with the additional advantage of excellent biocompatibility with human fibroblasts.² Beside irradiation intensity, printing parameters such as drop density, number of printed layers, and the permeability of the coated paper substrates can be modulated to finely tune the observed ΔT of printed GNS.³ Moreover, the nature and the thickness of the coatings can be tuned in order to avoid a close contact distance between GNS branches in printed patterns, thus preventing LSPR ibridization and maintaining the sharp shape of absorption bands. At a given set of printing parameters, this drives to a peaked trend of the observed ΔT vs irradiation wavelength (λ_{irr}) of the pattern, Figure 1. This allows either to write and read simple information using a single λ_{irr} (YES answer for $\Delta T >$ threshold) or to use multiple λ_{irr} to write and read complex information like thermal bar codes and anti-counterfeit signatures.⁴

Keywords: gold nanostars, photothermal effect, inkjet-printing, hyperthermia, encrypted writing

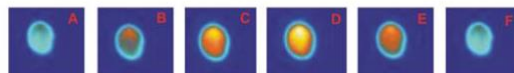
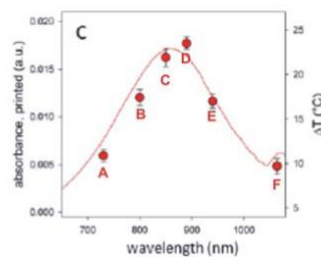


Figure 1: absorption spectrum (solid line) of an inkjet printed pattern of GNS on glass. Red points: observed T increase (vertical right axis) with laser sources having the same intensity but different λ_{irr} . Lowest row: photothermal images, (by thermocamera) of a laser beam impinging upon a printed pattern at the λ_{irr} corresponding to A-F points.

References:

1. Borzenkov, M., Pallavicini, P. et al. (2016) Fabrication of Inkjet Printed Gold Nanostar Patterns with Photothermal Properties on Paper Substrate, *ACS Appl. Mater. Interfaces*, 8, 9909-9916
2. Sarfraz, J., Pallavicini, P. et al (2018) Photo-thermal and cytotoxic properties of inkjet-printed copper sulfide films on biocompatible latex coated substrates, *Appl. Surf. Sci.* 435,1087-1095.
3. Borzenkov, M., Pallavicini, P. et al (2016), Photothermal effect of gold nanostar patterns inkjet-printed on coated paper substrates with different permeability, *Beilstein J. Nanotechnol.*, 7, 1480–1485.
4. Chirico, G., Pallavicini, P. et al (2018) Photothermally Responsive Inks for Inkjet-Printing Secure Information, *Part. Part. Syst. Charact.* 1800095

Graphene quantum dots as drug delivery systems for cancer therapy

R. Romeo,¹ D. Iannazzo,² A. Pistone,² C. Celesti,² S. V. Giofr ,¹ G. Visalli,³ A. Di Pietro³

¹Department CHIBIOFARAM, University of Messina, V.le Annunziata, 98168, Messina, Italy

²Department of Engineering, University of Messina, C.da Di Dio, 98166, Messina, Italy

³Department BIOMORF, University of Messina, Via Consolare Valeria, 98100, Messina, Italy

Abstract:

Graphene quantum dots (GQDs), fragments limited in size of a single-layer two-dimensional graphene, are considered as the next generation of carbon-based nanomaterials with enormous potential in biomedical field. Due to their outstanding physical, chemical and biological properties, these nanomaterials have shown promising applications in cancer therapy.¹ When compared with other carbon-based nanomaterials, GQDs exhibit biologically interesting properties, such as low toxicity, chemical inertness, water solubility and the ability to be internalized inside cells by endocytosis which make them ideal nano-carriers for drug delivery.² The quantum confinement, which confers fluorescence to these nanostructures, allows the simultaneous detection and treatment of cancer cells, making them suitable platforms for theranostic purposes.³ The surface/volume ratio and versatile surface functionalization allows their multimodal covalent and non-covalent conjugation with drugs, targeting ligands, and polymers, in order to improve their pharmacological profile.^{4,5}

GQD, synthesized by acidic oxidation and exfoliation of multi-walled carbon nanotubes (MWCNT) have been conjugated with anticancer agents and with targeting ligands that could specifically recognize specific receptors on the cells surface and induce receptor-mediated endocytosis in order to minimize the systemic toxicity and undesirable side effects typically associated with conventional therapy (Fig. 1). The reported results lead to targeted therapies for cancer treatment, opening new possibilities in the use of anticancer drugs

poorly soluble in water and endowed with systemic toxicity.

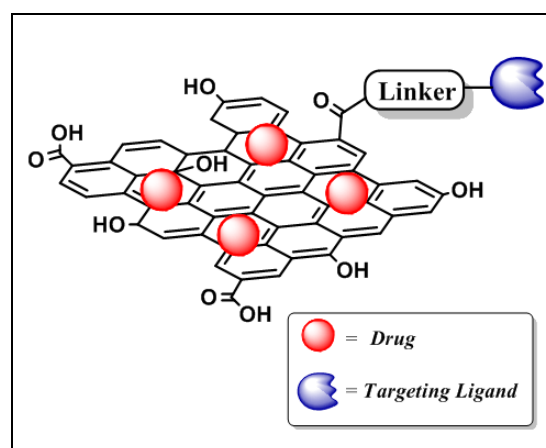


Figure 1: Drug Delivery Systems GQD based for targeted anticancer therapy

Keywords: Drug delivery system, graphene quantum dots, targeted delivery, anticancer activity

References:

1. Iannazzo, D., Ziccarelli, I., Pistone, A. (2017) Graphene quantum dots: multifunctional nanoplatforms for anticancer therapy *J. Mater. Chem. B*, 5, 6471-6489.
2. Wang, C., Wu, C., Zhou, X., Han, T., Xin, X., Wu, J., Zhang, J., Guo, S. (2013) Enhancing cell nucleus accumulation and DNA cleavage activity of anti-cancer drug via graphene quantum dots. *Sci. Rep.* 3, 2852.
3. Iannazzo, D.; Pistone, A.; Salam , M.; Galvagno, S.; Romeo, R.; Giofr , S.V.; Branca, C.; Visalli, G. (2017) Graphene quantum dots for cancer targeted drug delivery. *Int. J. Pharm.*, 518, 185-192.
4. Iannazzo, D., Pistone, A., Celesti, C., Triolo, C., Patan , S., Giofr , S. V. Romeo, R., Ziccarelli, I., et al. (2019) A Smart Nanovector for Cancer Targeted Drug Delivery Based on Graphene Quantum Dots, *Nanomaterials*, 9, 282.

Protein-nanoparticle interactions: effect of surface functionalization and pH of the medium

B. Meesaragandla,^{1,2,*} I. Garcia,³ L.M. Liz-Marzán^{3,4} and M. Delcea^{1,2}

¹ Institute of Biochemistry, University of Greifswald; ² ZIK HIKE, University of Greifswald, Germany;

³CIC biomaGUNE and CIBER de Bioingeniería, Biomateriales y Nanomedicina (CIBER-BBN), Paseo de Miramón 182, 20014 Donostia-San Sebastián, Spain

⁴Ikerbasque, Basque Foundation for Science, 48013 Bilbao, Spain

Abstract:

In recent times, nanoparticles (NPs) are widely used in medicine due to their unique physicochemical properties, such as small size, low toxicity and high reactivity. When used for the drug delivery applications, they can stimulate and/or suppress the immune response by interacting with blood proteins.¹ The conformational changes of proteins after conjugation with NPs are an important aspect for immunogenicity. The compatibility of the NPs with the immune system is mainly determined by their surface chemistry. In this work, we have studied the human serum albumin (HSA) protein-gold nanoparticle (AuNP) interactions focusing on the nature of AuNP surface and pH of the medium. HSA exhibits different isomeric forms and undergoes conformational changes at different pH conditions (e.g. pH 3.8, 7.4, and 9.3).²

AuNPs with different surface functionalization (citrate, PEG-OMe, PEG-COOH, PEG-NH₂, and glycan) were chosen to investigate the effect of surface functionalization on protein structure. Both UV-Vis and dynamic light scattering (DLS) measurements have confirmed the formation of protein corona. No significant change (or a slight red shift) is observed in the localized surface plasmon resonance (LSPR) position (at 523 nm), which may indicate the weak interaction between core AuNPs and HSA. Circular dichroism (CD) spectroscopy studies suggested that HSA conjugated to AuNPs undergoes a change in the secondary structure (decrease in alpha-helix) at various pH for all functionalized AuNPs. This change in protein secondary structure might be due to the type of dominant interaction between NPs and HSA (i.e. electrostatic, hydrogen bonding). Our results showed that both surface charge and pH of the medium influences the changes in HSA structure. For example, neutral PEG-OMe-AuNPs do not induce changes in protein

structure at all investigated pHs and may be considered safe for drug delivery applications, whereas positively charged PEG-NH₂-AuNPs induces conformational changes in HSA at all pH conditions, being therefore a non-safe system for delivery applications.

Keywords: gold nanoparticles, human serum albumin, protein corona, surface modification, pH, immunogenicity.

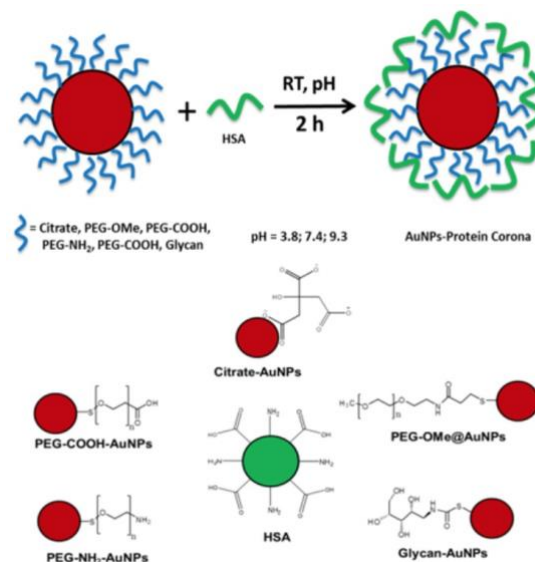


Figure 1: Schematic representation of the formation of AuNP-HSA corona at different pH conditions (top) and the variety of functional groups at the NPs surface (bottom).

References:

1. Dobrovolskaia, M. A., McNeil, S. E. (2007), Immunological properties of engineered nanomaterials, *Nat. Nanotechnol.*, 2, 469-478.
2. Chatterjee, T., Pal, A., Dey, S., Chatterjee B. K., Chakrabarti, P. (2012) Interaction of virstatin with human serum albumin: spectroscopic analysis and molecular modeling. *PLOS One.*, 7, e37468. doi: 10.1371/journal.pone.0037468.

Protein-nanoparticles interactions by microfluidic: A novel tool for biomedical applications

N. Orellana,¹ S. Torres,¹ S. Palma,^{1,2} M. L. Cordero,³ M. Kogan^{2,4} and N. Hassan¹

¹ Programa Institucional de Fomento a la I+D+I, Universidad Tecnológica Metropolitana. Edificio de Ciencia y Tecnología, Ignacio Valdivieso 2409, San Joaquín, Santiago, Chile

² Departamento de Química Farmacológica y Toxicológica, Facultad de Ciencias Químicas y Farmacéuticas, Universidad de Chile. Santos Dumont 964, Independencia, Santiago, Chile

³ Departamento de Física, Facultad de Ciencias Físicas y Matemáticas, Universidad de Chile. Av. Blanco Encalada 2008, Santiago, Chile

⁴ Advanced Center for Chronic Diseases (ACCDiS). Santos Dumont 964, Independencia, Santiago, Chile.

Abstract:

Metal nanoparticles have gained significant attention in recent years because of their unique physical and chemical properties, making them suitable for drug delivery and targeting, a together with cancer treatment. The surface of metal nanoparticles can be modified to target cancer cells, specifically by conjugating a specific targeting moiety to the surface of the metal nanoparticle (1). Currently, gold nanoparticles (AuNPs) are being used in drug delivery and cancer treatment, because of their potent photothermal effect responsible of a controlled drug delivery. Nanoparticles stability in a biological medium is crucial for its utilization as a drug delivery system. For this reason, several characteristics must be considered before utilizing this type of materials.

Microfluidic can provide evidence of the behaviour of the Protein-corona formation onto AuNPs when are subjected to hydrodynamic forces, in a hydrodynamic regime which can contrast the macroscopic scale (bulk) scenario (3).

In this work, we studied the interactions of gold nanospheres (AuNS) and gold nanorods (AuNR) functionalized with polyethylene glycol (PEG) and folic acid (FA) with different plasma proteins by microfluidic. We analyzed their behaviour in a hydrodynamic regime, mimicking the natural environment, comparing their behaviour in a macroscopic scale (Figure 1).

Protein-nanoparticles samples were analysed by different techniques: a) TEM to analyse the morphology, and homogeneity of the nanoparticles before and after of the interaction, b) Dynamic light scattering, to evaluate the hydrodynamic diameter and c) Zeta potential, to analyse how the surface charge change with the

presence of protein corona. D) UV-VIS-NIR spectroscopy, to analyse the surface plasmon resonance of the nanoparticles in presence of protein, e) Micro-BCA assay to quantify the protein attached to the nanoparticle, f) Atomic absorption to quantify the gold content interacting with the protein and g) Circular dichroism to analyse the secondary structure content of the protein before and after interaction with nanoparticles.

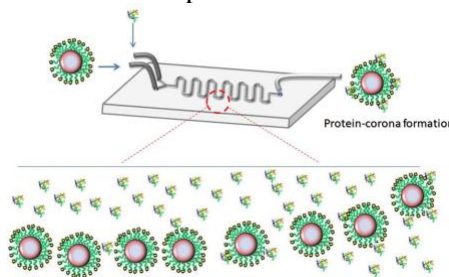


Figure 1: Schematic representation of the proposed work. Protein-corona formation by hydrodynamical parameters.

The results demonstrated that the AuNPS were coating by proteins in different manner depending on the flow rates.

Keywords: protein folding, biomaterials, biomedical applications, microfluidics, folic acid, gold nanoparticles, polyethylene glycol.

References:

1. Mout, R., Moyano, DF., Rana, S., Rotello, VM. (2012), Surface functionalization of nanoparticles for nanomedicine. *Chemical Society reviews* 41:2539-44.
2. Valencia, PM., Farokhzad, OC., Karnik, R., Langer, R. (2012) Microfluidic technologies for accelerating the clinical translation of nanoparticles, *Nat Nano* 7:623-9.

Targeting of Nano-Carriers in Atherosclerotic Arterial Bifurcation Sites

Maria Khoury, Mark Epshtein, Hila Zukerman and Netanel Korin

Department of Biomedical Engineering, Technion - IIT, Haifa, Israel

Abstract:

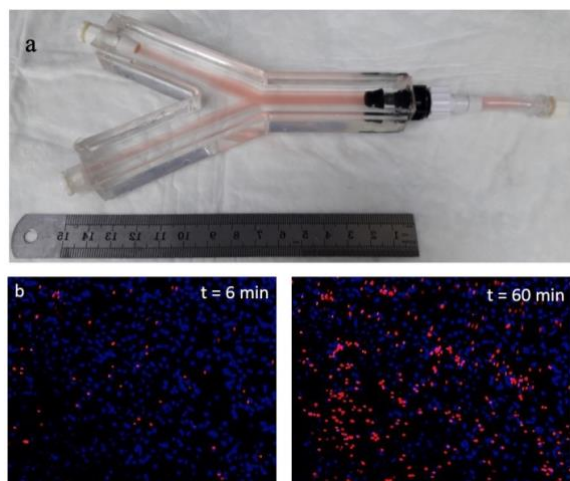
Cardiovascular diseases, including Atherosclerosis, are one of the leading causes of death in western society and there is a clinical need for new approaches for improved therapies [1]. Targeted nano-therapeutics to atherosclerotic sites can provide safer, more efficient and effective treatments through localization and release of encapsulated therapeutics specifically at the desired region [2]. Studies have shown that atherosclerotic lesions localize at specific regions that may include tight curves and bifurcations along the blood vessel [3]. The goal of our research is to understand particle dynamics, deposition and adhesion in models of arterial bifurcations under physiological conditions. We have designed and fabricated 3D real-sized arterial bifurcation models cultured with human umbilical vein endothelial cells (HUVECs). The models were connected to a programmable perfusion system for injection of particles. Our results show that different particles tend to localize at specific sites within the bifurcation based on hemodynamics and particles properties. These findings highlight the key role of hemodynamics and particle characteristics when developing targeted nano-carriers to the vasculature.

Keywords: Nano carriers, Drug targeting, Blood vessels, Atherosclerosis, Bifurcations, Hemodynamics, Vascular targeting

Figure 1: (a) a PDMS 3D real-sized model of the human carotid artery bifurcation, cultured with endothelial cells, (b) the deposition of $2\mu\text{m}$ particles (in red) to endothelial cells (nucli staining in blue) inside the model, at two different time points under physiological flow, showing the increase of adhesion of the particles as a function of time.

References:

1. Mozaffarian, Dariush, et al. "Executive Summary: Heart Disease and Stroke Statistics—2015 Update A Report From the American Heart Association." *Circulation* 131.4 (2015): 434-441.
2. Moghimi, S. Moein, A. Christy Hunter, and J. Clifford Murray. "Nanomedicine: current status and future prospects." *The FASEB journal* 19.3 (2005): 311-330.
3. Glagov, S., et al. "Hemodynamics and atherosclerosis. Insights and perspectives gained from studies of human arteries." *Archives of pathology & laboratory medicine* 112.10 (1988): 1018-1031.



Buccal permeating lipid-core micelles loaded on mucoadhesive films as a novel drug delivery system for biologic drugs

W-H. Chou,^{1,2} A. Galaz,^{1,2} M.O. Jara,^{1,2} J.O. Morales,^{1,2,3*}

¹ University of Chile, Department of Pharmaceutical Science and Technology, School of Chemical and Pharmaceutical Sciences, Santiago, Chile

² Advanced Center for Chronic Diseases (ACCDiS), Santiago, Chile

³ Luleå University of Technology, Pharmaceutical and Biomaterial Research Group, Department of Health Sciences, Luleå, Sweden

Abstract:

Lipid-core micelles (LCMs) are composed of lipid self-associated copolymers dispersed in aqueous solution and have been developed as drug delivery systems for poorly water soluble drugs, including cardiovascular and antineoplastic agents. On the other hand, the buccal route of administration is a non-conventional route for delivering drugs and elicits several advantages as an alternative for oral administration, including avoiding first-pass metabolism and low enzymatic activity, and therefore, this route can be exploited to deliver biological drugs. The goal of this research was to develop buccal mucoadhesive films loaded with rhodamine 123 (Rho) and human insulin (Ins)-loaded LCMs as a novel drug delivery system to deliver biologics through the buccal epithelium.

Synthesis of drug-loaded LCMs using GRAS excipients, and loading of those particles on the surface of buccal mucoadhesive films comprise the main steps of this research and were obtained by using novel low-energy hot emulsification and thermal inkjet printing processes, respectively (Figure 1). This research represents the first approach using this type of nanoparticles as drug delivery system loaded on mucoadhesive films for buccal nanocarrier permeation.

We have demonstrated a high association of Rho and Ins to LCMs, yielding nano-sized, spherical-shaped and monodispersed particles (Table 1). Furthermore, the surface charge of Ins-LCMs is less negative in comparison with Rho-LCMs, due to the interaction among positively-charged Ins and negatively-charged LCMs lipid constituents. *In vitro* release studies have demonstrated that the released amount of Rho and Ins loaded on LCMs after 72 h was 26% and 88%, respectively, at 37°C in PBS 7.4. On the other hand, HPMC mucoadhesive films loaded with Rho-LCMs elicited 30-times higher

permeation rate in comparison with a Rho-LCMs suspension control, after 6 minutes of contact by *ex vivo* permeation studies. Furthermore, the cumulative amount of Rho-LCMs that effectively crossed the buccal epithelium after 24 minutes is almost 15 times higher using a printed mucoadhesive film compared to a suspension. This enhanced permeation can be related to the increase of local disposition of LCMs, leading to a large concentration gradient, which favors LCMs transport. Therefore, we expect similar results for Ins permeation using Ins-LCMs-loaded mucoadhesive films, and consequently this research will lead to develop an alternative drug delivery system for biological drugs using the buccal route of administration.

Keywords: lipid-core micelle, buccal mucoadhesive film, rhodamine 123, insulin, permeation, drug delivery system, biological drug.

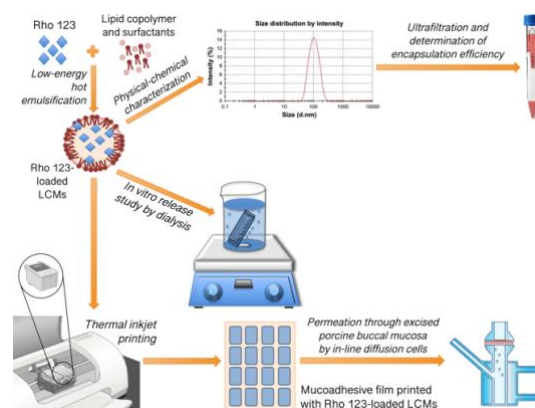


Figure 1: Diagram of synthesis and characterization of drug-loaded LCMs and elaboration of LCMs-loaded mucoadhesive films.

Table 1: Physical-chemical properties of drug-loaded LCMs. HD: hydrodynamic diameter, PDI: polydispersity index, ZP: zeta potential; EE: encapsulation efficiency.

Sample	HD (nm)	PdI	ZP (mV)	EE (%)
Rho-LCMs	26.2±2.5	0.25±0.11	-12.4±3.6	98.3±0.8
Ins-LCMs	16.6±1.0	0.20±0.05	-2.6±1.1	94.3±3.8

References:

1. M. Hillery and A. S. Hoffman, in *Drug Delivery: Fundamentals & Applications*, 2da Ed. (Taylor & Francis Group, 2017), pp. 1–21.
2. M. B. Brown and V. F. Patel, in *Drug Delivery: Fundamentals & Applications*, 2da Ed. (Taylor & Francis Group, 2017), pp. 201–14.
3. H. F. Fritz, A. C. Ortiz, S. P. Velaga, and J. O. Morales, *Drug Delivery and Translational Research* (2018).
4. M. Montenegro-Nicolini, V. Miranda, and J. O. Morales, *AAPS J* **19**, 234 (2017).

Hybrid nanostructure lipid capsules: A promising nano-vehicles to improve anticancer activity of curcumin

Sunil Kumar Yadava, Remya V, Jyotsnendu Giri*

Department of Biomedical Engineering, Indian Institute of Technology, Hyderabad India

Abstract

Curcumin has received immense interest among scientific community for its effectiveness to cancer cells as well as cancer stem cells. [1] High hydrophobicity and unsatisfactory bioavailability have been impeding clinical use of curcumin [2]. Recently, various nanoformulations are developed to overcome these limitations [2]. However, low entrapment efficiency, expulsion during storage, instability, burst release, tedious development process and formulation cost remains challenging to gain popularity for clinical use [3].

We developed curcumin loaded hybrid nanostructure lipid capsules (Cur-HnLCs) to meet the above challenges. Cur-HnLCs of 30 nm was prepared. Physicochemical properties of Cur-HnLCs such as particles size, zeta potential, encapsulation efficiency, *in-vitro* drug release kinetic, and stability was determined. Therapeutic efficacy of Cur-HnLCs was determined using different breast cancer cells such as MCF7, MDMB-231 as well as cancer stem cells.

Cur-HnLCs are shown narrow size distribution having ζ potential (-) 8.32 mV. The cur-HnLCs are stable for 60 days at 4 °C without change in their size and drug leaching. High encapsulation efficiency (>95 %) of curcumin was achieved and controlled release of curcumin from the HnLCs was observed. *In-vitro* anti-cancer efficacies of cur-HnLCs formulation toward different breast cancer cells were more than 2 times compared to free curcumin. The IC₅₀ values of Cur-HnLCs on MCF-7 after 24 hrs of treatment are nearly 2.5 μ M and 20 μ M measured by [³H] thymidine incorporation and MTT assay, respectively [Figure 1]. Cur-HnLCs formulation was observed to kill breast cancer stem cells effectively.

Keywords: Nanocapsules, Curcumin, Cancer, Cancer stem cell, Drug delivery

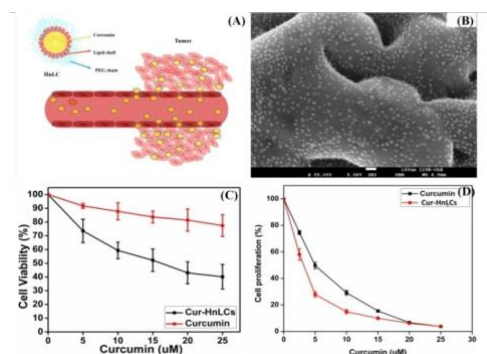


Figure 1: Schematic of Cur-HnLCs (A), Cryo SEM image of Cur-HnLCs (B), comparative cellular toxicity of curcumin, free and in HnLCs (C) and [³H] thymidine incorporation after treatment of cells with free curcumin and Cur-HnLCs for 24 hrs (D).

Novel curcumin nanoformulation (Cur-HnLCs) are developed with high drug encapsulation, stability and superior anticancer efficacy. The tunable and narrow size distribution of our nanoformulation will be suitable to enhance the accumulation of curcumin by EPR effect. The superior therapeutic efficacies toward cancer and cancer stem cells promise our nanoformulations for effective cancer therapy. However, *in-vivo* studies need to be performed to check the therapeutic efficacy of our cur-HnLCs, which is under process.

References

1. Elham Zendejdel et al. (2018), The molecular mechanisms of curcumin's inhibitory effects on cancer stem cells. *J Cell Biochem.* 1-9.
2. OrnochumaNaksuriya, et al.(2014), Curcumin nanoformulations: A review of pharmaceutical properties and preclinical studies and clinical data related to cancer treatment. *Biomaterials* 3365-3383.
3. JaisonJeevanandam, Yen San Chan*, Michael K. Danquah. Nano-formulations of drugs: Recent developments, impact and challenges. *Biochimie* 128-129 (2016) 99-112

A Novel Model based on Sphere-shaped Coulomb Explosion for the Study of Nano-particles of Gold in the Treatment of Brain Tumor

Zahid Hasan,^{1,*} Sagheer Abbas,¹ Muhammad Adnan Khan,¹ Kashif Iqbal,^{1,2} Zia Ahmad,¹,
Muhammad Mazhar Bukhari,¹

¹National College of Business Administration & Economics Department of Computer Science, Lahore, Pakistan

²GC University Lahore, Pakistan

Abstract:

Nanotechnologists, Pharmaceutical scientists and medical researchers are still engaged in a fighting against a high number of serious and complex diseases like brain tumor. The novel applications of Nanotechnology to the fitness of health increases high hopes and expectations. Nanotechnology exploits the enhanced too often novel physical, biochemical and organic or biologically dimensions of substantial at nanometer measurement and has the potential to empower early detection, prevention and recuperate analysis, treatment and follow through of illnesses.

In this research work, a model is proposed to design “Energy Distribution Control System” that will work as heat therapy for the treatment of the fatal tumor cells at molecular and Nano atomic level on the basis of “See and Treat” technique by controlling the intensity of heat by using the magical properties of coated Gold Nano-particles. This proposed model will be evaluated on the Thermo Phoresis Nt. The proposed model is concerned with the computer aided study of Nano-particles according to the requirement the different size of nanoparticles with diameter less than 100nm. The present study proposed a method to destroy the cancer tissues without touching the healthy cells of the body. The numerical results obtained in graphical form and show how Nano-particles of Gold preserve their energy as well as how they can be used in the treatment of cancer cells of Brain Tumor. The results are obtained by using MATLAB simulation.

Keywords: Nanotechnology, Gold Nanoparticles, Thermo Phoresis Nt, Heat Therapy, Nano atomic level

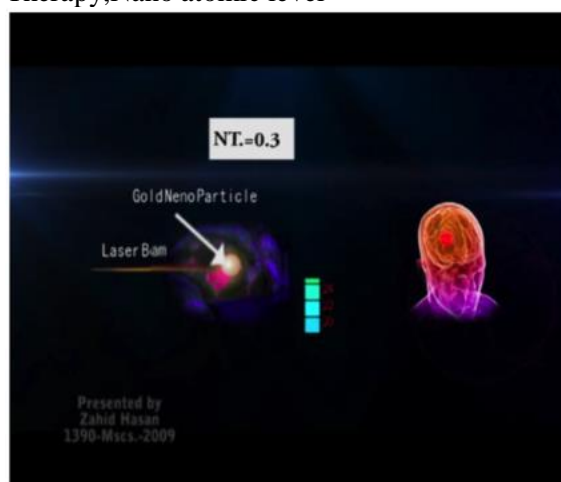


Figure 1: Figure illustrating the fundamental question that we are tempting to solve experimentally: what is the importance of the keypoint of Thermo Phoresis Nt how it preserve the heat energy and then it use for the treatment of cancer cells of Brain Tumour .

References:

1. Hashimoto, S., Werner, D., & Uwada, T. (2012). Studies on the interaction of pulsed lasers with plasmonic gold nanoparticles toward light manipulation, heat management, and nanofabrication. *Journal of Photochemistry and Photobiology C: Photochemistry Reviews*, 13(1), 28-54.
2. Vishwanathan, K., & Springborg, M. (2017). Effect of size, temperature, and structure on the vibrational heat capacity of small neutral gold clusters. *J. Mater. Sci. Eng*, 6, 325.

**Nanotech / Biotech -
Session II.C:
Nanomedecine-
Bioimaging / Diagnostics**

Nanoscale exploration of live brain tissue by single nanoparticle tracking and super-resolution imaging

Laurent Cognet

LP2N - Institut d'Optique, CNRS & University of Bordeaux, Talence, France
Email: laurent.cognet@u-bordeaux.fr

Abstract

Sub-wavelength localization of single nano-emitters is the basis of several super-resolution microscopy approaches (i.e. delivering images with resolution below the diffraction limit) which are now applied in different fields of science requiring nanoscale imaging performance. In complex systems like thick live biological tissues, it still remains a challenge to apply super-resolution imaging approaches. This is due to the limited brightness of fluorescent emitters, the optical aberrations induced by the samples and/or the poor penetration of the light at visible wavelengths. To circumvent these limitations, we recently developed several new approaches. More precisely, I will present SELFI, an original strategy to super-localise a single molecule *in 3D* which allowed 3D super-resolution microscopy to be achieved at unprecedented depths inside a biological tissue [1]. Finally, I will present another approach based on single quantum dot tracking [2] and single carbon nanotube tracking in the near-infrared to obtain super-resolved maps of the extracellular space within intact live brain tissues [3-4].

References

1. Bon et al *Nat. Methods.* (2018)
2. Varela, et al *Nat. Commun.* (2016)
3. Godin, et al *Nat. Nanotechnol.* (2017)
4. Paviolo, et al *Methods* (2019)

See also: www.cognet-research.com

Nanoparticles for multimodal imaging and phototherapy of cancer: towards theranostic

R.Rotomskis^{1,2*}

¹ Vilnius University, Biophotonics Group of Laser Research Center, Vilnius, Lithuania

² National Cancer Institute, Biomedical Physics Laboratory, Vilnius, Lithuania

Abstract:

While refinement of the conventional cancer treatment modalities is important, research has also focused on developing alternative treatment modalities that are safe and potent. The applications of nanoparticles in cancer therapy and diagnostics have been a major stride forward in solving some of the challenges associated with classic treatment and diagnostics modalities. A present status and prospects of nanoparticles related to the selectivity of cancer treatment, multimodality in diagnostics and unifying the process of diagnostics and treatment on one nanoparticle (theranostics) is discussed.

It is highly desirable to develop novel multifunctional nanostructured systems that can achieve simultaneous in vivo imaging and treatment, today named as theranostics.

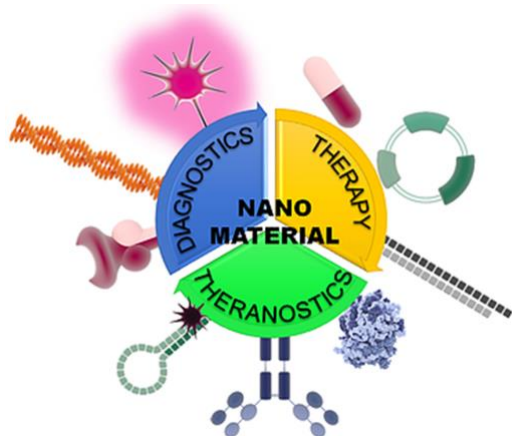


Figure 1: Figure illustrating the theranostic viewpoint envisages the combination of targeted therapeutic and diagnostic capabilities within a single entity.

By itself, theranostics predates the field of nanoscience; however, the advent of nanoparticles (NPs) with tunable physicochemical properties and subcellular size enabled the realization of multifunctional theranostic nanoplateforms.[1] Diagnostics-wise, NPs can serve as imaging contrast agents (optical, magnetic, X-ray, and photoacoustic)

and enriched with the therapeutic capacity, e.g. photothermal and photodynamic treatment.

Many kinds of nanostructures have been reported for bio-imaging, such as quantum dots, core/shell silica nanoparticles, polymer-coated gold nanoparticles, carbon nanotubes, magnetic nanoparticles. Photoluminescent (PL), magnetically active NPs are exceptionally well-suited contrast agents and can initiate therapeutic process. Quantum dots are bright PL nanoparticles which attached with photodrug can initiate the photodynamic therapy of cancer. Magnetic nanoparticles can be used as a contrast agent in the magnetic resonance imaging (MRI) and in case of applying of the variable magnetic field can induce thermal destruction of cancerous tissue. Rare earth-based nanoparticles (RENPs) have shown great merit as theranostic agents as their spectral properties can be fine-tuned and precisely controlled.[2] The unique advantage of RENPs lies within their ability to absorb near-infrared (NIR) radiation and convert it to light of both shorter and longer wavelengths, through anti-Stokes upconversion (UC) and Stokes downshifting (DS) processes, respectively. On one hand, DS emission within the biological optical transparency windows permits to visualize subcutaneous tissue layers, otherwise inaccessible to visible light. UC emission can be harnessed to photoinitiate drug release or production of reactive oxygen species (ROS), as in the case of photodynamic therapy of cancer (PDT). Upon the doping of different elements such as Gd and Sm into UCNPs structures, the prepared nanoparticles can also be endowed with more promising functions for multimodality imaging by the combination of fluorescent imaging with other imaging techniques.

Keywords: near-infrared, rare earth nanoparticles, theranostics, upconversion.

References:

1. J. Xie, S. Lee, X. Chen, Adv. Drug Delivery Rev. 2010, 62, 1064.
2. Skripka et al., Adv. Funct. Mater. 2018, 1807105.

Integrated optics devices in spectroscopy, biosensing and medical applications

B. Imran Akca

VU University of Amsterdam, LaserLab, Dept of Physics and Astronomy, Amsterdam, The Netherlands

Abstract:

Integrated optics is one of the fastest growing branches of optics which has several application areas including medical imaging, telecommunication, spectroscopy, astronomy and so on. By combining the basic components of integrated optics one can design an on-chip medical imaging system, a spectrometer, or an optical biosensor platform. We have demonstrated the first on-chip optical coherence tomography (OCT) on-chip in 2012 [1] which is one of the high-resolution optical imaging modality with a very wide application range. To do so, an optical spectrometer based on arrayed waveguide gratings (AWG) was designed and fabricated together with an optical wavelength-flattened beam splitter. Moreover, different on-chip spectrometers with novel features were designed for various applications and some of them experimentally demonstrated [2]. In addition to spectrometers, on-chip beam splitters and polarization splitters were designed and experimentally demonstrated that could be used in various medical imaging as well [3]. Besides imaging, integrated optics is an excellent technology for optical biosensing applications as it provides compact, power and cost-efficient devices with unique features. Our recent optical biosensor idea combines on-chip optical frequency combs- a Nobel prize winning idea with ring resonators in order to be used in early detection of lung cancer. Another emerging field is called reconfigurable integrated optics which allows to use the same on-chip components for different applications by changing specific properties of the waveguiding material without changing the device design. To do so, novel materials which show different responses to external stimulus are in high demand. In summary, it is possible to design custom devices by using integrated optics for different applications at a very small scale with unprecedented performance. Novel materials would allow novel functionalities in integrated optical devices, therefore interdisciplinary collaborations are necessary.

Keywords: integrated optics, spectrometers, optical biosensors, medical imaging, novel materials, compact, cost-effective, beam splitters, polarization splitters, reconfigurable

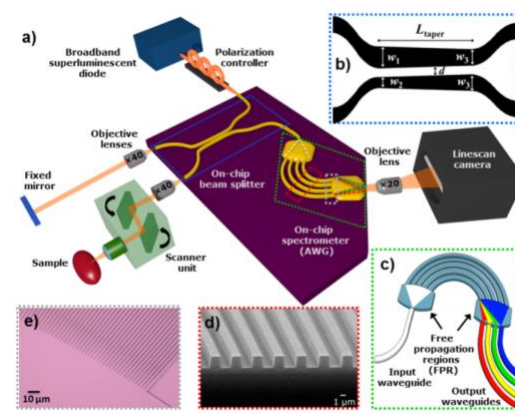


Figure 1: Schematic of the partially integrated spectral-domain (SD)-OCT system. (a) The complete SD-OCT setup comprising a broadband light source, the microchip with its optical circuitry consisting of a broadband beam splitter and the spectrometer (purple plate, magnified for viewing purposes), line-scan camera, and reference and sample arms, the latter including a scanner unit. (b) Details of the integrated broadband beam splitter, a 3-dB non-uniform adiabatic coupler (c) A conventional AWG which, in contrast to our device, includes output channels. (d) Scanning electron microscope image of the arrayed-waveguide section of the AWG before top-cladding deposition. (e) Optical microscope image of linear tapers at the waveguide/FPR interface of the fabricated AWG spectrometer.

References:

1. B. I. Akca et al. (2013) Miniature spectrometer and beam splitter for an optical coherence tomography on a silicon chip, *Opt. Express*, 21, 16648.
2. B. I. Akca, C. R. Doerr (2018) Interleaved Silicon Nitride AWG Spectrometers, *IEEE Photon. Technol. Lett.* PP(99):1-1.
3. E. Heemskerk, B. I. Akca (2018) On-chip polarization beam splitter design for optical coherence tomography, *Opt. Express*, 26, 33349.

Tracking stem cells and macrophages with gold and iron oxide nanoparticles—the choice of the best suited particle

Xing Sun, Neus Feliu, Wolfgang J. Parak

Center for Hybrid Nanostructures (CHyN), University of Hamburg, Hamburg

Abstract:

Cell-based therapies, which employ living cells as delivery systems or medicines, offer an attractive alternative to the traditional therapeutics. Nanoparticle (NP)-based cell imaging offers good potential for future diagnosis tools in medicine. Among them, gold and iron oxide NPs are good candidates, which can be used as contrast agents for imaging by computed tomography (CT) and magnetic resonance imaging (MRI), respectively. Therefore, cells which have been labeled with these NPs may also be tracked. This may be of great importance for in vivo tracking of administered or transplanted cells.

In this work, we optimized the conditions to label stem cells and macrophages with a library of gold and iron oxide NPs of different sizes (5 nm - 100 nm core diameter) and shapes. We investigated the amount of NPs which can be delivered to different cells, as well as their related toxic effects, in relation to the physicochemical properties of the NPs. Our study revealed that, in general, when cells are exposed to NPs at similar elemental concentration (e.g., Au or Fe), bigger NPs lead to higher internalized elemental amounts as compared to exposure with smaller sized NPs. While the exposure concentrations are limited concerning the onset of toxicity, bigger NPs lead to better labeling than smaller NPs, resulting in improved contrast for imaging with enhanced biocompatibility.

Keywords: gold nanoparticles, stem cells, cellular uptake, cell labeling.

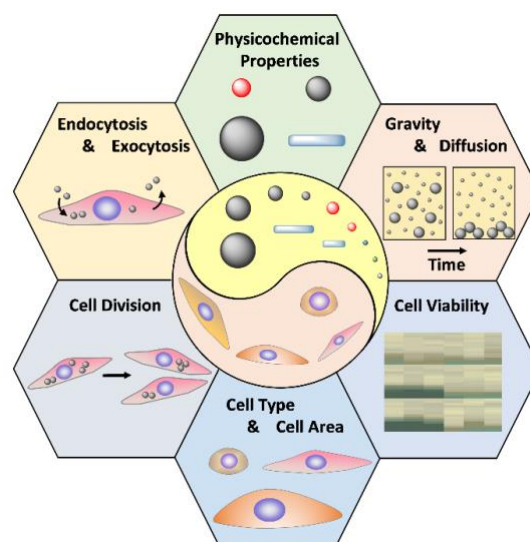


Figure 1: Scheme of the influencing factors in the cell uptake study.

References:

1. Xing Sun, Mahmoud Gamal, Philipp Nold, Alaa Said, Indranath Chakraborty, Beatriz Pelaz, Franziska Schmied, Kerstin von Pücklere, Jens Figiel, Ying Zhao, Cornelia Brendel, Moustapha Hassan, Wolfgang J. Parak, Neus Feliu, *Applied Materials Today*, 2018, In press.
2. Chithrani, B. D.; Ghazani, A. A.; Chan, W. C. W., Determining the Size and Shape dependence of gold nanoparticle uptake into mammalian cells. *Nano Lett.* 2006, 6 (4), 662-668.

Mesoporous Nickel Vanadate-Graphene Nanocomposite Integrated Microfluidic Biochip for Biosensing Application

Nawab Singh¹, Prabhakar Rai², Ashutosh Sharma², B. D. Malhotra^{3*}, and Renu John^{1*}

¹Department of Biomedical Engineering, Indian Institute of Technology Hyderabad-502285, India.

²Department of Chemical Engineering, Indian Institute of Technology Kanpur, Kanpur, 208016, India.

³Department of Biotechnology, Delhi Technological University, Shahbad Daultapur, Main Bawana Road, Delhi-110042, India.

Abstract:

Cardiovascular diseases (CVD) are currently the leading cause of death worldwide. Cardiac myoglobin (cMb) is a cardiac biomarker that is being exploited for early diagnosis of acute myocardial infarction (AMI). We report results of studies relating to the development of an electrochemical microfluidic biosensor for human cardiac myoglobin detection. The microfluidic chip was nanoengineered using L-cysteine modified mesoporous nickel vanadate-graphene nanocomposite (Cys-Ni₃V₂O₈-RGO) self-assembled on gold (Au) electrode followed by assembling polydimethylsiloxane microchannels. The Cys-Ni₃V₂O₈-RGO/Au surface was covalently functionalized with cardiac myoglobin antibodies (cMAb) via EDC/NHS coupling chemistry. This cMAb conjugated cysteine nickel vanadate-graphene based transducer (cMAb/Cys-Ni₃V₂O₈-RGO/Au) was used to detect the human cardiac myoglobin. The uniformly distributed nickel vanadate (Ni₃V₂O₈) nanospheres onto RGO nanosheets offered large surface area with mesoporous structure for enhanced loading of the cMAb. In addition, electroactive nature of Ni₃V₂O₈-RGO nanocomposite offers high mobility of electrons and good reaction kinetics resulting in a new sensor platform for the development of electrochemical microfluidic biosensor. This cMAb/Cys-Ni₃V₂O₈-RGO/Au microfluidic biochip showed lower detection limit of 0.02 ng mL⁻¹ for a wide range of concentration (0.02–400 ng mL⁻¹) of cardiac myoglobin protein (cMb) indicating high affinity to cMb. This microfluidic biosensor showed high stability, good selectivity and high reproducibility due to integration of microfluidic elements with mesoporous Ni₃V₂O₈-RGO. The results of these studies revealed the efficiency of the Cys-Ni₃V₂O₈-RGO/Au transducer as an excellent biosensing device for biomolecules detection. This microfluidic device can be applied to detect cardiac troponin I, B-type natriuretic peptide, cardiac troponin T and cardiac troponin C by immobilizing the specific antibody recognition elements and can be used for real point-of-care application in biomedicine.

Keywords: Cardiac Myoglobin, Ni₃V₂O₈ nanosphere, RGO nanosheets, Microfluidics, Acute Myocardial Infarction, Electrochemical.

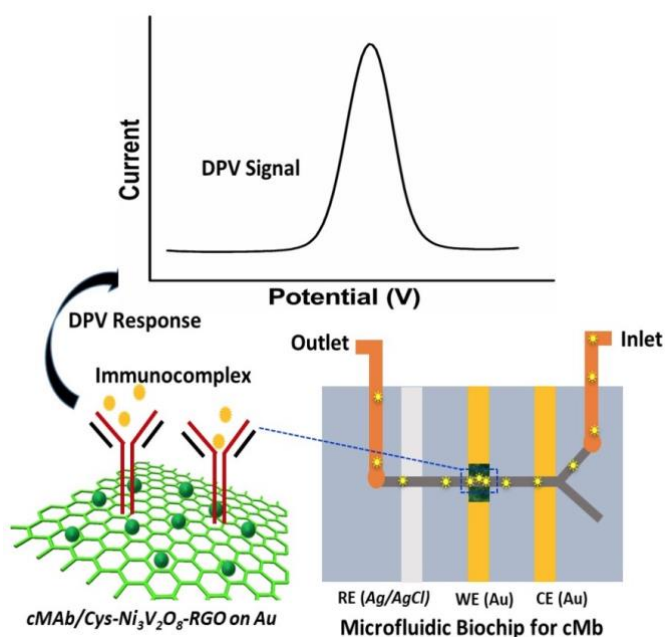


Figure 1: Graphical representation of the fabrication of microfluidic biochip for detection of cardiac myoglobin: The sensor using embedded Cys-Ni₃V₂O₈-RGO as a working electrode and functionalized with antibody of cMb molecules to specific detection of cardiac myoglobin.

References:

1. Sharma, Deepti, Jongmin Lee, and Heungjoo Shin. "An electrochemical immunosensor based on a 3D carbon system consisting of a suspended mesh and substrate-bound interdigitated array nanoelectrodes for sensitive cardiac biomarker detection." *Biosensors and Bioelectronics* 107 (2018): 10-16.
2. Zhang, Jun, et al. "Fundamentals and applications of inertial microfluidics: a review." *Lab on a Chip* 16.1 (2016): 10-34.
3. Sackmann, Eric K., Anna L. Fulton, and David J. Beebe. "The present and future role of microfluidics in biomedical research." *Nature* 507.7491 (2014): 181.

Enhanced Coupling Effect of Gold Nanoislands and Gold Nanoparticles for Optical Biochemical Sensing

Y.K. Chan, C.M.L. Wu*

City University of Hong Kong, Department of Materials Science and Engineering, Hong Kong SAR, P.R. China

Abstract:

It is known that gold nanoparticles (AuNPs) provide certain desirable features for nanotechnology applications. Our previous work on self-assembly gold nanoislands (AuNIs) formed on glass for localized surface plasmon resonance (LSPR) also showed that the nanoislands provided an excellent sensing platform for optical biochemical sensing [1]. In this work, we attempt to use AuNPs and AuNIs together to create electromagnetic coupling between them, to further improve the optical biochemical sensing capability. The study is based on our well-studied LSPR configuration with AuNIs formed after annealing a thinly deposited gold film on glass. Gold films of about 3.3 nm to 13.3 nm thick were deposited. The effect of variation of deposition thickness, annealing temperature and annealing time on size and separation of AuNIs were studied. The enhanced coupling effect between AuNIs and AuNPs provided high sensitivity of optical sensing. The proof of concept was demonstrated via the sensing of small molecules, using Pb(II) ions in drinking water as an example. In achieving this, a polymer receptor was required to provide linkage between AuNIs/AuNPs and Pb(II) ion. That is, the AuNIs surface was first functionalized with suitable receptors and AuNPs. The size and separation of AuNIs and the coupling effect were first characterized by the optical extinction spectrum. The change in the optical extinction spectrum, and in particular, red shifting of absorption band of various AuNIs was studied. The best red shifted AuNIs sample is that with 6.7 nm gold deposition thickness. The initial annealing temperature is critical to the size and separation of the AuNIs. Using the best red-shifted AuNIs substrate and coupled with AuNPs, optical chemical sensing of Pb(II) ions by our Common-Path Spectral Interferometry was carried out. It achieved 0.26 radians phase change for 1 ppb Pb(II) ions solution. This was slightly better than the phase change of 0.25

radian with a similar method [1]. Further, to demonstrate the biosensing capability with the AuNIs/AuNPs couple, sensing of human IgG antigen biomolecules was carried out, and the results will be presented in the conference.

Keywords: gold nanoparticles, self-assembly gold nanoislands, electromagnetic coupling effect, red shifting of optical extinction spectrum, localized surface plasmon resonance, opti-chemical sensing, biosensing, Pb(II) ions, human IgG.

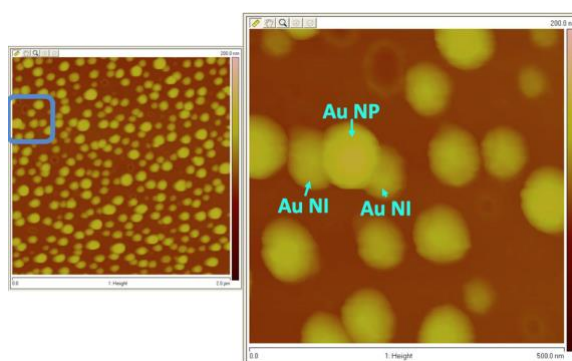


Figure 1: Atomic force microscope height scanning images of SAM-AuNIs with AuNPs. As an illustration, a AuNP was found on top of AuNIs.

References:

1. Qiu, G., Ng, S.P., Wu, C.M.L. (2017) Dielectric functionalization for differential phase detecting localized surface plasmon resonance biosensor, *Sensors & Actuators: B. Chemical*, 234, 247-254.
2. Qiu, G., Ng, S.P., Liang, X.Y., Ding, N., Chen, X.F., Wu, C.M.L. (2017) Label-free LSPR Detection of trace lead(II) ions in drinking water by synthetic poly(mPD-co-ASA) nanoparticles on gold nanoislands, *Analytical Chemistry*, 89, 1985-1993.

Construction of Functional Conical Nanopores in view of sensing applications

N. Arroyo,^{1,*} F. Picaud,¹

¹Laboratoire de Nanomédecine, Imagerie et Thérapeutiques, Université de Bourgogne-Franche-Comté, Besançon, France

Abstract:

Alzheimer is a distressing disease, which comes from an accumulation of protein aggregates such as amyloid fibrils. It inflicts a lot of pressure on both the patient and his family since no treatment exists for now. Amyloids and how they aggregate themselves seem to be a marker for the predisposition of Alzheimer¹. However, there is presently no dedicated equipment able to follow or analyze, in real time, the amyloid fibril formation. Single nanopore detection technology is considered as one of the major breakthroughs in the field of nanotechnology over the last decades². Indeed, the “Oxford Nanopore” company is able now to propose biological nanopores able to sequence DNA molecules³ with high performances. Unlike the biological ones, solid-state nanopores present advantages such as robustness and a diameter modulability ranging from a few to hundred of nm. This makes them good candidates for detecting objects from short DNA strands to nanoparticles⁴. However several factors should be overcome to detect small proteins such as amyloid fibril. We can cite for instance the unspecific adsorption of proteins in the nanopore, the nanopore lifetime, or the free energy barrier to enter or escape the nanopore. Here, we aim to use functionalized nanopores to measure the state of aggregation and allow an early medical supervision of the patient. The nanopore surface coverage by PEG molecules will help amyloids or other structures to enter and diffuse inside the nanopore. The measurement of the electrical intensity going through this nanopore could thus be the ideal way to quantify these amyloid translocations. By studying the intensity variation observed when a molecule structure translocates through the structure, it seems possible to have a better knowledge of what kinds of amyloid can be found in a patient blood sample. We develop in this study, numerical simulations on functionalized conical nanopores to take advantage of the ionic current rectification

effect. We present early work of nanofluidics obtained by molecular dynamics simulation on these nanocones. For this, we compare the behaviour of water molecules and of different ions under the presence or the absence of PEG functions on the nanopore surface. These preliminary results with only solvent molecules will allow us to determine the best geometrical functionalized nanopore to analyze the amyloid fibrils translocation inside the nanocone.

Keywords: functionalization, conical nanopore, molecular dynamics simulation, electrical detection.

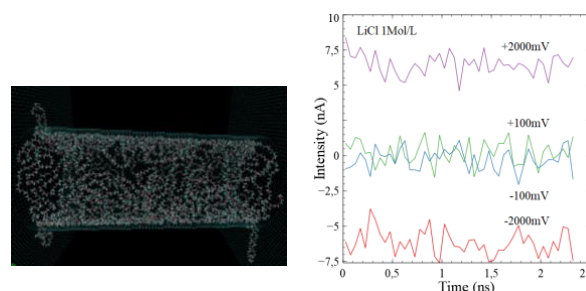


Figure 1: Left : side view of the conical nanopore functionalized by PEG molecules. Right : ionic currents through the nanopore caused by Li^+ and Cl^- diffusion under different electrical fields

References:

1. Chiti, F.; Dobson, C. M. *Annu Rev Biochem* **2006**, *75*, 333(b) Knowles, T. P. J.; Vendruscolo, M.; Dobson, C. M. *Nat Rev Mol Cell Bio* **2014**, *15*, 384.
2. Lepoitevin, M.; Ma, T.; Bechelany, M.; Janot, J. M.; Balme, S. *Advances in Colloid and Interface Science* **2017**(b) Wanunu, M. *Phys Life Rev* **2012**, *9*, 125.
3. Deamer, D.; Akeson, M.; Branton, D. *Nat Biotechnol* **2016**, *34*, 518.
4. Balme, S.; Coulon, P.-E.; Lepoitevin, M.; Charlot, B.; Yandrapalli, N.; Favard, C.; Muriaux, D.; Bechelany, M.; Janot, J. M. *Langmuir* **2016**, *32*, 8916.

Novel biosensing assay based on the integration of low refractive index resonant waveguide grating and upconversion nanoparticles

Y.-L. Gao,¹ J.-H. Lyu,¹ D.-T. Vu,¹ M. W.-Y. Chan,² L.-K. Chau,³ H.-C. Kan,¹ J.-Y. Lin,¹ C.-C. Hsu,^{1*}

¹National Chung Cheng University, Department of Physics, Chiayi, Taiwan, R.O.C.

²National Chung Cheng University, Department of Biomedical Sciences, Chiayi, Taiwan, R.O.C.

³National Chung Cheng University, Department of Chemistry and Biochemistry, Chiayi, Taiwan, R.O.C.

Abstract:

Highly luminescent 793 nm excited Nd³⁺-doped up-conversion nanoparticles (UCNPs) have shown great promise in bio-applications, benefiting from the high tissue penetration depth and low tissue overheating effect at 793 nm. Furthermore, as the Nd³⁺-doped UCNPs are deposited on a low refractive index (low-n) resonant waveguide grating (RWG) in aqueous environment, upconversion luminescence (UCL) generated from the UCNPs can be greatly enhanced thanks to the guided mode resonance (GMR) enhanced excitation field atop of the low-n RWG [1]. Therefore, the integration of UCNPs and low-n RWG can be a good platform for biosensing applications. Human cardiac troponin I (cTnI) is considered to be the gold standard for the diagnosis of myocardial infarction due to its presence only resulting from direct damage of myocardium. Herein, we synthesize Nd³⁺-doped UCNPs with multilayer core-shell structure (NaYF₄:Yb³⁺,Tm³⁺@NaYF₄:Yb³⁺,Nd³⁺@NaYF₄) as sensitive UCL bioprobes, and developed a sensitive extended sandwich-type strategy for the detection of cTnI with the help of GMR effect. The limit of detection was determined to be 2.5 fg/ml could meet the requirements for clinical application, and it can be used for early diagnosis of acute myocardial infarction.

Keywords: upconversion nanoparticles, low refractive index resonant waveguide grating, guided mode resonance, biosensing, human cardiac troponin I.

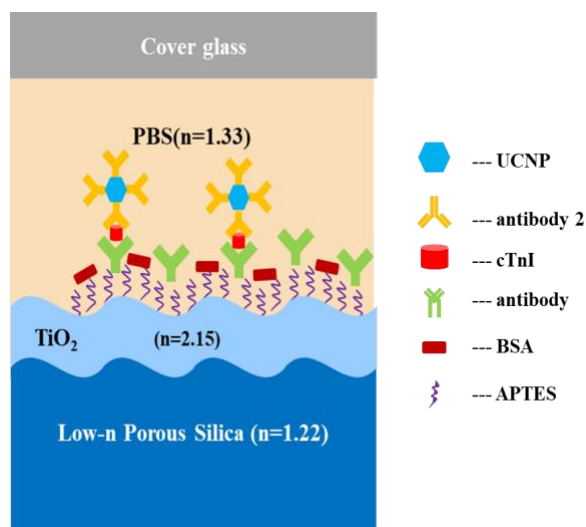


Figure 1: Schematic of sandwich type UCL based low-n RWG biosensing assay.

References:

1. Vu, D. T., Chiu, H. W., Nababan, R., Le, Q. M., Kuo, S. W., Chau, L. K., Ting, C. C., Kan, H. C., and Hsu, C. C. (2018) Enhancing upconversion luminescence emission of rare earth nanophosphors in aqueous solution with thousands fold enhancement factor by low refractive index resonant waveguide grating, *ACS Photonics*, 5, 3263-3271.

High-sensitivity wide-field fluorescent microscopy based on upconversion nanoparticles and resonant waveguide grating

T.-Y. Liu,¹ J.-H. Lyu,¹ M. W.-Y. Chan,² C.-C. Hsu,¹ H.-C. Kan,¹ J.-Y. Lin,¹

¹National Chung Cheng University, Department of Physics, Chiayi, Taiwan, R.O.C.

²National Chung Cheng University, Department of Biomedical Sciences, Chiayi, Taiwan, R.O.C.

Abstract:

Rare-earth (RE) lanthanide doped upconversion nanoparticles (UCNPs) can produce fluorescence that emits photons with frequencies higher than that of the excitation light via multi-photon transition process [1]. Since UCNPs mainly absorb near-infrared (NIR) light, auto-fluorescence and scattering can be suppressed and the photo-damage on biological cells can also be reduced. In addition, UCNPs are also with other advantages, e.g., good photo-stability, low photo-bleaching, high biocompatibility and water solubility and all these merits makes UCNPs suitable to serve as fluorescent tags to obtain high-contrast fluorescent imaging.

In this report, a novel type wide-field fluorescent microscopy using a low- n resonant waveguide grating (RWG) structure as a substrate and non-biotoxic UCNPs as fluorescent tags is successfully developed for observing high-resolution and high-contrast fluorescent images of bio-specimen. Resonant excitation of guided mode resonance (GMR) can form strong local fields on the top of RWG to enhance upconversion fluorescent emissions of the core/shell/shell UCNPs [2]. The nonlinear optical properties of UCNPs on RWG is fully characterized and the resonant condition of RWG excited by 793-nm laser is systematically optimized with the assistance of a spatial light modulator. UCF images of UCNPs are successfully taken via a home-built RWG-based upconversion fluorescence microscopy (UCFM) system with spatial resolution of ~ 230 nm, field of view of $\sim 86 \times 67 \mu\text{m}^2$, and image acquisition time of ~ 100 ms. Upconversion fluorescence (UCF) intensities of UCNPs at 450 nm and 475 nm are enhanced about 280 and 30 folds respectively when the low- n RWG is illuminated under resonant excitation condition (Figure 1). Periodic fringe pattern observed in UCF imaging under resonant excitation condition is ascribed to the strong local field distribution of the excitation light, which can be

applied to the development of structured illumination UCF microscopy.

Keywords:

rare-earth, upconversion nanoparticles, resonant waveguide grating, guided mode resonance, fluorescent microscopy

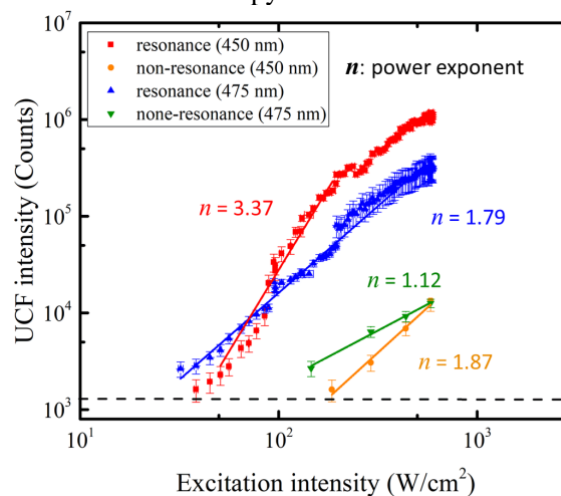


Figure 1: Excitation intensity dependence of 450 nm, 475 nm blue UCF emissions. Resonance represents oblique incidence at 16.1 degrees and non-resonance refers to normal incidence ($\theta = 0^\circ$) of the pump laser.

References:

1. Yang, L. W., Han, H. L., Zhang, Y. Y. and Zhong, J. X. (2009) White emission by frequency up-conversion in Yb^{3+} - Ho^{3+} - Tm^{3+} triply doped hexagonal NaYF_4 nanorods, *J. Phys. Chem.*, 113, 18995.
2. Lin, J. H., Liou, H. Y., Wang, C. D., Tseng, C. Y., Lee, C. T. Ting, C. C., Kan, H. C. and Hsu, C. C. (2015) Giant enhancement of upconversion fluorescence of $\text{NaYF}_4:\text{Yb}^{3+},\text{Tm}^{3+}$ nanocrystals with resonant waveguide grating substrate, *ACS Photonics*, 2, 530-536.

High-sensitivity detection of mesothelin by surface plasmon resonance

Erenildo F. Macedo, Dayane B. Tada*

¹ Federal University of São Paulo, UNIFESP, (Institute of Science and Technology), Sao Paulo, Brazil

Abstract

In this work, a new method with enhanced sensitivity was applied for detecting mesothelin by surface plasmon resonance (SPR) technique. This method was previously evaluated in the lectin detection and it is based on the functionalization of gold nanoparticles with an specific antibody followed by the incubation of these nanoparticles with a solution containing several types of molecules, including the molecule of interest. Then, the nanoparticles suspension was injected on a SPR biochip which contained different types of antibodies immobilized on the surface¹. This method was shown to be promissory in the analysis of proteins at very low concentration, which would be useful in the diagnosis of several diseases. Herein, this method was applied in the detection of mesothelin, which is an over-expressed protein in ovarian cancer and its cut-off point is 9 ng/mL (415 picomolar)^{2,3}. In order to detect mesothelin in a multi component solution at several concentrations, gold nanoparticles of 10 nm were functionalized with antibody anti-mesothelin and incubated with the solution for 30 min. Following, the solution was injected on a SPR biochip functionalized with antibody anti-mesothelin, BSA and antibody anti-CA 125 (negative controls). The results showed a detection limit of 35pM that was of great relevance demonstrating the efficiency of the sensor in detecting mesothelin at low concentration. This result demonstrated the potential of this method for future studies in detection of biomarkers, specially for cancer diagnosis.

Keywords: Surface Plasmon Resonance, biosensors, gold nanoparticles, enhanced sensitivity, mesothelin, biomarkers, ovarian cancer.

References:

1. Ferreira de Macedo, E., Ducatti Formaggio, D. M., Salles Santos, N., & Batista Tada, D. (2017). Gold Nanoparticles Used as Protein

Scavengers Enhance Surface Plasmon Resonance Signal. *Sensors*, 17(12), 2765.

2. Chang, M. C., Chen, Y. L., Chiang, Y. C., Chen, T. C., Tang, Y. C., Chen, C. A., ... & Cheng, W. F. (2016). Mesothelin-specific cell-based vaccine generates antigen-specific immunity and potent antitumor effects by combining with IL-12 immunomodulator. *Gene therapy*, 23(1), 38.
3. Hassan, R., Remaley, A. T., Sampson, M. L., Zhang, J., Cox, D. D., Pingpank, J., ... & Onda, M. (2006). Detection and quantitation of serum mesothelin, a tumor marker for patients with mesothelioma and ovarian cancer. *Clinical cancer research*, 12(2), 447-453.

Fast Detection of Bacterial Contamination in Fresh Produce Using Surface Modified Magnetic Nanoparticles and PCR

H.M.E. Azzazy¹, F. Farouk², S. Essam¹, A. Abdel Moteleb¹, R. El Shimy³, W. Fritzsche⁴

¹American University in Cairo, Department of Chemistry, New Cairo, Egypt

²Ahram Canadian University, Pharmaceutical Chemistrt Department ,Giza, Egypt

³National Organization for Drug Quality Control and Research, Giza, Egypt

⁴Leibniz Institute of Photonic Technology, Jena, Germany

Abstract:

Typical protocols for detecting bacterial contamination (*Salmonella typhi*, *Eschericia coli*, *Staphylococcus aureus*, *Klebsiella pneumoniae*, *Pseudomonas aerugenusa*, *Acenitobacter baumnii*) in food are lengthy encompassing initial bacterial enrichment on broth followed by plating and a subsequent molecular confirmation. This process requires at least 2 days. The aim of this work is to use modified magnetic nanoparticles (MNPs) for capturing bacteria followed by FTIR analysis, DNA extraction and PCR amplification for identification.

MNPs were synthesized and functionalized with oleic acid (OA) to impart surface hydrophobicity¹. The shape, size, crystallinity, and functionalization of OA-MNPs were characterized by TEM, SEM, zeta-sizer and FTIR. Strawberry samples were inoculated in broth media and incubated for 6 h at 37°C. MNPs were then added to the broth with gentel shaking for 3 min followed by collection using a magnet. Collected OA-MNPs (with immobilized bacteria) were Gram stained, FTIR scanned, and subjected to bacterial DNA extraction. Extracted DNA was assessed for purity, integrity, and quantity. PCR was performed using specific primers for *E. coli O157:H7* and *A. baumnii*.

The synthesized OA-MNPs were hydrophobic, spherical and crystalline with an average size of 5 – 15 nm. Microscopical examination of OA-MNPs (after Gram staining) revealed intact bacterial cells. The FTIR spectra of the immobilized bacteria were distinguishable from each other². A 2-3 fold increase in DNA extraction yield was achieved from immobilized bacteria compared to free ones; while maintaining the same purity. The extrctated DNA was amplified using *Rec A* or *STX 1/2* primers and yielded the specific amplicon bands for *A. baumnii* and *E. coli O157:H7*;

respectively. In conclusion, The developed protocol (Figure 1) can identify pathogenic bacteria contaminating strawberry in a short time (8 h) and enable a one working day decision on acceptability of fresh produce.

Keywords: Modified magnetic nanoparticles, Strawberry, PCR, Pathogenic bacteria.

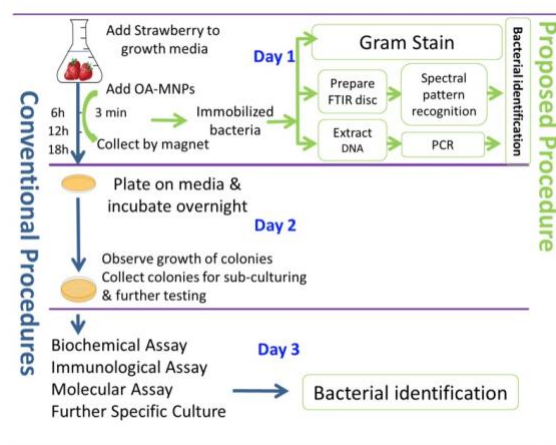


Figure 1: Proposed scheme for fast detection of pathogenic bacteria in fresh produce.

References

1. Shebl, R. I., Farouk, F., Azzazy, H. M. E. "Effect of Surface charge and hydrophobicity modulation on the antibacterial and antibiofilm potential of magnetic iron nanoparticles." *Journal of Nanomaterials* 2017 (2017). Article ID 3528295; <https://doi.org/10.1155/2017/3528295>.
2. Zarnowiec, P., Lechowicz, L., Czerwonka, G., Kaca, W. "Fourier transform infrared spectroscopy (FTIR) as a tool for the identification and differentiation of pathogenic bacteria." *Current medicinal chemistry* 22, no. 14 (2015): 1710-1718.

Acknowledgement

This work is funded by a grant from STDF, Egypt; GERF ID 23089.

NanoMatEn - Session II.D: Nanomaterials for Energy / Nanoelectronics

Inversion parameter in spinel Fe₃O₄/Mn₃O₄ core-shell nanoparticles at atomic resolution

P. Torruella,^{1,2} A. Ruiz-Caridad,^{1,2,3} M. Walls,³ A. G. Roca,⁴ A. López-Ortega,⁵ J. Blanco-Portals,^{1,2} L. López-Conesa,^{1,2,6} J. Nogués,^{4,7} S. Estradé,^{1,2} F. Peiró^{1,2}

¹LENS-MIND, Electronics and Biomedical Engineering Department, Universitat de Barcelona, E-08028 Barcelona, Spain

²Institute of Nanoscience and Nanotechnology (IN2UB), Universitat de Barcelona, Spain

³Laboratoire de Physique des Solides, Paris-Sud University, France

⁴Catalan Institute of Nanoscience and Nanotechnology (ICN2), CSIC and BIST, Campus UAB, Spain

⁵CIC nanoGUNE, Tolosa Hiribidea, 76, E-20018 Donostia-San Sebastián, Spain

⁶TEM-MAT, CCiT, Universitat de Barcelona, Spain

⁷ICREA, Pg. Lluís Companys 23, E-08010 Barcelona, Spain

Abstract:

In spinel oxides with AB₂O₄ structure, the A divalent cations usually occupy the tetrahedral positions (Th) and the B trivalent cations the octahedral (Oh) ones. This is just the opposite for inverse spinels as in Fe₃O₄. If some degree of inversion exists, the structure can be represented as (A_{1-x}B_x)[A_xB_{2-x}]O₄, where “()” denote Th positions in the structure and “[]” Oh positions, respectively, and x is the so called inversion parameter. The magnetic functional behavior of these oxides is highly dependent on the x value therefore, its measurement is of high relevance to understand the magnetic properties of these oxides. Conventional techniques such as x-ray and neutron diffraction refinement, Mössbauer spectroscopy, x-ray absorption or nuclear magnetic resonance can assess the coordination of chemical species with high precision, but without the spatial resolution required for complex systems such as core/shell nanostructures.

In this work, using scanning transmission electron microscopy (STEM) and near edge electron energy loss spectroscopy (EELS-ELNES), we calculate the cation inversion parameter of spinel oxides Fe₃O₄ and Mn₃O₄ in core/shell nanoparticle configuration with unprecedented spatial resolution [1]. First, we evaluate the oxidation state of transition metals by using the onset of the L3 peak [2], and the inversion parameter is determined from the L3 onset shift between octahedral and tetrahedral coordination sites. Alternatively, we carry out multivariate analysis (MVA) to reveal the 2+ and 3+ components and the corresponding score maps at atomic resolution. The cation inversion can then be estimated as the fraction of the 3+

ion signal in tetrahedral coordination positions. Both methods give results comparable to those from X-ray absorption on nanoparticle powder samples.

Keywords: spinel oxides, inversion parameter, electron energy loss spectroscopy, scanning-transmission electron microscopy.

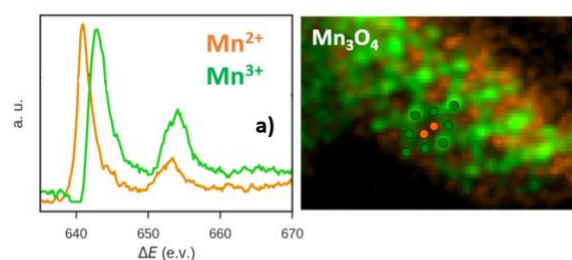


Figure 1: a) Spectral decomposition of the Mn L-edge with two main components corresponding to Mn²⁺ and Mn³⁺ species. The respective score maps are shown in b).

References:

1. Torruella, P., Ruiz-Caridad, A., Walls, M., Roca, A.G., Lopez-Ortega, A., Blanco-Portals, J., Lopez-Conesa, L., Nogués, J., Peiro, F., Estrade, S. (2018), *Nano Letters* 18, 5854-5861.
2. Tan, H., Turner, S., Yücelen, E., Verbeeck, J., Van Tendeloo, G (2011) *Phys. Rev. Lett.* 107, 107602.

Progress in nanoporous anodic alumina-based optical biosensors

L.F. Marsal^{1*}

¹Universitat Rovira i Virgili, Department of Electronic Engineering, Avda Paisos Catalans 26, 43007 Tarragona, Spain

Abstract

Nanoporous anodic alumina (NAA) is a nanostructured material suitable for developing complex and cost-effective biomedical applications like selective molecular separation, chemical/biological sensing, cell adhesion and culture, and drug delivery [1-2]. NAA is obtained by the electrochemical etching of aluminum and can be obtained in a self-ordered hexagonal pore distribution of parallel cylindrical nanopores with diameters between 10 and 300 nm [1-2]. Its geometric characteristics such as diameter, length and separation distance are controlled by the anodization conditions (voltage and time of anodization, temperature, and electrolyte concentration) [3-4]. Chemical resistance, thermal stability, and intrinsic photoluminescence are some of the outstanding properties of NAA [5]. Its highly effective surface area (hundreds of m^2/cm^3) makes of NAA an interesting platform for sensing and loading and releasing of active agents.

Here, we present some examples of NAA for advanced photonic structures for sensing applications [6]. The application of periodic variations of current or voltage during the anodization is transferred to the material as the periodic variation of the pore diameter with depth and consequently, to the periodic variation of the effective refractive index. In this way, we can engineer one-dimensional photonic crystals (1D-PC) with an enhanced optical response and stop bands tunable within the UV-VIS-NIR range. NAA 1D-PC biosensors were applied for the detection of substances of interest to the health and the environment like biomarkers or heavy metals. We deeply study the fabrication technological parameters that determine the properties of the optical response.

In addition, we demonstrated that the combination of NAA and selected aptamers can be used to prepare gated probes to detect specific substances. On these systems, the nanopores are loaded with a fluorescent reporter (rhodamine B) and functionalized with a short single-stranded DNA. The gated NAA was successfully applied to detect drugs, bacteria and fungus.

Acknowledgements: The Ministerio de Ciencia, Innovacion y Universidades (MICINN/FEDER) RTI2018-094040-B-I00, the Catalan authority AGAUR 2017SGR1527, and the ICREA Academia Award.

Keywords: nanoporous anodic alumina, optical properties, molecular gates, aptamer, photonic crystal, biosensor, biomaterials, biomedical applications.

References:

1. J. Ferré-Borrull, J., Pallarès, J., Macías, G., Marsal, L.F. (2014) Nanostructural engineering of nanoporous anodic alumina for biosensing applications, *Materials* 7, 5225.
2. Porta-i-Batalla, M., Xifré-Pérez, E., Eckstein, C., et al., (2017) 3D nanoporous anodic alumina structures for sustained drug release, *Nanomaterials* 7, 227
3. Santos, A., Formentín, P., et al., (2011) Structural engineering of nanoporous anodic alumina funnels with high aspect ratio, *J. Electroanal. Chem.* 655, 73 (2011).
4. Santos, A., Vojkuvka, L., Alba, M., Balderrama, V.S., et al., (2012) Understanding and morphology control of pore modulations in nanoporous anodic alumina by discontinuous anodization, *Physica Status Solidi (a)* 209, 2045.
5. Vojkuvkas, L., Santos, A., et al., (2012) On the mechanical properties of nanoporous anodized alumina by nanoindentation and sliding tests, *Surf. Coat. Technol.* 206, 2115 (2012).
6. Kumeria, T., Santos, A., Rahman, M.M., Ferré-Borrull, J. et al. (2014) Advanced structural engineering of nanoporous photonic structures: Tailoring nanopore architecture to enhance sensing properties, *ACS Photonics* 1, 1298 (2014).

Advanced Emerging Materials Applied in Next Generation Nano Electronic Devices

Hui-Lin Chang,^{1,2}

¹National Chiao Tung University, Department of Material Science and Engineering, HsinChu, Taiwan

²Micron Technology, Memory Development, Manassas, VA, USA

Abstract:

The integration of CNTs into Si-based metal-oxide-semiconductor field effect transistor (MOSFET) or new nanoelectronics remains a challenge in the fields of transistors and interconnections. CNTs are accepted as candidates for use in molecular electronics to overcome the physical limitation of current Si transistors and Cu interconnections [1-5]. Bundles of CNTs are naturally deposited in vertically direction, since they tend to adhere to each other vertically. The concept of the vertically aligned nanotube field-effect transistor (VCNTFET) has been proposed, to yield the characteristics of Si devices that will be required in the year of 2019, as set by the ITRS roadmap. The feasibility of realizing this vision depends on direct approaches to selective depositions in the trenches or holes of Si wafers. Bundles of CNTs in the trenches and holes can provide sufficient current density in the form of channels and conductors, respectively. In addition, CNTs orientation manipulation in either horizontal/vertical also plays key role for manufacturing. This study systematically elucidates the synthesis of CNTs by microwave plasma CVD (MPCVD). In this investigation, Fe catalyst and CoSi₂ film employed frequently as gate electrodes and a contact material in Si microelectronics are applied. The selective growth of CNTs in trench/hole/planar approaches is also examined. The morphology and nanostructures of CNTs are characterized. The field emission characteristics of CNTs deposited in the trenches and holes are investigated to determine electronic performance. Figure 1 shows the linkages among various carbon-based materials synthesized on Si wafers under the same microwave plasma chemical vapor deposition (MPCVD) system. The process parameters can be divided into three groups according to the structures of the synthesized materials, i.e. nanotube, nanowire and 2-D seaweed structure. The main parameters

include temperature, CH₄/H₂/N₂ gases, buffer layer application, additional Si source and patterning design for selective CNTs growth. With regard to the synthesis of catalyst-assisted carbon, wire/nanorod, and selective CNTs growth, three conditions, namely conditions 1, 2 and 3 were compared. Regard to the linkages of forming various kinds of carbon-based crystals and nanostructured materials, the following conclusions can be drawn: (1) The additional solid Si sources mainly contribute the Si component of Si-C-N crystals and nanotubes. Although some Si could be derived from the Si substrate, the solid Si columns ionized by plasma are highly active to participate in the reaction. (2) The nano-sized catalysts promote the formations of tubular, wire or rod morphology. The catalytic functions of the process environments without H₂ gas differ from those with H₂ gas. The catalysts are suggested to provide nucleation sites for Si-C-N crystal nucleation, and effectively reduce the energy of formation in the initial stage. The catalytic function is lost when the growing film covers the catalytic particle. In contrast, the role of the catalyst in forming Si-C-N tubes is similar to that described in the vapor-liquid-solid model. The tube grows by precipitating of graphite sheets from a super-saturated catalytic droplet. The formation of a curved graphite basal plane is energetically favorable, and so the tubular structure is formed. (3) The CH₄/H₂ ratio influences the formation of tubular and crystalline structures. A high ² CH₄/H₂ ratio favors the formation of C-sp bonding (graphite structure), whereas, a low ³ CH₄/H₂ ratio favors the formation of C-sp bonding (diamond structure). Therefore, carbon atoms surround and precipitate from catalysts with different CH₄/H₂ ratios form hollow tubes or solid nano-rods. (4) N₂ gas gives rise to

bamboo-like CNTs. Introducing N atoms into the carbon nanotube structure may induce distortion; change the bonding to that of pentagonal, heptagonal or other crystal lattices, and increase bending stress.

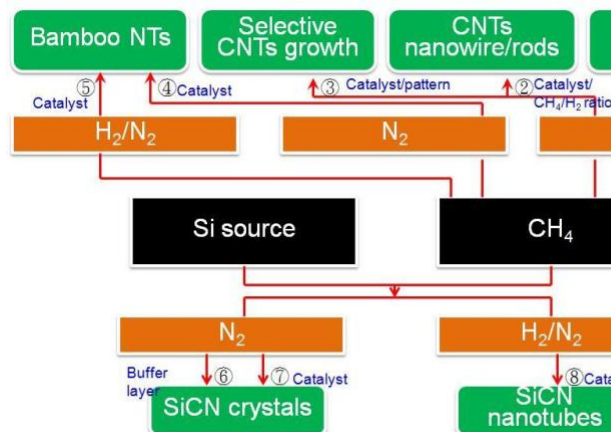


Figure 1: Figure 1 Process map of forming a variety of nanostructured materials

High Temperature Optical Metamaterials

M. Eich^{1,6}, M. Chirumamilla¹, P. Dyachenko¹, S. Lang¹, G. Shang¹, Q.Y. Nguyen², K. Knopp¹, G. Vaidhyanathan⁶, S. Molesky⁵, H. Renner¹, A. Yu Petrov^{1,5}, Z. Jacob⁴, M. Störmer,⁶ T. Krekeler⁷, M. Ritter⁷, G. Schneider²

¹Institute of Optical and Electronic Materials, Hamburg University of Technology, Eissendorfer Strasse 38, 21073 Hamburg, Germany

²Institute of Advanced Ceramics, Hamburg University of Technology, Denickestrasse 15, 21073 Hamburg, Germany

³University of Alberta, Department of Electrical and Computer Engineering, 9107 - 116 Street, T6G 2V4, Edmonton, Canada

⁴Birck Nanotechnology Center, School of Electrical and Computer Engineering, Purdue University, West Lafayette, IN 47906, USA

⁵ITMO University, 49 Kronverkskii Ave., 197101, St. Petersburg, Russia

⁶Institute of Materials Research, Helmholtz-Zentrum Geesthacht, Max-Planck-Strasse 1, 21502 Geesthacht, Germany

⁷Electron Microscopy Unit, Hamburg University of Technology, Eissendorfer Strasse 42, Hamburg 21073, Germany

Abstract

In order to tailor thermophotovoltaic emitters to match specific photovoltaic receivers we design and investigate spectrally selective high temperature stable emitters. We demonstrate selective band-edge emitters based on a W-HfO₂ refractive multilayer metamaterial stable up to 1400°C. Conditions for improved selectivity and thermal stability are discussed.

The stability of nanoscaled structured materials at very high temperatures is a scientific topic of fundamental importance in various fields of physical and materials sciences. Particularly, nanostructured emitters are considered to provide spectrally selective thermal emitters that avoid the emission of unwanted radiative energy in the infrared, thus, can efficiently convert thermal radiation into electricity in thermophotovoltaic devices. Since the emitted power scales with the fourth power of temperature and for better match with low band gap photovoltaic cells, very high temperatures well above 1000 °C become very important.

We propose a hyperbolic metamaterial for this purpose which changes its emission properties close to the topological transition of its isofrequency surface. At short wavelength the metamaterial has absorptivity close to one and thus efficiently absorbs and emits radiation. At longer wavelengths, beyond the topological transition, the thermally excited hyperbolic modes have large wavevectors and cannot leave metamaterial due to total internal reflection. To emit significant power at the wavelengths usable for photovoltaic conversion (below 2 μm) the far-

field emitter should be heated to high temperatures and thus should be thermally stable. We demonstrate selective band-edge emitters based on a W-HfO₂ layered metamaterial. The thicknesses of tungsten and hafnium oxide are 20 and 100 nm correspondingly. The metamaterial selectivity comes from the change in effective permittivity and does not rely on the phase matching condition. Thus the metamaterial exhibits almost angle independent selective emission. We present a detailed study of the thermal stability of this tungsten based thin film metamaterial at high temperatures and under various vacuum conditions. Elimination of the residual oxygen from the environment allows achieving unprecedented thermal stability up to 1400 °C without losing spectral functionality. We attribute this stability to a confined and edge-less geometry of thin tungsten films.

References

1. Dyachenko, P.N et al., *Nature Communications*, vol. 7, no. 11809, pp. 1–8, June 2016
2. Lang, S et al., *Scientific Reports*, vol. 7, no. 1, p. 13916–13916, October 2017
3. Leib, E.W et al., *Journal of Materials Chemistry C*, vol. 4, no. 1, pp. 62–74, January 2016
4. Biehs, S.-A. et al., *Physical Review Letters*, vol. 115, no. 17, p. 174301–174301, October 2015
5. Dyachenko, P.N. et al., *Optics Express*, vol. 23, no. 19, pp. A1236, August 2015
6. Chirumamilla, M. et al., *Nano Energy*, submitted 2018

Plasma Engineered Nanocomposite and Amorphous Films and Coatings for Energy Industries

Ronghua Wei, Ph.D. Program Director

Southwest Research Institute[®], San Antonio, Texas, USA

Abstract:

In this lecture, the research conducted at Southwest Research Institute[®] (SwRI[®]) in plasma surface engineering (PSE) is reviewed. In particular, thick nanocomposite and amorphous films and coatings are produced using PSE technologies for use in severe environments against erosion, abrasion, corrosion, or deposit of paraffin or scaling that are often encountered in energy industries including the oil and gas industry and the power generation industry. The nanocomposite films and coatings produced using a Plasma Enhanced Magnetron Sputtering (PEMS) technology have a nanocomposite microstructure. It is composed of nanocrystalline MeC_xN_{1-x} (Me=Ti, Zr, Cr, Al, V, etc. or a combination, thereof) with the grain size of 4-10 nm in a matrix of amorphous SiC_yN_z. The unique microstructure renders super-hardness with high fracture toughness. As a result, the coatings are able to withstand severe erosion and abrasion against sand, slurry, and liquid droplets. Due to the advantages of the PEMS technology, thick nanocomposite coatings over 500μm have been produced for a durable life time. These coatings have been applied to parts used in the oil and gas industry such as drill head inserts, mud pump plungers, ball valves and seats. They are also used in the power industry on valve stems and seats against both erosion and corrosion. On the other hand, the amorphous Diamond-Like Carbon (DLC) films produced by Plasma Immersion Ion Deposition (PIID) technology exhibit a very dense amorphous microstructure and are used for the oil and gas industry for corrosion protection. In addition, due to their inherent low surface energy nature they are used against icing, scaling, waxing and asphaltene accumulation for downhole tooling, oil tubular goods and heat exchangers. SwRI has developed the PIID technology for depositing the inner surface of 2X12m long pipes, and a total of over 50km length of these pipes have been installed worldwide.

In this paper we review the methods for preparing these coatings, discuss their microstructural, physical, mechanical and tribological properties, and present examples for practical applications. A few processes of these PSE technologies have been transferred to industries for production coating of their components.

Keywords: Plasma Surface Engineering, Nanocomposite films and coatings; Erosion, abrasion and corrosion protection; Energy Industries.

Effect of UV illumination on Surface Adsorbents in MoTe₂ Channel for Gas Sensing Applications

Kyle DiCamillo^{1*}, Asha Rani^{2*}, Sergiy Krylyuk^{3,4}, Albert V. Davydov³,
Mona E. Zaghoul² and Makarand Paranjape¹

¹Department of Physics, Georgetown University, Washington, DC 20057, USA.

²School of Engineering and Applied Science, The George Washington University, Washington, DC 20052, USA

³Materials Science and Engineering Division, National Institute of Standards and Technology, Gaithersburg, MD 20899, USA

⁴Theiss Research, Inc., La Jolla, CA 92037 USA

*These authors contributed equally to this research.

Abstract:

The effect of UV illumination on MoTe₂ channel is investigated for NO₂ and NH₃ sensing response. MoTe₂ crystals are grown via chemical vapor transport and mechanically exfoliated into few layer flakes for FET fabrication. The MoTe₂ FET devices used for this work showed p-type conducting behavior at gate biases between -60V to 60V. The sensitivity of both NO₂ and NH₃ gas improves under the influence of UV light. Photoresponse of fabricated MoTe₂ devices were tested but found to have unexplained drops in current following UV light exposure. A spike in current is observed after UV exposure followed by gradual decrease until it approaches saturation below the dark current, which is attributed to the release of surface adsorbates (such as oxygen and hydroxyl groups) which are known to dope MoTe₂ p-type. Passivation of the surface with a 10 nm Al₂O₃ film prevents changing of surface adsorbents and subsequently was found to eliminate the current drop under UV illumination. It was also found that passivation led to the device switching from p-type to n-type. This is believed to be due to the loss of surface adsorbates during the deposition of the Al₂O₃ film. Following the realization that the device behavior is heavily modified by surface adsorbents, variation of carrier gas between N₂ and dry breathing air is used during sensing tests. It is found that choice of carrier gas has a large effect on sensing performance for both NO₂ and NH₃ sensing. NO₂ sensing is found to yield better results using N₂ carrier gas while NH₃ sensing is found to yield better results using dry breathing air as the carrier gas.

Keywords: molybdenum ditelluride, two-dimensional materials, nanomaterials, surface

effects, UV illumination, passivation, aluminum oxide, gas sensing applications.

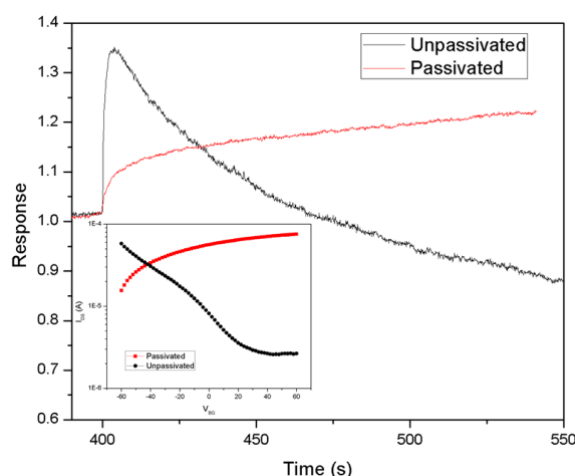


Figure 1: The response vs time for an MoTe₂ device before passivation (black curve) and after passivation (red curve). The inset shows the transfer characteristics of the same device before passivation (black curve) and after passivation (red curve).

References:

1. Chang, Y., Yang, S., Lin, C., Chen, C., Lien, C., Jian, W., Ueno, K., Suen, Y., Tsukagoshi, K., Lin, Y. (2018) Reversible and Precisely Controllable p/n-Type Doping of MoTe₂ Transistors through Electrothermal Doping, *Adv. Materials*, 30(13).

Plasmonic nano-gaps for light matter interactions on the nanoscale

Addison R. L. Marshall¹, Abdullah O. Hamza¹, Anthony P. Edwards¹, Francesco N. Viscomi¹, John E. Proctor^{1,2}, Johannes Gierschner³, Jean-Sebastien G. Bouillard^{1,4,5}, and Ali M. Adawi^{1,4*}

¹Department of Physics and Mathematics, University of Hull, Cottingham road, HU6 7RX, UK

²Materials and Physics Research Group, School of Computing, Science and Engineering, University of Salford, Manchester M5 4WT, United Kingdom

³Madrid Institute for Advanced Studies - IMDEA Nanoscience Calle Faraday 9, Ciudad Universitaria de Cantoblanco, 28049 Madrid, Spain

⁴G. W. Gray Centre for Advanced Materials, University of Hull, Cottingham road, HU6 7RX, UK

*a.adawi@hull.ac.uk

Abstract:

In this work we report on the design and fabrication of plasmonic nano-gaps consisting of a silver nanoparticle coupled to an extended silver film for the enhancements of the spontaneous emission, Förster resonance energy transfer and Raman scattering.

In the first part of this talk we show using FDTD calculations plasmonic nano-gaps are able to modify the spontaneous emission rate by more than a 100 times and the quantum efficiency of low quantum yield materials by 30 times [1]. Experimental studies on a range of representative structures confirm our modelling and reveal that such structures can modify the emission intensity by a factor of 30 times over the visible range.

In the second part of this talk we show theoretically and experimentally how plasmonic nano-gaps can be utilised to enhance Förster resonance energy transfer. In particular we considered nanoparticles of diameters 100 and 200 nm to form nano-gaps of width 30 nm doped with the molecular dyes Uranin and Rhodamine 6G as the donor-acceptor pair. We have found that the FRET rate can be enhanced by a factor of 3.6 times associated with retained FRET efficiency compared to vacuum. Further to that our work show that FRET rate in this type of nano-gaps is linearly dependent on the LDOS. These results are combined with 5 times enhancement in the emission rate of the acceptor and 14 times enhancement in its brightness as compared to structures without nano-gaps.

In the last part of this talk we present our results on the design and fabrication of plasmonic nano-gaps for single molecule Surface-Enhanced Raman Scattering (SERS) spectroscopy. Our calculations revealed that the enhancement in the SERS signal is mainly associated with the dipolar mode of the nano-gap and strongly affected by the particle size

which was found to be in direct agreement with our SERS measurements. Concentration dependent SERS measurements from our optimized nano-gaps doped with molecular dye Rhodamine 6G showed clear differences in the relative SERS peaks intensity at concentrations of 2×10^{-7} M compared to the SERS spectra measured from gaps doped with the same dye at higher concentrations 2×10^{-5} M. Those differences are attributed to the random orientation of the single molecular dye in the plasmonic gap, therefore highlighting the single molecule sensitivity of the optimised nano-gaps. In the single molecule regime, the SERS signal is dependent on the molecule orientation with regards to the field in the plasmonic nanostructure. The dipole moment derivative of the various Raman modes of the analyte were determined using DFT (Density Function Theory) calculations, and by convoluting this information with the known dipole moment of the plasmonic nanogap, we were able to recover the orientation of the single molecule within the nanogap [2].

Keywords: Spontaneous emission rate, Förster resonance energy transfer, Raman, SERS, FDTD, DFT, Plasmonic nano-gap.

References:

1. Anthony P. Edwards and Ali M. Adawi, J. Appl. Phys. 115, 053101 (2014)
2. Addison R. L. Marshall, Jamie Stokes, Francesco N. Viscomi, John E. Proctor, Johannes Gierschner, Jean-Sebastien G. Bouillard and Ali M. Adawi, Nanoscale 9, 17415–17421 (2017)

Tuning Fermi level pinning at metal/solid 2D/ Si heterostructure

J. Courtin,^{1,*} S. Le Gall,² P. Chrétien,² A. Moréac,¹ S. Tricot,¹ G. Delahye,¹ B. Lépine,¹ S. Ababou-Girard,¹ S. Guézo,¹ F. Solal,¹ P. Turban,¹ P. Schieffer,¹ J.-C Le Breton,¹

¹ Département Matériaux et Nanosciences, Institut de Physique de Rennes, Campus de Beaulieu, Bât 11E, Rennes, France

² Laboratoire de Génie électrique de Paris 11, rue Joliot Curie Plateau de Moulon 91192 Gif sur Yvette Cedex

Abstract:

The realization of metal/semiconductor contact with the low Schottky Barrier Height (SBH) represents a major interests for conventional and spin electronics. In fact, a low Schottky barrier height allow to realize ohmic-like contact on semiconductor therefore allow to reduce interface resistanc. Concerning spintronics the reduction of Shcottky barrier height improve the spin polarized current into semi-conductor.

However, Metal-Induced-Gap-States (MIGS) at silicon metal interface leads to Fermi level pinning close to valence band, therefore the SBH is large. Insertion of 2D materials at interface could resolve this problem.

We studied by x-ray photoemission spectroscopy and electrical characterisation (I(V) and C(V)) the electronic properties of metal/2D solid/Silicon interface. By these methods we have shown that adding graphene at the interface induces a high reduction of Schottky barrier height compared to Metal/Silicon intimate contacts [figure 1]. This large reduction of SBH allow to reduce interface resistance and to obtain an ohmic-like contact [figure 2]. In particulary we found that Fermi level is fully unpinned at graphene/Silicon interface, allowing to modulate the SBH by modification of graphene work function.

Keywords: silicon, graphene, boron-nitride, semi-conductor spintronic.

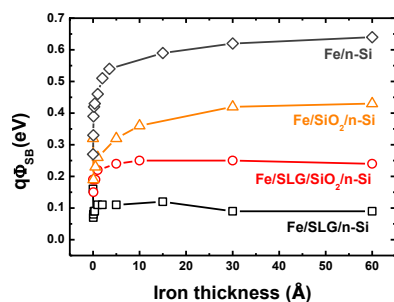


Figure 1: Schottky barrier height as a function of iron thickness determined by photoemission.

These measurements have been realized with silicon doping at 10^{16} cm^{-3}

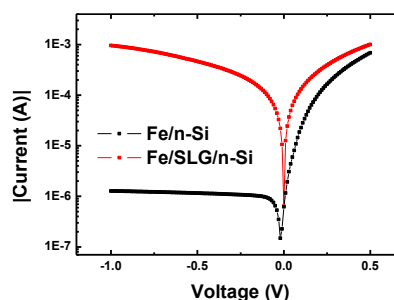


Figure 2: Current as a function of applied voltage with (red) and without graphene (black) at interface.

References:

1. S. Sze et K. K. Ng, « Metal-Semiconductor Contacts », in *Physics of Semiconductor Devices*, John Wiley & Sons, Ltd, 2006, p. 134- 196.
2. J. D. Albrecht et D. L. Smith, « Electron spin injection at a Schottky contact », *Phys Rev B*, vol. 66, n° 11, p. 113303, sept. 2002.
3. W. Mönch, « Barrier heights of real Schottky contacts explained by metal-induced gap states and lateral inhomogeneities », *J. Vac. Sci. Technol. B Microelectron. Nanometer Struct. Process. Meas. Phenom.*, vol. 17, n° 4, p. 1867- 1876, 1999.

Influence of Plate Acoustic Waves on Electronic Transport in Low Dimensional Nanostructures

V. Kolesov,¹ I. Kuznetsova,^{1,*} E. Soldatov,² A. Melnikov,² S. Dagesyan,²

¹ Kotelnikov Institute of Radio Engineering and Electronics of RAS, Moscow, Russia

² Lomonosov M.V. Moscow State University, Physics Department, Moscow, Russia

Abstract:

The acoustoelectric effect is the generation of an acoustoelectric current in a non-biased device by a piezoactive acoustic wave [1]. This effect has recently attracted the attention of researchers as a possible method to control the motion of massive objects in the quantum regime [2]. We suggest to use this effect for development of high sensitive nanoelectronic sensors. The sensitivity could be increased through the use of modulation mode of operation based on the acoustic pilot signal and the transition from quasi-stationary measurement to measurement at the modulation frequency. We have produced an acoustic delay line (DL) based on shear-horizontal acoustic wave of zero order (SH_0) with a resonant frequency of 2.77 MHz in Y-X lithium niobate plate. The DL consists of two interdigital transducers with 5 pairs of strips. The nanostructure presented in Figure 1 was placed in the center between the IDTs. The volt-ampere characteristics of this nanostructure in the presence and at the absence of the acoustic wave are presented in Figure 2. The analysis has shown that the presence of a piezoactive acoustic wave influences the electric current in a nanowire. We will provide a theoretical analysis of the obtained results. The work is partially supported by RSF 18-49-08005 in the frame of development of a hybrid acousto-nanoelectronic device and RFBR grant 19-07-01091 in the frame of development of a tunnel nanostructure.

Keywords: acoustoelectric effect, nanowire, volt-ampere characteristics, shear-horizontal acoustic wave, lithium niobate plate, sensor applications.

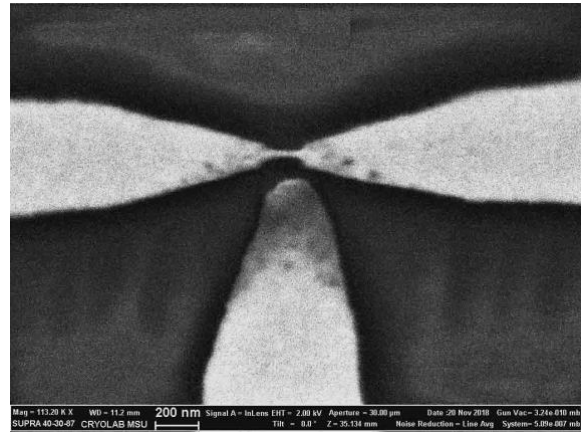


Figure 1: SEM image of the nanostructure.

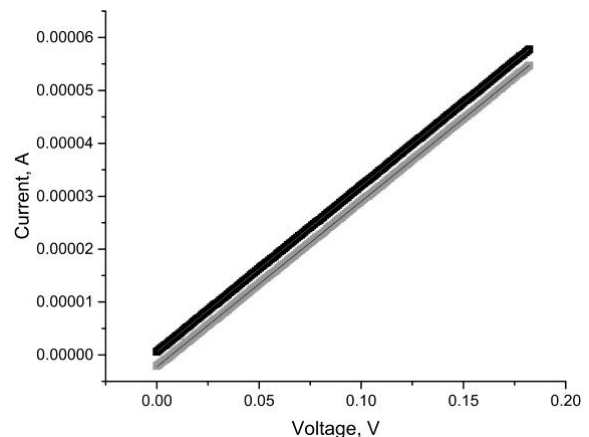


Figure 2: Volt-ampere characteristics of the produced nanostructure at the absence (black line) and in the presence (grey line) of the piezoactive acoustic wave.

References:

1. Entin-Wohlman, O., Levinson, Y., Galperin, Yu. (2000) Acoustoelectric effect in a finite-length ballistic quantum channel, *ArXiv*, cond-mat/0004428v1.
2. Chu, Y., Kharel, P., Renninger, W., Burkhardt, L., Frunzio, L., Rakich, P., Schoelkopf, R. (2017) Quantum acoustics with superconducting qubits, *Science*, 10.1126/science.aao1511.

Towards the Optimized Spintronic Response of Sn-Doped IrO₂ Thin Films

E. Arias-Egido,^{1,2*} M. A. Laguna-Marco^{1,2}, C. Piquer^{1,2}, R. Boada^{3,4},
and S. Díaz-Moreno⁴

¹Instituto de Ciencia de Materiales de Aragón, CSIC - Universidad de Zaragoza, Zaragoza, Spain

²Departamento de Física de la Materia Condensada, Universidad de Zaragoza, Zaragoza, Spain

³Universitat Autònoma de Barcelona, Department of Chemistry, 08193 Bellaterra (Barcelona), Spain

⁴Diamond Light Source Ltd, Harwell Science and Innovation Campus, Didcot, Oxfordshire OX11 0DE

Abstract:

IrO₂ has been proposed as the most promising material as spin-current detector.^[1] In order to explain and optimize the initial results observed by Fujiwara et al.,^[1] we prepared for the first time Sn-doped IrO₂ thin films, Ir_{1-x}Sn_xO₂ (x = 0–0.6), in the amorphous and polycrystalline states, by reactive magnetron co-sputtering. Choosing Sn as the dopant element is especially interesting, since SnO₂ presents an insulating behavior and, like IrO₂, it grows in the rutile structure. The only difference is an increase in the volume cell, which makes it easier for Sn to occupy Ir sites without any drastic structural change. The electrical response and strength of the spin-orbit coupling (SOC), both key properties involved in the spin-detection process, were carefully studied in order to better understand and tailor its performance as spin current detector material.

Overall, our work prove that the resistivity of IrO₂ can be tuned over several orders of magnitude by controlling the doping content in both the amorphous and the polycrystalline state. In addition, growing amorphous samples increase the resistivity, thus improving the spin-current to charge-current conversion. As far as the SOC is concerned, the system not only remains in a strong SOC regime but it seems to undergo a slight enhancement in the amorphous state, as well as in the Sn-doped samples.

Consequently, it points to a clear new direction/approach in the quest of optimized materials for spin current detection.^[2, 3] From the industrial application point of view, the good results obtained in the amorphous Ir_{1-x}Sn_xO₂ samples are especially relevant as they are easier to fabricate. Besides, taking into account the high price of Ir, Sn-doping also considerably reduces costs.

Keywords: iridates, spintronics, electrical properties, resistivity, spin-orbit coupling, thin films, co-sputtering.

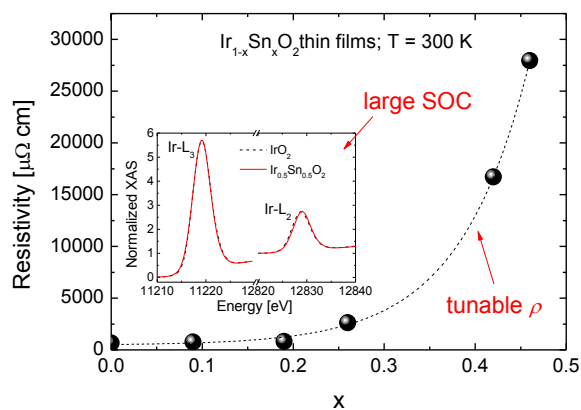


Figure 1: The electrical resistivity of the Ir_{1-x}Sn_xO₂ compound is proved to be tunable over several orders of magnitude, while the system remains in a strong SOC regime. Therefore, the two key properties involved in the spin-detection process are optimized.

References:

1. K. Fujiwara, Y. Fukuma, J. Matsuno, H. Idzuchi, Y. Niimi, Y. Otani, H. Takagi, *Nat. Commun.* 4, 2893, 2013.
2. K. Ando, E. Saitoh, *Nat. Commun.* 3, 629, 2012.
3. L. Vila, T. Kimura, Y. Otani, *Phys. Rev. Lett.* 99, 226604, 2007.

High concentration bolometric system with single-walled carbon nanotubes (SWCNT) absorber

Maranatha Andalis,¹ May Angelu Madarang,¹ Yuki Kuwahara,² Gail Tolentino,¹
Ralph Adrian Paragas,¹ Anfernee Harry Triol,¹ Mark Ilasin,¹ Takeshi Saito,² Ian Jasper Agulo,^{1,*}

¹Micro and Nano Innovations Laboratory, Department of Physical Sciences, College of Science,
University of the Philippines Baguio, Baguio City 2600, Philippines

²Nanomaterials Research Institute, National Institute of Advanced Industrial Science and Technology
(AIST), 1-1-1, Higashi, Tsukuba, Ibaraki 305-8565, Japan

Abstract:

We demonstrate a single-walled carbon nanotube (SWCNT)-based microbolometer with enhanced optical properties due to focused current-bias between two electrodes. The Au electrodes were deposited on an oxidized silicon substrate. The single-walled carbon nanotubes (SWCNT), synthesized using Enhanced Direct Injection Pyrolytic System (eDIPS) [1], were placed between two Au electrodes between the pointed tips with a gap of approximately 10 μm . The SWCNT was ascertained from Raman spectroscopy and optical absorption spectroscopy (OAS). The morphology and the thickness of the SWCNT film was estimated from atomic force microscopy.

We obtained a bolometer figure-of-merit temperature coefficient of resistance (TCR) of greater than -2.5% by measuring current-voltage (IV) characteristics from 20 $^{\circ}\text{C}$ to 100 $^{\circ}\text{C}$. An optical response of 580 V/W was obtained from a 5 mW 783 nm laser. The corresponding thermal time constant of 2.43 ms was estimated through the optical response from the modulation of the laser over a frequency range of 1 Hz to 1 kHz. From measurements of the voltage response vs temperature, we were able to estimate a thermal conductance, 0.23 $\mu\text{W}/\text{K}$, due to the oxide layer acting as a very good thermal isolation. The optical noise equivalent power (NEP) and optical detectivity of $4.81 \times 10^{-11} \text{W}/\sqrt{\text{Hz}}$ and $4.61 \times 10^8 \text{cm} \cdot \sqrt{\text{Hz}}/\text{W}$, respectively, were estimated from the responsivity, the spectral density, and area of the cell of the absorber, $4.9 \times 10^{-4} \text{cm}^2$.

We attribute the exceptional performance of the SWCNT microbolometer due to the increased current density between the tips of the electrode.

Keywords: zinc oxide; graphite; photocatalysis; solid-state reaction; time-resolved photoluminescence; time-integrated photoluminescence

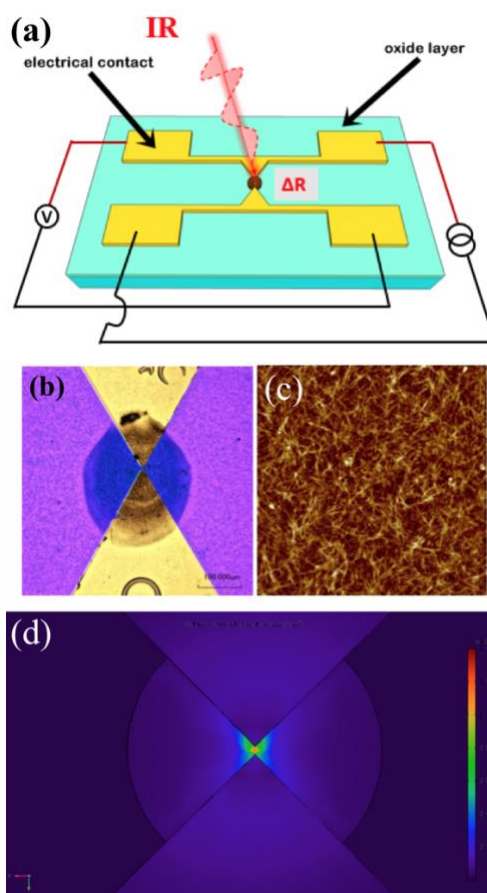


Figure 1: (a) Schematic diagram of the IR device. (b) Deposited CNT (blue) between the two tips of the electrodes (yellow) and the (c) AFM image of the SWCNT. (d) FEM simulation depicting the increased current density at the tips resulting to the enhanced bolometric response.

Reference:

1. Saito, T. Ohshima, S., Okazaki, T., Ohmori, S., Yumura, M., Iijima (2008), Selective diameter control of single-walled carbon nanotubes in the gas-phase synthesis, *J. Nanoscience and Nanotechnology*, 8, 6153-6157.

Theoretical study of the electronic flow between two metals through an insulator and under illumination: Applications at the nanoscales

M. Grosman, D. Duche, C. Reynaud, F. Michelini, JJ. Simon, and L. Escoubas

Aix Marseille Université, CNRS, Université de Toulon, UMR 7334 – IM2NP (Institut des Matériaux, de Microélectronique et des Nanosciences de Provence)

Abstract:

The purpose of this study is to derive a general formula for the electronic flow between two metals through an insulator and under illumination using a model based on photon assisted tunneling [1, 2, 3, 4]. We discuss the limitations of this model at the nanoscales, in particular when considering a Metal Insulator Metal (MIM) diode. When two electrodes are separated by a thin insulating film or by a molecule, and if the film is thin enough, an electron can flow between the two electrodes by tunnel effect. Schrödinger equations can be solved using a mode-space approach, which consists in separating the transport direction and the transverse confinement direction. Indeed, appearance of transverse modes is crucial to settle on the nanodevice working, which is of importance when considering a molecular or nano-electronic device. To the best of our knowledge, no electron transport model is available in the case of illumination.

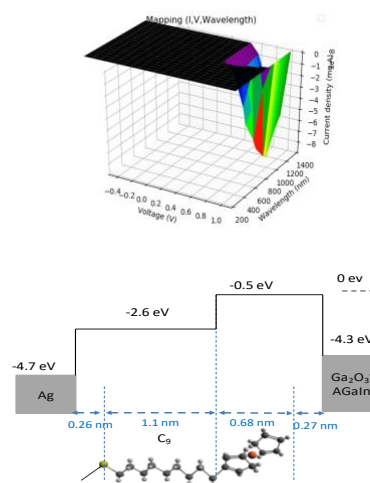
In our study, we assume a transfer Hamiltonian of the form $H = HL + HR + HT$, where HL and HR stands for the left and right electrode Hamiltonians respectively, and HT generates transitions between HL and $HR(t)$. $HR(t)$ describes the time-dependence of the right electrode under illumination. Then the resolution of the Schrödinger's equation is performed in cylindrical configuration. The results demonstrate an energy quantization and the appearance of transversal modes. Thus, the figure 1a shows the current flow between two metal electrodes through a 2 nm long insulating molecule considered as a 1 nm radius cylinder: one transversal mode is clearly visible and exhibits a region of high performances, and the figure 1b presents the energy level diagram of the considered nano-device.

In our model, the influence of the layer and the van der Waals interface on the current are

ignored and we suppose a 1nm cone - shaped tip contact. Our model is of interest for self-assembled molecular (SAMs) diodes where no lateral interaction occurs between the molecules, as for example ferrocenyl-alkanethiol based SAMs diodes showing high rectification ratios [5].

Keywords : nanoscale, diode, current flow, quantum, cylindrical configuration, photon assisted tunneling.

Figure: (a) Mapping of the current flow (in mA) through a 2nm long insulating molecule considered as a cylinder of “1” nm radius, versus the wavelength (in nm) of the incident light and the voltage applied between the two metallic electrodes. (b) Energy level diagram at open circuit used in our simulation.



References:

1. JG. Simmons, Generalized formula for the electric tunnel effect between similar electrodes separated by a thin insulating film. J Appl Phys. 1963
2. F. Grossmann, T. Dittrich, P. Jung, P. Hanggi, Phys. Rev. Lett. 67 (1991) 516

3. C. Cohen Tannoudji, B. Diu, F. Laloe, *Mécanique quantique*, Hermann, 1997
4. G. Platero et al, Photon-assisted transport in semiconductor nanostructures C.W.J. Beenakker, 2004
5. C. A. Nijhuis, et al, Mechanism of Rectification in Tunneling Junctions Based on Molecules with Asymmetric Potential Drops, *JACS*, 2010

Use of nanocarbons to provide ultra-fast charging of electric vehicles at 350kW to 1MW, so that drivers have the same experience of speed of recharge, cost and range as gasoline or diesel vehicles

Stephen Voller C.Eng
CEO & Founder ZapGo Ltd, Oxford, UK

Abstract

Gasoline (petrol) and diesel vehicles can be refueled in 5 minutes, and then travel 500 km or more. ZapGo has developed new energy storage technology capable of delivering the same driver experience in a battery electric vehicle, but without the need to upgrade the national grid infrastructure. ZapGo Ltd (Zap&Go) is a high technology business founded in Oxford, UK, in 2013. ZapGo has developed a solution to the problems encountered by all the current generation of appliances, devices and vehicles powered by lithium: slow charging. Called Carbon-Ion™ (C-Ion®), in contrast to Lithium-ion, this technology is based on carbon nano-materials. The technology and a growing patent portfolio is in part derived from Oxford University, and in part developed independently by Zap&Go's own scientists. The C-Ion cells are manufactured in China and Zap&Go is currently supplying grid energy storage solutions from their operations in Charlotte, NC in USA.

of the Guild of Entrepreneurs in the City of London.

Biography

Stephen Voller C.Eng is an experienced business leader and a recognised authority on energy storage technologies. He is the inventor of Carbon-Ion and he founded ZapGo Limited in 2013 to produce the next generation of energy storage devices based on this technology platform, with four core values: to be faster charging, safer, longer lasting and more recyclable than lithium batteries. Stephen has taken several technology businesses through concept, design and then into production. He launched the first ever CE-marked hydrogen fuel cell product. He previously ran a \$1bn business unit at IBM. He is a member of the Institute of Electrical and Electronic Engineers (IEEE) and is a Freeman

A high output flexible triboelectric nanogenerator based on polydimethylsiloxane/three-dimensional bilayer graphene composites

Dae Joon Kang

Department of Physics, Sungkyunkwan University, 2066, Seobu-ro, Jangan-gu, Suwon, Gyeonggi-do 16419, Republic of Korea

Abstract:

Ever since Wang *et al.*, reported a flexible triboelectric nanogenerator (FTENG) based on two different types of thin polymer, in 2012, for the first time,¹ extensive worldwide effort has been devoted to fabricating high output performance FTENG since it can convert mechanical energies (such as wind energy, human body activity, and water waves, etc) into electrical energy². In this study, the polydimethylsiloxane/three-dimensional bilayer graphene (PDMS/3D BLG) composites were successfully fabricated using carbon cloth (CC) as a low-cost flexible 3D substrate by a facile synthetic strategy. The Au/PET and PDMS/3D BLG/CC composites were employed as the top and bottom electrodes to fabricate flexible triboelectric nanogenerators (FTENG), demonstrating such FTENG have excellent output performance, evidenced by the maximum peak-to-peak output voltage, peak-to-peak current density, and output power density reaching up to 70 V, 9.3 $\mu\text{A cm}^{-2}$, and 0.65 mW cm^{-2} , respectively. Moreover, after 1000 bending cycles, the output performance of the FTENG retains 94.6% of the initial output performance, indicating its excellent flexibility. More importantly, such FTENG is able to instantaneously power up to 28 and 94 green light-emitting diodes (LEDs) with the device size of 1 x 3 cm^2 and 1 x 3 cm^2 , respectively as shown in Figure 1. These outstanding results demonstrate that the PDMS/3D BLG/CC composites are a promising candidate for flexible high

performance and wearable energy harvesting system.

Keywords: Triboelectric nanogenerator, 3D bilayer graphene, polydimethylsiloxane, carbon cloth, LEDs, flexible energy harvesting system.

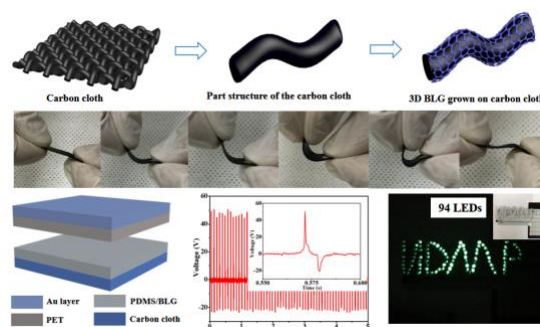


Figure 1: PDMS/ZnO/3D Gr/Ni foam based-hybrid energy harvester. The open-circuit voltage and short-circuit current density of the FTENG during repetitive compressive motions under the driving frequency of 3 Hz and various compressive forces after 1000 bending cycles.

References

1. F. R. Fan, Z. Q. Tian, Z. L. Wang, Flexible triboelectric generator, *Nano Energy*, 1 (2012) 328-334.
2. A. Jang, E. K. Jeon, D. Kang, G. Kim, B. Kim, D. J. Kang, H. S. Shin, Reversibly light-modulated dirac point of graphene functionalized with spiropyran, *ACS Nano*, 6 (2012) 9207-9213.

Control of thermal sensitivity stability of a hybrid magnetoresistive sensor using Zeeman energy

Mohamed Mahfoud,^{1,2} Quang Hung Tran,³ El Habib Belarbi,² Abdel Aziz Boukra,⁴ CheolGi Kim,⁵ and Ferial Terki¹

¹ Institut Charles Gerhardt Montpellier, UMR 5253, Université de Montpellier France

² Synthesis and Catalysis Laboratory LSCT, Tiaret University, Tiaret, Algeria

³ Sensors R&D&C, eV-Technologies, 14000 Caen, France

⁴ Laboratoire de Structure, Élaboration et Application des Matériaux Moléculaires, SEA2M, Université Abdelhamid Ibn Badis, Mostaganem, Algérie

⁵ Department of Emerging Materials Sciences, DGIST-Daegu Gyeongbuk Institute of Science and Technology, Daegu 42988, South Korea

Abstract:

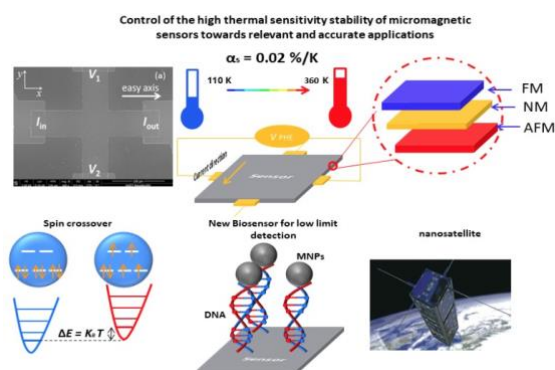
In the wide range of magnetic sensor applications, the thermal stability of sensor sensitivity is a crucial parameter that must be precisely controlled to get reliable measurements. In particular space¹, automotive², and bio-sensing³ applications where the temperature could strongly varies from 4 K to 473 K. Therefore, characterization of the magnetic properties of nano-materials^{4,5} give rise to precious information that could be decisive. Here we present a novel method to stabilize the sensitivity of an ultrahigh sensitive planar Hall effect (PHE) sensor by controlling Zeeman energy, in a wide temperature range from 110 K to 360 K. This thermal stability of the sensor sensitivity has been understood through the keys physical parameters such as the anisotropic resistivity, the magnetization easy axis, the exchange bias field and the coercivity field. Using this controlling method we optimized the thermal stability of our PHE sensor down to 0.02 %/K, which is very high thermal stability compared to others such as a PHE sensor without any controlling method (0.1%/K); giant magnetoresistance sensor (-0.18 %/K) and an anisotropic magnetoresistance sensor (-0.32 %/K)⁶.

Figure 1. Novel method to stabilize the sensitivity using Zeeman energy for highly precise measurements.

Keywords: thermal stabilization, sensitivity, Zeeman energy.

References:

1. Cochrane, C. J. *et al.* (2016), Vectorized magnetometer for space applications using electrical readout of atomic scale defects in silicon carbide. *Sci. Rep.* 6, 37077.
2. Kapser, K., Weinberger, M., Granig, W., and Slama, P., in *Giant Magnetoresistance (GMR) Sensors* (Springer, 2013), pp. 133–156.
3. Gaster, R. S. *et al.* (2011), Quantification of protein interactions and solution transport using high-density GMR sensor arrays. *Nature Nanotech.* 6, 314–320.
4. Hung, T.Q. *et al.* (2013), Room Temperature Magnetic Detection of Spin Switching in Nanosized Spin-Crossover Materials. *Angew. Chem.* 52, 1185.
5. Kamara, S. *et al.* (2017), Magnetic Susceptibility Study of Sub-Pico-emu Sample Using a Micromagnetometer: An Investigation through Bistable Spin-Crossover Materials. *Adv. Mater.* 29, 1703073.
6. See <http://www.sensitec.com>.



Zinc-tin oxide diodes with distinct resistive switching modes: from RRAM to neuromorphic applications

J. Martins¹, N. Casa Branca¹, J. Deuermeier¹, J. Goes², E. Fortunato¹, R. Martins¹, A. Kiazadeh^{1*}, and P. Barquinha¹

¹ i3N/CENIMAT, Department of Materials Science, Faculty of Science and Technology, Universidade NOVA de Lisboa and CEMOP/UNINOVA, Campus de Caparica, 2829-516 Caparica, Portugal

² Department of Electrical Engineering, Faculty of Science and Technology, Universidade NOVA de Lisboa and Centre for Intelligent Robotics, UNINOVA, Campus de Caparica, 2829 – 517, Portugal

*asal.kiazadeh@gmail.com

Abstract:

For filamentary resistive switching (1D-RS), defect-rich high- k dielectrics are widely reported as an optimal choice. However, area-dependent resistive switching (2D-RS) has been drawing increased attention lately as it relies on non-destructive switching events, causing less device-to-device variations. 2D-RS requires resistive switching matrices that can change their resistance globally. For this, amorphous oxide semiconductors (AOS) are an ideal choice given, for example, the possibility of tremendous on/off ratios in thin-film transistors. Low temperature processing makes this class of materials an ideal choice for System-On-Panel architectures and allows the use of inexpensive flexible substrates. Zinc-tin oxide (ZTO) is a promising sustainable variant by avoiding critical elements such as indium and gallium (as in the conventional indium-gallium-zinc oxide) while still enabling high performance.¹

In this work we present ZTO resistive switching diodes produced without thermal treatment. These devices can operate in distinct modes depending on the voltage polarity applied during memristor device initialization: conventional 1D-RS operation is achieved when the device sets (switches ON) in the reverse polarity of the diode, Figure 1 (a). 2D-RS is obtained when set occurs in forward polarity, Figure 1 (b). Offering a large memory window, the latter allows analog control of multilevel cell (MLC) operation, Figure 2. Such characteristics can emulate the behavior of the human synapses which is essential for neuromorphic computing applications.

Keywords: resistive switching, zinc tin oxide, low-temperature electronics, neuromorphic computing, artificial synapse.

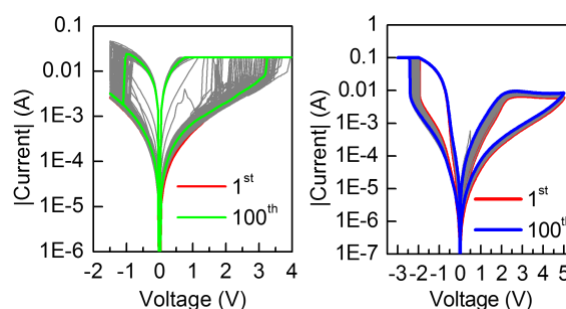


Figure 1: Endurance of ZTO memristors set in: (a) reverse polarity, (b) forward polarity.

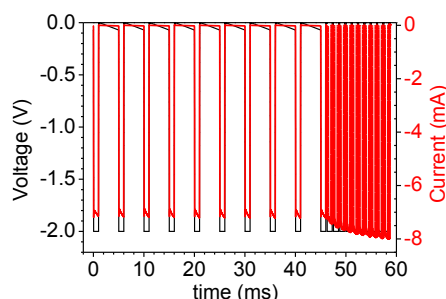


Figure 2: Gradual set process in forward bias with 1 ms pulses using pulse intervals of 4 ms and 0.15 ms. ($V_{\text{pulse}} = -2$ V).

References:

1. Fernandes, C.; Santa, A.; Santos, Â.; Bahubalindrani, P.; Deuermeier, J.; Martins, R.; Fortunato, E.; Barquinha, P. (2018) A Sustainable Approach to Flexible Electronics with Zinc-Tin Oxide Thin-Film Transistors, *Adv. Electron. Mater.*, 4, 1800032.

Multifunctional Zinc Tin Oxide Nanostructures: From Photocatalysis to Electronic Applications

A.Rovisco,* J. Martins, A.d.Santos, J. Neto, R. Branquinho, E.Fortunato, R. Martins and P. Barquinha

i3N/CENIMAT, Department of Materials Science, Faculty of Science and Technology, Universidade NOVA de Lisboa and CEMOP/UNINOVA, Campus de Caparica, 2829-516 Caparica, Portugal

Abstract:

Looking at the actual technology development, we are facing an increasing demand for smart and multifunctional surfaces on all sorts of objects and shapes. With this, flexible and transparent electronics is being pushed to unprecedented performance and integration levels.¹ Thus appears the necessity for a new generation of materials combining sustainability, low dimensions and still a wide range of properties compatible with its application on transistors, memories, sensors or even energy-harvesting components. For this end, indium-free multicomponent oxide nanowires (NWs) such as zinc-tin oxide (ZTO) are some of the most promising material systems for an upcoming generation of sustainable yet high performing transparent nanoelectronics.

Being a ternary oxide ZTO is a multifunctional material, which can crystallize in Zn_2SnO_4 and $ZnSnO_3$ phase, with different types of structures being possible for each phase. Consequently, due to their different properties each type of structure for this material has a wide applicability in for example photocatalysis, nanoelectronics, sensors and energy harvesting. And this work presents these applications using different ZTO nanostructures (Figure 1).

The nanostructures were produced by a seed-layer free hydrothermal synthesis at temperatures of only 200 °C.^{2,3} Nevertheless, the results obtained for the different applications show the similarity of the properties of these nanostructures when compared with the ones produced by vapor phase methods (at high temperatures). Moreover, the hydrothermal method used here proved to be a low-cost, reproducible and highly flexible route to obtain multicomponent oxide nanostructures, namely Zn_2SnO_4 nanoparticles and $ZnSnO_3$ nanowires (with length \approx 600 nm).

Keywords: ZTO, Zn_2SnO_4 , $ZnSnO_3$, nanostructures, nanoparticles, nanowires.

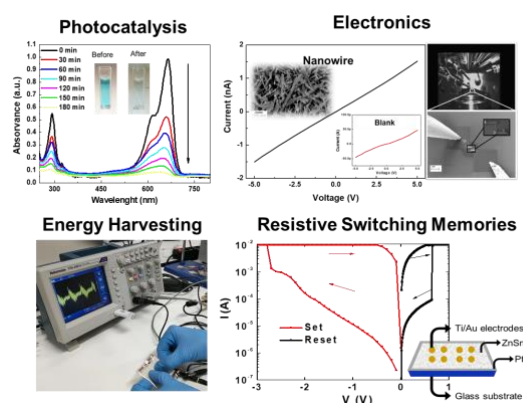


Figure 1: Several applications of ZTO nanostructures produced by hydrothermal synthesis.

References:

1. Roselli, L.; Borges Carvalho, N.; Alimenti, F.; Mezzanotte, P.; Orecchini, G.; Virili, M.; Mariotti, C.; Goncalves, R.; Pinho, P. (2014) Smart Surfaces: Large Area Electronics Systems for Internet of Things Enabled by Energy Harvesting. *Proc. IEEE*, 102, 1723–1746.
2. Rovisco, A., Branquinho, R., Martins, J., Oliveira, M.J., Nunes, D., Fortunato, E., Martins, R. and Barquinha, P. (2018) Seed-layer free zinc tin oxide tailored nanostructures for nanoelectronic applications: effect of chemical parameters, *ACS Appl. Nano Mater.*, 1, 3986–97.
1. Rovisco, A., Branquinho, R., Martins, J., Fortunato, E., Martins, R. and Barquinha, P. (2018) Growth mechanism of seed-layer free $ZnSnO_3$ nanowires: effect of physical parameters, under submission.

The Electrical Transport Characteristics of Ag-NP/n-Si nano Schottky Diodes using Conducting Atomic Force Microscope

Y. Abbas, A. Rezk, I. Saadat, A. Nayfeh, M. Rezeq,*

Khalifa University, PO Box 127788, Abu Dhabi, UAE

Abstract:

Recently, the miniaturization of semiconducting devices is intensively investigated to achieve higher density devices as well as to reduce the power consumption in production lines. Further reduction to the feature size of devices has required the use of photolithography and electron beam lithography. Also monodispersed NPs (NPs) on a substrate can provide an excellent platform for the fabrication of such devices in nanoscale as well as allowing lower power consumption. The unique properties of NP as compared to their bulk counterpart validate them promising candidate for the next generation of high-speed nanoscale devices.

The previous works on the Schottky diodes are mostly based on devices with a large contact area between metal and semiconductor interfaces. These studies did not investigate the effect of nanojunctions on the electrical characteristics. Therefore, a detailed investigation and understanding of Schottky diodes in the nanoscale regime is needed to be studied thoroughly.

In order to investigate the localized behavior of nano Schottky diode [1-2] we performed the electrical characteristics of Schottky device by means of conductive atomic force microscope (CAFM). The Schottky diodes are realized by approaching gold coated tip (Au-tip), with 30-40 nm radius, on the surface of n-Si substrate. The diode characteristics are also extracted by placing a silver (Ag) NP, with a 5-7 nm radius, between the Au-tip and n-Si substrate.

The Ag NPs are dispersed on the HF cleaned n-Si substrate by spin coating method. The nano-Schottky diode characteristics are carried out in the nanoscale stacking of Au-tip/n-Si as well as in Au-tip/Ag-NP/n-Si. During all electrical measurements the bias voltage is applied on the substrate while the CAFM tip is kept at a virtual ground as shown in Figure 1a.

The tapping mode topography of AFM revealed that the NPs are monodispersed on the substrate and the size of NPs are confirmed as ~5 nm in radius from the height tracing of the surface

(Figure 1b). From the electrical characteristics of the devices, as shown in Figure 1c, we inferred that the enhanced reverse bias current for Au-tip/Ag-NP/n-Si device is higher than that of Au-tip/n-Si, this is primarily due to enhanced tunneling [3]. During the tunneling process the Ag-NP allows more band bending at the Ag-NP/n-Si interface, due to electric field enhancement on the surface of the NP. Whereas, the forward biased current was lower in case of the Au-tip/Ag-NP/n-Si stacking device. This is due to the fact that electrons face a dual junction, the n-Si/Ag-NP and Ag-NP/tip junctions, which naturally creates greater barrier for the flow of electric current. The electrical characteristics and the insets of AFM topography and energy band structure of the measured junctions are shown in figure 1.

Keywords: Nano-Schottky diode, band bending, Ag-NPs, CAFM.

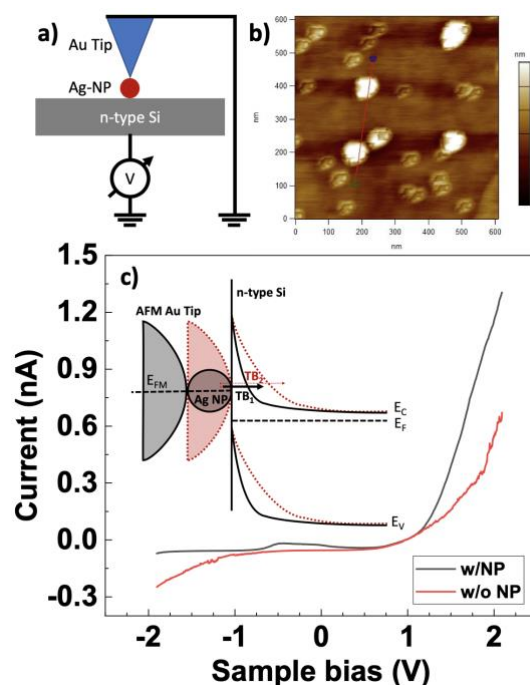


Figure 1: a) AFM schematics for electrical measurement setup. b) AFM topography of Ag-NPs on n-Si substrate. c) The IV characteristics for both junctions. Black solid curves

correspond to tip/NP/n-Si junction and red dotted curves correspond to tip/n-Si junction. The inset figure shows the corresponding energy band diagram at reverse bias for both junctions highlighting the barrier narrowing due to the NP.

References:

1. M. Rezeq, K. Eledlebi, M. Ismail, R. K. Dey, and B. Cui (2016) Theoretical and experimental investigations of nano-Schottky contacts, *Journal of Applied Physics* 120, 044302.
2. C S Pathak, M. Garg, J P Singh and R Singh (2018) Current Transport Properties of Monolayer Graphene/n-Si Schottky Diodes, *Semicond. Sci. Technol.* 33 055006
3. Erjuan Guo, Zhigang Zeng, Xiaobo Shi, Xiao Long, and Xiaohong Wang (2016), Electrical Transport Properties of Au Nanoparticles and Thin Films on Ge Probed Using a Conducting Atomic Force Microscope, *Langmuir*, 2016, 32 (41), pp 10589–10596

Light-Trapping Modes in Lossy Plasmonic Waveguides

Syed Muhammad Anas Ibrahim, Kyoung-Youm Kim*

Department of Optical Engineering, Sejong University, Seoul 05006, Korea

Abstract:

Achieving slow light has been a topic of great interest for researchers for the past few decades. Many techniques have been proposed based on the use of photonic crystal nanocavities, tapered waveguides, cold atomic gases, and metamaterials. Recently, slow light propagation or trapping of light via the light-trapping modes in plasmonic waveguides has been studied extensively. In lossless plasmonic waveguides, we can obtain such a light-trapping mode (whose group velocity approaches zero) when the overall power flow of a mode is reduced to zero (there are two opposite power flows inside the waveguide). However, it was shown that lossy plasmonic waveguides cannot support light-trapping modes. This conclusion was derived from the analysis adopting a complex wave vector to take metallic loss into account. In this work, we analyze the light-trapping mode in lossy conditions using an alternative approach which adopts a complex frequency. We show that (1) light-trapping modes can exist even if there is metallic loss and (2) their overall power flow is no longer reduced to zero as in the lossless case. We expect that these light-trapping modes will pave way for many applications in nanotechnology.

Keywords: waveguide, waveguide mode, slow light, trapping of light, plasmonics, plasmonic waveguide.

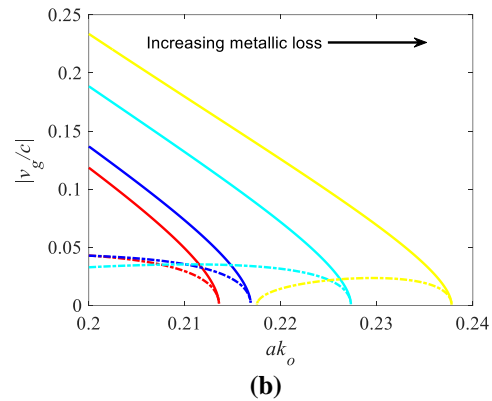
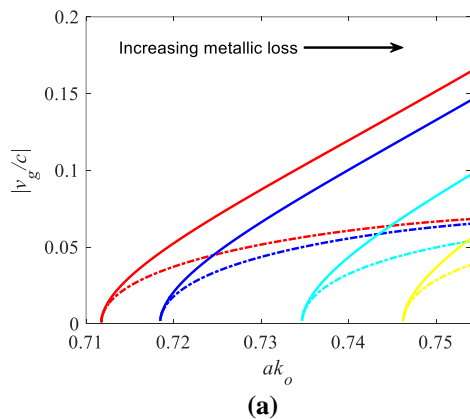


Figure 1: Group velocity of (a) antisymmetric plasmonic modes in a MIM waveguide and (b) symmetric modes in an IMI waveguide. Solid and dotted lines indicate that the corresponding modes are forward and backward, respectively.

References:

1. Tsakmakidis, K. L., Boardman, A. D., Hess, O. (2007), 'Trapped rainbow' storage of light in metamaterials, *Nature*, 450, 397-401.
2. Park, J., Kim, K.-Y., Lee, I.-M., Na, H., Lee, S.-Y., Lee, B. (2010), Trapping light in plasmonic waveguides, *Opt. Express*, 18, 598-623.

Acknowledgment:

This work was supported by the Basic Science Research Program through the National Research Foundation of Korea funded by the Ministry of Science, ICT and Future Planning (NRF-2016R1D1A1B03931510).

Multi-scale Defect Mechanics for Reliability of High Performance Electronic Devices in Radiation Environments

M. Paing, H. Y. Kim, Y. E. Pak*

Department of Mechanical Engineering, State University of New York, Korea

Abstract:

One of the many technical challenges of running a satellite in orbit comes from dealing with the harsh radiation environments of outer space. Specifically, electronic devices exposed to radiation degrade their performance over time, and in other cases cause unwanted transient events that alter or even destroy the function of the device. This research is specifically interested in analyzing the radiation conditions of a CubeSat placed in Low Earth Orbit, where trapped protons from the Van Allen belt are the main source of radiation [1]. Knowing the radiation environment includes finding proton flux data at various energy levels mapped out in a diagram using a software called SPENVIS (Space Environment Information System). Afterwards, a particle simulation program called GEANT4 was used to simulate the interaction of moving protons to a semiconductor device and calculate how much energy was deposited into the medium at various points in space (Figure 1) [3]. The test was done at various proton incident energy levels that represents the radiation environment and with two types of shielding to see the effect it has on its ability to absorb the radiation or redirect its path. The two models are an aluminum plate and an arbitrary CubeSat model chosen from the internet. With the energy deposition data obtained from GEANT4, this can then be used as reference to see the effectiveness of the shielding from CubeSat and possibly quantify the three effects of radiation that serves as a basis to aid the further steps found in RHA.

Keywords: energy deposition data, radiation conditions, GEANT4, shielding, satellite systems

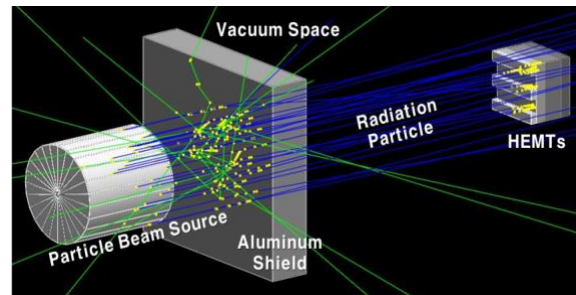


Figure 1: GEANT4 simulation of particles through an aluminum shield and high electron mobility transistors (HEMTs) [3]

References:

1. 2017 IEEE Nuclear and Space Radiation Effects Conference Short Course Notebook Radiation Hardness Assurance for Satellite Systems - From Macro to Nano.
2. Martines, Luz Maria S., "Analysis of LEO Radiation Environment and its Effects on Spacecraft's Critical Electronic Devices" (2011). Dissertations and Theses. 102.
3. Seo, Y., Mishra, D., Kang, K., Kim, J., and Pak, Y.E. Development of Defect Mechanics-based Multi-scale Simulation Techniques for Reliability Study of High Performance Electronic Devices in Radiation Environments. (2018)

NanoMatEn - Session II.E: Nanotechnology for Environmental Application / Water treatment

Compositional and Microstructural Engineering of Transition Metal Phosphides for Improved Electrocatalytic Performance

Lifeng Liu,* Junyuan Xu

¹International Iberian Nanotechnology Laboratory (INL), 4715-330 Braga, Portugal

Abstract:

Water splitting has been proposed to be a promising approach to renewable energy storage through converting the off-peak solar or wind energy to hydrogen fuels. Presently, one of major challenges facing widespread deployment of water splitting devices is their high cost, which primarily results from the use of precious and scarce noble metal catalysts.

In this talk, I will present our recent efforts towards compositional and microstructural engineering of transition metal phosphide (TMP) electrocatalysts, with an aim to improve their electrocatalytic performance for hydrogen and/or oxygen evolution reactions (HER & OER). I will showcase three examples: 1) Trends in the OER activity of TMP nanoparticles [1]. We have investigated the alkaline OER electrolysis of a series of TMP catalysts and observed a notable trend in OER activity which follows the order of FeP < NiP < CoP < FeNiP < FeCoP < CoNiP < FeCoNiP. Our results show that the introduction of a secondary metal(s) to a mono-metallic TMP can remarkably boost the OER performance. This promotional effect can be ascribed to the enhanced oxidizing power of bi- and tri-metallic TMPs. 2) RuCoP nanoclusters showing superior HER performance in alkaline solution [2]. The RuCoP clusters were prepared by wet chemical reduction of metal cations followed by a low-temperature phosphorization treatment. When used to catalyze the HER, they show exceptional activity with a very low overpotential (η) of 23 mV to reach -10 mA cm^{-2} and a high turnover frequency (TOF) value of 3.85 s^{-1} at $\eta = 100 \text{ mV}$. The superior HER performance can be attributed to the partial electron transfer from CoP to Ru, which substantially improves the HER kinetics on active Ru sites. Theoretical calculations also show that the adsorption energy of $-\text{OH}$ on RuCoP is lower than that on pristine Ru clusters and that water dissociation happens on RuCoP more easily, both contributing to the improvement of HER activity. 3) Hollow CoP

octahedron (OCH) nanostructures with well-defined exposed crystal facets [3]. The hollow CoP OCH NPs were prepared by solution phase synthesis of CoO OCH precursors, followed by a post-phosphorization treatment and subsequent chemical etching process. They show excellent intrinsic electrocatalytic performance for the OER, substantially outperforming CoP nanospheres without any preferentially exposed facets.

Keywords: transition metal phosphide, electrocatalysis, water splitting, hydrogen evolution reaction, oxygen evolution reaction, composition engineering, microstructure engineering.

References:

1. J.Y. Xu, J. J. Li, D.H. Xiong, B.S. Zhang, Y.F. Liu, K.H. Wu, I. Amorim, W. Li, L.F. Liu (2018), Trends in activity for the oxygen evolution reaction on transition metal (M = Fe, Co, Ni) phosphide pre-catalysts, *Chem. Sci.*, 9, 3470.
2. J.Y. Xu, T.F. Liu, J.J. Li, B. Li, Y.F. Liu, B.S. Zhang, D.H. Xiong, I. Amorim, W. Li, L.F. Liu (2018), Boosting the hydrogen evolution performance of ruthenium clusters through synergistic coupling with cobalt phosphide, *Energy Environ. Sci.*, 11, 1819
3. J.Y. Xu, Y.F. Liu, J.J. Li, I. Amorim, B.S. Zhang, D.H. Xiong, N. Zhang, S.M. Thalluri, J.P. Sousa, L.F. Liu (2018), Hollow cobalt phosphide octahedral pre-catalysts with exceptionally high intrinsic catalytic activity for electro-oxidation of water and methanol, *J. Mater. Chem. A*, 6, 20646.

Recent advances of nanocomposites for radioactive contaminants removal from nuclear wastes and beyond

Changhyun Roh,^{1,2,3*}

¹ Decommissioning Technology Research Division, Korea Atomic Energy Research Institute, 989-111 Daedukdaero, Yuseong, Daejeon, 34057, Republic of Korea.

² Biotechnology Research Division, Advanced Radiation Technology Institute (ARTI), Korea Atomic Energy Research Institute (KAERI), Jeonbuk, 56212, Republic of Korea.

³ Radiation Biotechnology and Applied Radioisotope Science, University of Science and Technology (UST), 217, Gajeong-ro, Daejeon 34113, Republic of Korea

Email: chroh@kaeri.re.kr

Abstract:

After the Fukushima Daiichi Nuclear Power Plant disaster in Japan in 2011, the demand drastically increased for efficient technology for the removal of radioactive contaminants. Many researchers have suggested using physical adsorption methods to remove radioactive contaminants from contaminated environment. For example, polymers, nanocomposites, and clay have all previously been investigated for their capacity to remove radioactive cesium through the interaction between the negatively charged surfaces of naturally occurring adsorbents and the positive charge of radioactive cesium. However, these adsorbents cannot be used to treat contaminated water in a real, open environment because there is no easy way to collect the adsorbents after they are used. In particular, adsorbents can cause blocking phenomena, which could be addressed by encapsulating the adsorbents with suitable modification that could alleviate the clogging and resolve the post-treatment separation problem. Therefore, novel solid adsorbents are needed to allow easy separation of the materials from the contaminant environment to prevent secondary contamination. In my talk, recent efforts in our research group, utilizing both organic and inorganic composites safe design and fabrication to aiming at removing radioactive contaminants from environment. And I will introduce new challenges of key issues to such novel nanocomposites based on recent advances for environmental applications.

Keywords: nanocomposites, radioactive contaminants, nuclear energy, nuclear wastes

References:

1. Lee I, Kang, S.-M., Jang S.-C., Lee, G.-W., Shim, H.-E., Rethinasabapathy, M., Huh, Y.-S., Roh, C. (2019) One-pot gamma ray-induced green synthesis of a Prussian blue-laden polyvinylpyrrolidone/reduced graphene oxide aerogel for the removal of hazardous pollutants. *J. Mater. Chem. A*, 7, 1737-1748.
2. Rethinasabapathy, M., Kang, S.-M., Lee, I., Lee, G.-W., Hwang, S.-K., Huh, Y.-S., Roh, C. (2018) Layer-Structured POSS-Modified Fe-Aminoclay/Carboxymethyl Cellulose Composite as a Superior Adsorbent for the Removal of Radioactive Cesium and Cationic Dyes *Ind. Eng. Chem. Res.* 57, 13731-13741
3. Jang S.-C., Kang, S.-M., Kim, G.-Y., Rethinasabapathy, M., Haldorai, Y., Lee, I., Han, Y.-K., Renshaw, J.C., Huh, Y.-S., Roh, C. (2018) Versatile Poly(Diallyl Dimethyl Ammonium Chloride)-Layered Nanocomposites for Removal of Cesium in Water Purification, *Materials* 11(998), 1-10.

Photocatalytic Activity of Nanostructured ZnO for Water Purification

Y. Leprince-Wang*, N. Martin, M. Le Pivert, M. Capochichi-Gnambodoe

Université Paris-Est, UPEM, ESYCOM (CNRS FRE2028), Champs sur Marne, France.

*corresponding author, e-mail : yamin.leprince@u-pem.fr

Abstract:

Drinkable water is a precious and limited resource. With the ever-increasing human and industrial needs, it becomes more and more necessary to find new cheap, environmental friendly and efficient ways to refine industrial and urban wastewaters, ensuring the availability of clean drinkable water in the future. The semiconductor-based photocatalysis is a well-known and efficient process for achieving water depollution, with very limited rejects in the environment. Metallic oxides, such as ZnO, are excellent photocatalysts [1,2], able to mineralize a large scale of organic pollutants in water, under UV irradiation that can be enlarged to visible range by doping nontoxic transition metal elements such as Ag and Fe [3]. With high surface/volume ratio, the nanostructured ZnO shows enhanced photocatalytic efficiency (Figure 1). ZnO nanostructure is also a promising candidate in microfluidic application for their easy-controllable synthesis and integration in a microfluidic system (Figure 2)[4].

Keywords: ZnO nanostructures, photocatalysis, water purification, doping, microfluidics.

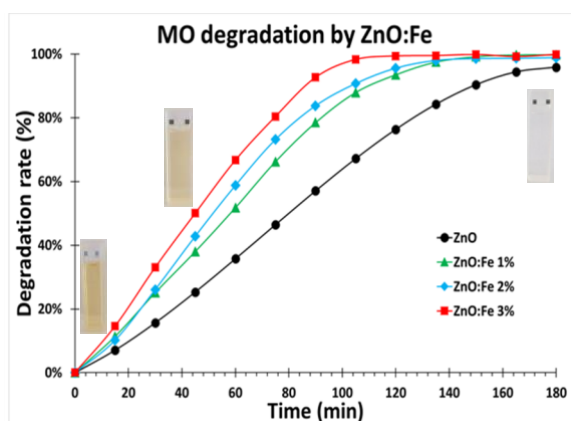


Figure 1: Photo-degradation of Methyl Orange (MO) solution under UV illumination: ~ 100% degradation rate of MO has been achieved for 1-3% mole Fe-doped ZnO NWs.

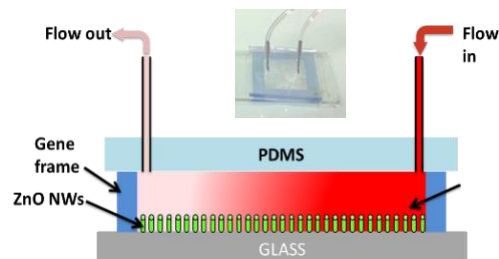


Figure 2: Microfluidic device with integrated ZnO nanostructure.

References:

1. Habba, Y.G., Capochichi-Gnambodoe, M., Serairi L., Leprince-Wang, Y. (2016) Enhanced photocatalytic activity of ZnO nanostructure for water purification, *Physica Status Solidi B*, 253, 1480-1484.
2. Habba, Y.G., Capochichi-Gnambodoe, M., Leprince-Wang, Y. (2017) Enhanced photocatalytic activity of iron-doped ZnO nanowires for water purification, *Applied Sciences*, 7, 1185.
3. Martin, N., Capochichi-Gnambodoe, M., Le Pivert, M., and Leprince-Wang, Y. (2018) A comparative study on the photocatalytic efficiency of ZnO nanowires doped by different transition metals, *Acta Physica Polonica A*, in Press.
4. Azzouz, I., Capochichi-Gnambodoe, M., Habba, Y.G., Marty, F., Leprince-Wang, Y., and Bourouina T. (2018) Zinc Oxide nano-enabled microfluidic reactor for water purification and its application to Volatile Organic Compounds, *Microsystems & Nanoengineering*, 4, 17093.

Strategy of functionalization for micropollutants electrochemical detection

Imer Sadriu^{1,2}, Emilie Mathieu-Scheers¹, Céline Grillot¹, Sarra Bouden¹, Jimmy Nicolle¹, Fetah I. Podvorica², Catherine Berho³, Valérie Bertagna¹, Christine Vautrin-UI¹

¹ ICMN Interfaces, Confinement, Matériaux et Nanostructures, UMR7374 - Université d'Orléans – CNRS, 1b rue de la Férollerie, 45071 Orléans Cedex 2, France.

² Chemistry Department of Natural and Mathematical Sciences Faculty, University of Prishtina, rr. “Nëna Tereze” nr. 5, 10000 Prishtina, Kosovo.

³ BRGM Bureau de Recherches Géologiques et Minières, 3 Avenue Claude Guillemin, 45100 Orléans

Abstract:

The monitoring of ground and surface water quality showed many aquifers contamination by a lot of micropollutants. It is therefore crucial to develop rapid, sensitive and selective analysis methods for the in-situ monitoring of these pollutants in real-time in order to be able to implementate the WFD of European Union [1-2].

ICMN Laboratory's activities in the field of the environmental metrology are focused on the development of electrochemical sensors based on fonctionalized carbon materials, to detect electroactive micropollutants in aqueous media. Electrochemical sensors have to possess physicochemical properties to allow sensitive and selective measurement of water micropollutants but also reliability, stability, robustness for in-situ analyses. This presentation will deal with the different strategies of functionalization adopted to develop organic and metallic micropollutant sensors: such as electrochemical grafting or molecular imprinting electro-polymerization. The results obtained regarding the electrochemical detection of pesticides (figure 1), polycyclic aromatic hydrocarbide (PAH) and metallic cations will be shown.

involving different steps:

1. Electropolymerization of monomer,
2. Template extraction (removal),
3. Adsorption process (rebinding),
4. Electrochemical detection.

Keywords: Micropollutants analysis ; Isoproturon ; HAP ; Electrochemical detection; Environmental monitoring ; Molecularly Imprinted Polymer (MIP) ; electrochemical grafting .

References:

1. Directive 2000/60/EC of the European Parliament and of the Council establishing a framework for the Community action in the field of water policy.
2. Directive 2013/39/EU of the European parliament and of the council of 12 August 2013 amending Directives 2000/60/EC and 2008/105/EC as regards priority substances in the field of water policy.
3. D. Pally, V. Bertagna, B. Cagnon, M. Alaaeddine, R. Benoit, F.I. Podvorica, C. Vautrin-UI, , J. Electroanal. Chem. 817 (2018) 101–110.

Acknowledgements

We really appreciate the financial support provided to the PIVOTS and the CAPEL-MIP projects by the Region- Centre Val de Loire (ARD 2020 and CPER 2015-2020 program) and French Ministry of Higher Education and Research (CPER 2015- 2020 and the public service grant to the CNRS and the University of Orléans) and the European Union. We also acknowledge the Embassy of France in Kosovo for financial support.

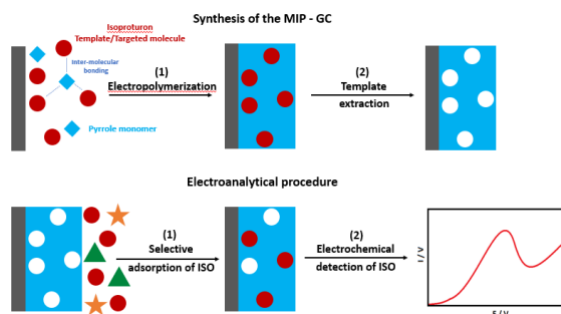


Figure 1: The procedure that describes how a molecularly imprinted polymer sensor works

Carbon dots' photoluminescence technique to detect total Chromium in industrial wastewater

R. Sinha,^{1*} T. K. Mandal,^{1,2}

¹ Indian Institute of Technology Guwahati, Department of Chemical Engineering, Assam, India

² Indian Institute of Technology Guwahati, Centre for Nanotechnology, Assam, India

Abstract:

Carbon nanomaterials namely carbon dots (CDs) have drawn much attention in recent years with their wide range of applications. These CDs basically have sizes below 10 nm and consist of sp^2 hybridized carbon with crystalline or amorphous core and an oxidized carbon surface with large number of carboxyl ($-COOH$) groups. One of the most significant characteristics of CDs is their ability to show photoluminescence property when excited with light of a particular wavelength. The quenching of the photoluminescence of the CDs can be very much useful to sense the presence of heavy metals in a water bodies. In this work, we report the synthesis of photoluminescent CDs from indigenous potato sources by simple heating reaction to detect chromium ions in industrial wastewater (Figure 1). The presence of $-COOH$ functional group was confirmed by FTIR characterization. These carboxylic acid groups are actually responsible for their extraordinary water-solubility. The X-ray diffraction (XRD) spectra confirmed the amorphous nature of the synthesized CDs and also these CDs exhibited a quantum yield (QY) of 6.08%. The quenching of photoluminescence of thus synthesized CDs was utilized to develop a sensing probe for detection of total Chromium in industrial wastewater (Tannery wastewater) in the form of Cr^{6+} . Initially the sample of Tannery wastewater was diluted with DI water (1:1) and then the diluted solution was treated with H_2O_2 followed by UV-exposer to oxidise Cr^{3+} into Cr^{6+} ions. The proposed method is able to detect the chromium concentration even lower than $0.1 \mu M$.

Keywords: Heating reaction, Carbon dot, Photoluminescence, Quenching of photoluminescence, Quantum yield, Chromium detection.

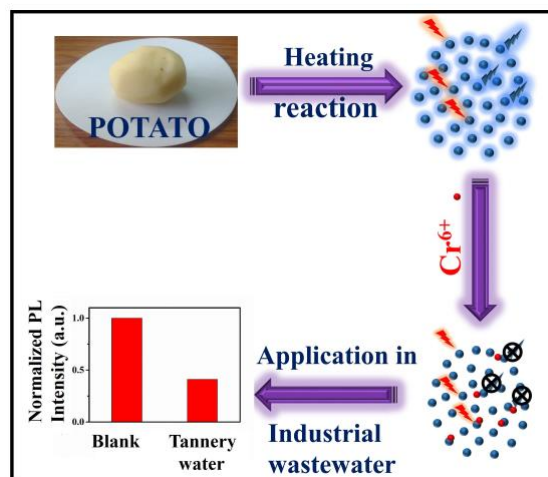


Figure 1: Figure explaining the overall process of synthesizing CDs from potato by simple heating reaction and the use of these CDs as a sensing probe to detect total chromium ion in industrial wastewater (Tannery water) by utilizing the property of quenching of photoluminescence of CDs.

References:

1. Sahu, S., Behera, B., Maiti, T. K., Mohapatra, S. (2012), Simple one-step synthesis of highly luminescent carbon dots from orange juice: application as excellent bio-imaging agents, *Chem. Commun.*, 48, 8835-8837.
2. Goswami, U., Dutta, A., Raza, A., Kandimalla, R., Kalita, S., Ghosh, S. S., Chattopadhyay, A. (2018), Transferrin-Copper Nanocluster-Doxorubicin Nanoparticles as Targeted Theranostic Cancer Nanodrug, *ACS Appl. Mater. Interfaces*, 10, 3282-3294.

Preparation of a Floating Photocatalyst-adsorbent Composite *via* TiO₂ Deposition on Silicalite-1 Coated-Hollow Glass Microspheres

Supinya Nijpanich^{1*}, Takeshi Hagio^{1,2}, Yuki Kamimoto², Ryoichi Ichino^{1,2}

¹Nagoya University, Department of Chemical Systems Engineering, Nagoya, Japan

²Nagoya University, Institutes of Innovation for Future Society, Nagoya, Japan

Abstract:

Wastewater generated from daily activities, hospitals, industries contains plenty of organic pollutants which cannot be easily decomposed in nature. These organic pollutants have an adverse effect on plants, animal and human. Various processes have been applied to purify the wastewater before disposal to the nature source, such as adsorption process, ozone degradation and photocatalysis. Adsorption process has been attracted interest since it does not generate the secondary waste, while photocatalysis is a green technology for treatment of environmental organics pollutants. However, adsorption suffer from saturation and photocatalysts do not have the ability to attract the pollutants to decompose. Furthermore, the conventional adsorbent and photocatalyst are normally available in powdery form which still present some lacks such as difficulty in separation after treating process. In the present work, we report the incorporation of two processes, adsorption and photocatalysis, for preparing a floating photocatalyst-adsorbent which can be easily separated and also directly contact with the UV source enhancing the photocatalytic performance of material (figure 1). Silicalite-1, which is a siliceous MFI-type zeolite, was chosen to be an adsorbent in our work due to its high hydrophobicity proficient to adsorb the organic molecules contaminated in wastewater. Firstly, silicalite-1 was crystallized on a hollow glass microsphere and then the TiO₂ precursor was introduce to deposit TiO₂ on the surface. The optimum condition to prepare the floating catalyst-adsorbent composite was investigated. The preliminary study on the adsorption-photocatalytic performance was done by methylene blue experiment under ultraviolet irradiation. It was found that the prepared floating photocatalyst-adsorbent composite could degrade the methylene blue *via* adsorption

of the molecules on the surface follow by degradation through photocatalytic reaction.

Keywords: adsorption, photocatalysis, silicalite-1, titanium dioxide

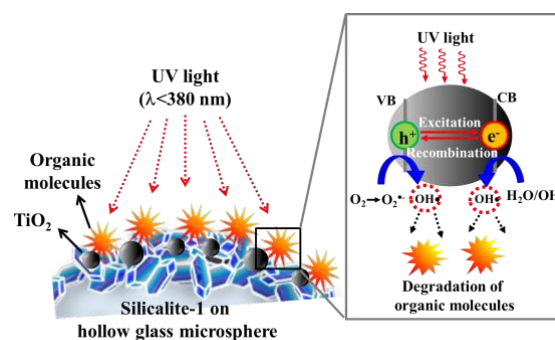


Figure 1: Figure illustrating the adsorption and degradation mechanism of the floating photocatalyst-adsorbent for organic molecules removal in wastewater.

References:

1. Brião, G.V., Jahn, S.L., Foletto, E.L. and Dotto, G.L. (2017) Adsorption of crystal violet dye onto a mesoporous ZSM-5 zeolite synthesized using chitin as template. *Journal of colloid and interface science*, 508, 313-322.
2. Hamed, A.K., Dewayanto, N., Du, D., Ab Rahim, M.H. and Nordin, M.R. (2016) Novel modified ZSM-5 as an efficient adsorbent for methylene blue removal. *Journal of Environmental Chemical Engineering*, 4(3), 2607-2616.

Corrugated Graphene Channels for Seawater Desalination via Capacitive Deionization

Madhavi Dahanayaka,^{1,2} Bo Liu,^{1,3} Zhongqiao Hu,³ Zhong Chen,⁴ Adrian Wing-Keung Law,^{1,5} Kun Zhou*^{1,3}

¹ Environmental Process Modeling Center, Nanyang Environment and Water Research Institute, Nanyang Technological University, 50 Nanyang Avenue, Singapore 639798, Singapore

² Interdisciplinary Graduate School, Nanyang Technological University, 50 Nanyang Avenue, Singapore 639798, Singapore

³ School of Mechanical and Aerospace Engineering, Nanyang Technological University, 50 Nanyang Avenue, Singapore 639798, Singapore

⁴ School of Material Science and Engineering, Nanyang Technological University, 50 Nanyang Avenue, Singapore 639798, Singapore

⁵ School of Civil and Environmental Engineering, Nanyang Technological University, 50 Nanyang Avenue, Singapore 639798, Singapore

Abstract:

Shortage of potable water is one of the main challenges faced by many countries across the world where seawater desalination has become the key approach in addressing the issue due to the abundance of seawater. Recently, capacitive deionization (CDI) has emerged as a promising technology for desalination that has a high recovery rate with the ability to remove a wide range of ionic contaminants and benefits in terms of energy efficiency and cost effectiveness. In CDI, particles with opposite charges are adsorbed into two electrodes under the effect of an external electric field. These electrodes are made from porous materials and the process efficiency depends on the characteristics of the materials. Graphene (GE) has excellent properties in terms of its high electrical conductivity, surface area, mechanical stability and chemical inertness, thus has been identified as an exceptional choice for CDI. Using molecular dynamics simulations, this study reports the effect of electric field and surface morphology of corrugated GE layers on their CDI process. Deionization performances are evaluated in terms of water flow rate and ion adsorption and explained by analysing the water density distribution and radial distribution function. Simulation results reveal that corrugation of GE layers reduces the water flow rate but largely enhances the ion adsorption in comparison to the flat GE layers. Such enhancement is mainly due to the adsorption of ions inside the GE layers as a result of anchoring effect at the regions with wide interlayer distances. Moreover, it reveals that the entrance configuration of the GE channel also has significant effect on the performance of deionization. Overall, the results from this study

will be helpful in designing effective electrode configurations for CDI.

Keywords: Graphene, Nanochannels, Capacitive deionization, Water Desalination, Molecular dynamics simulation.

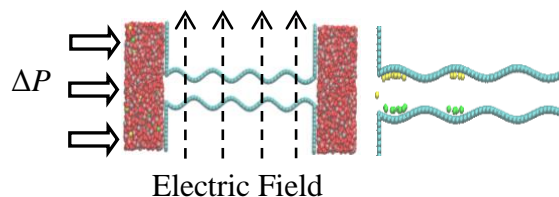


Figure 1: (Left) Schematic of the simulation model. (Right) Ion distribution inside the channel. Cyan, grey and red colours represent carbon, oxygen and hydrogen atoms, respectively. The sodium and chlorine ions are represented by yellow and green colours, respectively.

References:

1. Anderson, M. A., A. L. Cudero and J. Palma (2010). "Capacitive deionization as an electrochemical means of saving energy and delivering clean water. Comparison to present desalination practices: Will it compete?" *Electrochimica Acta* 55(12): 3845-3856.
2. Bao, W., F. Miao, Z. Chen, H. Zhang, W. Jang, C. Dames and C. N. Lau (2009). "Controlled ripple texturing of suspended graphene and ultrathin graphite membranes." *Nature nanotechnology* 4(9): 562-566.
3. Cohen-Tanugi, D. and J. C. Grossman (2012). "Water Desalination across Nanoporous Graphene." *Nano Letters* 12(7): 3602-3608.
4. Fasolino, A., J. H. Los and M. I. Katsnelson (2007). "Intrinsic ripples in graphene." *Nat Mater* 6(11): 858-861.

Smart micro and nano sensors for ambient air quality monitoring

F. Udrea

Engineering Department, Cambridge University, Cambridge CB2 1PZ

Abstract

The sensor field has seen tremendous changes in the last decade. The traditional large and bulky devices have been largely replaced by a new class of low power, ultra-small size sensors with higher sensitivity, higher selectivity and often controlled by sophisticated ASICs. This talk covers the concepts and the development of micro and nano sensors in environmental monitoring. In particular the case of miniaturised gas sensors using chemical and optical techniques for ambient air quality analysis will be highlighted. Finally the talk will give an example of a University spin off company in this field. The talk will finish with an outline of the challenges for the ambient air quality future and a vision of different technologies for the next 10 years.

Keywords: smart gas sensors, gas sensors, air quality sensors, optical sensors

References:

1. Udrea, F.; Luca, A.D. CMOS technology platform for ubiquitous microsensors. 2017 International Semiconductor Conference (CAS), 2017, pp. 43–52.
2. De Luca, A.; Cole, M.T.; Hopper, R.H.; Boual, S.; Warner, J.H.; Robertson, A.R.; Ali, S.Z.; Udrea, F.; Gardner, J.W.; Milne, W.I. Enhanced spectroscopic gas sensors using in-situ grown carbon nanotubes. *Applied Physics Letters* 2015, 106

Durability study of the photocatalytic efficiency of Fe and Ag-doped ZnO nanowires

N. Martin,^{1,*} M. Le Pivert,¹ M. Capochichi Gnambodoe,¹ Y. Leprince-Wang¹

¹ Université Paris-Est, ESYCOM, UPEM, 5 Bd Descartes, 77454 Marne-la-Vallée, France

*corresponding author, e-mail : nathan.martin@u-pem.fr

Abstract:

Water is a widely-used liquid, in the industry or in everyday life. Being essential for living beings in general, and humans in particular, maintaining clean water supplies is vital to the perpetuation of the environment and to human health.

Photocatalysis is a promising process for water depollution, as it is an easy, efficient, low cost and sustainable way for the degradation of organic pollutants from urban and industrial effluents. Among all the photocatalysts, ZnO nanowires have attracted particular attention with their high efficiency under UV-light¹ and their biocompatibility. The last obstacles for the use of ZnO nanowires under visible-light are their large band-gap (3.37 eV) and their high electron-hole recombination rate.

To enhance the photon absorption by the ZnO nanowires, thus their photocatalytic efficiency, transition-metal doping has proven its efficiency². In this work, we investigated the Fe and Ag-doping effect on the photocatalytic efficiency of supported ZnO nanowires hydrothermally grown on Si-wafers. The dopants elements Fe and Ag were chosen by their environmentally-friendly feature.

The samples were doped with different concentrations of each metal (from 1 mol% to 3 mol%) and tested on the photocatalytic degradation of a model organic molecule: Methyl Orange (MO), an organic dye widely found in textile industry wastewater, reputed as one of the most difficult to degrade compared to the other dyes such as Methylene Blue (MB) or Acid Red 14 (AR14)¹. Every photocatalytic experiment was performed for three hours, this being the time needed to attain a quasi complete dye degradation with all the doped-samples during the first experiments.

The reproducibility of our results and the durability were tested by re-using our samples for several successive identical experiments, with or without annealing between each photocatalytic experiment.

As shown in Figure 1, all of our doped samples showed better efficiency than undoped ZnO, and the Ag-doped samples exhibited very good reproducibility, as well as excellent durability even without in-between-experiments-annealing. For the Fe-doped samples, even with an annealing between the photocatalysis, the efficiency decreases over time. The annealing only allows to lessen the decrease. This effect seems more prominent for the higher doping concentrations, especially the 3%-doped samples.

Keywords: ZnO, Nanowires, Doping, Transition metal, Photocatalysis, Organic dyes degradation, Water depollution, Reproducibility.

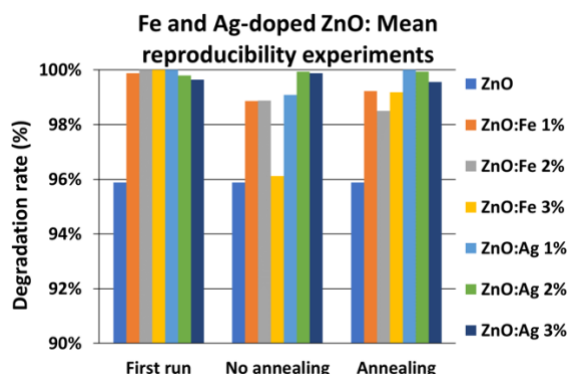


Figure 1: Mean reproducibility results of Fe and Ag-doped ZnO nanowires with and without post-photocatalysis annealing, compared to undoped ZnO efficiency.

References:

- Habba, Y. G., Capochichi-Gnambodoe, M., Serairi, L., Leprince-Wang, Y. (2016), Enhanced photocatalytic activity of ZnO nanostructures for water purification, *Phys. Status Solidi B.*, 253, 1480-1484.
- Qi, K., Cheng, B., Yu, J., Ho, W. (2017), Review on the improvement of the photocatalytic and antibacterial activities of ZnO, *J. Alloys Compd.*, 727, 792-820.

Novel FeVO₄/BiOCl Nanocomposite for Efficient Photocatalytic Dye Degradation and Cr(VI) Reduction Under Visible Light Irradiation

Auttaphon Chachvalvutikul¹, Sulawan Kaowphong^{1,2*}

¹ Department of Chemistry, Faculty of Science, Chiang Mai University, Chiang Mai, Thailand

² Center of Excellence in Materials Science and Technology, Chiang Mai University, Chiang Mai, Thailand

Abstract:

Heterogeneous photocatalysis is an efficient method for the oxidation of a variety of organic compounds as well as for the reduction of toxic metals from aqueous solutions. Herein, photocatalytic oxidation of organic dyes (rhodamine B and methylene blue) and reduction of Cr(VI) by a novel FeVO₄/BiOCl nanocomposite under visible light irradiation were reported for the first time. Results showed that the amount of FeVO₄ remarkably influenced the photocatalytic activity of the FeVO₄/BiOCl nanocomposites. The FeVO₄/BiOCl nanocomposite with 6.25% wt of FeVO₄ exhibited the highest photocatalytic activity; 99.8% and 87.2% of the RhB and MB degraded within 360 min, respectively. Moreover, the 6.25% wt-FeVO₄/BiOCl also possessed an excellent activity in the photocatalytic reduction of Cr(VI) in acidic solution. This photocatalyst potentially reduced 97.8% and 85.5% of Cr(VI) at solution pH values of 3 and 5, respectively. Based on the results from UV-vis DRS, photoluminescence, XPS, and active species trapping experiments, a synergistic mechanism between FeVO₄ and BiOCl nanoparticles for the improved photooxidation of rhodamine B was proposed (Figure 1). The improved photocatalytic activity could be ascribed to the increased absorption in the visible-light range and the enhanced charge separation efficiency at the interface of FeVO₄ and BiOCl nanoparticles. The FeVO₄/BiOCl photocatalyst fabricated herein is being further evaluated by removing other pollutants and has great potential in wastewater purification.

Keywords: FeVO₄/BiOCl; nanocomposites; photocatalytic activity; visible light

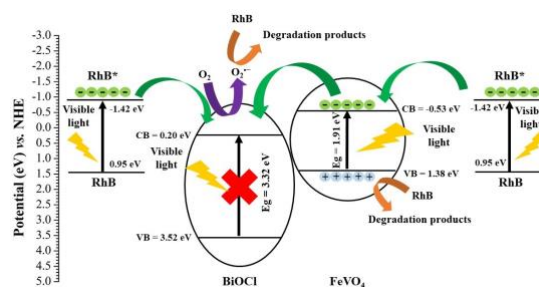


Figure 1: A synergistic mechanism between FeVO₄ and BiOCl nanoparticles for the improved photooxidation of rhodamine B.

Enhancement of Photocatalytic Dye Degradation and Hydrogen Evolution of a Z-scheme $\text{Bi}_2\text{WO}_6/\text{ZnIn}_2\text{S}_4$ Composite

Tawanwit Luangwanta¹, Auttaphon Chachvalvutikul¹, Sulawan Khaophon^{1,2,*}

¹ Department of Chemistry, Faculty of Science, Chiang Mai University, Chiang Mai 50200, Thailand

² Center of Excellence in Materials Science and Technology, Chiang Mai University, Chiang Mai, Thailand

Abstract:

In this research, $\text{Bi}_2\text{WO}_6/\text{ZnIn}_2\text{S}_4$ composite was synthesized by a facile modified wet-impregnation method for photocatalytic degradation of organic compounds (salicylic acid and methylene blue) in aqueous solutions and H_2 evolution. The synthesized samples were characterized by various techniques, including XRD, SEM, TEM, UV-vis DRS, XPS and BET methods. Effect of weight percentages (% wt) of the Bi_2WO_6 in the $\text{Bi}_2\text{WO}_6/\text{ZnIn}_2\text{S}_4$ composite on the photocatalytic activity was investigated. The $\text{Bi}_2\text{WO}_6/\text{ZnIn}_2\text{S}_4$ composite with 12.5 % wt of Bi_2WO_6 exhibited the highest photocatalytic degradation activity of the organic compounds, where 71.9% of salicylic acid and 98.6% methylene blue were degraded after exposure to LED light for 300 min. Moreover, the optimal 12.5% wt- $\text{Bi}_2\text{WO}_6/\text{ZnIn}_2\text{S}_4$ sample was capable of producing 7.91 μmol of H_2 after 180 min. The stability and reusability tests for hydrogen production were evaluated for practical applications. A direct Z-scheme charge transportation process between ZnIn_2S_4 and Bi_2WO_6 contact interface was revealed by the optical analyses and the radical trapping experiments. The enhanced photocatalytic activity of the $\text{Bi}_2\text{WO}_6/\text{ZnIn}_2\text{S}_4$ photocatalyst was due to the increased ability to absorb visible light, and the enhanced charge separation and transportation between Bi_2WO_6 and ZnIn_2S_4 through the Z-scheme mechanism. The $\text{Bi}_2\text{WO}_6/\text{ZnIn}_2\text{S}_4$ composite is a promising photocatalyst for treating organic pollutants in wastewater and producing hydrogen gas from water splitting.

Keywords: $\text{Bi}_2\text{WO}_6/\text{ZnIn}_2\text{S}_4$; heterostructure; Z-scheme; visible light

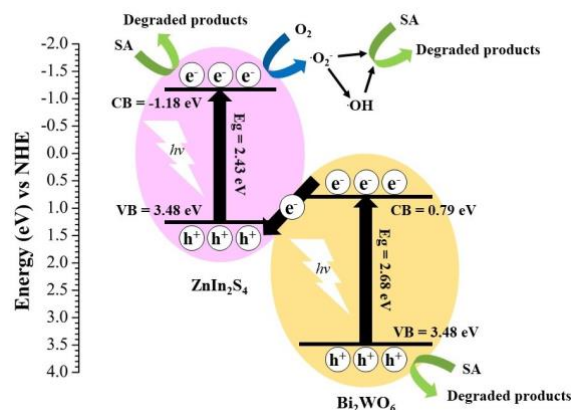


Figure 1: A direct Z-scheme charge transportation process between ZnIn_2S_4 and Bi_2WO_6 contact interface.

Application and Characterization of Polyethylene-Blended Polystyrene Nanofibrous Sorbents in the Removal of Crude Oil Spills

M. Alazab Alnaqbi, A. Al Blooshi, Y.E. Greish¹

¹United Arab Emirates University, Department of Chemistry, Alain, UAE

Abstract:

The combined advantage of polymer blends enables them to be generally identified to have enhanced properties over their respective pristine polymers. In the current work, hydrophobic polymers blends were prepared, characterized and evaluated for their efficiency in the removal of crude oil spills from aqueous media. The matrix polymer used is Polystyrene (PS), while polyethylene (PE) was blended with PS with proportions of 5-20 wt%. As shown by their scanning electron micrographs, blends were electrospun into beaded-free microfibers with interconnected porosities. The presence of PE increased the hydrophobicity of the blends' fibrous sorbents fabricated afterwards. Upon investigating their efficiency in the removal of crude oil spills, PE-PS blends showed superior sorption capacities when compared with pure PS blends' fibrous sorbents. The currently made fibrous sorbent were highly superior showing 5 times higher sorption capacity compared with commercially available polypropylene crude oil fibrous sorbent. These results indicate the potential of using fibrous sorbents made of PE-PS blends as sorbents for the removal of rude oil spills.

Keywords: polymer blends, polystyrene, polyethylene, electrospinning, crude oil sorption, nanofibrous sorbents

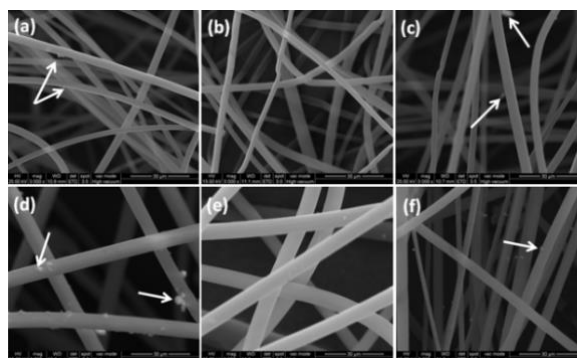


Figure 1: Figure illustrating the scanning electron micrographs of PE-PS fibrous sorbents containing 5 wt% (a,d), 10 wt% (b,e) and 20 wt% (c,f) of each of the additives.

References:

1. Markovic G, Visakh PM. Polymer blends: state of art. Recent developments in polymer macro, micro and nano blends: preparation and characterization, pp 1-15, 2017.
2. M. Alazab Alnaqbi, Y.E. Greish, M. Mohsin, E. J. Elumalai, A. Al Blooshi (2016) Morphological Variations of Micro-nanofibrous Sorbents Prepared by Electrospinning and Their Effects on the Sorption of TOTAL Crude Oil. J. Env. Chem. Eng., 4: 1850–1861

Nickel-Alumina and Zinc-Alumina Aerogels: Powerful Highly Porous Adsorbents for a Broad Spectrum of Toxic Effluents

M. Chaaban, J. Mallah, H. El-Rassy*

American University of Beirut, Department of Chemistry, Beirut, Lebanon

Abstract:

The numerous toxic effluents discharged nowadays in waterways from various sources without any prior treatment could seriously lead to several environmental and health problems. Among others, organic dyes, toxic metals, and inorganic anions represent major categories of these water pollutants. Although multiple physical, chemical, and biological processes are widely used to treat any contaminated water body, the physical adsorption at the solid-liquid interface remains as one of the easiest, efficient, and economically interesting technique since it does not require too much expertise by the end user when it comes to its implementation in wastewater treatment plants. We report herein the first use of alumina and metal-substituted alumina highly porous aerogels as adsorbents for these pollutants from wastewater. These highly porous materials were obtained via a fast and easy epoxide-initiated sol-gel process and dried under supercritical carbon dioxide conditions. The aerogels were later calcined at different temperatures and the effect of calcination on the chemical, structural, and surface properties of the aerogels was evaluated. The aerogels were texturally and structurally characterized before being tested for the removal of various azo-dyes and inorganic anionic species from simulated wastewater, where the effect on adsorption of the substitute metal, pH, temperature, calcination, and initial adsorbate concentration were investigated. The results revealed the outstanding potential of these aerogels for water remediation. We found also that the substitution of alumina by some other metals boosts the adsorption capacity of the aerogel. These materials showed higher adsorption capacities than most of the adsorbents reported in literature. For instance, the maximum monolayer adsorption capacity of Congo Red on nickel-substituted alumina aerogels was calculated to be 1660 mg.g^{-1} . A full thermodynamic and kinetic study was performed on these adsorbents.

Keywords: Aerogel, Alumina, Sol-Gel, Remediation, Adsorption, Wastewater, Toxic Effluents.

Biosynthesis of Clusters and Nanoparticles by extracellular electron transfer-capable bacteria and their application in catalysis

R. Jimenez-Sandoval,^{1*} S. Pedireddy,¹ P. Saikaly¹

¹ King Abdullah University of Science and Technology, Water Desalination and Reuse Center, Thuwal, Saudi Arabia

Abstract

The rising demands of global energy, environmental pollution from fossil fuel burning, depletion of fossil fuels, pressurize the scientific community to develop low-cost and efficient renewable energy technologies. Chemical method is the most commonly used for the synthesis of metal nanoparticle catalysts. However, this approach results in low yields, it is unsustainable, and generates large amounts of hazardous wastes. To overcome this situation, the biological approaches, which make use of renewable resources like bacteria, fungi, and plant extracts as source for reduction of metals, paves a clean and alternative route to traditional physical and chemical methods.

In this work, *Geobacter sulfurreducens* serves as the biological component to produce noble metal nanoparticles via reduction of metal precursors for electrocatalytic applications. For example monodispersed platinum cluster/nanoparticles are synthesized using, *Geobacter sulfurreducens* as a reducing agent (Figure 1). For electrocatalytic applications, we in-situ reduced graphene oxide on the surface of bacteria to confer a conductive surface. We performed detailed physicochemical characterizations to know the metal concentrations, visualize the metal nanoparticles and evaluated their electrochemical performance towards oxygen evolution reaction (OER) and hydrogen evolution reaction (HER). Moreover, these catalysts could be applied in wastewater treatment to catalyze the electrolysis of toxic organic wastes. This study will allow us to produce through biological synthesis electrocatalytic nanoparticles following the principles of green chemistry and will have the potential to substitute traditional catalysts.

Keywords: noble metal nanoparticles, electrocatalysis, *Geobacter sulfurreducens*, reduced graphene oxide, oxygen evolution reaction, hydrogen evolution reaction, biological synthesis, green chemistry.

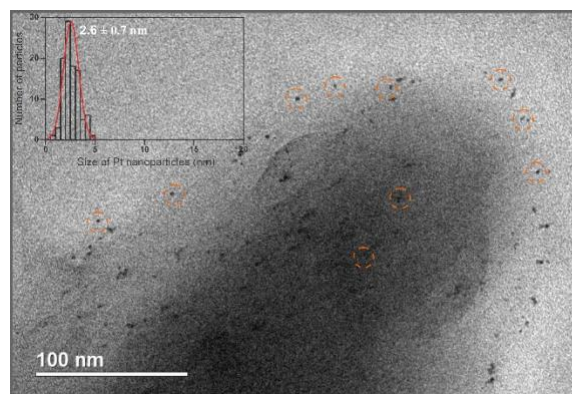


Figure 1: Transmission electron microscopy image of *Geobacter sulfurreducens*/Pt hybrid. This figure shows well dispersed platinum nanoparticles of 2-3nm of diameter in the outer membrane of *Geobacter sulfurreducens*.

References:

1. Sheldon, R. A., Arends, I. W. and Hanefeld, U. (2007). Introduction: Green Chemistry and Catalysis. In *Green Chemistry and Catalysis* (eds R. A. Sheldon, I. W. Arends and U. Hanefeld).
2. Singh, J., Dutta, T., Kim, K. H., Rawat, M., Samddar, P., & Kumar, P. (2018). 'Green' synthesis of metals and their oxide nanoparticles: applications for environmental remediation. *Journal of nanobiotechnology*, 16(1), 84.

Atomistic simulation of water pumping and desalination process through carbon nanotubes using Rayleigh traveling waves

A. Zhuldassov¹, N. Zhakiyev¹, Z. Insepov^{1,2,3*}

¹ Nazarbayev University, Nur-Sultan, Kazakhstan

² Purdue University, West Lafayette, IN USA

³ National Nuclear Research University (MEPhI), Moscow, Russia

Abstract:

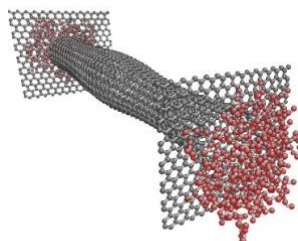
A nanopumping method proposed for simple atomic gases in our previous paper [1] was further applied to a system containing water molecules and salt ions. Hydrated ions have a bigger mass than water molecule that can prevent ions from pumping through CNT under surface acoustic waves.

Water molecules can pass through tube at very high flow rates due to smooth and hydrophobic inner walls of CNTs. By applying various Rayleigh wave frequencies, an optimal salt rejection and high water flow rate mode have been obtained. The new water pumping concept seems to be more energy efficient than that based on a traditional reverse osmosis desalination via 2-dimensional membranes.

Atomistic modeling and simulation of nanofiltration process was carried out using large scale atomistic/molecular massive parallel simulation (LAMMPS) software package [2]. Armchair CNTs with chirality (10, 10), lengths (10^2 - 10^4 Å) and radius of 13.5 Å were used for simulation. TIP3P water potentials used for modeling water molecules and salt ions Na^+ and Cl^- were used for modeling water desalination process under the Rayleigh waves (Fig. 1). CHARMM interatomic potentials were used for salt ions, with cutoff potential radius 10 Å. Electrostatic interactions were described by Ewald summation method [3]. An NVE ensemble was used to solve the equations of motion.

The traveling waves ranged was from 1 to 50 THz, with periodic conditions along the Z axis. The water flow rate and velocities were calculated and compared with the results of other pumping methods [4, 5].

Keywords: CNT, water nanopumping, desalination, surface acoustic wave, LAMMPS.



Time = 1 ns

Figure 1. Process of water transportation in CNT actuated by surface acoustic wave after 1 ns.

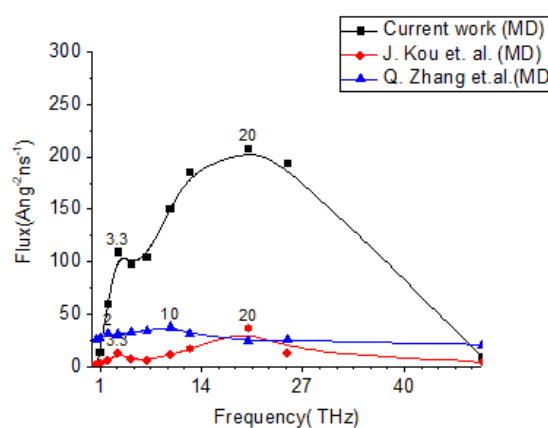


Figure 2. Comparison of our results with other works [4, 5].

References:

1. Z. Insepov, D. Wolf, A. Hassanein, Nano Lett, 6, 1893-1895 (2006).
2. <http://lammps.sandia.gov/>
3. A.D. MacKerell, "Atomistic Models and Force Fields" in Comput. Biochem. and Biophys., Dekker Inc. NY, p. 7-38 (2001).
4. J. Kou, H. Lu, F. Wu et al, Electricity Resonance-Induced Fast Transport of Water through Nanochannels, Nano Lett. 14, 4931-4936 (2014).
5. Q. Zhang, W. Jiang, J. Liu, et al, Water transport through carbon nanotubes with the radial breathing mode. Phys. Rev. Lett. 110, 254501 (2013).

Water pumping through microchannels

Z. Ramazanova¹, N. Zhakiyev¹, K.B. Tnyshtykbayev³, Z. Insepov^{1,2,3*}

¹ Nazarbayev University, Astana, Kazakhstan

² Purdue University, West Lafayette, IN USA

³ National Nuclear Research University (MEPhI), Moscow, Russia

Abstract:

Experimental results and finite element modeling were presented on water actuation via a sub-millimeter thin tube by surface acoustic waves (SAW). Basic principles of water actuation techniques for water transport in micron scale tubes are discussed. In experiment, the tube walls were exposed the frequency of acoustic waves of 27 kHz that showed a substantial increase in the flow rate of water and fountaining at a resonant frequency. Experimental observations of acoustic streaming and pumping effects via sub-millimeter tubes were confirmed by numerical finite-element simulations of water flows under acoustic waves.

It was observed that for the same values of the immersion depths of the tubes, the water level increased with the decreasing of the tube diameter. For the full range of diameters there was a local maximum of water level at the immersion depth.

As input data in the simulation model, the following parameters were specified: a frequency of the wave, sound speed in water, the radius of the tube; and the density of liquid. The flow rate and the mean flow velocities in the inlet and outlet openings were evaluated in the calculations and compared with experiment.

Keywords: water actuation technique, acoustic pressure, finite element modeling, liquid pumping.

**Nanotech / Biotech Joint
Session III.A:
NanoBioApplications /
Nanosafety**

Magneto-Plasmonic Nanoparticle Based-Approaches for Cancer Treatment: Therapy and Biodegradation

A. Abou-Hassan

Sorbonne Université, CNRS, Physico-chimie des Electrolytes et Nanosystèmes Interfaciaux, F-75005 Paris, France

Abstract:

The use of multi-functional therapeutic modalities in a single nanostructure has become an important and promising strategy to combined tumour targeted-therapy and imaging, which offer great promise for the future of cancer prevention, diagnosis and treatment. Moreover, these multi-approaches can also offer new insights to overcome limitations of current cell therapies tools. Thermal nanotherapies are non-invasive approaches for tumor ablation, where localized heat generation is mediated by magnetic and photothermal nanomaterials. However, the intended therapeutic application requires optimal heating efficiency in the intratumoral environment, where cellular confinement effects play an important role in the final heat-generating performance. Here, we proposed combined therapeutic approaches based on nanothermal treatments and photoactivatable therapies combined on a single magneto-plasmonic nanohybrid. We show that heating is cumulative when combining both modalities into a single nanohybrid and the efficiency is maintained even in Vivo. Moreover, as one of the most challenging issues of tomorrow's nanomedicine is the long-term fate of nanomaterials once they have completed their mission in the biological environment. We have investigated the intracellular biotransformations of these nanomaterials through the study of their physical and chemical modifications at the nanoscale over the time in a 3D tissue model. We demonstrated clearly using microscopic metrics correlated at the nanoscopic level by other analysis methods the shielding effect of gold protecting iron oxide cores from biodegradation.

Keywords: magneto-plasmonic nanohybrids, magnetic hyperthermia, photothermal therapy, bimodal therapy, cellular degradation

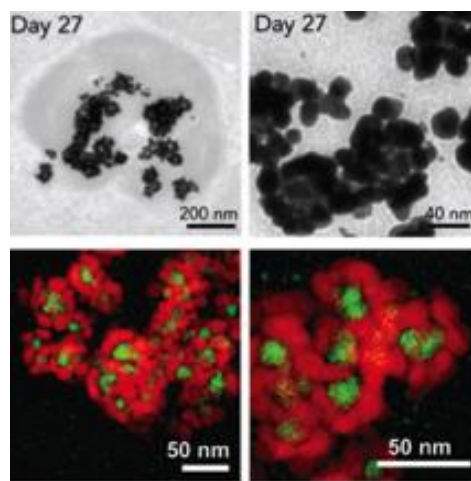


Figure 1: TEM and STEM-EELS maps during the degradation of the magneto-plasmonic iron oxide@Au nanohybrids on day 27 inside endosomes.

References:

1. A. Espinosa, M. Bugnet, G. Radke, S. Neveu, G. Botton, C. Wilhelm, A. Abou-Hassan, *Nanoscale*, 7, 18872-18877.
2. F. Mazuel, A. Espinosa, G. Radtke, M. Bugnet, S. Neveu, Y. Lalatonne, G.A. Botton, A. Abou-Hassan, C. Wilhelm, *Advanced Functional Materials*, 27, 1605997
3. A. Curcio, A. K. Silva, S. Cabana, A. Espinosa, B. Baptiste, N. Menguy, C. Wilhelm C, A. Abou-Hassan, *Theranostics*, 9, 288-1302

Aerosol dynamics and dispersion modelling for workplace nanoparticle exposure

Miikka Dal Maso^{1,*}, Alexander Christian Østerskov Jensen², Niko Leskinen¹, Ismo K Koponen³

¹Tampere University, Aerosol Physics Unit, Tampere, Finland

²Now at: Scania AB, Stockholm, Sweden

³Now at: Force Technology, Copenhagen, Denmark

Abstract:

Occupational and environmental exposure to aerosol particles are much-studied field of study. Strongly localized particulate matter sources require careful characterization, and both the aerosol concentration and size distribution vary temporally and spatially with the workplace activities. In many cases, background aerosol is present which further complicates the picture. [1]. Adding to such heterogeneous sources, several aerosol processes such as coagulation, agglomeration, diffusional deposition, and gravitational settling affect the evolution of the aerosol number size distribution in the workplace. It is also likely that that gas-phase vapour compounds condense or partition to the particle phase, changing its composition and toxicity.

Quantification of aerosol exposure requires understanding of the particle size distribution, because deposition to the respiratory system is a particle size-dependent process. Understanding the dispersion and dynamic evolution of the aerosol size distribution once it has been released requires simultaneous solving of the aerosol general dynamic equation (GDE)[2] and dispersion equations. This usually requires discretization or making some assumptions and simplifications, for example regarding the mixing and dilution of the room or its compartments [3], or using simplifying parameterizations in the case of particle coagulation and aggregation [4].

Here, we will present comparisons of different modelling approaches (Gaussian dispersion[5], the near field/far field model, and multicompartment modelling[6], see Fig 1.) for workplace sources, and discuss their applicability for detailed aerosol dynamics modelling and for estimating both workplace concentrations and assessment of personal exposure. We will also discuss methods and model sensitivity to including particle size information and conversion between mass, surface, and number-based metrics.

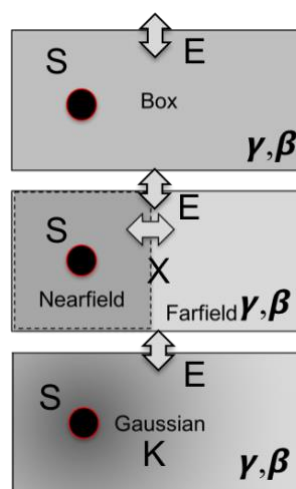


Figure 1: Modelling the dispersion of an aerosol. Top: a single-box model; middle: a two-box (NF/FF) model; bottom: Gaussian dispersion. S refers to the source, E and X to air exchange, K to turbulent diffusion. γ and β are parameters for to aerosol dynamics.

We will discuss considerations that should be made when choosing the modelling approach, and the sensitivity of the models to different parameters, especially in case of source characterization.

Keywords: aerosol modelling, workplace aerosol, exposure assessment

References:

1. Brouwer, D. et al., *Toxicology* 2010, 269, 120–127.
2. Seinfeld & Pandis, *Atmospheric Chemistry and Physics*, Wiley, 1998
3. Jensen, A. C Ø, et al., *Environments*, 5(5), 52, 2018
4. Lehtinen, K. E. J., et al., *J. Coll. Int. Sci.* 1996, 182 (2) , 606–608.
5. Cheng, K.-C. et al *Environmental Sci & Tech* 2011, 45 (9): 4016–4022.
6. Jensen, A.C.Ø, et al., *Aeros. Air Qual. Res.*, 2019, doi: 10.4209/aaqr.2018.08.0322

Bio-inspired Single-Molecule Electrical Contacts

I. Díez-Pérez,^{1,2,*} A. C. Aragonès¹, M. Ruiz,¹ E. Ruiz², J.C. Cuevas³, R. Perez³, G. Vilhena³, Linda A. Zotti³

¹ Department of Chemistry, Faculty of Natural & Mathematical Sciences, King's College London, Britannia House, 7 Trinity Street, London SE1 1DB, United Kingdom

² Institute of Theoretical and Computational Chemistry, University of Barcelona, 1 Marti i Franques, Barcelona 08028, Spain

³ Departamento de Física Teórica de la Materia Condensada C5, Universidad Autónoma de Madrid, Spain

Abstract:

Bioelectronics is rapidly moving towards designing nanoscale electronic platforms that allow *in vivo* determinations. Such devices require interfacing a complex biomolecular moiety as the active sensing unit to an electronic platform for signal transduction. Inevitably, a true systematic design goes through a bottom-up understanding of the structurally related electrical signatures of such hybrid biomolecular circuits, which will ultimately lead us to tailor its electrical properties and exploit them as high performance bioelectronic devices with a wide variety of applications in organic electronics, sensing, biomanufacturing, *etc.*

In this contribution, we will present our latest efforts to try to understand and control charge transport in a single-protein junction. The first part of the contribution will consist on a quick survey on how we build electrical connections with individual molecules between two macroscopic metal electrodes under near physiological conditions. Here we will particularly focused on new methodologies to trap redox proteins in a tunneling junction in a more “gentle” manner [1,2]. Then the presentation will move on to the main core where we will try to show the feasibility to study charge transport in a single-protein junction using a simple redox protein model such as a bacterial blue Cu-Azurin. We will start showing the main observed electrical signatures of these systems that make them particularly efficient in translocating charge as compared to any other synthetic macromolecular homologous. We will then move to our latest results where we start bioengineering the outer protein surface through point-site mutagenesis to try to understand the transport mechanisms through the protein backbone. It is suggested that such modifications allow us tuning the

extension of the electrical coupling between the protein and the metal electrodes [3]. These latest results are slowly leading us towards paving the way to rationally design the protein/electrode communication in a nanoscale hybrid bioelectronic device. The contribution will conclude by showing how our novel approach that might help in the future to understand complex biomolecular functions such as enzymatic catalysis. In particular, the concept of *electrostatic catalysis* of a well-known coupling reaction is demonstrated in a single-molecule junction [4].

Keywords: protein conductance, single-protein junctions, bioengineered protein wires, transport mechanisms in redox proteins

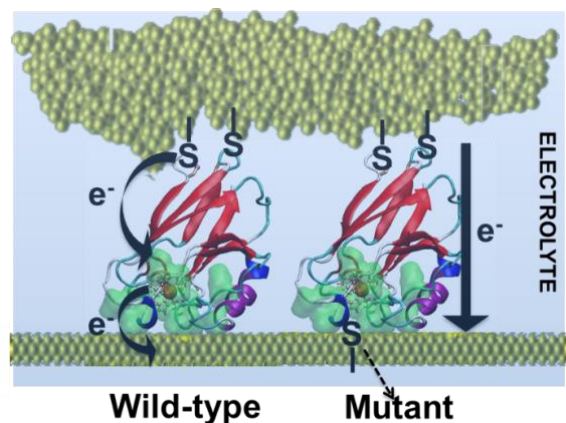


Figure 1: Schematic representation of a single protein junction of wildtype and mutant variants of a Cu-Azurin. The charge transport is modulated from 2-step sequential tunneling to an off-resonant coherent tunneling.

References:

1. Díez-Pérez *et al.* Nat. Chem. 1, 635 (2009)
2. A.C. Aragonès *et al.* Nano Letters 14, 4751 (2014)
3. M.P. Ruiz *et al.* JACS 139, 15337 (2017)
4. A.C. Aragonès *et al.* Nature 531, 88 (2016)

Cleaning, activation and coating nanotechnologies for functional surfaces in food processing

K. Horn,^{1*} M. Fröhlich,² C. Stancu,²

¹ INNOVENT e.V., Technology Development, Jena, Germany

² Leibniz Institute for Plasma Science and Technology Greifswald, Germany

Abstract:

Food production today is one of the major industries worldwide. The basis for meeting the demand for foodstuffs are, in addition to natural raw materials and processing formulas, suitable technologies. These technologies are designed to meet the requirements of good shelf life and perfect hygienic and health aspects while at the same time preserving important natural characteristics of the food. There is a great need for technologies for the technical design and care / maintenance of production facilities and the production environment as well as food packaging. Product-friendly surface modifications play an important role and can be realized by means of atmospheric plasmas, flame treatment and sol-gel coating. Fine cleaning and antibacterial treatment as well as nano-coatings allow e.g. a hygienic production environment, barrier coatings for corrosion protection and as gas barrier, easy-to-clean properties and labeling functionalities (Figure 1). In this study noted technologies incl. application examples are presented. The focus is on work within the Surface4Food network and the CleanBand project, which emerged from the network. The Network Surface4Food unites research institutes, companies and institutions with the overlying goal of enhancing surfaces in the food industry production and processing procedures using innovative surface technologies to allow for more efficient and effective cleanability and have a prophylactic effect against recontamination. The CleanBand project investigated new possibilities for antimicrobial surface treatment of conveyor belts in the food industry (Figure 2). Herein the focus was on shortening downtimes in production due to time-consuming and chemical-intensive cleaning cycles and on the sealing and antibacterial finishing of customized cut edges of the conveyor belts to extend the service life.

Keywords: atmospheric pressure plasma, PYROSIL®, CVD coating, Sol-Gel technology,

barrier coatings, silica-based marker coatings, inline functionalization, antibacterial applications, healthcare.



Figure 1: local hydrophil/hydrophob surface functionalization preparing antibacterial and easy-to-clean properties.

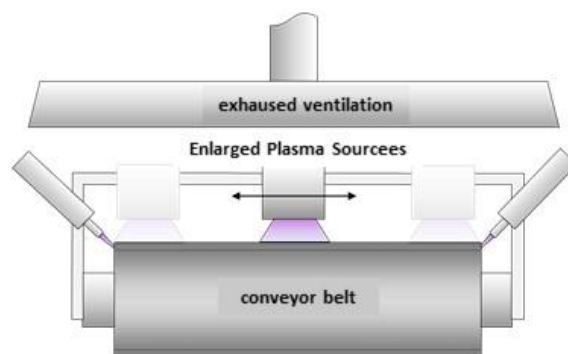


Figure 2: Technical solution for an inline module to be developed in the project for the cleaning, disinfection and coating of conveyor belts.

References:

1. Beier, O., Pfuch, A., Horn, K., Weisser, J., Schnabelrauch, M., Schimanski, A. (2013) Low Temperature Deposition of Antibacterially Active Silicon Oxide Layers Containing Silver Nanoparticles, Prepared by Atmospheric Pressure Plasma Chemical Vapour Deposition, *Plasma Process. Polym.* 10, 77–87
2. Gerullis, S., Pfuch, A., Spange, S., Kettner, F., Plaschkies, K., Küzün, B., Kosmachev, V. P., Volokitin, G. G., Grünler, B. (2018) Thin antimicrobial silver, copper or zinc containing SiO_x films on wood polymer composites (WPC) applied by atmospheric pressure plasma chemical vapour deposition (APCVD) and sol-gel technology, *Eur. J. Wood Prod.* 76, 229

Gadolinium-loaded liposome safety: *in vitro* study in human liver cells and macrophages

P.Šimečková,¹ F. Hubatka,² J.Slavík,¹ O.Kováč,¹ J.Neča,¹, P.Turánek-Knötigová,² J.Mašek,²
K.Pěňčíková,¹ J.Procházková,¹ J.Turánek,² M.Machala,¹

¹Department of Chemistry and Toxicology and ²Department of Pharmacology and Immunotherapy, Veterinary Research Institute, Brno, Czech Republic

Abstract:

Gadolinium-based contrast agents (GBCA) are extensively used for magnetic resonance imaging. Gadolinium is chelated in relatively stable complexes, and thus believed to be non-toxic. However, recently, GBCA have been shown to induce side effects, such as nephrotoxicity, neurotoxicity and hepatotoxicity. Liposomes are studied as potential carriers of both magnetic resonance contrast agents, including gadolinium, and drug molecules, such as thrombolytic agents. Therefore, liposomes can serve as diagnostic as well as theranostic agents for imaging and treatment of various pathological states and illnesses including stroke. They also

exhibit favourable platform for a new generation of targeted diagnostic and theranostic systems.

As compared to low molecular gadolinium complexes, the biodistribution of gadolinium chelates formulated into liposomes can significantly differ after their administration to the patients. Therefore, a more intensive study of potential toxicological effects of gadolinium formulations on different organs and cell types including liver cells and immune cells seems to be necessary.

In this study, liposomes containing PE-DTPA gadolinium chelator were tested for its potential toxicological effects.

The cytotoxicity of gadolinium-loaded nanoliposomes (Gd-L) was tested by neutral red uptake in human liver cancer Hep G2 cells, liver progenitor (non-differentiated) HepaRG cells and HepaRG cells differentiated into two cell populations, hepatocyte-like and biliary epithelial cells, which is a liver model closest to primary hepatocytes and well established model for drug-induced human hepatotoxicity studies. The concentration of gadolinium ranged between 1 μ M and 100 μ M, and we found no cytotoxicity up to 72 h. Next, we used complex system of general biomarkers of toxicity, including induction of early response genes, heat shock, ER stress, oxidative stress, and DNA damage

responses and modulation of xenobiotic-metabolizing enzymes. Differentiated HepaRG cells were exposed to Gd-L (total lipid concentration 25 μ g/ml) for 24 h and changes in mRNA expression were measured by RT-PCR. Finally, pro-inflammatory effects of Gd-L were studied. The amount of eicosanoids released from HepaRG, exposed to Gd-L, into the cultivation medium was determined by LC/MS-MS. Activation of inflammasome was detected using activated THP1 (model human macrophages).

We did not detect any changes in any tested parameters, which indicates that Gd-L were not toxic to liver HepaRG cells, also, that they not induce inflammasome activation. In conclusion, we established a complex system highly suitable for *in vitro* identification of major possible toxic responses with possible implications in evaluation of nanosafety.

Acknowledgement: This project was supported by the Ministry of Education, Youth and Sports OPVVV PO1 project "FIT" (Pharmacology, Immunotherapy, nanoToxicology), no. CZ.02.1.01/0.0/0.0/15_003/0000495 (JT) and the Ministry of Health CZ AZV-ČR 16-30299A (JT, JM).

Keywords: gadolinium, liposomes, MRI, nanotoxicity, cytotoxicity, early response genes, heat shock response, ER stress, oxidative stress, DNA damage, inflammation, CYPs.

Fabrication of Layer-by-Layer Bionanocomposite Scaffold for *In-vitro* Skin Regeneration after Chronic Burns

F. El-Shishiny,¹ W. Mamdouh^{1*}

¹The American University in Cairo (AUC), Department of Chemistry, School of Sciences and Engineering, Cairo, Egypt

Abstract:

Skin burn wounds is a definitive issue that can affect a patient's life quality and may drive to Disability-Adjusted Life-Years (DALYs) and cause of death in chronic cases. WHO reported annual global death of 265,000 patients due to skin burns that often take place in low and middle-income countries. This study aims to fabricate novel tri-layered asymmetric porous bio-nanocomposite that can mimic the natural skin layers. The upper layer is composed of a nano-fibrous mat and imitative the skin epidermal layer and protects against a wide range of pathogens strains. While the lower layer is in the form of xerogel and mimics the skin dermal layer and provides physical support. Both layers are stick together using effective natural adhesive material that can keep the whole fabricated scaffold intact and stable. A consistent characterization was performed for each layer individually using specific standard techniques. Structural morphology was analyzed using scanning electron microscopy and image j that revealed the existence of significant pore distribution among the electrospun and xerogel layers confirmed by the method of Brunauer-Emmett-Teller. Chemical and functional groups of the utilized components were confirmed using fourier transform infrared spectroscopy. The innovated scaffold exhibited promising swelling capacity that appropriates for absorbing wound exudates, followed by constant biodegradability over time ($P < 0.0001$). Nearly 98% of the *in-vitro* induced gap was healed in the presence of the three scaffold asymmetrical layers using mouse embryonic fibroblasts. The innovated asymmetric scaffold reveals promising biological features for skin regeneration after chronic burns with potential for clinical applications.

Keywords: skin burns, third-degree burns, wound healing, nanofibers, xerogels, biocomposite, scaffold, tissue-engineered skin, tissue culture, biomedical applications.

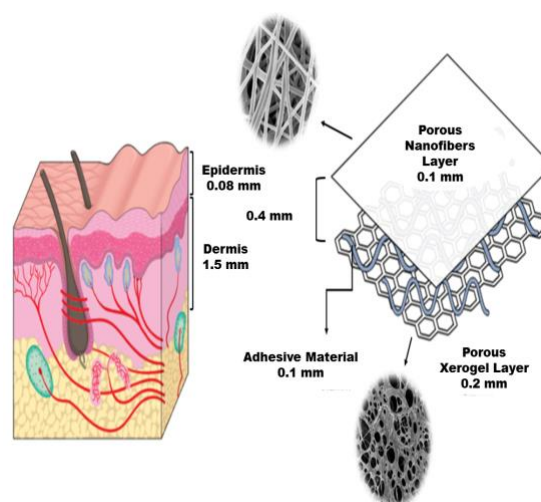


Figure 1: Figure illustrating the engineered design of tri-layered asymmetric porous bio-nanocomposite scaffold that mimics the natural skin layers. The upper layer consists of the porous nanofibrous sheet with an average thickness of 0.1mm. The lower layer constitutes of the xerogel mat with an average thickness of 0.2 mm. The middle layer is composed of an adhesive material (0.1mm). The whole scaffold was engineered to a thickness of 0.4 mm to facilitate the taken by the normal skin.

References:

1. Dias, J. R., Granja, P. L., & Bártolo, P. J. (2016). Advances in electrospun skin substitutes. *Progress in Materials Science*, 84, 314-334.
2. Kheiri, A., Amini, S., Javidan, A. N., Saghafi, M. M., & Khorasani, G. (2017). The effects of *Alkanna tinctoria* Tausch on split-thickness skin graft donor site management: a randomized, blinded placebo-controlled trial. *BMC complementary and alternative medicine.*, 17(1), 253.

NanoMatEn - Session III.B: Nanomaterials for Clean and Sustainable Technology

Nanoscaled Structure Determination of Functional Materials

Shin-ichi Shamoto^{1*}

¹ Japan Atomic Energy Agency, Advanced Science Research Center, Tokai, Japan

Abstract:

Many functional and industrial materials have been tailored in nanoscales from thin films to bulk materials. Some of them are composed of multi-phases in nanoscales. Traditional solder is a typical example with various ingredients for a specific application. They usually contain local strains due to the multi-phases and disorders. Even a single phase suffers the disorders from the strains by dopings. These disordered local structures closely related to their functional physical properties, based on the electronic structure modifications. The current nanoscience challenges standard crystallographic analysis based on a space group, which fails to observe the specific disorders in the crystal structures. Here, two methods will be introduced. One is the atomic pair distribution function analysis by using traditional total scattering [1]. This method has often been used for amorphous materials. The other is the surface structure analysis of single layer materials by using total-reflection high-energy positron diffraction (TRHEPD) [2]. The high sensitivity to a surface structure enables the single unit cell structure determinations such as a single unit cell β -FeSe superconductor (Figure 1) [2]. Although the bulk β -FeSe has low superconducting transition temperature T_c of 6 K, high- T_c above 60 K has been reported in a single unit cell β -FeSe [3]. Our analysis reveals that the single unit cell is strongly compressed along the normal direction of Fe layer [2]. The asymmetric Fe-Se layer heights are possibly optimized in average.

Keywords: Nanoscale materials characterization, Atomic pair distribution function analysis, Total-reflection high-energy positron diffraction, Neutron scattering, High- T_c iron-based superconductor.

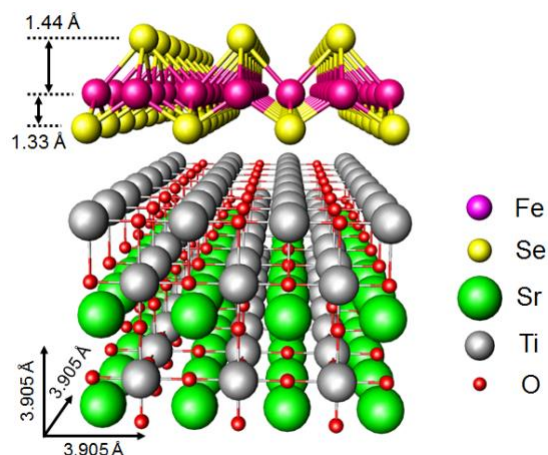


Figure 1: Surface structure of 1 unit cell FeSe on a SrTiO₃(001) substrate determined by TRHEPD [2]. Red and yellow spheres indicate Fe and Se atoms respectively. Green, silver, and red spheres are Sr, Ti, and O atoms, respectively. The asymmetric displacements of top-Se atoms are magnified by 1.5 times for clarity.

References:

1. S. Shamoto (2019), Local Structure in Functional Solids, *J. Phys. Soc. Jpn., Special Issue "New Frontiers in Physics with Spin, Orbital, and Atomic Correlations Studied by Neutron Scattering"* in press.
2. Y. Fukaya, G. Zhou, F. Zheng, P. Zhang, L. Wang, Q.-K. Xue, S. Shamoto (2019), Asymmetrically optimized structure in a high- T_c single unit-cell FeSe Superconductor, *J. Phys. Cond. Mat.* 31-5, 055701.
3. S. He, J. He, W. Zhang, L. Zhao, D. Liu, X. Liu, D. Mou, Y.-B. Ou, Q.-Y. Wang, Z. Li, L. Wang, Y. Peng, Y. Liu, C. Chen, L. Yu, G. Liu, X. Dong, J. Zhang, C. Chen, Z. Xu, X. Chen, X. Ma, Q. Xue, & X. J. Zhou, (2013), Phase diagram and electronic indication of high-temperature superconductivity at 65 K in single-layer FeSe films. *Nature Mater.* 12, 605-610.

Micro- and nanometer scale Cu(In,Ga)Se₂ for photovoltaic devices

Sascha Sadewasser

International Iberian Nanotechnology Laboratory, 4715-330 Braga, Portugal

Abstract:

Cu(In,Ga)Se₂ (CIGSe) is used as absorber layer in thin film solar cells with the highest efficiencies. However, the scarce elements In and Ga raise concerns for their large-scale deployment. We present results on the development of device concepts employing micro and nanometer scale structures of CIGSe allowing materials savings and/or efficiency improvements.

Ultra-thin CIGSe solar cells were realized introducing a point-contact passivation layer, consisting of a thin Al₂O₃ on the Mo back contact and with a regular hole pattern (~200 nm). An increase from 8% to 11.8% for devices with only 240 nm thick absorber layer was achieved [1,2]. On the other hand, micro-scale CIGSe islands were electro-deposited into holes in a SiO₂ matrix and completed into solar cell devices [3], which can be used as micro-concentrator solar cells by adding a micro lens array.

CIGSe nanowires growing on top of a polycrystalline base layer were prepared by co-evaporation. This composite structure is interesting for improved light absorption [4]. We also prepared CIGSe quantum dots (QDs) using migration-enhanced epitaxy on GaAs(111)A substrates. Transmission electron microscopy confirmed their epitaxial growth with the (112) plane of CIGSe parallel to the (111) plane of GaAs. The QDs exhibit a pyramidal shape with four facets formed by {112} planes.

Keywords: protein folding, nanoporous sol-gel glasses, silica-based biomaterials, circular dichroism spectroscopy, surface hydration, crowding effects, micropatterning, biomedical applications.

References:

1. B. Vermang, J.T. Wätjen, Ch. Frisk, V. Fjällström, F. Rostvall, M. Edoff, P. Salomé, J. Borme, N. Nicoara, S. Sadewasser, *IEEE J. Photovoltaics* 4, 1644 (2014).
2. P.M.P. Salomé, B. Vermang, R.-Ribeiro Andrade, J.P. Teixeira, J.M.V. Cunha, M.J. Mendes, S. Haque, J. Borme, H. Aguas, E. Fortunato, R. Martins, J.C. Gonzalez, J.P. Leitão, P.A. Fernandes, M. Edoff and S. Sadewasser, *Adv. Mater. Interf.* 5, 1701101 (2018).
3. S. Sadewasser, P. Salomé, and H. Rodriguez-Alvarez, *Sol. Energy Mat. Sol. Cells* 159, 496 (2017).
4. H. Limborço, P.M.P. Salomé, J.P. Teixeira, D. Stroppa, R.-Ribeiro Andrade, N. Nicoara, K. Abderrafi, J. Leitão, J.C. González, and S. Sadewasser, *CrystEngComm* 18, 7147 (2016).

Nanomaterials: Towards New Application Opportunities in the Field of Energy

A. Taleb,^{1,2,*}

¹ Chimie ParisTech, PSL University, CNRS, Institut de Recherché de Chimie Paris, Paris, France

² Sorbonne université, 4 place Jussieu, Paris, France

Abstract:

Over the last century, the development of nanomaterial science provided new technological opportunities in different fields including energy, environment and health. These developments would suely contribute to the postfossil energy era. In fact, hybrid nanomaterials are uniquely positioned to offer the possibility to fine tune their properties, using their size, shape, functionalisation and assembly (Figure 1); in order to fit a specific application requirements. These new possibilities are not only limited to the optimization of existing properties, but go beyond to introduce and create new properties.

In this context, the energy sector would greatly benefit from these developments, and offer a new renewable, sustainable and friendly alternatives to fossil resources, which has been proven to be a serious threat to the future of the planet, through its contribution to global warming.

In this regard, and due to their properties, nanomaterials have been well explored to improve the energy conversion and storage efficiency.

In this study, we will introduce the new challenges faced by these new nanomaterials in the energy field. Furthermore, we will review the fundamentals and the most recent developments in the synthesis and characterization of nanomaterials, as well as their applications in the energy conversion by solar cells, and the storage in Li-ion batteries. In addition, we will show how this new class of materials hold the promise of enabling an optimized balance between: low-cost, high-efficiency requirements, smart renewable, clean energy harvesting as well as the storage.

Keywords: nanomaterials synthesis, nanomaterials characterizations, energy applications.

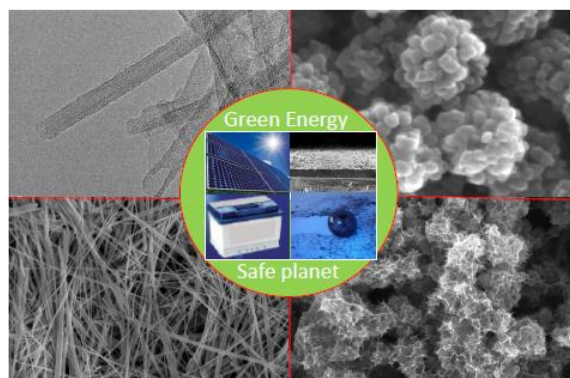


Figure 1: illustration of nanomaterials involved in different fields of energy.

References:

1. Taleb, A., Mesguich, F., Yanpeng, X., Colbeau-Justin, C., Dubot, P. (2016) Optimized TiO₂ nanoparticles packing for photovoltaic applications, *Solar Energy Materials and Solar Cells*, 148, 52.
2. Taleb, A., Mesguich, F., Yanpeng, X. (2014) Effect of cracking and aggregation on the efficiency of DSSC, *IEEE (IRSEC)*, 1-4.
3. Mehraz, M., Taleb, A., Światowska, J., Dubot, P., Bezzazi, B. (2019) Hydrothermal synthesis of TiO₂ aggregates as a negative electrode for lithium-ion batteries: the role of specific surface and pore size. submitted

Perovskite Solar Cells Based on Self-assembled Monolayer of Conjugated Polyelectrolyte as Hole-Extraction Material

Chi-Yuan Chang,¹² Wei-Che Wang,¹ Yang-Fang Chen,^{*12} Leeyih Wang^{*13}

¹ Center for Condensed Matter Sciences, National Taiwan University, Taipei 10617, Taiwan.

² Department of Physics, National Taiwan University, Taipei 106, Taiwan.

³ Institute of Polymer Science and Engineering, National Taiwan University, Taipei 10617, Taiwan

Abstract:

Stability and reproducibility are two major issues affecting the commercialization of solar cells. Herein, we adopted P3HT-COOH to replace PEDOT:PSS as the hole extracting material of perovskite solar cells. The measurement of photoelectron spectrometer indicated P3HT-COOH possesses a more desirable match of work function (-5.32 eV) to perovskite layer compared with PEDOT:PSS (-5.25 eV). Meanwhile, the more hydrophobic surface of P3HT-COOH induced the growth of perovskite crystals into a larger grain size, leading to the increment of J_{sc} from 17.11 to 20.68 mA/cm². This work also presents a facile method to prepare a homogeneous hole-extraction-layer simply through dipping the ITO substrate into the polyelectrolyte solution that greatly simplifies the fabrication process and reduces materials consumption. **Figure 1** depicts the contact angle and schematic representation of spin-coated and self assembled P3HT-COOH. The solar cell prepared from the traditional spin coating (SC-cell) process exhibited an average power conversion efficiency (PCE) of 17.01% with an open-circuit voltage of 1.04 V; on the other hand, the one from the self-assembled method (SA-cell) had a relatively higher PCE of 18.37% with an open-circuit voltage of 1.08 V. More importantly, the SA-cell possessed a small standard deviation of PCE (0.25%), which is apparently smaller than that (0.47%) of the SC-cell. Moreover, the former maintained more than 80% of its initial PCE after 1-month storage in a chamber with a relative humidity of ~55%.

Keywords: hole extraction material, perovskite solar cells, self-assembled monolayer, hole extraction material, stability.

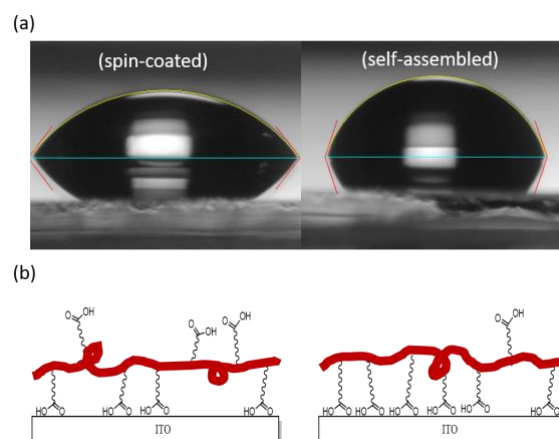


Figure 1: (a) Contact angle of deionized water on P3HT-COOH prepared by SP and SAM. (b) Schematic representation of spin-coated and self-assembled P3HT-COOH.

References:

1. W. Yan, S. Ye, Y. Li, W. Sun, H. Rao, Z. Liu, Z. Bian and C. Huang, 2016, **6**, 1600474.
2. Y. Wu, X. Yang, W. Chen, Y. Yue, M. Cai, F. Xie, E. Bi, A. Islam and L. Han, *Nature Energy*, 2016, **1**, 16148.

Nitrogen doped graphene as a filler in chitosan anion exchange membranes for ethanol fuel cell applications

M. Božič^{1,2}, B. Kaker¹, S. Hribernik^{1,2}, K. Stana-Kleinschek^{1,2,3}, E. Pavlica⁴, A. Motealleh⁵, S. Eqtesadi⁵, R. Wendellbo⁵, S. Jessie Lue⁶

¹University of Maribor, Faculty of Mechanical Engineering, Smetanova 17, 2000 Maribor, Slovenia, mojca.bozic@um.si

²University of Maribor, Faculty of Electrical Engineering and Computer Science, Koroška cesta 46, 2000 Maribor, Slovenia

³Graz University of Technology, Institute for Chemistry and Technology of Materials (ICTM), Stremayrgasse 9, 8010 Graz, Austria

⁴University of Nova Gorica, Laboratory of Organic Matter Physics, Ajdovščina, Slovenia

⁵Abalonyx AS, Forskningsveien 1, 0373 Oslo, Norway

⁶Chang Gung University, Department of Chemical and Materials Engineering, Kweishan, Taoyuan 33302, Taiwan

Abstract:

Direct alkaline ethanol fuel cells have recently received increasing attention since in principle they allow for the use of non-precious metal catalysts, which dramatically reduces the cost per kilowatt of power in fuel cell devices.¹ The heart of a DAFC is an anion exchange membrane (AEM) formed by sandwiching a multi-layered structure (i.e. anode diffusion layer, anode catalyst layer and AEM) between an anode and a cathode.

In this work, a series of novel nitrogen doped graphene oxide derivatives (N-GO) were successfully synthesized and blended with chitosan polymer in order to produce anion exchange composite membranes. To investigate their applicability in direct ethanol fuel cells, the membranes were characterized in terms of their structural properties, chemical and alkaline stability and ionic properties. The incorporation of N-GO suppressed ethanol permeability and improved ionic conductivity. Impedance analysis indicated that some hydrated membranes could exhibit a conductivity up to 0.08 S cm^{-1} . Newly developed membranes have been shown to exhibit potential for use in alkaline direct methanol fuel cell application.

Keywords: nitrogen doped graphene oxide, chitosan membrane, direct alkaline ethanol fuel cells

Acknowledgements

The authors would like to acknowledge the financial support received in the frame of M-era.NET program (NanoEIEm - Designing new renewable nano-structured electrode and

membrane materials for direct alkaline ethanol fuel cell - <http://nanoelmem.fs.um.si/>, grant number C3330-17-500098).

References:

1. Dekel D.R., (2018) Review of cell performance in anion exchange membrane fuel cells. *J Power Sources*, 375(31), 158-169.

Analytical Solution for Predicting Electrical Power Generation in Piezoelectric Thin Film Multilayer Energy Harvesting System

A. T. Nguyen,* Y. E. Pak

SUNY Korea, Department of Mechanical Engineering, Incheon, Korea

Abstract:

Piezoelectric multilayers have various application in high-performance sensors, actuators and energy damping systems [1,4]. Recently, a generalized analytical model of a piezoelectric multilayer having arbitrary crystal orientations under the influence of thermal expansion coefficient and lattice mismatches between the film layers has been derived [2,3]. This model provides a closed-form expression that predicts the curvatures and the normal strains of the piezoelectric multilayer in different growth orientation when subjected to externally applied mechanical and electrical loads [4]. In this research, the aforementioned model of piezoelectric thin films will be further expanded by including dynamic effects of the external loading conditions. As a result, an analytical dynamic model of a simple piezoelectric multilayer thin films system is obtained to predict the amount of energy harvested from the system due to external vibration. To simplify the problem, a bilayer of piezoelectric thin films deposited on a substrate that is subjected to a quasi-static harmonic excitation will be first studied, which will lay the foundation for the generalized analytical model for n-layer of thin films. By using the recursive relations, the derived formulations can model any number of layers, thus minimizing the computation time. The predicted strain and the electric field obtained from this model are to be confirmed by using Finite Element Method for some energy harvesting systems. A user-friendly MATLAB code based on the model will also be created for designers and engineers to quickly calculate the predicted performance of a piezoelectric energy harvesting device subjected to a given external vibration.

Keywords: energy harvestings, multilayer thin film, piezoelectricity, electroelastic fields, vibration

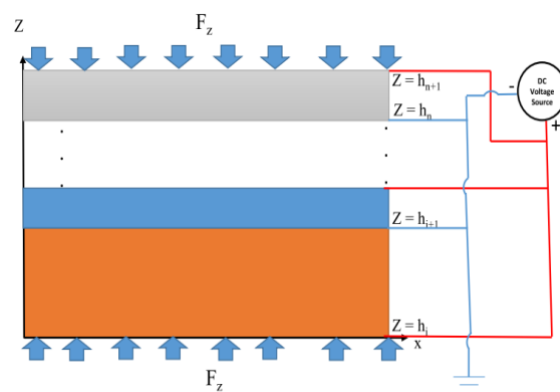


Figure 1: Schematic representation of piezoelectric multilayer beam under externally applied force and electric potential. [4]

References:

1. Ahn, J. H., Shin, D. J., Seo, C. E., Cho, K. H., Koh, J. H. (2016) Energy Gathering from the Multi-Layered Piezoelectric Energy Damping System Based on (Bi,Sc)O₃–(Pb,Ti)O₃ Ceramics. *J. Nanosci. Nanotechnol.*, 16, pp. 12894-12896(3)
2. Gao, C., Zhao Z. and Li, X. (2015) Modeling of thermal stresses in elastic multilayer coating systems. *J. Appl. Phys.*, 117, 055305
3. Mishra, D., Lee, S. H., Seo, Y. and Pak, Y. E. (2017) Modeling of stresses and electric fields in piezoelectric multilayer: Application to multi quantum wells. *AIP Advances*, 7, 075306, 1-14
4. Mishra, D., Yoon, S., Seo, Y. and Pak, Y.E. (2018) Analytical Solutions of Electroelastic Fields in Piezoelectric Thin Film Multilayer: Applications to Piezoelectric Sensors and Actuators. (submitted to *Acta Mech.*)
5. Xu, T. B., Siochi, E. J., Kang, J. H., Zuo, L., Zhou, W., Tang, X. and Jiang, X. (2013) Energy harvesting using a PZT ceramic multilayer stack. *Smart Mater. Struct.*, 22, 065015
6. Zhao, S. and Ertuk, A. (2014) Deterministic and band-limited stochastic energy harvesting from uniaxial excitation of a multilayer piezoelectric stack. *Sens Actuators A Phys.*, 214, 58-65

Vanadium oxide nanosheets for flexible dendrite-free hybrid Al-Li-ion batteries with excellent cycling performance

Xuefei Gong, Pooi See Lee*

School of Materials Science and Engineering, Nanyang Technological University, 639798, Singapore
Email: pslee@ntu.edu.sg

Abstract

Although lithium (Li) ion batteries have been the focus of research in energy storage devices for the last decades and significant progresses have been made towards high energy densities and improved safety, the dendrites formation with lithium metal as anodes remains a persistent challenge. In contrast, aluminum (Al) ion batteries with Al anodes inherently possess the advantages of no dendrite growth and offer low cost option, which make Al-ion batteries attractive as an alternative to beyond Li-ion batteries. In addition, based on the three electron transfer redox reactions, Al delivers high volumetric and gravimetric capacities, and provides promising applications in cost-effective and large-scale energy storage systems. However, the development of Al ion batteries is restricted by the sluggish kinetics of Al^{3+} ions diffusion and insertion/extraction, due to the strong electrostatic force between intercalation framework of host materials and trivalent Al^{3+} ions. It can lead to decreased intercalation sites in host materials and consequently capacity decays quickly.

A concept of hybrid Al-Li-ion battery has been proposed, which utilizes the fast Li^+ ions intercalation/deintercalation into/from the cathode materials compared to Al^{3+} and Al stripping/deposition on the surface of aluminum anode due to higher redox potential of Al/Al^{3+} (-1.67 V vs. SHE) compared to Li/Li^+ (-3.04 V vs. SHE). Our approach circumvents the sluggish kinetics and maintains the dendrite-free formation of Al-ion batteries. Subsequently, a hybrid Al-Li-ion battery, composed of vanadium oxides nanosheets on carbon fibers as cathode, Al foil as anode and $[\text{EMIM}][\text{Cl}]/\text{AlCl}_3/\text{LiCl}$ as electrolytes, has been successfully fabricated. This hybrid battery delivered a high volumetric capacity of 32.5 mAh/cm^3 at a current density of 100 mA/cm^3 (based on the total volume of cathode including carbon fibers as current collectors) and maintains 21.5 mAh/cm^3 even at 1 A/cm^3 .

More impressively, the capacity could be retained 70.1% after 3000 cycles, much better than other Al-ion batteries reported. The excellent electrochemical performance could be attributed to the improved kinetics with the introduction of Li^+ ions into the electrolyte as well as the 3-D porous structures of cathode materials. Moreover, structural integrity under different bending conditions could be achieved. Therefore, this work demonstrates a safe, cost-effective and flexible hybrid Al-Li-ion battery that exhibits highly competitive advantages among various energy storage devices.

Posters Session I: Nanomaterials synthesis, characterization/Nanomet rology and properties

Magnetic Abrasive Polishing of Nano Film Coated Pyrex Glass Using Acoustic Emission

Hyo-Jeong Kim¹, Hee-Hwan Lee¹ and Seoung-Hwan Lee^{2,#}

¹Hanyang University, Graduate School, Department of Machine Design, Seoul, South Korea

²Hanyang University, Department of Mechanical Engineering, Ansan, South Korea

#Corresponding Author/E-mail: sunglee@hanyang.ac.kr, TEL: +82-31-400-5288

Abstract:

To apply amorphous (transparent conductive oxide, TCO) thin film to high end electronic devices including organic light emitting device (OLED) displays, surface finishing is important. For the surface uniformity of thin films with nanometer thickness, nanoscale ultra-precision machining, such as magnetic abrasive polishing (MAP), is necessary. In addition, to effectively monitor the polishing process, a sensing scheme with nanoscale sensitivity, e.g., acoustic emission (AE), is essential. The purpose of this research was to develop a practical methodology for the control of surface characteristics utilizing in-process monitoring of the nanoscale finishing of thin film coated surfaces. Using a specially-designed MAP and AE monitoring setup, experiments were carried out on indium-zinc-oxide (IZO)-coated Pyrex glass. Based on the results from preliminary experiments, three major polishing parameters (gap, rpm and abrasive size) were selected for the application of design of experiment (DOE) to the finishing setup. Both the AE rms and surface roughness values from the experiments were compared and examined using analysis of variance (ANOVA) (Figure 2-3). The experimental results demonstrate strong correlations between the AE (rms) signals and surface roughness variations during MAP. With the proposed scheme, controlled nano-finishing and in process monitoring of surface characteristics are feasible.

Keywords: IZO film, magnetic abrasive finishing, acoustic emission, surface roughness, analysis of variance.

References:

1. Wu, C. C., Wu, C. I., Sturm, J. C., Kahn, A. (1997). Surface modification of indium tin oxide by plasma treatment: An effective method to improve the efficiency, brightness, and reliability of organic light

emitting devices. *Applied Physics Letters*,70(11), 1348-1350.

2. Lee, H. H., Lee, S. H. (2017). Analysis of the Material Removal Rate in Magnetic Abrasive Finishing of Thin Film Coated Pyrex Glass. *Surface Review and Letters*, 24(supp01), 1850004.

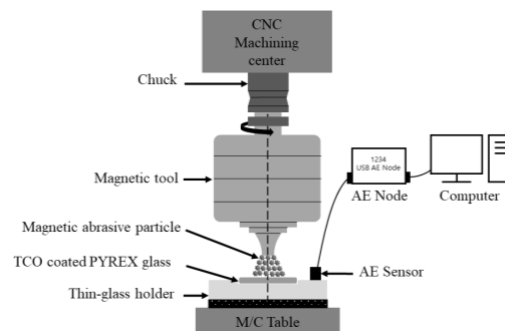


Figure 1 Schematic of polishing system

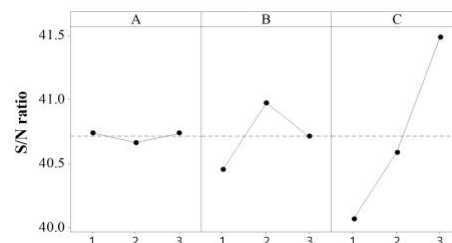


Figure 2 S/N ratio during MAP (Surface roughness (Ra), larger the better, 3 levels, A:RPM, B: Gap (mm), C: Particle size (μm))

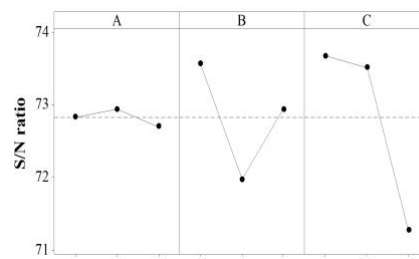


Figure 3 S/N ratio during MAP (AE RMS, smaller the better)

Citric Acid Coated Magnetic Iron Oxide Nanoparticles (Fe_3O_4): Synthesis, Characterization and Applications

E.A. Moacă,^{1,2,#} C. Farcaș,^{1,3,#} D. Coricovac,^{1,*} F. Loghin,³ C. Dehelean,¹ C. Păcurariu,²

¹“Victor Babes” University of Medicine and Pharmacy, Faculty of Pharmacy, Department of Toxicology and Drug Industry, Timisoara RO-300041, Romania

²Politehnica University Timisoara, Faculty of Industrial Chemistry and Environmental Engineering, Timisoara RO-300006, Romania

³“Iuliu Hatieganu” University of Medicine and Pharmacy Cluj-Napoca, Faculty of Pharmacy, Department of Toxicology, Cluj-Napoca RO-400012

dorinacoricovac@umft.ro

- E.A. Moacă and C. Farcaș contributed equally to this work

Abstract:

Magnetic iron oxide nanoparticles (MIONPs) obtained via the combustion method constitute the ideal raw material for the preparation of biocompatible magnetic colloidal suspension suitable for tumor cells hyperthermia approach, whose viability is known to be sensitive to mild hyperthermic treatment. The aim of the present study was: i) the development and characterization of a biocompatible magnetic colloidal suspension based on Fe_3O_4 nanoparticles coated with CA and ii) the *in vitro* assessment of Fe_3O_4 @CA nanoparticles under standard and hyperthermic conditions, on two distinct breast adenocarcinoma cell lines (MDA-MB-231; MCF-7) as well as a non-tumorigenic cell line (MCF-10A). The surface of magnetic nanoparticles (MNPs) has been functionalized by citric acid (CA) coating and easily dispersed in distilled water, leading to a stable biocompatible colloidal suspension. The surface functional groups of Fe_3O_4 @CA colloidal suspension were investigated by FT-IR. The biocompatible magnetic colloidal suspension was characterized in terms of dynamic light scattering (DLS), transmission electron microscopy (TEM) and magnetic measurements. The intensity distribution of the particle size suggests that the Fe_3O_4 @CA nanoparticles have a hydrodynamic diameter of 101 nm.

The results indicate that the uptake of Fe_3O_4 @CA into the cells was strongly enhanced under hyperthermic conditions. The usefulness of this MNPs as heat mediators being confirmed.

Keywords: magnetic iron oxide nanoparticles, combustion method, biocompatible colloidal suspension, cytotoxicity, Fe_3O_4 @CA cellular uptake, hyperthermia.

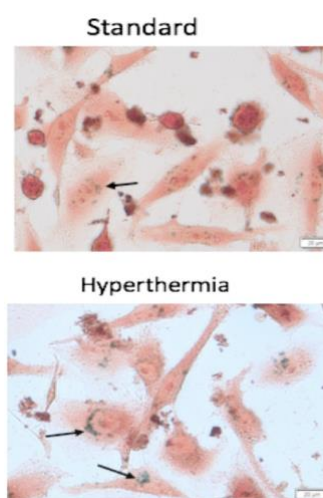


Figure 1: Cellular internalization of Fe_3O_4 @CA NPs inside MDA-MB-231 cells (indicated by black arrows) under standard and hyperthermic conditions. The cells were visualized by bright field microscopy, at magnification 40x.

Acknowledgement:

This work was supported by a grant of Ministry of Research and Innovation, CNCS-UEFISCDI, project number PN-III-P4-ID-PCE-2016-0765, within PNCDI III.

References:

1. Ianoș, R., Tăculescu, A., Păcurariu, C., Lazău, I. (2012) Solution Combustion Synthesis and Characterization of Magnetite, Fe_3O_4 , Nanopowders, *J. Am. Ceram. Soc.*, 95, 2236-2240.
2. Kobayashi T. Cancer hyperthermia using magnetic nanoparticles. *Biotechnol. J.* 2011, 6, 1342–1347.

High-Speed Sinter-Bonding of a Semiconductor Die by Addition of Ag Nanoparticles in 2-Micron Ag-coated Cu Particles

Sung Yun Kim, Eun Byeol Choi, Jong-Hyun Lee

Seoul National University of Science and Technology, Department of Materials Science & Engineering, Seoul, Republic of Korea

Abstract:

Ag-finish dies were attached on Ag-finish substrates through sinter-bonding at below 250 °C by addition of Ag nanoparticles in 2-micrometer Ag-coated Cu (Cu@Ag) particles for the attaining a bondline which do not melt or can sustain mechanical stability even at the temperature exceeding 300 °C, alike solder alloys. The nanoparticles were used with the aim of prompt filling of the spaces between the Cu@Ag particles during the sinter-bonding. The content of Ag in Cu@Ag particles was 20 wt.% and the average thickness of Ag shell was 256 nm. The average size of Ag nanoparticles was 100 nm, however, the nanoparticles were severely aggregated with large size deviation. After mixing with α -terpineol at a specific wight ratio of Cu@Ag particles and nanoparticles, the paste were printed on the substrate. The Ag shells in Cu@Ag particles were dewetted by instability at the interface of Ag layer/Cu core during heating for the attachment of a die, which was beneficial for the sinter-bonding. The added Ag nanoparticles were also sintered under reaction with the dewetted Ag, which induced significant enhancement in the density of bondline compared with that of bondline sintered only with Cu@Ag particles. Thus, the sinter-bonding speed was outstandingly faster than that of pure Ag or Cu particles, even though nanoparticles were added in usage of the pure particles. Consequently, sufficient shear strength exceeding 20 MPa was obtained even after short bonding for 30 s at 250 °C. The increase of added Ag nanoparticles from 20 to 40 wt.% strengthened adhesion at the bondline/substrate interface, resulting in the increase of shear strength.

Keywords: die attach, sinter-bonding, Ag-coated Cu particle, Ag nano-shell, Ag dewetting, Ag nanoparticles, shear strength.

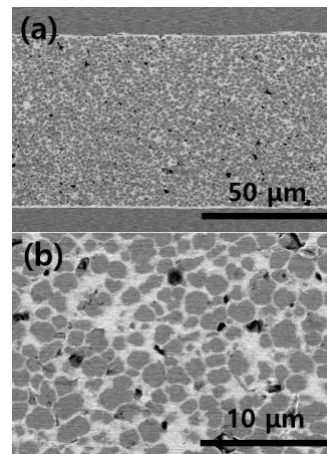


Figure 1: Cross-sectional BSE images showing a bondline between a Ag-finished die and substrate sinter-bonded at 250 °C for 30 s under 20 MPa using a mixture of 20 wt.% Ag-coated Cu particles and Ag nanoparticles at weight ratio of 8:2; (a) low and (b) high magnification.

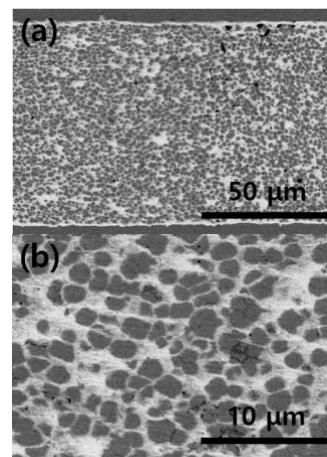


Figure 2: Cross-sectional images showing a bondline sinter-bonded at 250 °C for 30 s under 20 MPa using a mixture of 20 wt.% Ag-coated Cu particles and Ag nanoparticles at weight ratio of 6:4; (a) low and (b) high magnification.

References:

1. Lee, C.H., Choi, E.B., Lee, J.-H. (2018) Characterization of novel high-speed die attachment method at 225 °C using submicrometer Ag-coated Cu particles, *Scr. Mater.*, 150, 7-12.

Structural Development and Crystallization Kinetics of Bismuth Germanate Glass Embedded with Bi_2GeO_5 Crystals Prepared by the Modified Incorporation Method

S. Panyata,^{1,2} P. Intawin,¹ A. Kraipok,^{1,2} S. Eitssayeam,¹ T. Tunkasiri,¹ U. Intatha,³ K. Pengpat,^{1,*}

¹ Department of Physics and Materials Science, Faculty of Science, Chiang Mai University, Chiang Mai 50200, Thailand

² Graduate PhD's Degree Program in Materials Science, Faculty of Science, Chiang Mai University, Chiang Mai 50200, Thailand

³ School of Science, Mae Fah Luang University, Chiang Rai, 57100, Thailand

Abstract:

Newly ferroelectric crystal phases and glass matrices have been widely investigated in order to develop the properties of the materials that are suitable to perform in multifunctional purposes. The bismuth germanate system has provided many of interesting phases, such as $\text{Bi}_4\text{Ge}_3\text{O}_{12}$, $\text{Bi}_{12}\text{GeO}_{20}$ and Bi_2GeO_5 , which possess valuable properties. In the field of ferroelectric, glass-ceramic embedded with Bi_2GeO_5 crystals is one of particular interest as it has a high probability of being ferroelectric as reported for the first time by Pengpat and Holland. However, the formation of Bi_2GeO_5 phase exhibited the surface crystallization. It was determined that the crystallites formed a one-dimensional growth of crystals during the crystallization process. This type of crystal growth may not be preferable due to its anisotropic property. In this work, we have an attempt to fabricate and modify bulk crystallization of glass ceramics based on bismuth germanate containing Bi_2GeO_5 crystals. Glasses have been prepared from $\text{BiO}_{1.5}\text{-GeO}_2\text{-BO}_{1.5}$ ternary glass system on the region of $58.4\text{BiO}_{1.5}\text{-}23.4\text{GeO}_2\text{-}18.2\text{BO}_{1.5}$ (mol%) by using the modified incorporation method. X-ray diffraction result of glass-ceramics suggested that the main peak of glass-ceramics matched the orthorhombic structure of the pure Bi_2GeO_5 phase. Differential thermal analysis (DTA) would give useful quantitative information with regard to the nucleation and crystallization mechanism. The important kinetic parameters such as Avrami exponent (n) and Crystallization activation energy (E_c) were investigated by non-isothermal method using DTA measurements at different heating rates. Microstructure of the obtained glass-ceramics showed the crystallites formed on the surface and they could diffuse in

to the bulk structure indicating that crystallization mechanism in this glass is between two and three-dimensional crystal growth (Figure 1 (b.)) which supported the results of Avrami exponent studies. The modified incorporation method can effectively modify the crystallization mechanism of Bi_2GeO_5 glass-ceramics, resulting in the improvement of this Bi_2GeO_5 glass-ceramic embedded with a desired crystal dimension.

Keywords: bismuth germanate, Bi_2GeO_5 , glass-ceramics, crystallization kinetics

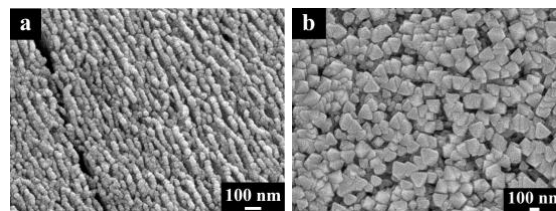


Figure 1: SEM micrographs of the $58.4\text{Bi}_{1.5}\text{-}23.4\text{GeO}_2\text{-}18.2\text{BO}_{1.5}$ glass-ceramics prepared by using two different methods (a) glass-ceramics prepared by using conventional method and (b) glass-ceramics prepared by using the modified incorporation method.

References:

1. Pengpat, K., Holland, D. (2003) Glass-ceramics containing ferroelectric bismuth germinate (Bi_2GeO_5), *J. Eur. Ceram. Soc.*, 23, 1599-1607.
2. Panyata, S., Eitssayeam, S., Rujjanagul, G., Tunkasiri, T., Pengpat, K. (2017) Non-isothermal crystallization kinetics of bismuth germinate glass ceramics, *Ceram. Int.*, 43, S407-S411.

Transparent BST Glass ceramic Nanocomposites: Fabrication Crystallization Kinetics and Properties

P. Intawin,¹ S. Panyata,^{1,2} A. Kraipok,^{1,2} S. Eitssayeam,¹ T. Tunkasiri,¹ M. Kamnoy,^{1,2}
S. Inthong,^{1,2} K. Pengpat,^{1,*}

¹ Department of Physics and Materials Science, Faculty of Science, Chiang Mai University, Chiang Mai 50200, Thailand

² Graduate PhD's Degree Program in Materials Science, Faculty of Science, Chiang Mai University, Chiang Mai 50200, Thailand

Abstract:

A nanocomposite material consisting of crystallites inside a glass-like matrix has been synthesized using the glass crystallization method. In this study, we have studied the structural, optical, dielectric and ferroelectric properties of crystals embedded in a glassy matrix, the $\text{Ba}_{0.7}\text{Sr}_{0.3}\text{TiO}_3$ (BST) – Na_2O – B_2O_3 – SiO_2 system prepared by the melt quenching technique. In order to change the prepared glass to glass-ceramic samples, heat treatment technique was employed using temperatures ranging between 650 and 850 °C. The X-ray diffraction patterns showed the presence of the amorphous phase and the precipitation crystalline phase in the amorphous matrix. The morphology of the crystals was studied by scanning electron microscope. The important kinetic parameters such as Avrami exponent (n) and Crystallization activation energy (E_c) were investigated by non-isothermal method using DTA measurements at different heating rates. All glass-ceramic samples confirm the spherical-like nanocrystals structure (Figure 1). The microstructure, with cluster of spherical crystal structure, indicates a typical three-dimensional crystallization mechanism, which agrees with the above analysis of Avrami exponent ($n = 4.2$) for glass sample at T_c . It was found that the crystal size and crystallinity increased with increasing heat treatment temperature. Optical, dielectric and ferroelectric properties of the synthesized samples depend upon their morphology and crystallinity.

Keywords: Transparent glass ceramic; Ferroelectric glass ceramic; Nanocomposite; crystallization kinetics

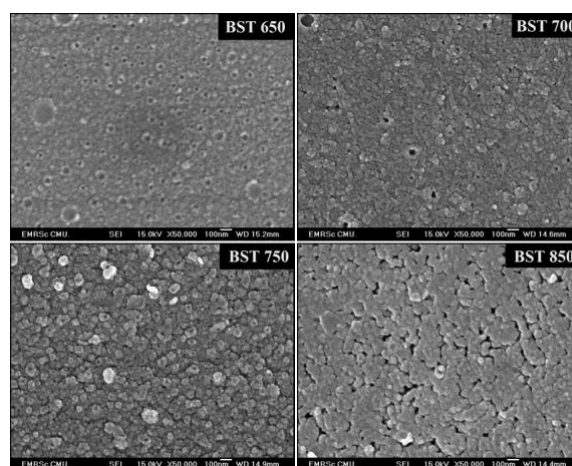


Figure 1: The fine microstructures with many spherical-like nanocrystals of homogeneously dispersed in the glass matrix are clearly displayed. However, it was found that with the increase in heat-treatment temperature, both the crystal volume fractions as well as the size of the crystals increased.

References:

1. E.P. Gorzkowski, M.J. Pan, B. Bender, M. Wu (2007), Glass-ceramics of barium strontium titanate for high energy density capacitors, *J. Electroceram* 18, 269–276.
2. P. Mukherjee, K.B.R. Varma (2004), Crystallization and physical properties of LiTaO_3 in a reactive glass matrix (LiBO_2 – Ta_2O_5), *Ferroelectrics* 306, 129–143.
3. V.V. Golubkov, O.S. Dymshits, A.A. Zhilin, A.V. Redin, M.P. Shepilov (2001), Crystallization of glasses in the $\text{K}_2\text{ONb}_2\text{O}_5$ – SiO_2 system, *Glass Phys. Chem.* 27, 504–511.

Mixed Monolayer Semiconductor Nanocrystals for Optimized Nanocomposites

S. Fernández de Ávila^{1,*}, F. Rodríguez-Mas¹, J.C. Ferrer¹, J.L. Alonso¹

¹ University Miguel Hernández, Department of Communications Engineering, Elche, Alicante, Spain.

Abstract:

This contribution reports on the synthesis of semiconductor nanocrystals (NCs) functionalized with two mixed organic ligands, thiophenol and decanethiol, with variable ratios, and their influence on the optical properties of nanocomposites obtained from the integration of these NCs into a polymer matrix.

Hybrid nanocomposites consisting of organic polymers hosting inorganic semiconducting nanocrystals combine the ease of polymers processing, and the stability and properties of NCs, such as size dependent optical absorption and light emission, and improved electronic characteristics. However, the optimal integration of the NCs in the hosting polymer as well as the optical and electrical properties, and morphology of the resulting nanocomposite strongly depend on the ligands used to stabilize the nanocrystals.

We report here the results obtained with two ligands with very distinct characteristics:

Decanethiol is an organic radical with isolating nature which length hinders the charge transfer from the NCs to the surrounding material. Nevertheless, this ligand is soluble in toluene or chlorobenzene as most of the polymers often used as semiconducting matrix.

Thiophenol, instead, is a shorter molecule more suitable when charge transport is required, but unfortunately, thiophenol stabilized NCs are insoluble in most of the polymer compatible solvents.

Mixed monolayer PbS and CdS nanocrystals have been synthesized following different chemical routes with several combinations of both organic ligands. Influence of the composition of the mixed monolayer on the optical properties of nanocrystals is presented.

Nanocomposites prepared blending these mixed monolayer NCs with polymer solutions are also studied to evaluate their potential for integration in optoelectronic devices.

Keywords: semiconducting nanocrystals, chalcogenides, hybrid nanocomposites, organic

ligands, optical properties, optoelectronic applications.

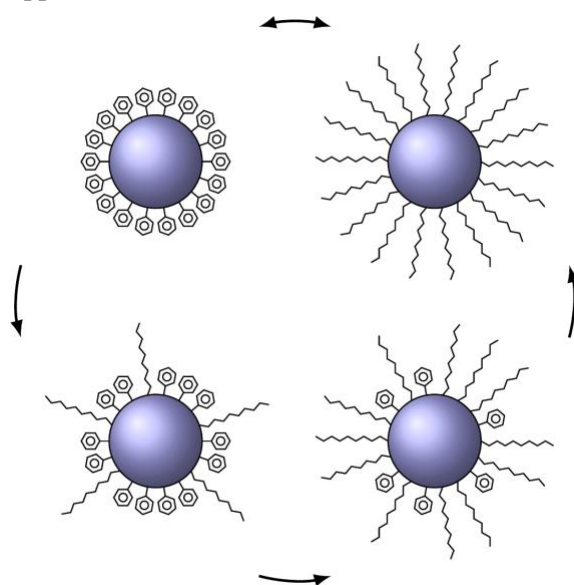


Figure 1: Figure illustrating several Nanocrystals with decreasing ratio of thiophenol ligands. Identical NCs with only thiophenol or decanethiol ligands (upper part) and mixed monolayer NCs (lower part)

References:

1. Merg, A.D., Zhou, Y., Smith, A.M., Millstone, J.E., Rosi, N.L. (2017) Ligand exchange for controlling the surface chemistry and properties of nanoparticle superstructures, *Chem. Nano. Mat.*, 3, 745-749.
2. Bousquet, A., Hiorns, R. C., Dagron-Lartigau, C. and Billon, L. (2017). Hybrid Conjugated Polymer–Inorganic Objects: Elaboration of Novel Organic Electronic Materials. In *Hybrid Organic-Inorganic Interfaces* (eds M. Delville and A. Taubert). doi: [10.1002/9783527807130.ch6](https://doi.org/10.1002/9783527807130.ch6).

Study Of La doped ZnS Thin Films Properties synthesized by Chemical Bath Deposition Technique (CBD) in acidic medium

^{1,*} H. Haddad, ^{1,2,*} H. Merzouk, ^{1,*} D. Talantikite ^{1,*} A. Tounsi

¹ Abderrahmane Mira University, Chemical Department, Bejaia, Algeria

² Abderrahmane Mira University, Physics Department, Bejaia, Algeria

*Genius Laboratory of environment), Bejaia University , Algeria

Abstract:

To our knowledge So far no author has reported the effect of lanthanum doping on the thin layers of zinc sulphide elaborated by the Chemical Bath technique (CBD) in acidic medium where as the studies made up to now are developed in a basic medium. In this work, Undoped and La-doped ZnS thin films have been produced on glass substrates using the Chemical Bath deposition technique (CBD) in acidic medium (PH=4). The Lanthanum concentration was varied from 0% to 10%, keeping other deposition parameters constant {(T=80°C), t=2hours, [Zn²⁺]=0.2M, [S²⁻]=0.4M

. [Na₂EDTA]=0.055M, La_x (1-10%)}. The XRD analysis present amorphous structures for all deposits and no peak was awarded which means that the crystallinity of the deposited layers is insignificant. Spectroscopic analysis have shown significant improvement of both optical gap and transmittance of the deposited layers especially in the visible range, the films with a La-doping content of 1% have the better optical transmittance over 80 % in the visible range and a wide band gap energy (E_g) of 3.815 eV. For the other samples the transmittance was varying from 75 to 80% while the band gap energy(E_g) remains the same. The Infrared characteristic of undoped ZnS vibration peaks were observed at 1105, 640, and 452 cm⁻¹.

Keywords: , La-doped ZnS thin films, chemical bath deposition (CBD) technique, acidic medium, optical transmittance visible range. XRD analysis present amorphous structures for all deposits and no peak was awarded. Spectroscopic analysis have shown significant improvement of both optical gap and transmittance of the deposited layers especially in the visible range, the films.

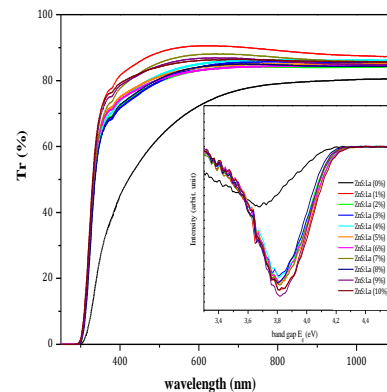


Figure 1: Figure is illustrating the fundamental question that we are tempting to solve experi

mentally: what is the importance of lanthanum concentration on ZnS thin films transmittance prepared by CBD Technique in acidic medium. The insert figure inside Fig1 shows a plot of $dT/d(hv)$ versus the band gap energy E_g

References:

1. Xie Hai-Qing; Chan Yuan; Huang Wei-Qing Huang(2018) Optical characteristics of La-doped ZnS thin films. IOP science
2. T.E.Manjulavalli, A.G Kannan Department of Physics, NGM College, Pollachi-642 001, Tamilnadu, India(2015) Structural and optical of ZnS Thin Films Prepared By Chemical Bath Deposition, Int journal of ChemTech Research CODEN (USA).

Structure, Morphology, Thermal and Electrochemical Studies of Electrochemically Synthesized Polyaniline/Copper Oxide Nanocomposite for energy storage device

Ashokkumar S P, Yesappa L, Vijeth H, Niranjana M, Vandana M, Devendrappa H*

Department Of Physics, Mangalore University, Mangalagangothri 574199, India

*Corresponding Author: dehu2010@gmail.com

Abstract:

In this abstract paper discussed about the synthesis, characterization and supercapacitor and energy storage device applications. Polyaniline (PANI) doped Copper oxide (CuO) nanocomposite (PCN) was prepared by electrochemical deposition method. The Polyaniline nanocomposites were characterized by using X-ray diffraction (XRD), Thermo gravimetric analysis (TGA), Differential scanning calorimetry (DSC), Field emission scanning electron microscope (FESEM) and Cyclic Voltammetry (CV) methods. The XRD result reveals the change in the structural phase due to metal nanoparticles. The TGA graph shows that the thermal decomposition occurs in two steps, first decomposition about 14.03% in the region 78.91-102°C due to moisture and water on the surface of the material and second stage between 110-650°C is caused the loss of the doping acid and the weight loss. As increases the concentration of nano composite in the PANI matrix leads to decrease in the degradation temperature. DSC results reveal an enhanced thermal stability of the PANI nanocomposites with the addition of concentration and the melting temperature of PANI is found to be 135°C, whereas PCN nano composite increased to 145°C. These results show the PCN nano composite have higher thermal stability than the PANI. FESEM confirms the shape changes from grain to rod like structure due to addition of nano concentration. The electrochemical performance of cyclic voltammetry technique with three-electrodes system in 1M aqueous H₂SO₄ solution as an electrolyte in the potential window from -4 to 2V at various scan rates 100 - 500mV/s. The high specific capacitance obtained because of large surface to volume ratios, which is clearly evidenced by its unique nano rod like structure may provide the fast electron mobility, and they are favourable to pseudocapacitor behavior. These obtained

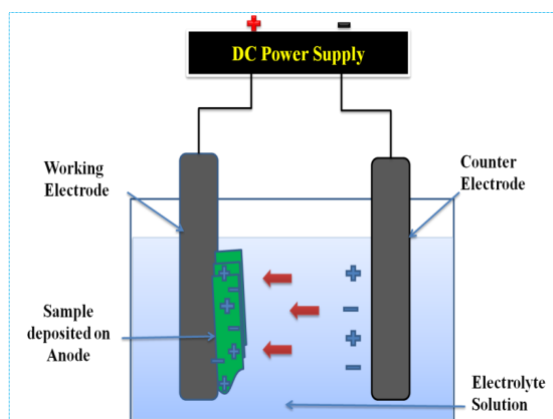
results were confirmed that PANI nanocomposite is suitable candidature for supercapacitor, electrodes and energy storage applications.

Keywords: Conducting polyaniline, nano composite, electrochemically synthesized, Structure, Surface morphology, thermal and electrochemical studies.

Experimental Methods:

Schematic. Schematic diagram represents the electrochemically deposition of polyaniline copper oxide nanocomposites.

PANI CuO (PCN) nanocomposites was



synthesized by electrochemical deposition method with applied voltage is 2 volt for deposition time allowed is 900 seconds. The sample were characterized by X-ray diffraction (XRD) Riga Ku 600 Miniflex bench top, Field emission scanning electron microscopy (FESEM) and Thermal properties like Thermo gravimetric analysis (TGA), Differential scanning calorimetry (DSC).

FESEM images:

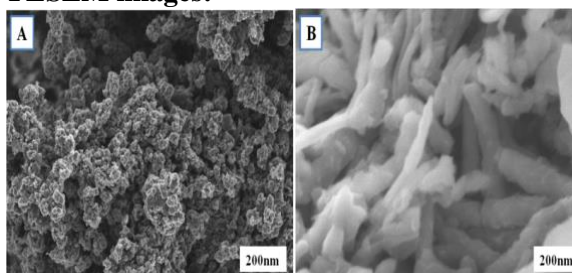


Figure 1: FESEM images of PANI and PCN nanocomposite.

The Fig. 1 (A) and (B) is the PANI and 0.15wt % of PCN nanocomposite respectively. FESEM images of PANI and PCN nanocomposites shows the homogeneous distribution and morphology changes from grains to rod like structure [1] is clearly visible in (A) & (B) images. The Fig. 2 (B) displays the rod like shape and which is randomly dispersed due to increase in wt% of CuO to PANI as a results most significant morphology of PCN nanocomposite. Hence from grain to rod structure changes confirms, this material can be usable for making an energy storage application [2].

References:

1. Archana, K., Raghu, S., & Devendrappa, H. (2016), Methyl blue dyed polyethylene oxide films: Optical and electrochemical characterization and application as a single layer organic device, *Optical Materials*, 51, 213-222.
2. Qin, Q., & Zhang, R. (2013). A novel conical structure of polyaniline nanotubes synthesized on ITO-PET conducting substrate by electrochemical method, *Electrochimica Acta*, 89, 726-731.

Improvement of Contact Resistance Characteristics between Graphene-carbon Nanotube for Carbon Semiconductor

Eunmi Choi,² Yinhua Cui¹, Yuan Gao¹, Sung Gyu Pyo¹

¹ School of Integrative Engineering, Chung-Ang University, Seoul, Korea

² Materials & Energy Measurement Center, Korea Research Institute of Standards and Science, Daejeon 34113, Korea

Abstract:

Recently, the era of the technology node of less than 10 nm has dawned to achieve multi-function and high-performance devices beyond Moore's Law. However, it has a reliability issue caused by the poor film coverage of the barrier/seed layers and thermomechanical stress that is caused by sharply increased aspect ratio (AR) and decrease in pitch and interconnect size. Also, it has a problem such as resistance(R)-capacitance(C) delay with resistance increase by boundary scattering and a lower mean free path that is caused by grain effect in nano-thickness of Cu and thermo-mechanical reliability due to the difference in the coefficient of thermal expansion (CTEs) between Si and Cu. So, the development of new materials is required for less than 10 nm technology node. To overcome the problem, nano-carbon semiconductors based on vertical carbon nanotube (CNT) interconnects and graphene lines as base materials have attracted attention.

CNT has characteristics such as high thermal conductivities, high mechanical strength and high aspect ratio. In addition, CNT has a high electromigration (EM) resistance characteristic compared to Cu due to the high maximum current density of 10^9 A/cm². On the other hand, graphene has characteristics high thermal conductivities and high mechanical strength. Also, it is expected that RC delay degradation by highest carrier mobility of 200,000 cm²/vs and enhanced EM resistance characteristics by high maximum current density of 2×10^8 A/cm².

Many researchers expect a technology age of less than 5 nm that is highly reliable with improved RC delay and EM resistance using the highest carrier mobility and very high f_T characteristics of the horizontal graphene line and the high AR of the vertical CNT interconnect. However, The problem must

be solved such as a random defect in graphene surface, control of physical properties according to the structure of CNTs, patterning technology for control of electrical characteristics of graphene, and contact resistance of graphene and CNT in order that ideal carbon semiconductor.

The research that is about contact resistance improvement is early stage compared with the continuous progress of research on Graphene defect and CNT structure control.

On the other hand, the contact resistance issue of Graphene-CNT has a large influence on the overall resistance of the device because it follows the quantum resistance due to the contact area of ~ 1 nm. Therefore, it is required to understand and reduce the contact resistance of contact resistance between vertical CNT interconnect and horizontal graphene line in order to realize a device with high reliable. In addition, the research about contact resistance is required when applied metal electrodes or metal lines in vertical CNT interconnects.

Generally, the contact resistance of CNT-metal and CNT-graphene have been measured using test structure of CNT TFETs.

To make the TFET structure, there are two methods of forming the electrode. First, forming an electrode after growing the CNT. Second, transferring the CNT after forming the electrode.^{14, 15} However, both methods have limitations on the reliability of measured values because side contacts measured rather than 'real end contacts' between the vertical CNT interconnect -electrode. Therefore, a new measurement method that can measure 'real end contact' intuitively is required. In this study, we propose a 'real end contact' measurement method of CNT-graphene without using a test structure. In addition, discuss the possibility of applying a metal layer to improve contact resistance characteristic.

Keywords: carbon semiconductor, contact resistance, CNT-Graphene contact

Structural, magnetic and electromagnetic wave absorption properties of La-BaM/PANI nanocomposites

N. Tran, Y. J. Choi, M. Y. Lee, T. L. Phan, B. W. Lee¹

¹Department of Physics and Oxide Research Center, Hankuk University of Foreign Studies, Yongin 17035, South Korea

Abstract:

$\text{Ba}_{1-x}\text{La}_x\text{Fe}_{12}\text{O}_{19}$ ($x = 0-0.5$) nanocrystalline samples were synthesized by using coprecipitation method combining with heat treatment. Sample-shapes were being in the nano-hexaplates with size 100 – 300 nm and thickness ~50nm. Then, their composites with polyaniline (PANI) were prepared with hexaferrites (H) and PANI (P) ratio H/P = 9/1. The composites together with 7% wt. epoxy were pressed in to toroidal (with $D = 7$ mm and $d = 3$ mm) followed by drying at 170 °C for 0.5h. Both X-ray diffraction (XRD) and Raman spectroscopy (RS) studies indicated that all composites mainly crystallized into the M-type hexaferrite structure (the space group $P6_3/mmc$). Specifically, the composites with $x \leq 0.2$ were single phase without any impurity while those with $x > 0.2$ had a trace of a secondary phase Fe_2O_3 . The magnetic properties of these composites have been studied by using a vibrating sample magnetometer (VSM) with the external field up to 10 kOe. The results show that the saturation magnetization M_s of the composites with $x \leq 0.3$ were almost unchanged, about 35~37 emu/g, while the coercivity H_c increased from 4.22 kOe for $x = 0$ to 4.86 kOe for $x = 0.1$ then decreased to 4.23 kOe. For the composites with $x > 0.3$, M_s gradually decreased to 25.5 emu/g for $x = 0.5$. This can be attributed to the appearance of Fe_2O_3 . Notably, composite with $x = 0.5$ had lowest magnetization ($M_s = 25.5$ emu/g) and highest coercivity ($H_c = 5.02$ kOe). Electromagnetic wave absorption properties of these composites were studied by PNA-X Network Analyzer in the frequency range from 0.1 – 18 GHz. By doping, reflection loss (RL) of composites has been changed. Undoping composite had low RL (– 3 dB at 7.7 and 9.1 GHz). All doping composites had RL below – 5dB (~68.4% microwave absorption). Especially, the bandwidth of microwave RL below – 10 dB (~90% microwave absorption) is obtained in 6.65 – 8.14 GHz with the minimum

RL = – 14.2 dB at 7.4 GHz for composite with La-doping concentration $x = 0.1$ (thickness 3.5 mm). This makes $\text{Ba}_{0.9}\text{La}_{0.1}\text{Fe}_{12}\text{O}_{19}$ /PANI nanocomposite can be a potential microwave absorption candidate.

Keywords: M-type hexaferrites, PANI, composites, electromagnetic wave absorption

*Corresponding author: bwlee@hufs.ac.kr

Hydrothermally Synthesized Titanium dioxide (TiO₂) Nanotubes Based Sensor for Brain Signals Extraction

Santhosh Kumar N, Naveen Kumar S K*

Department of Electronics, Mangalore University, Mangalagangothri, Mangalore, Karnataka -574199, India.

*Corresponding author email: nave12@gmail.com

Abstract:

Titanium dioxide (TiO₂) nanotubes have been synthesized by using hydrothermal method. The changes in the structure of the TiO₂ nanoparticles by the effect of hydrothermal temperature are described in this work and it is mainly focused on the metal oxide semiconductor (MOS) structure or sensor for brain signal extraction. The properties of the hydrothermally synthesized TiO₂ nanotubes were characterized and carried out the optical absorption studies using UV-Visible spectrophotometer, structural changes using X-ray diffractometer, surface morphology by field emission scanning electron microscope (FESEM) and thermal properties by thermo gravimetric analysis (TG/DTA) and from these studies, it is confirmed that TiO₂ nanotubes are applicable in the signal extraction process. The capacitance versus voltage (CV) and current versus voltage (IV) characteristics are performed and it has been revealed that the TiO₂ nanotubes can be used to fabricate MOS structure then that leads to work as a sensor. A setup for electrical study of MOS structure was shown in the Fig.

Keywords: Hydrothermal, TiO₂ nanotubes, CV, IV, MOS, Sensor.

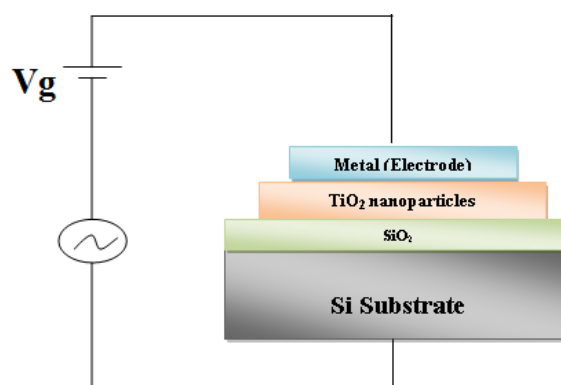


Figure 1: A setup for electrical study of MOS structure

References:

1. Hossein eslani, et al., (2015) hydrothermal synthesis and characterization of TiO₂ derived nanotubes for biomedical applications, *Synthesis and Reactivity In Inorganic, Metal-Organic, and Nano-Metal Chemistry*, 46, 1149-1156.
2. Prajith, R.P, Ganesan R, Gobalakrishnan (2013), Design of electroencephalogram sensor for long term bio signal measurement, *Int. J. latest trends in engineering and technology*, 2, 198-206.

ZnO:Ga nanoscintillator for X-ray induced photodynamic therapy

E. Mihóková¹, L. Procházková,^{1,2} I.T. Pelikánová,² R. Dědic,³ and V. Čuba²

¹Institute of Physics, Czech Acad. of Sci., Department of Optical Materials, Prague, Czech Republic

²Czech Technical University, Faculty of Nuclear Sciences and Nuclear Engineering, Prague, Czech Republic

⁴Charles University, Faculty of Math. and Physics, Dept. of Chemical Physics and Optics, Prague, Czech Republic

Abstract:

Active research in luminescent and scintillating materials in recent years is mainly driven by emerging applications, such as those in biomedicine. Photodynamic therapy (PDT) is treatment in which visible or near-infrared light is used to activate a photosensitizer (PS), administered to target a diseased tissue of interest. In the presence of ground state oxygen, the light-activated PS creates reactive oxygen species, especially highly cytotoxic singlet oxygen, that can induce tissue death [1]. X-ray induced PDT (PDTX) is a combination of radiotherapy and PDT providing more efficient tumor cell killing than the radiotherapy alone [2]. After the X-ray energy is absorbed by a scintillating nanoparticle, it is either radiatively or nonradiatively transferred to the PS molecule. To observe a cytotoxic effect at therapeutic radiation doses, the light yield of scintillating nanoparticle, the efficiency of energy transfer to the photosensitizer and the cellular uptake of the nanoparticles, all need to be fairly well optimized [3]. The nanoparticle uptake by tumor blood vessels can be improved by enhanced permeability and retention (EPR) effect promoted, among others, by suitable nanoparticle size.

We synthesize a prospective core-shell nanocomposite for PDTX based on ZnO:Ga scintillating core. The core is synthesized by the UV photochemical method [3], coated by amorphous silica shell using the sol-gel technique, facilitating a functionalization by a photosensitizer, protoporphyrin IX (PpIX) molecules. Combined results of steady state and time resolved spectroscopy suggest the presence of an energy transfer between the ZnO:Ga core and PpIX outer layer. In particular, i) emission of the core is almost completely suppressed in the RL spectrum of functionalized particle, ii) PL spectrum features characteristic emission of

PpIX in the red spectral region under the core excitation, iii) PL decay features PpIX decay under the core excitation. The results indicate that the mechanism of energy transfer is more likely to be nonradiative.

The singlet oxygen generation in the system is demonstrated by the 3'-(p-aminophenyl) fluorescein (APF) chemical probe sensitive to the singlet oxygen presence. Observed features of nanocomposite studied indicate its considerable potential for PDTX application.

Keywords: nanocomposites, bioconjugates, photodynamic therapy, scintillator, singlet oxygen, biomedical applications.

References:

1. Agostinis, P., Berg, K., Cengel, K.A., Foster, T.H., Girotti, A.W., Gollnick, S.O., Hahn, S.M., Hamblin, M.R., Juzeniene, A., Kessel, D., et al. (2011), Photodynamic therapy of cancer: An update, *CA Cancer J. Clin.* 61, 250–281.
2. Retif, P., Pinel, S., Toussaint, M., Frochet, C., Chouikrat, R., Bastogne, T., Barberi-Heyob, M. (2015), Nanoparticles for radiation therapy enhancement: the key parameters, *Theranostics*, 5, 1030–1044.
3. Morgan, N.Y., Kramer-Marek, G., Smith, P.D., Camphausen, K., Capala, J. (2009), Nanoscintillator conjugates as photodynamic therapy-based radiosensitizers: calculation of required physical parameters, *Radiat. Res.*, 171, 236–244.
4. Prochazková, L., Gbur, T., Čuba, V., Jarý, V., Nikl, M., (2015), Fabrication of highly efficient ZnO nanoscintillators, *Opt. Mater.*, 47, 67–71 (2015).

Fabrication of MEMS based blackbody for calibration of infrared camera using black silicon and MWCNTs

Seolhui Hwang,^{1,*} Jaehyuk Lee,² Taegy Kim,³ Jonggul Ok,² Jongkwang Lee,¹

¹Hanbat National University, Department of Mechanical Engineering, Daejeon, Republic of Korea

²Seoul National University of Science And Technology, Department of Mechanical and Automotive Engineering, Seoul, Republic of Korea

³Chosun University, Department of Aerospace Engineering, Gwangju, Republic of Korea

Abstract:

Optical cameras are not uniform in output characteristics due to high temperature-low temperature repetition and repetitive operation-non-operation. This is a fatal disadvantage which deteriorates the performance of the optical camera, and a blackbody is used to solve this problem. Figure 1 shows a blackbody system based on MEMS developed by Chosun University. Black silicon (BSi) and multi-walled carbon nanotubes (MWCNTs) were proposed for fabricating of MEMS-based blackbody surface on upper side of a silicon wafer of this system. To fabricate the BSi, we used the cryogenic and Bosch processes in the DRIE process [1]. The detailed experimental variables of the cryogenic process are : SF_6 / O_2 gas = 40 / 18 sccm, RF power : 1000 W, pressure : 10 mTorr, process time : 15 minutes, process temperature : -110 °C. Also, the detailed experimental variables of the Bosch process are : SF_6 / C_4F_8 gas = 200 / 200 sccm, RF power : 2000 W, SF_6 / C_4F_8 pressure : 30 / 40 mTorr, SF_6 / C_4F_8 pulse time = 3 / 0.5 seconds, bottom power : 40 W. The total process time is 5 minutes.

MWCNTs were cultivated using a chemical vapored deposition (CVD) process. In order to cultivate MWCNTs, a catalyst layer was required, and Aluminum oxide (Al_2O_3) 10 nm and iron (Fe) 1 nm were used as catalysts. Then, the substrate was placed in a furnace and Ar was supplied at 400 sccm, H_2 at 200 sccm, and C_2H_4 at 100 sccm for 10 ~ 15 minutes at a temperature range 725 °C ~ 775 °C [2]. Figure 2 (a) is a cryogenic process, (b) is a SEM image of MWCNTs cultivated in BSi produced through Bosch process. Figure 3 shows the reflectance results of BSi fabricated through another process and MWCNTs cultivated on BSi. As a result, it was found that the high reflectance of BSi in the infrared range was greatly reduced to less than 2% in MWCNT cultivation.

Keywords: Black silicon (BSi), Multi-wall

carbon nanotubes (MWCNTs)

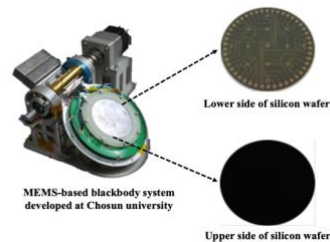


Figure 1: The entire system of MEMS blackbody

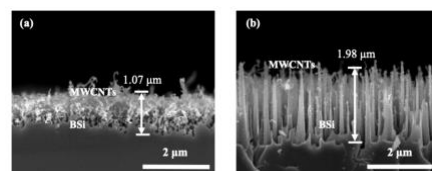


Figure 2: SEM images of fabricated MWCNTs at BSi. (a) is BSi fabricated by cryogenic process and (b) is BSi fabricated by Bosch process

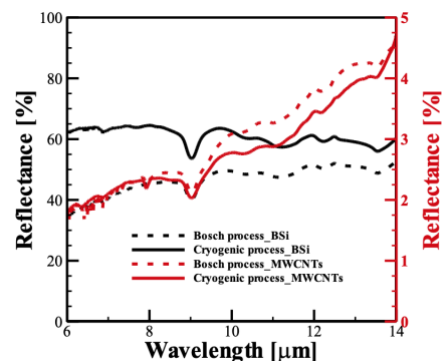


Figure 3: Comparison of FT-IR reflectance results of BSi and MWCNTs

References:

1. Pradeep Dixit and Jianmin Miao (2006) Effect of SF_6 flow rate on the etched surface profile and bottom grass formation in deep reactive ion etching process, *Int. MEMS Conference.*, 34, 22-26
2. Rajesh Purohit, Kuldeep Purohit, Saraswati Rana, R. S. Rana and Vivek Patel (2014) Carbon Nanotubes and Their Growth Methods, *Procedia Materials Science.*, 6, 716-728

BERGMAN'S SPECTRAL REPRESENTATION : A POWERFUL FRAMEWORK FOR EXTRACTING THE DIELECTRIC PROPERTIES OF NANOPOWDERS

A. Nzie,^{1,*} C. Blanchard,¹ D. De Sousa Meneses,¹

¹ CNRS, CEMHTI UPR3079, Univ. Orléans, F-45071 Orléans, France

Abstract:

Being able to master the electromagnetic properties of finely divided heterogeneous media, i.e. when the size of the heterogeneities of the material is much smaller than the wavelength of the radiation [1], is imperative when it comes to optimizing their optical properties for targeted applications in both materials science and industrial sector. The design process generally necessitates the knowledge of the dielectric function of the constituting parts. Finding these data entries can represent the tricky part of the whole problem when the phases composing the heterogeneous structure are nanoobjects. In fact, the dielectric properties of nanograins are often significantly different from their bulk counterpart due to the presence of confinement or defects. The complexity of these systems makes it indispensable to develop new numerical tools as well as experimental means devoted to their characterization.

We present a new procedure based on sets of experimental spectra to retrieve the dielectric function of one of the homogeneous nanophases composing a binary mixture, as well as information on the spatial distribution of the material. Several effective medium approaches like Maxwell-Garnett, Felderhof, Bruggeman, Lichtenecker and more particularly Bergman's general theory have been developed to compute the optical response of mixtures [2]. The latter has an integral form and separates mathematically the influence of the spatial distribution of the matter (through a spectral density function) from the one induced by the nature of the phases in presence. This theory is mathematically expressed by the following relationship :

$$F(s) = 1 - \frac{\epsilon_{eff}}{\epsilon_m} = \frac{A_0}{s} + \int_{0^+}^1 \frac{m_f(z)}{s-z} dz, \text{ where } s = \frac{\epsilon_m}{\epsilon_m - \epsilon_i}$$

spectral density function
chemical Composition

where, ϵ_m and ϵ_i are the dielectric function of the matrix and inclusions, respectively. The parameter A_0 is a measure of the percolation strength of the inclusions. Through this formulation, we have the possibility to determine one of the four quantities (ϵ_m , ϵ_i , ϵ_{eff} , m_f) from the knowledge of the three others. The capability of the proposed procedure is presented through the study of the dielectric and structural properties of amorphous silica pellets manufactured from nanopowders with different porosity levels and KBr pellets containing a low concentration of SiO₂ nanoparticles. Transmittance and reflectivity measurements performed on a set of samples were fitted as a whole by solving a nonlinear optimization problem based on the Bergman's theory. The outputs are the wanted dielectric function of the silica nanoparticles ϵ_i and the spectral density function m_f associated to the pellets. The behaviour of the percolation strength of the SiO₂ nanoparticles in the porous matrix are also estimated and porosities extracted using Bergman's theory are compared to those obtained by density measurements. The dielectric function of the silica nanograins is discussed at the light of that of bulk silica and a comparison with predictions made with other effective media approximations is also given.

Keywords: Effective medium theories, SiO₂ nanopowder, Spectral density function.

References:

1. Milton G W, McPhedran R C, McKenzie D R 1981 Transport properties of arrays of intersecting cylinders *Appl. Phys.* **25** 23–30
2. Bergman D J and Stroud D 1992 Physical Properties of Macroscopically Inhomogeneous Media *Solid State Physics* vol 46 (Elsevier) pp 147–269

Composites based on poly(2, 2'-bithiophene) and TiO₂ nanoparticles: from chemical synthesis to optical properties and their applications in the leather and textile materials field

I. Smaranda^{1*}, M. Stroe¹, A. Radu¹, R. Constantin¹, C. Gaidau², L. Chirila², M. Baibarac¹

¹National Institute of Materials Physics, Lab. of Optical Processes in Nanostructured Materials, Atomistilor street 405A, Magurele, Romania

²National Institute and Development Institute for Textiles and Leather, 16 Lucretiu Patrascanu street, 030508, Bucharest, Romania

Abstract:

Optical properties of composites based on poly(2, 2'-bithiophene) (PBTh) and TiO₂ nanoparticles, prepared by the chemical polymerization of the monomer 2, 2'-bithiophene in the presence of semiconductor nanoparticles, were reported. As increasing the TiO₂ nanoparticles concentration in the synthesis mixture mass, the PBTh/TiO₂ composites shown: i) an intense Raman line in the 1400-1600 cm⁻¹ spectral range with a maximum which is down-shifted from 1454 cm⁻¹ to 1430 cm⁻¹ and ii) a photoluminescence (PL) complex band in the 550-750 nm spectral range, consisting from two emission bands peaked at 629 and 670 nm, whose intensity increase from 3.5 x 10⁵ counts/sec to 1 x 10⁶ counts/sec. In the presence of the VIS light, a gradual decrease in the relative intensity of the two emission bands in the case of PBTh and its composites with TiO₂ nanoparticles is reported. The functionalization of leather and cotton fabrics with the PBTh and its composites with TiO₂ nanoparticles was performed by the direct chemical interaction in aqueous dispersions. After drying of leather and textile material, the weight increasing of PBTh and its composites with TiO₂ nanoparticles was assessing by the Raman spectroscopy. In the case of the cotton fabrics functionalized with PBTh or the PBTh/TiO₂ composites, a decrease of the ratio between the Raman lines peaked at 1097 and 1458 cm⁻¹, belong to the cotton and composite material, respectively, was reported to occur from 2.55 to 0.61 as a

consequence of the increasing of the PBTh or PBTh/TiO₂ layer onto textile material surface. Regardless of the PBTh/TiO₂ composite material weight onto leather surface, the Raman spectra show in the 500-3500 cm⁻¹ spectral range only the Raman lines of the polymer. Photocatalytic activity of the leather and cotton fabrics with the PBTh/TiO₂ composites was evaluated by photodegradation efficiency of methylene blue dye. The leather and cotton fabrics functionalized with the PBTh/TiO₂ composites have shown improved self-cleaning properties in the comparison with those treated with the alone PBTh. The performances of these composites will be highlight in comparison with the TiO₂ nanoparticles [1] and other composites such as polyaniline/TiO₂ [2].

Keywords: composites, TiO₂ nanoparticles, polymer, Raman scattering, cotton fabrics, photodegradation.

References:

1. Saadoun, M., Chorfi, H., Bousselmi, L., Bessais, B., (2007), Polymer supported porous TiO₂: application to photo-catalysis, *Phys. Status Solidi C*, 4, 2029-2033.
2. Nosrati, R., Olad, A., Najjari, H. (2017), Study of the effect of TiO₂/polyaniline nanocomposite on the self-cleaning property of polyacrylic latex coating, *Surf. Coat. Tech.*, 316, 199-209.

Indirect to Direct Bandgap Transition in Two-dimensional SnS₂ Monolayer by Nickel Doping: First-Principles Calculations

S. Batjargal,^{1,2,*} M. Hayashi,^{1,2}

¹ Center for Condensed Matter Sciences, National Taiwan University, Taiwan

² Center of Atomic Initiative for New Materials, National Taiwan University, Taiwan

Abstract:

Direct bandgap semiconductors play a critical role in optoelectronics. In this regard, SnS₂ is a two-dimensional (2D) layered semiconductor which has ignited intensive attention due to its semiconducting nature and nontoxicity. The pristine SnS₂, however, has an indirect bandgap. For a more widespread use, it is highly desired to translate SnS₂ into direct bandgap semiconductors by controlling external parameters. Utilizing first-principles calculation methods with accurate HSE hybrid functional, we show the possibility of indirect to direct bandgap transition in SnS₂ single layer via nickel doping (Figure 1). A substitutional nickel-dopant on the tin site of SnS₂ generates new band lines at the bottom of the conduction band due to strong orbital hybridization with states of its nearby sulfur atoms. Consequently, the direct bandgap can be achieved in SnS₂; moreover, the bandgap size is narrowed as the number of nickel-dopants increases.

Keywords: Two-dimensional (2D) nanomaterials, electronic property, band structures, first-principles calculations.

point. Ni-SnS₂ sheets become direct bandgap semiconductors with reduced values.

References:

1. Batjargal, S., Hayashi, M. (2019), Possible Indirect to Direct Bandgap Transition in SnS₂ via Nickel Doping, *Chemical Physics*, 522, 59-64.

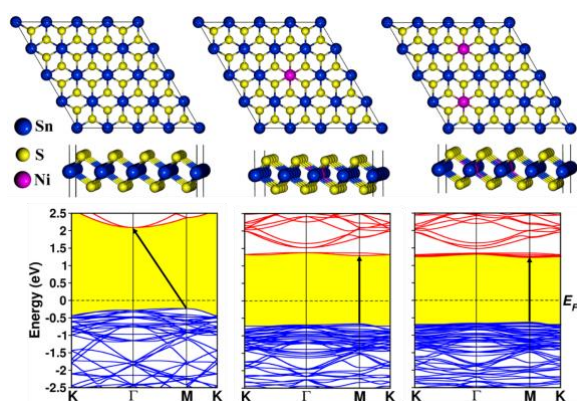


Figure 1: Band structures of (a) pure SnS₂, and (b) one and (c) two nickel-doped SnS₂. The blue, yellow and magenta balls represent the tin, sulfur and nickel atoms, respectively, whereas the solid arrows indicate the bandgap transitions. Pristine SnS₂ has an indirect bandgap with the transition between Γ and M

Generation of new photo-responses in the visible domain due to morphological imperfections

A. Ben Gouider Trabelsi,^{*a, b} F. V. Kusmartsev,^{a, c} M. B. Gaifullin,^a D. M. Forrester,^d A. Kusmartseva^a and M. Oueslati^e

^a Department of Physics, Loughborough University, Loughborough, LE11 3TU, UK.

^b Department of Physics, Princess Nourah bint Abdulrahman University, Riyadh, PO Box 84428, Saudi Arabia KSA.

^c Micro/Nano Fabrication Laboratory, Microsystem & Terahertz Research Centre of CAEP, Chengdu, P.R. China

^d Department of Chemical Engineering, Loughborough University, Loughborough, UK

^e Unité des Nanomatériaux et Photonique, Faculté des Sciences de Tunis, Université de Tunis El Manar Campus Universitaire, El Manar, 2092 Tunis, Tunisia
Email: amira.bengouider@gmail.com

Abstract:

Epitaxial graphene grown on 6H-SiC (000-1) shows remarkable photo-physical phenomena. The electrical resistance of graphene increases under light illumination in contrast to conventional materials where it normally decreases. The resistance shows logarithmic temperature dependences which may be attributed to an Altshuler–Aronov effect. We show that the photoresistance depends on the frequency of the irradiating light, with three lasers (red, green, and violet) used to demonstrate the phenomenon (Figure 1). The counterintuitive rise of the positive photoresistance may be attributed to a creation of trapped charges upon irradiation. We argue that the origin of the photoresistance is related to the texture formed by the graphene flakes. Photovoltage also exists and increases with light intensity. However, its value saturates quickly with irradiation and does not change with time. The saturation of the photovoltage may be associated with the formation of a quasi-equilibrium state of the excited electrons and holes associated with a charge redistribution between the graphene and SiC substrate. The obtained physical picture is in agreement with the photoresistance measurements: X-ray photoelectron spectrometry “XPS”, atomic force microscopy “AFM”, Raman spectroscopy and the magnetic dependence of photoresistance decay measurements.

Keywords: Epitaxial growth, graphene, oxidation, photoluminescence, X-ray photoelectron spectrometry “XPS”, atomic force microscopy “AFM”, Raman spectroscopy, photoresistance and magnetic dependence of photoresistance.

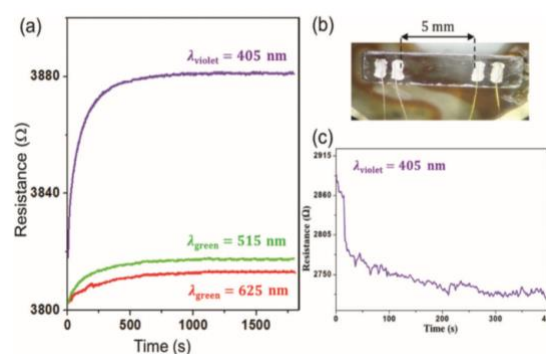


Figure 1: (a) Time dependence of the photoresistance of epitaxial graphene grown on 6H-SiC face terminated carbon (000-1), under continuous light irradiation: the purple, green and red curves correspond to the different illumination photon frequencies, from violet (405 nm), green (515 nm) and red (625 nm) lasers respectively; (b) optical image of the sample highlighting the four-probe contacting method for resistance measurements; (c) the time dependence of the photoresistance of a 6H-SiC substrate without graphene control, taken under continuous light irradiation from a violet laser.

References:

1. F. Wang, G. Liu, S. Rothwell, M. Nevius, A. Tejada, A. TalebIbrahimi, L. C. Feldman, P. I. Cohen and E. H. Conrad, *Nano Lett.*, 2013, 13, 4827–4832.
2. F. Joucken, Y. Tison, P. Le Fevre, A. Tejada, A. TalebIbrahimi, E. Conrad, V. Repain, C. Chacon, A. Bellec, Y. Girard, S. Rousset, J. Ghijsen, R. Sporken, H. Amara, F. Ducastelle and J. Lagoute, *Sci. Rep.*, 2015, 5, 14564.

Processing at different pressures and characterization of the ceramic superconducting $(\text{Bi}_{1.6}\text{Pb}_{0.4})\text{Sr}_2\text{Ca}_1\text{Cu}_2\text{O}_y$

I. Martínez-Ramírez^{1*}, E. Díaz-Valdéz¹, C. Mejía-García¹, T. Molina-Mil¹, A. M. Paniagua-Mercado¹.

¹ Escuela Superior de Física y Matemáticas, Instituto Politécnico Nacional, , Department of physics, Ciudad de México, Mexico.

Abstract:

This work shows the effect of compaction pressures on structural properties and critical current density of $(\text{Bi}_{1.6}\text{Pb}_{0.4})\text{Sr}_2\text{Ca}_1\text{Cu}_2\text{O}_y$ samples. Ceramic powders were prepared by conventional solid-state reaction method and sintered at 840°C after compaction at five different pressures 300, 450, 600, 750 and 900 MPa. The obtained samples were characterized by resistance vs. temperature (R-T) by four-point probe method, critical current density vs. applied magnetic field, (J_c -H), material density vs. pressure, (ρ - P), XRD, and by scanning electron microscopy (SEM). The results of this study showed that the quality of electrical and structural properties of Bi-2212 bulk superconductors strongly depends on the compaction pressure. X-ray diffraction patterns show the main reflections of the phase Bi-2212 for all samples, varying slightly in intensity. SEM shows the morphology of the grains present in the samples observing a decreasing in porosity at high compaction pressures (Figure 1). The aim of this work was to find the optimal compaction pressure for BSCCO ceramic superconductors in order to be used as superparamagnetic nanostructured superconductor with Au nanoparticles.

Keywords: Bi-based superconductors, Compaction pressure, X-ray diffraction.



Figure 1: Meissner effect of the Bi-2212 superconducting sample at 300 Mpa with a thermal treatment at 840°C for 36 hours and its characteristic microstructure (SEM).

References:

1. Kemal Kocaba, Melis Gökçe, Muhsin Çiftçiöğ lu Özlem Bilgili, (2010), Effect of Compaction Pressure on Structural and Superconducting Properties of Bi-2223 Superconductors, *J Supercond. Nov Magn* (2010) 23: 397–410.
2. M. Tepe, I. Avcı, and D. Abukay, (2003), Effect of pelletization pressure on structural properties and critical current hysteresis of ceramic superconducting $\text{Bi}_{1.7}\text{Pb}_{0.3}\text{Sr}_2\text{Ca}_2\text{Cu}_3\text{O}_y$, *Phys. Stat. Sol. (a)* 198, No. 2, 420– 426 (2003).

Bright-Excitons Splittings in CsPbX₃ (X= Cl, Br, I) Nanocrystals

R. Ben Aich,^{1*} K. Boujdaria,¹ L. Legrand,² M. Chamarro,² and C. Testelin²

¹ Université de Carthage, Faculté des Sciences de Bizerte, LR01ES15, Laboratoire de Physique des Matériaux : Structure et Propriétés, 7021 Zarzouna, Bizerte, Tunisia

² Sorbonne Université, CNRS-UMR 7588, Institut des NanoSciences de Paris, INSP, 4 place Jussieu, F-75005, Paris, France

Abstract:

A precise understanding of the excitonic fine structure is an essential step in view of the applications at the single object scale of all-inorganic perovskite nanocrystals in domains like nanophotonics or quantum optics. This new kind of colloidal materials has emerged recently as potential alternatives to II-VI semiconducting nanocrystals thanks to their defect-tolerance behaviour. In this work, the contribution of the long-range exchange interaction to the bright-exciton splittings is computed in strong and weak confinement regimes by using the group theory and **k.p** arguments. We show that the interplay of the shape anisotropy and the crystalline phase of a nanocrystal define the energy splitting between the fine structure components and then the emission characteristics. Different regimes are explored from weak to strong exciton confinement. In the weak confinement regime, splittings are inversely proportional to the cube of the exciton Bohr radius and we observe an increase of the splittings from iodide, to bromide, then chloride perovskite compounds. However, in the strong confinement regime, splittings increase inversely proportional to the nanocrystal volume and, for a given nanocrystal size, the splitting values are comparable for the three halide perovskite materials. This study provides crucial informations to seek the optimization of nanophotonic quantum devices manipulating the excitonic fine structure.

Keywords: Excitons, Inorganic perovskites, Nanocrystals

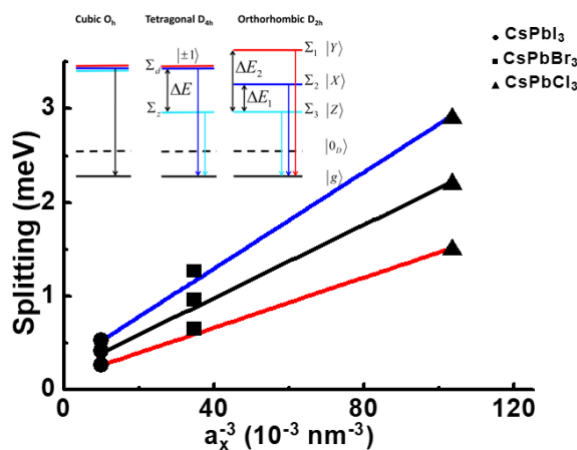


Figure 1: Energy labeling of the fine structure states and the dependence of the splitting on a_x^{-3} in the weak confinement regime.

Effect of nanoparticles of Titanium Dioxide in Technique Textiles

A. Paniagua-Mercado^{1*}, A. Mauro-Nolasco², C. García-Mejía¹, E. Díaz-Valdés¹, J. Ibarra-Báez¹.

¹Instituto Politecnico Nacional, 'Escuela Superior de Física y matemáticas, México D. F.

²Instituto Politecnico Nacional, Escuela Superior de Ingeniería Textil México D. F.

Abstract

Samples of ceramic fiber textile, with glass insert that supports 640°C, were characterized. Samples were prepared with 5% and 10% of titanium oxide nanoparticles, respectively, through starch impregnation method; later they were burned at different temperatures (400°C, 700°C, 800°C and 1100°C) during 24 h. The weight of each one was obtained, and it was observed that some samples lost more weight than the others. Friction test was conducted to evaluate wear. Macroscopic observations indicated that with 5% TiO₂ nanoparticles, the samples were not eroded 100% as the others without nanoparticles, but after being burned above 700°C an opaque film is formed, and at 1100°C they became slightly yellowish and diffused corresponding to a change from clinostatite to MgSiO₃; the insert was more resist to temperature, the samples become brittle from 800°C. The phases formed and the effect of TiO₂ nanoparticles at the surface was determined by XRD, EDS-X, analysis, abrasion test, Macrographs, Micrographs and EDS. Finally, oxides formed a protective film in the fiber depending of size of titanium dioxide and the temperatures, the insert was more resist to temperature, the fiber was protected of any photocatalytic activity by titanium dioxide and can attack dangerous and toxic chemicals; those nanoparticles are adhered to textile surfaces, converting this textile in new textile fiber.

Keywords: Ceramic fiber textile, nanoparticles, impregnation, titanium dioxide, clinostatite.

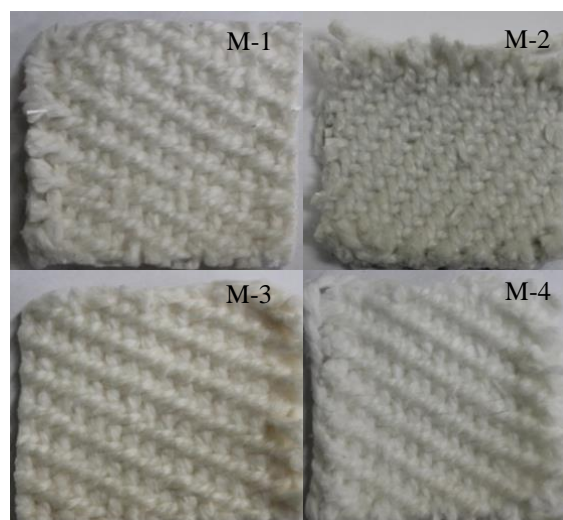


Fig 1 Samples of group 1

Figure 1: This figure is the natural textile fiber without nanoparticles, only was burned to 400 °C M-1, 700 °C M-2, 800 °C M-3 and 1100 °C M-4, when is protected with TiO₂, change the properties.

References:

1. Garcia, G. (2015) Textiles Panamericanos, color radiante, textiles tecnicos con nanopartículas, nuevos avances en materiales tecnicos, html. Copyright, Billian Publishing Inc.
2. Quian, L., Hines, J. (2004) Journal of textile and Apparel, Technology and Management, vol.4 issue 1, p.p. 3.
3. Quian, L., Hines, J. (2004) Journal of textile and Apparel, Technology and Management, vol.4 issue 1, p.p. 5
4. Functionality of nano titanium dioxide on
5. 6789/781/1/559_2005_ESIT_MAESTRIA_karina_alvarado.pdf

Characterization of Nanoparticles and related Metals in Tattoo Ink using Asymmetrical Flow Field-Flow Fractionation coupled with MALS and ICP-MS

G. Heinzmann^{1,*}, F. Meier¹, R. Drexel¹, T. Pfaffe¹, E. Moldenhauer¹, T. Klein¹

¹ Postnova Analytics GmbH, Landsberg, Germany

E-Mail: info@postnova.com

Abstract:

With increasing applications for nanoparticles in various consumer products, there is an urgent need for accurate and robust characterization methods for these materials also in complex matrices. Field-Flow Fractionation (FFF) is a particle separation and characterization technique that works over a broad size range, usually from 1 nm to 30 μm [1,2]. Coupled with Multi Angle Light Scattering (MALS) and Inductively-coupled Plasma Mass Spectrometry (ICP-MS), FFF not only enables the fractionation of sample constituents according to their size, but also provides information about elemental distributions across particle size distributions [3-4].

Metal and metal oxide nanoparticles are added to tattoo inks to enhance color vibrancy, but cutaneous allergies may occur due to the presence of toxic metals in inks.

This presentation demonstrates the use of Asymmetrical Flow FFF (AF4) coupled with MALS and ICP-MS to characterize several types of commercial tattoo ink by metal nanoparticle composition [5]. Particle size and element distributions of various metals (Al, Ti, Cu) were measured to study the composition of ink ingredients as a function of particle size, and dissolved versus particulate metal components.

Keywords: Tattoo ink, field-flow fractionation, ICP-MS, nanoparticle analysis, complex matrices

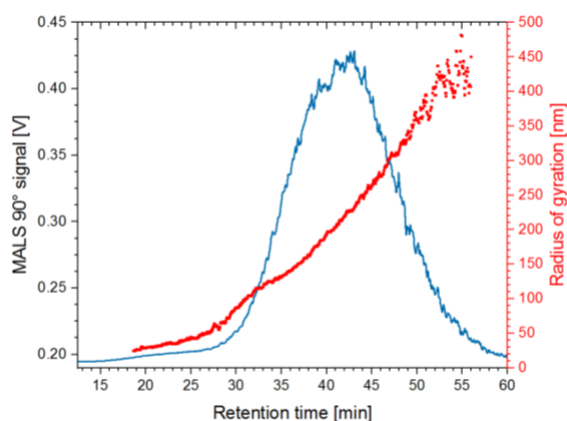


Figure 1: Particle size distribution of a nanoparticle containing, commercial tattoo ink determined by AF4-MALS.

References:

1. Giddings J.C., Ratanathanawongs S.K., Barman B.N., Moon M.H., Liu G.Y., Tjelta B.L., Hansen M.E., *Adv Chem Ser*, **1994**, 234, 309.
2. Giddings J.C., *Science*, 1993, 260, 1456.
3. Heroult, J., Nischwitz V., Bartczak D., Goenaga-Infante H., *Anal Bioanal Chem*, **2014**, 406(16), 3919.
4. Cascio C., Geiss O., Franchini F., Ojea-Jimenez I., Rossi F., Gilliland D., Calzolari L., *J Anal Atom Spectrom*, **2015**, 30(6), 1255.
5. Bocca B., Sabbioni E., Micetic I., Almonti A., Petrucci F., *J. Anal. At. Spectrom.*, **2017**, 32(3), 616-628.

High sensitivity aerosol mass concentration measurements by Corona charger : $PM_{0.1}$ down to pg/m^3

Wen-Cheng Gong^{1,2}, Chuen-Jinn Tsai², Nicolas Jidenko¹ and Jean-Pascal Borra^{1*}

¹Lab Phys Gaz & Plasmas, CNRS, Univ. Paris Sud, CentraleSupélec, Univ. Paris-Saclay, France

²Institute of Environmental Engineering, National Chiao Tung University, Hsinchu 300, Taiwan

Abstract

Air quality is a major issue, especially in terms of suspended particles, for health and atmospheric impact. Development of reliable and sensitive measurements of size and concentration is still under investigation especially below 100 nm, with recent development below 30 nm¹ (e.g. to study initial phases of nucleation on single digit nanometer sized particles reported in the atmosphere² and toxicological effects of nanoparticles). A high sensitivity aerosol mass concentration monitor is developed based on aerosol corona charger, size selection by impactors and measurement of the current of charged aerosol per size range. Doing so aerosol concentration can be derived from these currents if the mean charge per particle (\bar{q}_p) and aerosol penetration ($P = N_{out}/N_{in}$) versus particle size are defined as presented here.

A needle-to-cylinder direct corona charger with injection of aerosol in the discharge gap has been designed to achieve high mean charge per particle and high aerosol penetration. A flowrate of 16.7 L min⁻¹ (transit time of 15 ms). The discharge voltage (V_{corona}) is set from 3.6 to 8 kV to achieve a stable corona ion source with current from 1 to 30 μ A. Monodisperse NaCl particles with modal diameters (d_p) from 30 to 100 nm ($N_p \sim 10^4$ cm⁻³) are tested.

As expected from charging laws³⁻⁵, the mean charge per particle increases with particle diameter, probably due to a combined diffusion and field charging mechanism, even for particle as small as 30 nm. Despite higher charge for larger particles, the electrical mobility decreases with lower electro-collected fraction (higher penetration, cf. Figure 1). Such efficient charging of nanometer sized particles with fA detection limit of commercial electrometers, allows one to estimate the number concentration of the inlet sampled aerosol from current measurements, taking into account the losses by diffusion and electro-collection and the mean charged per particle versus particle diameter (cf. table 1). The related mass concentration can then be evaluated assuming water density of atmospheric particles.

The designed needle-to-cylinder direct corona charger is thus suitable to reduce the detection limit

of $PM_{0.1}$, down to pg/m^3 , while traditional filter based gravimetric measurement methods are limited to $\mu g/m^3$ mass concentration range. Moreover, these electrical measurements of mass concentration are suitable for quasi-real time measurement (response time ~ 0.1 ms). However, space charge electric field due to charged particles, affects electrical losses, i.e. the penetration required for mass concentration evaluation. This affects the accuracy of calculated $PM_{0.1}$ for higher particle concentrations and/or for larger particles mixed with particles smaller than 0.1 μ m, which still has to be addressed to define the concentration range of the apparatus.

Keywords: Aerosol, $PM_{0.1}$, corona charger,

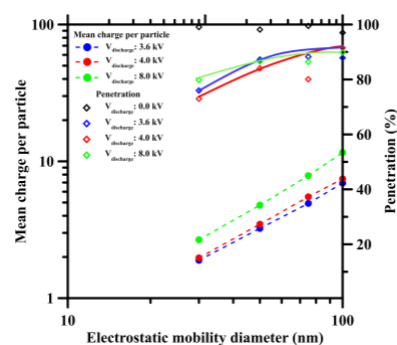


Figure 1: Aerosol penetration and mean charge per particle versus particles size at various V_{Corona}

D_p (nm)	detection limit	
	number conc. (#/cm ³)	mass conc. (pg/m ³)
5	112*	2*
30	14	200
50	8	500
100	4	2000

Table 2: Detection limits versus monodisperse particle size (*extrapolated values)

References

1. Kulmala M (2012) *Nat Prot.* 7-9 p1651
2. Carnerero, et al. (2018) *Atmos. Chem. Phys. Discuss.* <https://doi.org/10.5194/acp-2018-173>
3. Lawless, P. A. (1996). *J.A Sci.* **27**:191–215
4. Marquard A et al. (2006). *JAS* **37**:1052–68
5. Huang C.-H. et al. (2012) *JAWMA* **62**(1)87

Simple Sonochemical Synthesis of CuO Nanoparticles

N. Hassan^{1,*}, N. Silva², Y. Quintero³, S. Ramírez⁴, I. Díaz⁵, M. Colet⁵, A. Garcia^{3,*}.

¹ Programa Institucional de Fomento a la I+D+i, Universidad Tecnológica Metropolitana, San Joaquín, Chile

² Facultad de Diseño, Universidad del Desarrollo. Las Condes, Chile.

³ Advanced Mining Technology Center (AMTC), Universidad de Chile, Chile;

⁴ Department of Materials Chemistry, Faculty of Chemistry and Biology, Universidad de Santiago de Chile, Estación Central, Chile.

⁵ Department of Chemical Engineering and Biotechnology, Faculty of Physical and Mathematical Sciences, Universidad de Chile, Chile.

Abstract:

Copper oxide nanoparticles (CuONPs) were synthesized in air by reducing copper (II) sulfate pentahydrate salt ($\text{CuSO}_4 \cdot 5\text{H}_2\text{O}$) in the presence of sodium borohydride. The reaction was stabilized with Hexadecyltrimethylammonium bromide (CTAB) in a basic medium and using ultrasound waves. Different molar ratios of CTAB: Cu^{2+} and NaBH_4 : Cu^{2+} were explored [1]. Optimum conditions to generate spherical, stable, and monodispersed nanoparticles with hydrodynamic diameters of 36 ± 1.3 nm were obtained, using 16 mM CTAB and 2 M NaBH_4 (molar ratios Cu^{2+} :CTAB: NaBH_4 of 1:6:10). After to addition of NaBH_4 into CTAB: Cu^{2+} solution, an intense color change from colorless to dark brown was observed and abundant foam formation indicated the metallic copper particles formation, which was oxidized rapidly by the oxygen in the ambient. The TEM micrographs (Figure 1a) revealed that the first dark brown colloidal suspension corresponded to metal clusters of 3.6 ± 1.4 nm. By the DLS measurements, we obtained a distribution size number for CuNPs of 2 ± 0.3 nm with high polydispersity index (PDI) value of 0.592. The DLS measurements suggest that while NaBH_4 continues to react, the colloidal suspension would be polydispersed. This could be explained by the presence of metallic nuclei, and micelles of dynamic sizes. Figure 1b shows the TEM micrographs that were obtained after 72 hr in the yellow colloidal suspension of copper oxide, in which spherical particles 34 ± 12 nm in diameter and homogeneously distributed, were observed. Similar results were observed with DLS, where a distribution size number of 36 ± 1.3 nm and a PDI of 0.150, with a Zeta potential value of $+37 \pm 1.5$ mV, were attained.

X-ray diffraction (XRD) was implemented, and a monoclinic CuO crystal system was formed. This demonstrated a monoclinic crystal system corresponding to CuO. The diffraction peaks were identified and confirmed according to their selected area electron diffraction (SAED) patterns.

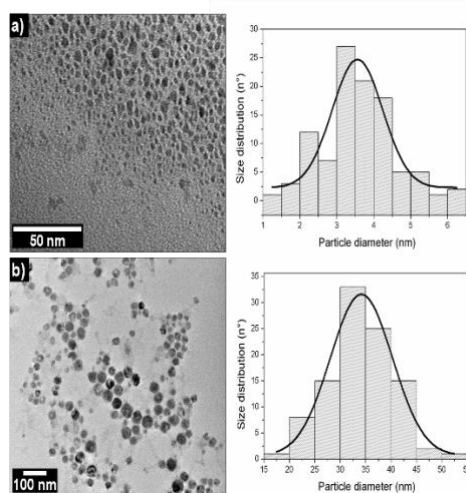


Figure 1: Transmission Electron Microscopy (TEM) micrographs of a) CuNPs and b) CuONPs with their respective particle size distribution histograms.

Funding: This research was funded by the Associative Research Program of the National Commission of Science and Technology, CONICYT, PIA Project ACM170003 and Fondecyt de Iniciación 11170849.

References:

1. N. Silva, S. Ramírez, I. Díaz, A. Garcia, N. Hassan (2019). Easy, quick and reproducible Sonochemical synthesis of CuO Nanoparticles. *Materials*. 12, 804-817.

Posters Session II: NanoBioMedecine / Nanosafety

Interaction of iron oxide nanoparticles with transferrin: effect on stability and iron uptake

Ulrike Martens^{1,2}, Ali Abou-Hassan³ and Mihaela Delcea^{1,2}

¹ University of Greifswald, Institute for Biochemistry, Greifswald, Germany

² University of Greifswald, Centre for Innovation Competence - Humoral Immune Reactions in Cardiovascular Diseases, Greifswald, Germany

³ Sorbonne Université, Laboratoire PHENIX, Paris, France

Abstract:

Recent research demonstrated that nanoparticles (NPs) can enhance or suppress the immune response by binding to proteins of the blood stream [1].

We focused on superparamagnetic iron oxide nanoparticles (SPIONs) which have received an increasing interest in the last decades due to their numerous applications as theranostics in nanomedicine [2]. They present many advantages related to their magnetic properties, including magnetic manipulation and separation. One important blood protein is transferrin whose main role is to deliver iron to all biological tissues. Transferrin is composed of two distinct domains, each containing an iron binding site.

We investigated by various biophysical techniques the interactions of SPIONs, namely maghemite $\gamma\text{-Fe}_2\text{O}_3$ NPs modified with different coatings (e.g. citrate, dextran) with transferrin. In particular, dynamic light scattering measurements as well as SDS-PAGE analyses revealed protein corona formation of our model protein transferrin on the NPs. Transferrin acted as a stabilizing agent of the colloidal suspension as verified by zeta potential measurements. In addition, the influence of the NPs on the iron binding site of transferrin in comparison to the binding to iron-free transferrin (apotransferrin) was studied *via* UV-Vis spectroscopy and urea PAGE.

Further, we characterized functionalized-NP and identified structural changes of the proteins upon interaction with nanoparticles using circular dichroism spectroscopy. The secondary structure of transferrin is not altered due to the iron-loading. The iron-saturation of the protein strongly affects the formation of the bioconjugate. The iron-free form results in a threefold increase of the hydrodynamic diameter compared to the partly iron-saturated transferrin.

Keywords: iron oxide nanoparticles, transferrin, apotransferrin, protein corona, nanoparticle-protein interaction, circular dichroism spectroscopy, stability, iron uptake.

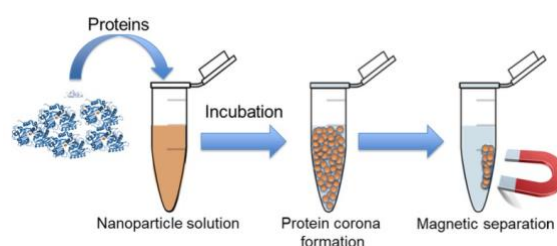


Figure 1: Schematic of the formation of bioconjugates consisting of magnetic nanoparticles with attached protein corona. The loaded magnetic nanoparticles were isolated by applying a magnetic field.

Funding by BMBF (NanoImmun-FKZ 03Z22C51) is acknowledged.

References:

1. M. A. Dobrovolskaia et al. (2007) *Nat. Nanotech.* 2, 469.
2. M. Mahmoudi et al. (2011) *Advanced Drug Delivery Reviews* 63, 24–46.

Live Animal Imaging of a Labeled Chlamydia Recombinant Protein Encapsulated in PLGA Nanoparticles

V. A. Dennis,^{1,*} R. Sahu,¹ S. R. Singh,¹

¹ Alabama State University, Center for Nanobiotechnology Research, Montgomery, USA

Abstract:

Advancement in the nanomaterial field related to nanoparticle formulation and their use as therapeutic agents in biomedical applications for drug delivery, vaccine and targeting is being explored. To develop nanoparticles for these critical applications, it is important to understand their uptake and intracellular allocation for processing. The intracellular activity of nanoparticles is vital for biosafety and therapeutic efficacy. We have developed a *Chlamydia trachomatis* nanovaccine by encapsulating its immunologically dominant recombinant MOMP (major outer membrane protein) in biodegradable PLGA (poly (lactic-co-glycolic acid) nanoparticles (PLGA-rMOMP). *Chlamydia* is the leading cause of bacterial sexually transmitted infections worldwide, and vaccine development is needed to reduce its infections. The aim of this study was to investigate the uptake and intracellular distribution of the nanovaccine by live imaging in mice. We encapsulated FITC- or Infrared (IR)-labeled rMOMP in PLGA nanoparticles followed by subcutaneous injection of mice. Imaging of the labeled rMOMP encapsulated in PLGA nanoparticles was monitored daily up to 15 days using a live imaging system. Our results show that the encapsulated labeled rMOMP localized to regional lymph nodes and induced an early antibody response in mice, suggesting protein release and its capacity to induce an adaptive immune response.

Keywords: PLGA nanoparticles, Live imaging, Chlamydia nanovaccine, Bacteria, rMOMP, FITC, Infrared, Lymph nodes, Antibody.

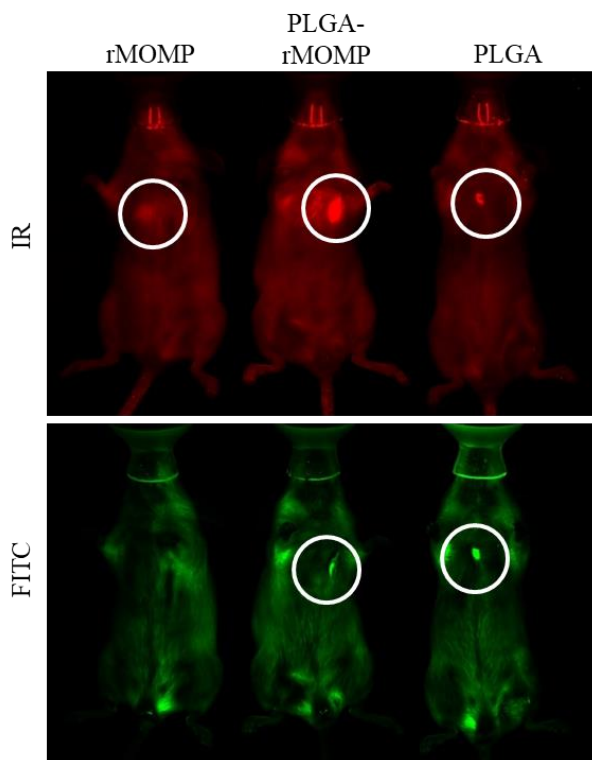


Figure 1: Trafficking of a labeled (IR or FITC) Chlamydia recombinant major outer membrane protein (rMOMP) encapsulated in PLGA nanoparticles to regional nodes in mice. White circles show the protein in regional lymph nodes after day 15 of injecting mice with the labeled rMOMP, PLGA-encapsulated labeled rMOMP (PLGA-rMOMP) or labeled PLGA nanoparticles alone.

References:

1. Stacie J. Fairley, Shree R. Singh, Abeyayehu N. Yilma, Alain B. Waffo, Praseetha Subbarayan, Saurabh Dixit, Murtada A. Taha, Chino D. Cambridge, Vida A. Dennis. *Chlamydia trachomatis* recombinant MOMP encapsulated in PLGA nanoparticles triggers primarily T helper 1 cellular and antibody immune responses in mice: a desirable nanovaccine candidate. *Int. J. Nanomedicine* 2013; 8:2085-99. doi: 10.2147/IJN.S44155.

Study on phase transformation pathways of iron sulfide minerals

Yen-Hua Chen* and Ding-Teng Jhan

National Cheng Kung University, Department of Earth Sciences, Tainan, Taiwan

Abstract:

Iron sulfide is the common mineral on the natural Earth, and the changes in its chemical composition would lead to different iron sulfide mineral-phases (mackinawite: FeS, greigite: Fe₃S₄, pyrrhotite: Fe_{1-x}S, pyrite: FeS₂, etc.). There has been increasing attraction in iron sulfide minerals because of its importance in geology. For example, pyrrhotite geothermometry is applied to determine the temperature of ore bodies. Greigite is acted as a reference for the presence of methane in natural gas hydrate. It is also imperative for paleomagnetic and environmental magnetic investigations. The growth process and phase transition of iron sulfides also have a significance in the global sulfur-cycle and the origin of life. Owing to the geological importance of iron sulfides, detailed understanding of their phase transition pathways and their mineral properties would be valuable. However, the formation pathways of iron sulfides are still not fully understood.

In this study, iron sulfide minerals are synthesized via hydrothermal methods under anoxic conditions (adjusting the effects on the pH values, growth temperature and reaction time, ratio of Fe/S in the raw materials). It was observed that it was against for greigite growth at a higher reaction temperature and greigite and pyrrhotite favored to exist under the acidic environment. Moreover, the sufficient sulfur-source (a higher ratio of S/Fe) would enhance the phase transformation from greigite to smythite or pyrite. It was also found that the phase transition sequence was in the order of FeS → Fe₃S₄ → Fe₉S₁₁ → Fe₇S₈ during the crystal growth and this order was agreed with the natural phenomenon. This suggested that pyrrhotite was the final stable phase under this anoxic condition.

Keywords: iron sulfide mineral, hydrothermal method, phase transformation pathway.

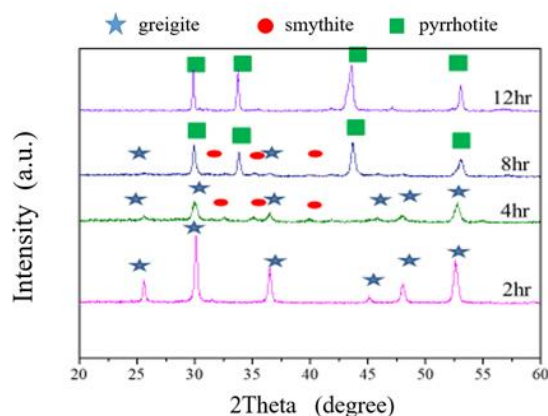


Figure 1: The XRD pattern of iron sulfide minerals under the synthetic parameters of 135°C, Fe/S = 3/4 with different reaction time.

References:

1. Bouchloukh, W., Jouenne, B. (2012) Characterization of biofilms formation in urinary catheters, *Amer. J. Infect. Control.*, In Press. Rickard, D, Lither, G.W. (2007) Chemistry of iron sulfides, *Chem Rev* 107: 514–562.
2. Devey, A.J. (2009) Computer modelling studies of mackinawite, greigite and cubic FeS. PhD thesis, University College London.

Membrane affinity of fluorescently labelled and drug-conjugated peptides

E. Pári^{*1}, É. Kiss¹, G. Gyulai¹, K. Horváti^{2,3}, Sz. Bősze²

¹Eötvös Loránd University, Institute of Chemistry, Laboratory of Interfaces and Nanostructures, Budapest, Hungary

²MTA-ELTE Research Group of Peptide Chemistry, Budapest, Hungary

³Eötvös Loránd University, Institute of Chemistry, Budapest, Hungary

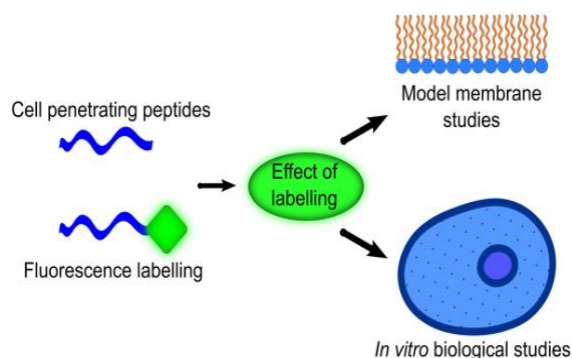
*pari.edit@gmail.com

Abstract:

Recently cationic amphiphilic and antimicrobial peptides have considerable attention as possible agents against drug resistant pathogens [1]. Cell penetrating peptides (cpps) and several synthetic derivatives are also in the focus of research and therapeutic applications because of their promising ability to transport nonpermeable drugs into live cells [2]. Further assistance might be provided by attaching a fluorescent moiety to a bioactive component to follow the transport, distribution, cellular uptake, internalisation processes in biological systems [3].

The aim of the present work was to investigate the membrane affinity of a series of peptides and comparing the effect of fluorescent labelling and drug-conjugation on them. The studied peptides contains some cell penetrating peptides such as Penetratin and Transportan, antimicrobial peptides like Magainin and Melittin, synthetic cationic peptides such as OT20, a shorter derivative of CrotaMin and Dhvar4 a synthetic derivative of Histatin. These original peptides, their 5(6)-carboxyfluorescein (Cf) derivatives and their isoniazid (INH) drug conjugates were investigated. The peptide-lipid interactions were characterized and compared applying Langmuir monolayer cell membrane models. Zwitterionic DPPC, negatively charged DPPC+DPPG and DPPC+mycolic acid mixed lipid monolayers were used.

It was found that the membrane affinity to the neutral lipid layer was increased by Cf-conjugation in the case of the most hydrophobic Magainin, Melittin and Transportan. Enhanced membrane affinity was found using DPPC+DPPG model membrane for both unlabelled and Cf-labelled peptides



due to the interplay of the hydrophobic and electrostatic interactions. Peptide-lipid interactions also increased as a result of INH conjugation particularly in the case of Transportan and Magainin with DPPC+mycolic acid mixed monolayer.

The understanding the interactions of bioactive peptides and drug-carrier conjugates with cell membrane might contribute to design more effective therapeutic systems.

Keywords: cell penetrating peptides, membrane affinity, lipid monolayer, penetration, fluorescent labelling, drug-conjugation

References:

1. Nyström, L., Malmsten, M. (2018), Membrane interactions and cell selectivity of amphiphilic anticancer peptides, *Curr. Opin. Colloid. In.*, 38, 1-17.
2. Reissmann, S. (2014), Cell penetration: scope and limitations by the application of cell-penetrating peptides, *J. Pept. Sci.* 20, 760-784.
3. Kiss, É., Gyulai, G., Pári, E., Horváti, K., Bősze, Sz. (2018), Membrane affinity and fluorescent labelling: comparative study of monolayer interaction, cellular uptake and cytotoxicity profile of carboxyfluorescein-conjugated cationic peptides, *Amino Acids* 50, 1557-1571.

Optical Sensing by Plasmon Resonance Effects of Gold Nanoparticles

Geon Joon Lee,^{1,*} Myeongju Kang,² Eun Ha Choi,¹ Younghun Kim,²

¹ Kwangwoon University, Department of Electrical and Biological Physics, Seoul 01897, Korea

² Kwangwoon University, Department of Chemical Engineering, Seoul 01897, Korea

Abstract:

Photon localization has attracted intense interest since it was first proposed as the analogue of electron localization. Nanostructured materials have unique physical and chemical properties as a result of their small size. These properties differ from those of the corresponding bulk materials. If the electromagnetic wave is coupled to a collective oscillation of surface electrons around metal nanoparticles, surface plasmon wave is generated and localized strongly in the vicinity of nanoparticle. Experimentally, there have been many research efforts devoted to the structural, electrical, and optical properties of low dimensional structures, such as quantum dots, quantum wells, nanoparticles, nanowires, and nanotubes. Among them, metallic nanostructures have drawn considerable attention because of surface plasmon resonance effects, selective photoabsorption, photoluminescence enhancement, Raman enhancement, large optical nonlinearity, and ultrafast response. Otto *et al.* studied the surface-enhanced Raman spectra of DNA bases due to plasmon resonance effects of roughened silver film[1]. Lee *et al.* investigated the optical properties of nucleobase thin films by attenuated total reflection and surface-enhanced Raman spectroscopy[2]. In this research, we examined the optical sensing properties of gold nanoparticles (AuNPs) prepared by reduction method using citrate and gold chloride (Figure 1). The size of AuNPs was adjusted by Ostwald ripening mechanism. The optical and structural properties of AuNPs were measured by dynamic light scattering, transmission electron microscopy (TEM), UV-visible absorption and Raman spectroscopy. The optical sensing properties of AuNPs were studied by comparing the Raman spectra of biomaterials and/or functional materials incubated on AuNPs with those on glass.

Keywords: gold nanoparticles, plasmon resonance, surface-enhanced Raman scattering, optical sensing, functional materials, biomaterials.

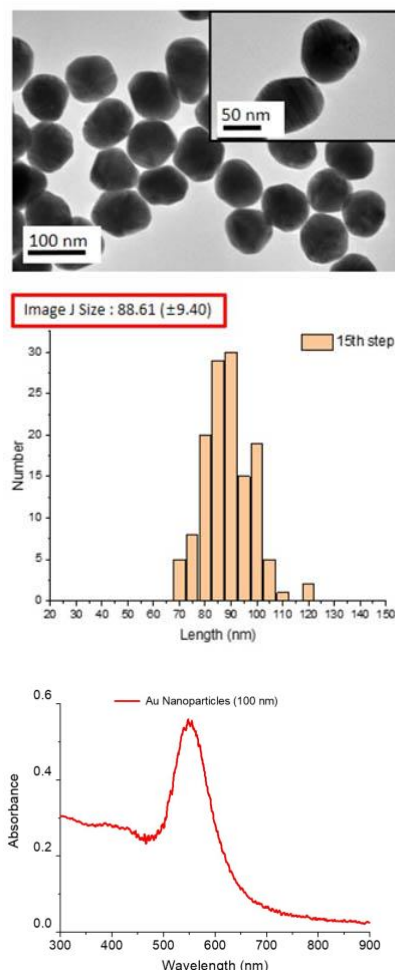


Figure 1: TEM image, particle size distribution and absorption spectrum of gold nanoparticles prepared by citrate reduction method and Ostwald ripening.

References:

1. C. Otto, T. J. J. Tweel, F. F. M. de Mu1 and J. Greve (1986), Surface-Enhanced Raman Spectroscopy of DNA Bases, *J. Raman Spec.*, 17, 289-298.
2. M. Kim, W. K. Ham, W. Kim, C. K. Hwangbo, E. H. Choi, G. J. Lee (2018), Optical properties of nucleobase thin films as studied by attenuated total reflection and surface-enhanced Raman spectroscopy, *Opt. Mater.*, 78, 531-577.

Improvement of photoactivity of modified-chlorin photosensitizer by its conjugation to metallic and bimetallic nanoparticles

J. A. Magalhães^{1*}, B. C. Nunes¹, A. U. Fernandes², D.C. Arruda³, E. R. Camargo⁴, D. B. Tada¹

¹Federal University of São Paulo, Department of Science and Technology, Sao Paulo, Brazil

²Anhembi Morumbi University, Institute of Biomedical Engineering, Sao Paulo, Brazil

³University of Mogi das Cruzes, Integrated Nucleus of Biotechnology, São Paulo, Brazil

⁴Federal University of São Carlos, Department of Chemistry, Sao Paulo, Brazil

*jmagalhaes@gmail.com

Abstract:

Although Photodynamic Therapy (PDT) of cancer has been continuously improved, its efficiency is still limited by the high toxicity in the absence of irradiation, aggregation and deactivation by biomolecules of the most common photosensitizers (PS). The association of PS to nanoparticles (NPs) can be a promising tool to overcome these limitations and also to enhance PS tumor selectivity. In addition, the association of PS to metallic and bimetallic NPs may provide the enhancement of PS photoactivity due to the electronic coupling with NPs plasmon effect. Herein we investigate the physicochemical properties and cytotoxicity of two types of NPs: gold NPs (AuNPs) and gold-platinum NPs (AuPt NPs) functionalized with a chlorin molecule modified with a thiol group. AuNPs were obtained by the Turkevich method¹ whereas AuPtNPs were obtained by the co-reduction of gold and platinum salts². TEM images were used to investigate morphology and size of the NPs and dynamic light scattering (DLS) was used to determine the size distribution and ζ -potential of coated and uncoated NPs. NPs composition was determined by XRD analysis, and ICP-OES was used to quantify the metals in the NPs. Finally, cytotoxicity of coated and uncoated NPs was evaluated by the MTT assay. For AuNPs, images of TEM showed nearly spherical NPs, with a mean diameter of 19 ± 8 nm, whereas the hydrodynamic diameter obtained by DLS was of 14.4 ± 0.4 nm. AuNPs presented satisfactory colloidal stability, as indicated by the ζ -potential of -47 ± 1 mV. XRD analysis showed the characteristic peaks of gold with FCC

crystalline structure, without contaminants, and metal concentration of 1.9 mM which was obtained by ICP-OES. The plasmon band of AuNPs was visible at 525 nm by UV-Vis spectrometry. The functionalization of AuNPs with the chlorin-modified molecule was successful since the characteristic peaks of modified-chlorin (408 nm and 670 nm) and the displacement of the gold plasmon band were observed in the UV-Vis spectrum of chlorin-AuNPs. Moreover, it was observed a decrease in ζ -potential (-36 ± 4 mV) and an increase of hydrodynamic diameter (17.0 ± 0.8 nm) compared to the AuNPs. In the case of AuPt NPs, the hydrodynamic diameter could not be measured by DLS due to the very small size of these NPs. Therefore AuPt NPs were characterized by TEM. The images showed spherical NPs with mean diameter of 2.2 ± 0.9 nm. Individual peaks of gold and platinum did not match with the peaks observed by XRD analysis, indicating an alloy structure of the NPs. ICP-OES indicated the molar proportion of 80% Au and 20% Pt. After functionalization, the presence of the modified chlorin peaks in UV-Vis spectrum confirmed the presence of chlorin in the AuPt NPs although the ζ -potential did not change significantly. In the MTT assay the incubation of melanoma cells (B16-F10Nex2) with functionalized NPs and chlorin in solution followed by laser irradiation of 660 nm and 102 J/cm² resulted in cytotoxicity of chlorin-AuNPs and chlorin-AuPtNPs 56% and 25% higher, respectively compared to chlorin in solution. At the same concentration of chlorin and under laser irradiation of 660 nm and 102 J/cm², chlorin-AuNPs were twice more toxic to B16-F10Nex2 cells (41%) than chlorin-

AuPtNPs (70%). Therefore, both types of NPs improved the phototoxicity of the modified-chlorin molecule in comparison with chlorin free in solution. Comparing the two types of NPs, it was possible to conclude that gold NPs provided higher increase in the photoactivity of chlorin. It is noteworthy that in the absence of irradiation, both types of NPs were able to reduce chlorin toxicity. The cell viability of functionalized NPs in the absence of irradiation was about 88% and 106% whereas the chlorin in solution resulted in 96% of cell viability. In conclusion the functionalization of AuNPs and AuPt NPs with modified-chlorin resulted in promising platforms to be used in the PDT of cancer since they showed enhanced photoactivity and lower toxicity in the dark.

Keywords: photodynamic therapy, gold nanoparticles, gold-platinum nanoparticles.

References:

1. B. Enustun, J. Turkevich, Coagulation of colloidal gold, *Journal of the American chemical society* 85 (21) (1963) 3317-3328.
2. Y. Zhao, C. Ye, W. Liu, R. Chen, X. Jiang, Tuning the composition of AuPt bimetallic nanoparticles for antibacterial application, *Angewandte Chemie International Edition* 53 (31) (2014) 8127-8131.

Target Catalyzed Toehold-mediated DNA Strand Displacement Events for Universal MicroRNA Detection

Y. Park,¹ C. Y. Lee,¹ S. Kang,¹ H. Kim,¹ K.S. Park,² H. G. Park,^{1*}

¹ KAIST, Department of Chemical and Biomolecular Engineering, Daejeon, Republic of Korea

² Konkuk University, Department of Biological Engineering, Seoul, Republic of Korea

Abstract:

Herein, we developed a label-free, and enzyme-free method for the colorimetric detection of microRNA (miRNA). The system utilizes a detection probe that specifically binds to the target miRNA and sequentially releases a catalyst strand (CS) used for the triggering of the subsequent TMSD reaction. Thus, in the presence of target miRNA, CS, which mediates the formation of an active G-quadruplex DNAzyme that is initially caged and inactivated by a blocker strand, is released. Additionally, a fuel strand that is supplemented for the recycling of the CS induces another round of TMSD events, consequently leading to the generation of a large number of active G-quadruplex DNAzymes. As a result, a distinct colorimetric signal is produced by the ABTS oxidation promoted by the peroxidase mimicking activity of the free G-quadruplex DNAzymes. Based on this novel strategy, we detected miR-141, a promising biomarker for human prostate cancer, with high selectivity. The diagnostic capability of this system was demonstrated by reliably determining target miR-141 in human serum, showing its great potential towards real clinical applications. Importantly, the proposed approach involves separate target recognition and signal transduction modules. Therefore, it could be extended to analyze different target miRNAs by simply redesigning the detection probe while keeping the same signal transduction module as a universal signal amplification unit, which was demonstrated by analyzing a second target miRNA, let-7d.

Keywords: miRNA detection, colorimetric biosensor, biomarker detection, toehold-mediated strand displacement, enzyme-free, label-free, G-quadruplex DNAzyme

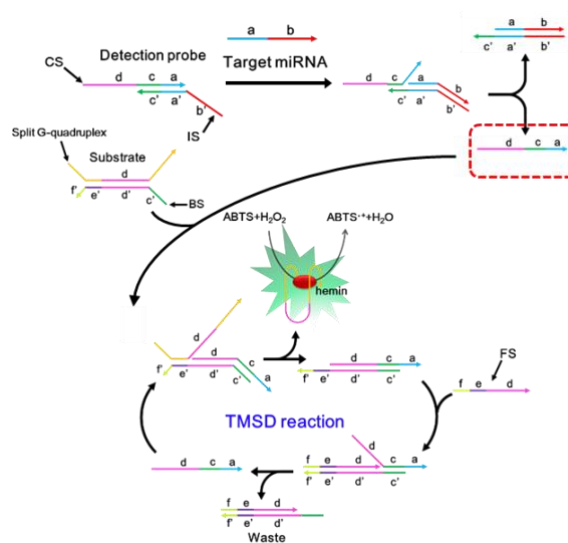


Figure 1: Schematic illustration of the target miRNA detection system based on the target-triggered TMSD reaction (The 3'-end is denoted by an arrow).

References:

1. Bartel, D.P., (2004) MicroRNAs: genomics, biogenesis, mechanism, and function, *Cell*, 116, 281-297.
2. Bi, S., Zhang, J., Hao, S., Ding, C., Zhang, S., (2011) Exponential Amplification for Chemiluminescence Resonance Energy Transfer Detection of MicroRNA in Real Samples Based on a Cross-Catalyst Strand-Displacement Network *Anal. Chem.*, 83, 3696-3702.
3. de Planell-Saguer, M., Rodicio, M.C., (2011) Analytical aspects of microRNA in diagnostics: A review *Anal. Chim. Acta* 699, 134-152.

Target-responsive DNA polymerase activity based fluorescence aptasensor for protein detection

Y. Jung¹, C. Y. Lee¹, K. S. Park,² and H. G. Park^{1,*}

¹ KAIST, Department of Chemical and Biomolecular Engineering (BK 21+ program), Daejeon, Republic of Korea

² Konkuk University, Department of Biological Engineering, College of Engineering, Seoul, Republic of Korea

Abstract:

Herein, a novel detection method for target protein based on the target-responsive DNA polymerase activity was described. In principle, the detection probe consisting of two different types of DNA aptamers specific to the target protein and DNA polymerase, regulates DNA polymerase activity in response to the target protein. The presence of target protein enables destabilization of the detection probe and recovery of DNA polymerase activity. Consequently, the activated DNA polymerase triggers the primer extension reaction on the target-specific DNA aptamer, which recycles the target protein for repetitive activation cycle of DNA polymerase. Also, DNA polymerase initiates the multiple primer extension reactions on the primer/template complex, leading to the release of the fluorophore from TaqMan probe and dramatic fluorescence enhancement (Figure 1). Based on this strategy, we successfully determined a model target protein, lysozyme (Lys) with a limit of detection as low as 0.8 nM and demonstrated the practical applicability of this system by analyzing Lys in human serum.

Keywords: DNA aptamer, DNA polymerase activity, Aptamer-protein interaction, Protein detection, Biosensor

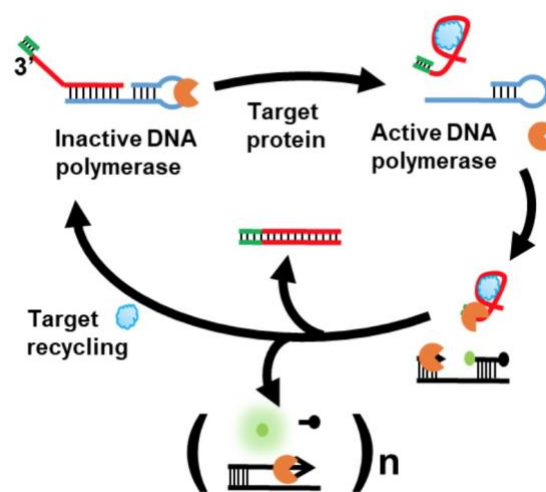


Figure 1: Schematic illustration of the protein detection method based on the target-responsive DNA polymerase activity.

References:

1. Park, K. S., Lee, C. Y., Park, H. G. (2015) Target DNA induced switches of DNA polymerase activity, *Chem. Commun.*, 51, 9942-9945.
2. Tan, Y., Guo, Q., Zhao, X., Yang, X., Wang, K., Huang, J., Zhou, Y. (2014) Proximity-dependent protein detection based on enzyme-assisted fluorescence signal amplification, *Biosens. Bioelectron.*, 51, 255-260.
3. Fu, R., Jeon, K., Jung, C., Park, H. G. (2011) An ultrasensitive peroxidase DNzyme-associated aptasensor that utilizes a target-triggered enzymatic signal amplification strategy, *Chem. Commun.*, 47, 9876-9878.

Effect of Nano-Scale and Micro-Scale Zero-Valent Iron on Inferring Metabolic Pathways in Freshwater Bacteria

N. H.A. Nguyen*, R. Špánek, A. Ševců

Technical University of Liberec, Institute for Nanomaterials, Advanced Technologies and Innovation, Liberec, Czech Republic

Abstract:

In recent years, research interest in metagenomics using next-generation sequencing (NGS) has been increasing in the environmental field. In particular, the NGS of 16S rRNA gene has been applied for the toxicity study of nanomaterials on freshwater microorganisms. A question arising is whether NGS data can be further applied for the description of metabolic pathways. Up to now, no such study has investigated this possibility. Bowman has introduced the term ‘inferring metabolic pathways’, which is based on a phylogenetic placement approach of 16S rRNA gene sequence collections and MetaCyc pathway ontology¹. We have applied the Bowman method (Paprica framework) to analyse NGS data from our recent publication, where the nano-scale ZVI (nZVI) dynamically changed freshwater bacterial communities compared to less influencing micro-scale ZVI (mZVI)². This encouraged us to ask questions concerning bacterial metabolic pathways: which were significantly involved or how they changed due to different effect of nZVI and mZVI (Figure 1)? Our first results revealed that 268 metabolic pathways played significant roles ($p < 0.05$) in bacterial metabolisms. The 50 most influenced pathways were chosen for further investigation and included 30 for degradation, 15 for biosynthesis, 3 for biosynthesis/degradation and 2 for detoxification. Additionally, we applied three methods for evaluation of inferring metabolic pathways: i) Bowman, ii) DESEQ2 and iii) our own method ‘Špánek’, and obtained 8 common and significant pathways. These pathways showed similar trend between mZVI treatment and the control. nZVI treatment affected acetoin degradation and hydrogen oxidation, both highly decreased after 7 days and increased again after 21 days; six other pathways: octane oxidation, propanoyl CoA degradation II, methylsalicylate degradation, chlorosalicylate degradation and Entner-Doudoroff pathway I highly increased after 7 days and decreased after 21 days. Investigation of inferring metabolic pathways based on 16S

rRNA sequencing is very promising, though it has to be verified by transcriptomic analysis.

Keywords: inferring metabolism, mZVI, nZVI, bacterial communities, reservoir water.

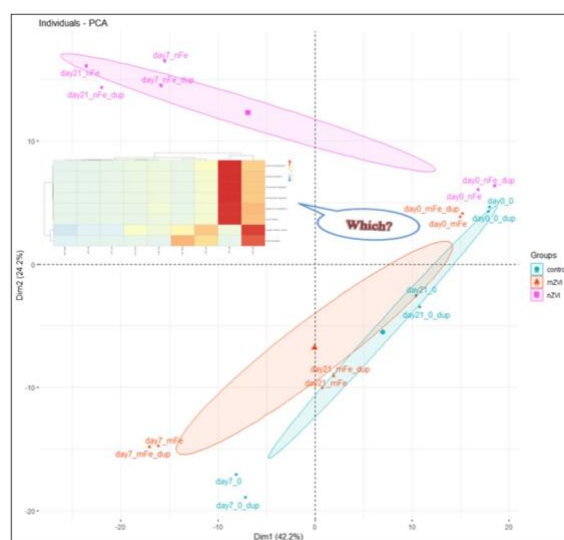


Figure 1: Illustration of the fundamental question of which metabolic pathways were significantly involved or changed due to the different effect of mZVI and nZVI on bacterial communities in reservoir water. An inserted heatmap shows 8 significant metabolic pathways affected by ZVI.

References:

1. Bowman J.S., Ducklow, H. W. (2015), Microbial communities can be described by metabolic structure: a general framework and application to a seasonally variable, depth-stratified microbial community from the coastal west antarctic peninsula, *PLoS One*, 10,1–18.
2. Nguyen, N. H. A., Špánek, R., Vojtěch K., Ribas, D., Vlková, D., Řeháková, H., Kejzlar, P., Ševců, A. (2018), Different effects of nano-scale and micro-scale zero-valent iron particles on planktonic microorganisms from natural reservoir water, *Environ. Sci.: Nano*, 5,1117-1129.

Food Matrices-ZnO Nanoparticle Interactions and their Effects on Biological Systems

Hye-rin Jin,¹ Yu Jin,¹ Soo-Jin Choi,¹

¹ Seoul Women's University, Department of Food Science & Technology, Seoul, Republic of Korea

Abstract:

Nanotechnology have been applied to various fields such as electronic products, consumer goods, pharmaceutical, and food industry (Luykx et al.; 2008). ZnO nanoparticles (NPs) are widely used as dietary supplements, food additives, and food packaging materials due to their nutritional value and antimicrobial property. Therefore, humans are more likely to be exposed to ZnO NPs (Yan et al.; 2015). However, there are little study on the interaction between ZnO NPs and food matrices, which can affect their toxicity and biological responses. Indeed, food additive ZnO NPs are directly added to food matrices composed of various components. In this study, we investigated the interactions between food matrices (saccharides and proteins) and ZnO NPs by characterizing their changes in physicochemical properties. Quantitative analysis of the interactions was performed by HPLC and fluorescence quenching. Moreover, the interaction effects on biological responses were evaluated in terms of cytotoxicity (Figure 1), cellular uptake, intestinal transport, oral absorption, protein deformation, and digestive efficiency. The results show that ZnO NPs were interacted with saccharides and proteins in food matrices, but the interaction effects on biological responses were highly dependent on the type of food components. Interestingly, the interactions did not affect protein structure or digestive efficiency. These findings will be useful to elucidate and understand potential toxicity of ZnO NPs in the food industry.

Keywords: zinc oxide nanoparticles, interaction, saccharide, protein, food matrix, cytotoxicity, intestinal transport, oral absorption, protein deformation, digestive efficiency.

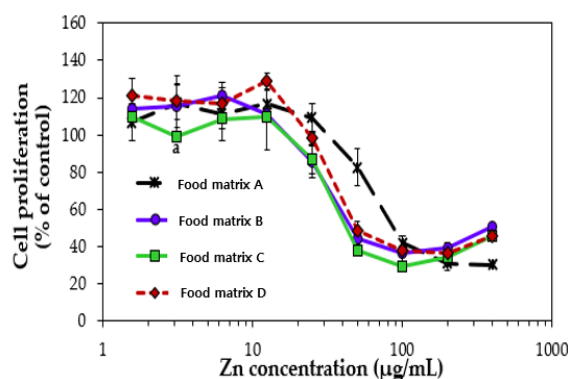


Figure 1: Cytotoxic effect caused by the interaction between ZnO NPs and food matrices.

References:

1. Luykx, D. M., Peters, R. J., van Ruth, S. M., Bouwmeester, H. (2008) A review of analytical methods for the identification and characterization of nano delivery systems in food, *J. Agr. Food Chem.*, 56, 8231–8247.
2. Yan, X., Rong, R., Zhu, S., Guo, M., Gao, S., Wang, S., Xu, X. (2015) Effects of ZnO nanoparticles on dimethoate-induced toxicity in mice, *J. Agr. Food Chem.*, 63, 8292–8298.

Detection of Zinc Oxide Nanoparticles in Food Matrices Using Cloud Point Extraction Approach

Ye-Rin Jeon,¹ Soo-Jin Choi¹

¹ Seoul Women's University, Department of Food Science & Technology, Seoul, Republic of Korea

Abstract:

Zinc oxide (ZnO) have been used in diverse food products as food additives because of its nutritional value (Faiz *et al*; 2015). Recently, the use of zinc oxide nanoparticles (ZnO NPs) in food products is increasing along with nanotechnology development. However, study on physicochemical changes of ZnO NPs in food matrices and their effects on biological responses has not been extensively explored. Moreover, it is important to separate and detect ZnO NPs as particulate forms to determine their fate in food products. In this study, we developed separation and detection method of ZnO NPs in food matrices using cloud point extraction (CPE) approach (Figure 1)(Majedi *et al*; 2012), followed by characterization by dynamic light scattering (DLS) and field emission scanning electron microscopy (FE-SEM) analysis. Quantitative analysis of ZnO NPs and zinc ion was performed with inductively coupled plasma atomic emission spectroscopy (ICP-AES). The CPE method was also applied to determine their biological fate in human intestinal cells. The results show that particle size distributions and morphology of ZnO NPs obtained after CPE in food matrices were not significantly different from those of pristine. The recovery of ZnO NPs in foods using CPE was more than 80% with primarily particulate forms. These findings will be useful to determine the fate of ZnO NPs in food matrices and biological samples, and provide basic information about their safety aspect in food products.

Keywords: cloud point extraction, zinc oxide, food additive, size distribution, food matrices, cellular fate.



Figure 1: Schematic illustration for separation and quantification of ZnO NPs in food matrices using CPE method.

References:

1. Faiz, H., Zuberi, A., Nazir, S., Rauf, M., Younus, N. (2015) Zinc oxide, zinc sulfate and zinc oxide nanoparticles as source of dietary zinc: comparative effects on growth and hematological indices of juvenile grass carp (*ctenopharyngodon idella*), *Int. J. Agric. Biol.*, 17, 568-574.
2. Majedi, SM., Lee, HK., Kelly, BC. (2012) Chemometric analytical approach for the cloud point extraction and inductively coupled plasma mass spectrometric determination of zinc oxide nanoparticles in water samples, *ACS Anal. Chem.*, 84, 6546-6552.

Safety Evaluation of Food Additives Titanium Dioxide and its Quantitative Analysis in Food Matrices

Ji-Soo Hwang,¹ Soo-Jin Choi,¹

¹ Seoul Women's University, Department of Food Science & Technology, Seoul, Republic of Korea

Abstract:

The use of nanoparticles as food additives has been increasing due to the development of nanotechnology in the food industry (He *et al.*; 2016). Titanium dioxide (TiO₂) are used in various food products to improve functionality as a coloring agent (Peters *et al.*; 2014). However, study on the safety aspects of food additive TiO₂ as well as their physicochemical properties and quantitative analysis in food matrices has not been well explored. In this study, physicochemical properties of food additive TiO₂ particles from various manufacturers were characterized by measuring hydrodynamic radii and zeta potentials, and their cytotoxicity was investigated in human intestinal cells. Quantitative analysis of TiO₂ in simulated and commercial food products were performed by optimizing pretreatment conditions, followed by inductively coupled plasma-atomic emission spectroscopy (ICP-AES) analysis (Figure 1). The results demonstrate that the hydrodynamic radii of food additive pristine TiO₂ particles were larger than 100 nm. There is little cytotoxicity caused by TiO₂ in terms of cell proliferation and membrane damage, except oxidative stress induction. Their intestinal transport was found to be extremely low. The presence of food additive TiO₂ in various commercial food products was confirmed, showing similar physicochemical properties to pristine TiO₂. These findings will provide basic information about safety aspect of food additive TiO₂.

Keywords: titanium dioxide, food additives, physicochemical property, cytotoxicity, quantitative analysis.

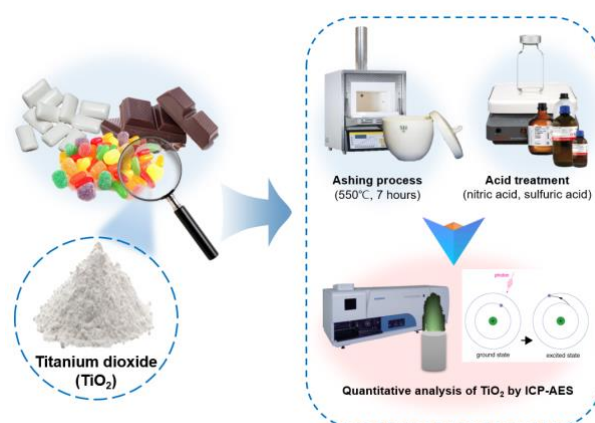


Figure 1: Schematic illustration for quantitative analysis of TiO₂ by ICP-AES after pretreatment such as ashing process and acid treatment.

References:

1. He, X., Hwang, H. (2016), Nanotechnology in food science: functionality, applicability, and safety assessment, *J. Food. Drug Anal.*, 24, 671-681.
2. Peters, R., Bommel, G., Rivera, Z., Helsper, H., Marvin, H., Weigel, S., Tromp, P., Oomen, A., Rietveld, A., Bouwmeester, H. (2014), Characterization of titanium dioxide nanoparticles in food products: analytical methods to define nanoparticles, *J. Agric. Food Chem.*, 62, 6285-6293.

Size Distribution, Cytotoxicity of Food Additive Silicon Dioxide and Establishment of their Quantitative Analytical Methods in Commercial Food Products

Ye-Hyun Kim¹, Soo-Jin Choi¹

¹ Seoul Women's University, Department of Food Science & Technology, Seoul, Republic of Korea

Abstract:

Silicon dioxide (SiO₂) nanoparticles have been widely used as food additives to prevent powders or food products from clumping during storage, namely, for anticaking effect (Dekkers *et al.*; 2011). Therefore, information on the potential toxicity of food additive SiO₂ and establishment of accurate quantitative analytical methods for their detection in food matrices is required (Yang *et al.*; 2014). In this study, we analyzed the size distribution of commercially available food additive SiO₂ from various manufacturers. Cytotoxicity and intestinal transport of SiO₂ were evaluated in human intestinal cells and 3D cell culture models. Furthermore, quantitative analysis of SiO₂ was performed in commercial food products by optimizing pretreatment conditions, followed by molybdenum blue analysis (Figure 1). The results demonstrate that SiO₂ was found to be aggregated in distilled water and food matrix solution, although its primary particle size was less than 100 nm. Although no significant effects of food additive SiO₂ on cytotoxicity exposed in short-term, long-term exposure investigated cytotoxicity. On the other hand, quantitative analytical results from commercial food products were highly affected by food matrices, indicating the necessity of different pretreatment methods depending on food matrix type. These findings will provide practical information for safety aspect of food additive SiO₂ and their fate in food matrices.

Keywords: silicon dioxide, food additive, size distribution, cytotoxicity, intestinal transport, quantitative analysis, food matrices.

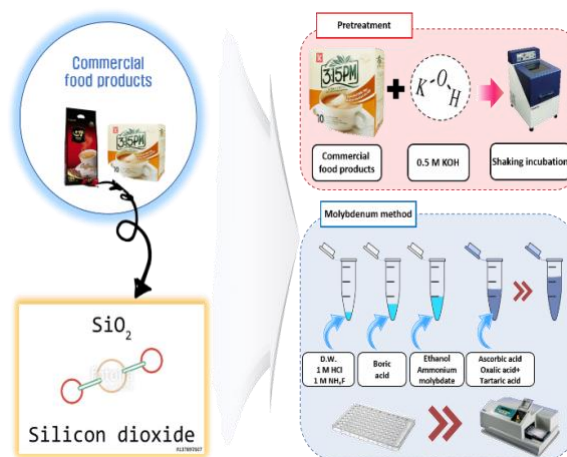


Figure 1: Schematic illustration for quantitative analysis of food additive SiO₂ nanoparticles in various commercial food products.

References:

1. Dekkers S., Krystek P., Peters R.J.B., Lankveld D.P.K., Bokkers B.G.H., van Hoeven-Arentzen P.H., Bouwmeester H., Oomen A.G.. (2011) Presence and risks of nanosilica in food products, *Nanotoxicology* 5, 393–405.
2. Yang Y. X., Song Z. M., Cheng B., Xiang K., Chen X. X., Liu J.H., Cao A., Wang Y., Liu Y., Wang H. (2014), Evaluation of the toxicity of food additive silica nanoparticles on gastrointestinal cells, *J. Appl. Toxicol.* 34, 424–435.

The effect of novel silver alloys nanoparticles on soil bacteria

K. Hrnčířová,¹ N. A.H. Nguyen,¹ A. Ševců¹

¹ Institute for Nanomaterials, Advanced Technologies and Innovation, Technical University of Liberec, Czech Republic

Abstract:

Silver metal alloy nanoparticles (NPs) are developed for biomedical applications because of their antibacterial properties. However, these NPs may accidentally end in the environment. Therefore we investigated an impact of silver metal alloy NPs on bacteria commonly present in soil environment. Two different silver alloys NPs were produced by pulsed laser ablation in liquid (PLAL) – silver cobalt (AgCo) and silver iron (AgFe). Toxicity of these NPs was tested on gram-positive *Bacillus subtilis* and gram-negative *Pseudomonas putida*. Tested NPs were modified by ligands (i.e. glutathione) which can cause different toxicity. Bacteria were exposed to NPs in 96 well microplates in different concentrations for short exposure time (3 h) and longer exposure time (24 h). Then we performed 'spot test' on agar growth medium for visualization of cell viability by their colony forming ability (Figure 1). Minimal inhibition concentration (MIC) was determined for each NPs.

Silver metal alloys NPs were more toxic towards to *B. subtilis* than *P. putida*. MIC of AgCo and AgFe for *B. subtilis* was 1.5 mg/L after 3h or 24h. MIC of AgCo and AgFe for *P. putida* was 6.25 mg/L and 12.5 mg/L after 3h, respectively. The MIC of two NPs was lower after 24h, AgCo: 3.125 mg/L and AgFe: 1.5 mg/L.

Our results revealed negative effect of silver metal nanoalloys on soil bacteria, the gram-positive cells being more affected. Moreover, 24-h exposure caused stronger effect, most probably due to released Ag of Fe ions.

Keywords: silver metal alloy, silver cobalt alloy, silver iron alloy, nanoparticles, toxicity, nanotoxicity, bacteria



Figure 1: Spot test – viability of *Pseudomonas putida* exposed to AgFe nanoparticles for 3 hours. Cells were transferred onto toxicant-free agar medium and incubated at 30°C for one day. Cell viability was estimated by colony forming ability.

References:

1. Pandey et al. (2014). Silver nanoparticles synthesized by pulsed laser ablation: as a potent antibacterial agent for human enteropathogenic Gram-positive and Gram-Negative bacterial strains, *App. Biochem. and Biotech.*, 174, 3, 1021–103.
2. Suppi et al. (2015), A novel method for comparison of biocidal properties of nanomaterials to bacteria, yeasts and algae, *J. of Haz. Mat.*, 286, 75–84.

Analysis of oxidative stress biomarkers for estimation of nZVI ecotoxicity toward various organisms

Jaroslav Semerad^{1,2}, Monika Moeder³, Jan Filip⁴, Martin Pivokonsky⁵ and Tomas Cajthaml^{1,2,*}

¹ Institute of Microbiology, Czech Academy of Sciences, v.v.i., Vídeňská 1083, CZ-142 20, Prague 4, Czech Republic

² Institute for Environmental Studies, Faculty of Science, Charles University, Benátská 2, CZ-128 01, Prague 2, Czech Republic

³ Helmholtz-Center for Environmental Research – UFZ, Department of Analytical Chemistry, Permoserstr. 15, 04318, Leipzig, Germany

⁴ Regional Centre of Advanced Technologies and Materials, Palacký University, Šlechtitelů 27, CZ-783 71, Olomouc, Czech Republic

⁵ Institute of Hydrodynamics of the Czech Academy of Sciences, Pod Patankou 30/5, CZ-166 12, Prague 6, Czech Republic

Abstract:

Nanomaterials attracted research attention in recent decades due to their unique chemical properties to which their enhanced chemical reactivities could be attributed, which also made these nano-scale materials increasingly useful for various applications, including remediation technologies.

Despite the fact that nZVI was proved to be generally harmless during application to contaminated groundwater aquifers, certain concern regarding the use of a new nano-scale substance still persist. Note-worthy, there is still a lack of a suitable, comprehensive and standardized set of tests for the ecotoxicological evaluation of novel nanomaterials in order to determine whether the new materials are more or less harmful. The problem lies in the particularity of nanomaterial mode of action when classical ecotoxicity tests are not useable. Therefore, the aim of this contribution was to test feasibility of a newly developed protocol for evaluation of potentially negative effects caused by nanoparticles represented by nZVI and to investigate whether the assay can be employed for the estimation of oxidative stress using organism from different Kingdoms.

The assay was realized via analysis of cell compartment damage products mainly represented by GC-MS detection of aldehydes created after oxidation of membrane lipids and proteins. The tested organisms included bacteria, fungi and algae. The results showed that various degradation products e.g. formaldehyde, acrolein, methional, glyoxal, and benzaldehyde etc. could be detected after nZVI exposition (Figure 1). The results showed that

the products were detected in a dose-dependent manner that proved reliability of the assays.

Keywords: oxidative stress, nZVI, toxicity assay, malondialdehyde, remediation, reactive oxygen species.

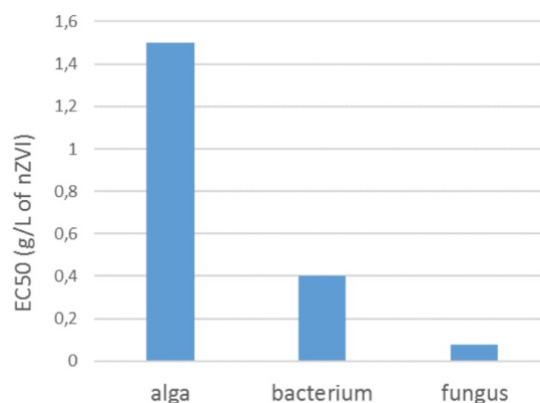


Figure 1: EC50 values of formaldehyde production for various organisms after exposition to nZVI.

References:

1. Semerad, J., Cajthaml, T. (2016), Ecotoxicity and environmental safety related to nano-scale zerovalent iron remediation applications, *Applied Microbiology and Biotechnology*, 100, 9809-9819.
2. Semerad, J., Cvancarova, M., Filip, J., Kaslik, J., Zlota, J., Soukupova, J., Cajthaml, T. (2018), Novel assay for the toxicity evaluation of nanoscale zero-valent iron and derived nanomaterials based on lipid peroxidation in bacterial species, *Chemosphere*, 213, 568-577.
3. Sevcu, A., El-Temsah, Y. S., Joner, E. J., Cernik, M. (2011), Oxidative Stress Induced

in Microorganisms by Zero-valent Iron Nanoparticles. *Microbes and Environments*, 26, 271-281.

4. Nemecek, J., Pokorny, P., Lhotsky, O., Knytl, V., Najmanova, P., Steinova, J., Cernik, M., Filipova, A., Filip, J., Cajthaml, T. (2016), Combined nano-biotechnology for in-situ remediation of mixed contamination of groundwater by hexavalent chromium and chlorinated solvents. *Science of the Total Environment* 563, 822-834.

Effect of gold nanoparticles on virus infection in a respiratory cell model

M. Marchetti,^{1*} B. De Berardis,¹ F. Superti¹

¹ Istituto Superiore di Sanità, National Centre for Innovative Technologies in Public Health, Rome, Italy

Abstract:

The “Project on Emerging Nanotechnologies” (2013, <http://www.nanotechproject.org/cpi/about/analysis/>) has shown that gold is one of the most common nanomaterial among consumer products. The growing production and use of these engineered nanoparticles (NPs) result in an increasing number of exposed workers and consumers. Due to their aerodynamic diameter < 0.1 μm , NPs show high deposition in the lower respiratory tract and can cause oxidative stress, peribronchial inflammation, progressive interstitial fibrosis, chronic inflammatory responses, and create a favorable substrate to respiratory infections. Moreover the NP higher surface reactivity can act as carrier for copollutants of biological origin, such as bacteria and viruses. Adenoviruses are a common cause of upper and lower respiratory tract infections and have been frequently associated with exacerbation of inflammatory airway diseases (1). At present there is no information about the impact of viral infection on the toxicological effects of AuNPs or vice versa. The aim of this study is to assess the influence of NP exposure on viral infection in a respiratory cell model: the alveolar basal epithelial cell line A549.

The interaction between NPs and respiratory cells has been investigated by electron microscopy (Figure 1a), whereas Adenovirus infection has been studied using cytological, virological, and ultrastructural methods (Figure 1b).

Results of this research indicate that NP exposure can enhance virus infectivity suggesting that viral respiratory infections have to be considered as another potential NP risk to human health.

Funding: This work has been supported by the BRIC-INAIL project through the grant ID 53

Keywords: nanoparticles, cytotoxicity, viral infection assays, transmission electron microscopy.

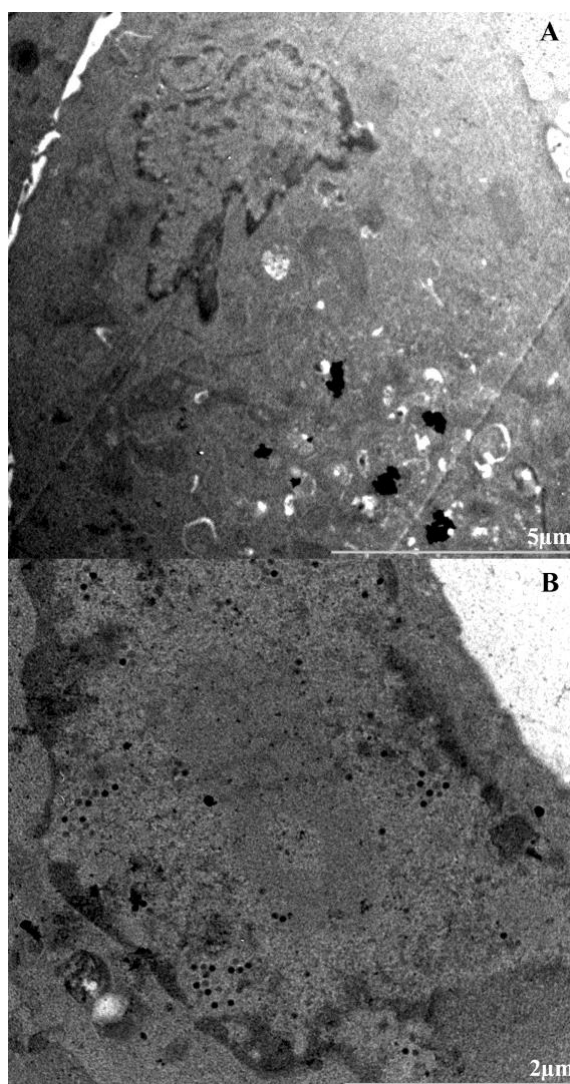


Figure 1 A549 cells: TEM micrographs showing NPs inside the cytoplasm (A) and viral particles inside the nucleus (B).

References:

1. Frickmann, H., Jungblut, S., Hirche, T.O., Groß, U., Kuhns, M., Zautner, A.E. (2012) Spectrum of viral infections in patients with cystic fibrosis, *Eur J Microbiol Immunol (Bp)*. 2, 161-175.

Characterization of nano scale zero valent iron (nZVI) in different aqueous media

Cheryl Soo Yean. Yeap,¹ Nhung H.A. Nguyen¹, Alena Sevcu¹

¹ Technical University of Liberec, Institute for Nanomaterials Advanced Technologies and Innovation, Liberec, Czech Republic

Abstract:

Nanoscale zero-valent iron (nZVI) has gained notable recognition for its application in remediation of environmental hazards mainly chlorinated ethenes and BTEX from polluted aquifers. With the increasing use of nZVI, there is still uncertainty with respect to their potential environmental impacts and toxicological effects, especially at molecular levels. The aim of this study was to elucidate potential effect of nZVI on the soil bacterium, *Pseudomonas putida* at its transcriptomic level. Preliminary studies have been performed to compare (1) various RNA extraction methods from seven different companies to effectively extract RNA from *Pseudomonas putida* in control and nZVI spiked media; (2) nZVI behaviour in four different aqueous media, particularly carbonate buffer pH 8, environmental reservoir water pH 7, physiological solution (NaCl 0.85%) and 10% tryptone soy broth (TSB) by the use of differential centrifugal sedimentation (DCS) and UV-Vis spectrophotometer analysis. Among the seven, RNA extraction by the phenol-chloroform method using RNAzol (MRC, Inc.) has shown to be able to recover both small RNA and large RNA while RNA extraction by using most of the commercial column kits are often unable to elute both the RNA species in a single elution. The UV-Vis absorbance peak of nZVI was at around 210 nm in most of the aqueous media except submerged condition in TSB which is shown at 245 nm. DCS analysis revealed that nZVI increasingly agglomerates from the beginning until 25 hours in the carbonate buffer and physiological solution while, to our surprise, nZVI in TSB showed a relatively stable particle state throughout the exposure. Based on the collected data so far, we will set-up the most appropriate nZVI conditions for the transcriptomic analysis.

Keywords: RNA extraction, nano scale zero valent iron (nZVI), differential centrifugal sedimentation, uv-vis spectroscopy

Biodegradable and Biocompatible Polymeric Nanoparticles from fruit & vegetables wastes and their biomedical applications

Sherine S. Metwally^{1*}, Wael Mamdouh²

^{1,2} The American University in Cairo (AUC), Department of Chemistry, School of Sciences and Engineering (SSE), AUC Avenue, P.O. Box 74, New Cairo 11835- Egypt

*Correspondence: sherineelhosiny@aucegypt.edu, phone +202 01009278959

Abstract:

The emergence of many resistant bacteria causing serious bacterial infections has spread the threat of infectious diseases. These threats have increased the alertness to discover natural products to be used as antimicrobials (1). New drugs from natural products, will counterfeit the chemical diversity of chemical medications. The synthetic antimicrobials have many side effects, while, naturally produced antimicrobials have fewer side effects. Moreover, they have superior benefits in the biocompatibility with human body and high therapeutic value (1, 2). Another big problem of concern in this research was food waste management. Egypt as well as many developing countries is facing environmental and sanitary problems because of the incomplete food waste management. Wastes from food processing industries (fruits and vegetables) ranked the second one in generation of wastes after household sewage wastes (3). However, these wastes have vast economical potentials and recently have shown great interest to researchers, yet, are considered pollutants if not well utilized. New trends have shown food waste products are natural antimicrobial, prebiotics and antioxidants. Peels and seeds which are the major byproducts from fruits and vegetables, were reported to be rich with high amounts of phenolic compounds which have the antimicrobial and antioxidant properties (4).

Nanotechnology is a widely spread field, that grabs the scientific attention from different aspects. It is that technology that deals with materials that have at least one of their dimensions in the Nano-size range (1nm-100nm) (5). The new capability to see and move atoms in this nanoscale have shown a vast array of applications which implements science, industry, economy and human health, etc. Nanoparticles show great interest in food waste

management as it may enhance solubility, facilitate controlled release, improve bioavailability, and protect the stability of phytochemicals during processing, storage, and distribution, etc (5). Nowadays industries have realized the potential applications of nanotechnology in Food sector and are making their efforts in research and development in this area.

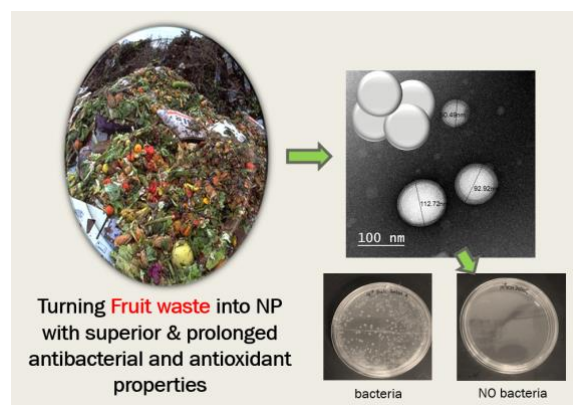


Figure 1: Figure illustrating the potentials of food waste managements, through preparing fruit waste loaded Nano-particles with enhanced properties, higher biocompatibility and lesser side effects.

As shown in figure 1, this work aimed to provide a beneficial use from certain fruit wastes by extracting its phytochemicals and preparing fruit waste loaded Nano-particles with enhanced properties, higher biocompatibility and lesser side effects.

The formulated nanoparticles were characterized for size, & morphology using different techniques such as Zeta sizer, IR & TEM. Different factors were studied during processing to determine the impact of these factors over the nanoparticles characteristics. Entrapment efficiency, invitro release profile, and its biomedical applications were also studied. The prepared nanoparticles showed

unique properties than that of the bulk-sized by-products.

Utilization of food wastes by-products by this advanced new technology will have a great impact on the economical level in developing countries as well as in their environmental level, by reducing pollutants. The new sciences of Nanotechnology involved in this study will aid its vast applications and flourish this big array of research in food waste utilization.

Keywords: Polymeric Nanoparticles, Hydrophobic fruit by-products, Fruit Waste management, Natural antibiotics, Enhanced antioxidant activity, prolonged antioxidant activity, Sustained Release systems, nutraceuticals & food supplements, biomedical applications.

References:

1. Ayukekbong, James A., Michel Ntemgwa, and Andrew N. Atabe. "The threat of antimicrobial resistance in developing countries: causes and control strategies." *Antimicrobial Resistance & Infection Control* 6, no. 1 (2017): 47.
2. Gyawali, Rabin, and Salam A. Ibrahim. "Natural products as antimicrobial agents." *Food control* 46 (2014): 412-429.
3. Thi, Ngoc Bao Dung, Gopalakrishnan Kumar, and Chiu-Yue Lin. "An overview of food waste management in developing countries: current status and future perspective." *Journal of environmental management* 157 (2015): 220-229.
4. Joshi, V. K., Ashwani Kumar, and Vikas Kumar. "Antimicrobial, antioxidant and phyto-chemicals from fruit and vegetable wastes: A review." *International Journal of Food and Fermentation Technology* 2, no. 2 (2012): 123.
5. Sozer, Nesli, and Jozef L. Kokini. "Nanotechnology and its applications in the food sector." *Trends in biotechnology* 27, no. 2 (2009): 82-89.

Highly Sensitive Lactate Sensors Based on Carbon MEMS (CMEMS)

Shahrzad Forouzanfar¹, Fahmida Alam¹, Nezhil Pala^{1*}, Chunlei “Peggy” Wang^{2**}

¹Department of Electrical and Computer Engineering, Florida International University, , Miami, FL, USA

²Department of Mechanical and Materials Engineering, Florida International University, Miami, FL, USA

Abstract:

L-Lactic acid is one of the important metabolites produced during the anaerobic phase of glycolysis, making its precise determination highly important in various fields such as clinical diagnosis, sport, and military activities. Lactate plays a crucial role in several areas of human health, including heart failure, hepatic dysfunction, shock, respiratory insufficiency, and systemic disorders. In sports medicine, knowledge of optimal blood lactate levels is vital to ensuring the maximum performance of an athlete during intensive exercise and endurance-based activities.

Various methods have been developed for determining lactate levels, such as optical, nuclear magnetic resonance, liquid chromatography, fluorimetry, and amperometry. Among these methods, electrochemical ones possess advantages such as simple instrumentation, low detection limit, and wide dynamic range, as well as high selectivity and stability. A Carbon-microelectromechanical system (C-MEMS) is one in which Carbon is synthesized through pyrolysis of micropatterned photoresist polymer in an oxygen-free environment under high temperatures. Carbon possesses various remarkable properties such as a wide electrochemical window, low non-specific adsorption of biomolecules, excellent biocompatibility, and low cost. Furthermore, carbon-based materials exhibit good electrical conductivity, as well as good tolerance toward bio-fouling. The surface of the carbon can be functionalized efficiently via various physical, chemical, or electrochemical treatments. C-MEMS devices circumvent the major drawbacks associated with commercialized screen-printed carbon electrodes such as low resolution and miniaturization.

We developed an electrochemical C-MEMS-based sensing platform to detect L-Lactic Acid.

The sensing platform of the biosensor—interdigitated carbon micro fingers—was synthesized by pyrolyzation of photo-patterned photoresist polymer in oxygen-free and high-temperature conditions. The surfaces of the fingers were functionalized by an oxidation pretreatment technique involving oxygen reactive ion etching (RIE) to form $-\text{COOH}$ on glassy carbon. Taking advantage of having high concentrations of this carboxylic group on the surface of the carbon, we immobilized Lactate Oxidase (LOx) on the surfaces of the interdigitated carbon micro fingers without any other surface pretreatments. We employed various analytical characterization methods such as Fourier-transform infrared spectroscopy (FTIR) and Scanning Electron Microscopy (SEM) for material characterization. Sensing capabilities were measured by cyclic voltammetry (CV), electrochemical impedance spectroscopy (EIS). The carbon capacitive sensor demonstrated detection of lactate over a wide dynamic range of 50 nM-5 mM for the electrode area of $0.5 \times 0.5 \text{ cm}^2$. The sensitivity of this linker-free lactate sensor was found to be 40 nM / cm^2 , making it the first carbon capacitive L-lactate sensor with such high sensitivity.

Keywords: Lactic Acid; Electrochemical; Enzymatic; Carbon MEMS

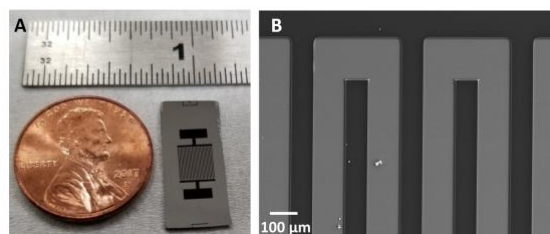


Figure 1 A) Digital picture of PDC_{RIE} and one cent coin. B) SEM picture of PDC_{RIE} .

1.

Enhanced light absorption in porous silicon with nanocrystalline TiO₂ deposited by metal-organic chemical vapor deposition (MOCVD)

D. Hocine¹, S. Oussidhoum¹, M. Bensidhoum², A. Crisbasan³, D. Chaumont³, E. Bourenane⁴, A. Moussi⁵, E. Lesniewska³, N. Geoffroy³, M.S. Belkaid¹

¹Laboratory of Advanced Technologies of Electrical Engineering (LATAGE), Faculty of Electrical and Computer Engineering, Mouloud Mammeri University (UMMTO), BP 17 RP, 15000 Tizi-Ouzou, Algeria

²Laboratoire de Vision Artificielle et Automatique des Systèmes, Faculty of Electrical and Computer Engineering, Mouloud Mammeri University (UMMTO), BP 17 RP, 15000 Tizi-Ouzou, Algeria

³Laboratoire ICB (UMR CNRS 6303), Université de Bourgogne Franche-Comté, BP 47870, 21078 Dijon, France

⁴Laboratoire Electronique, Informatique et Image, LE2I

University of Burgundy, 9 Av. Alain Savary, B.P. 47870, 21078 Dijon Cedex, France

⁵DDCS Division, Research Center for Semiconductor Technology for Energy (CRTSE), 02 Bd. Frantz Fanon, B.P 140 Alger –7 Merveilles Algiers – Algeria

Abstract:

Titanium dioxide (TiO₂) is very employed as antireflective layer in solar cells due to its interesting optical properties allowing high device performances. In this work, nanocrystalline TiO₂ thin films were successfully deposited on porous silicon (PSi) by metal organic chemical vapor deposition (MOCVD) technique using titanium tetra-isopropoxide (Ti(OC₃H₇)₄) as precursor at temperature of 550°C for different periods of times: 5, 10 and 15 min. The objective was to improve the optical absorption properties of the porous layers dedicated for photovoltaic application. The structural, morphological and optical properties of the elaborated TiO₂/PSi samples were analyzed by means of X-ray diffraction (XRD), scanning electron microscopy (SEM), energy dispersive X-ray spectroscopy (EDX), atomic force microscopy (AFM), photoluminescence (PL) and UV-Visible absorption spectroscopy methods. The effect of deposition time on the microstructural properties which influence the optical characteristics of the obtained samples was also examined. The XRD analysis confirms the nanocrystalline structure of the deposited TiO₂ composed only by anatase. The SEM characterization evidenced an increase in the TiO₂ film thickness showing more uniform surfaces as the deposition time rises. Correspondingly, the surface roughness increases with the particle size and film thickness as indicated by AFM studies. The PL measurements indicate an intensive emission of porous silicon in the visible range of the solar spectrum with a peak at 685 nm corresponding to 1.8 eV which is the band gap energy of PSi [2].

Moreover, it was observed a decrease in the PL signal of TiO₂/PSi indicating a reduced carriers recombination rate. The UV-Vis measurements showed a considerable enhancement in optical absorption of porous silicon after the deposition of nanocrystalline TiO₂ films. Indeed, the TiO₂ coatings deposited on PSi for 15 min with thickness of 200 nm have the best structure quality and exhibit, consequently, the highest absorption. From these interesting results, we demonstrate the viability of the use of the MOCVD as reproducible process for the elaboration of highly efficient antireflective layers.

Keywords: Porous silicon, MOCVD, TiO₂, optical properties, structural properties, microstructure, photoluminescence.

Simulation of Crossbar Architecture for Memristor Based Nano-Memory

Meenal Negi, Seshan Srinivasan, and Lili He

San Jose State University, Department of Electrical Engineering, San Jose, USA

Abstract:

Crossbar architectures can be used to construct large memory arrays. The non-volatile characteristic nature of Memristor allows the crossbar design to store values. For this paper, the authors have considered simulation of a 4x4 crossbar array thereby reading and writing 16 bits to the memory subsystem. The model for memristor and the memristive crossbar for this paper were generated in SIMULINK software. The Memristor was characterized with initial parameters using a MATLAB function. The memory subsystem signals for read and write were generated using MATLAB. Memristors are considered as the fourth basic passive element after resistors, capacitors and inductors. Memristors are passive nano-electronic devices similar to resistors. Memristors exhibit non-volatility characteristics[1]. In this paper, a 4x4 crossbar memory array was simulated using Memristors in Simulink software. Crossbar architectures are considered the easiest for nano-structure memory in terms of fabrication. Crossbar architecture have good noise tolerance capabilities. The amount of power consumed grows linearly with the size of the crossbar matrix due to alternate current paths thus lowering the overall effective resistance. Memristor based crossbar arrays are considered the basic building block for ultra high density memories [2]. With high density comes the problem of high power consumption. The power consumption increases dramatically with increase in size of the crossbar size. The power draw is high because of the alternating paths for current to flow in a crossbar architecture. The alternating current paths might lead to read errors at such a high density memory module.

Keyword: memristor, crossbar memory, nano-structure, MATLAB simulation

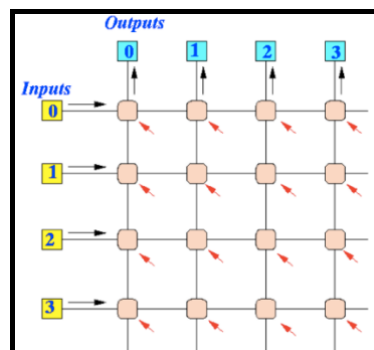


Figure 1: Figure show the schematic of a 4 x 4 cross-bar nano-structure [3]. Crossbar switches are created when two wires overlap each other at any angle other than zero. In a 4x4 crossbar matrix, there would be total of 16 intersections. Each intersection contains 1 memristor. A 4x4 crossbar matrix is capable of storing 16 bits. Read and Write signals required for reading/writing data into and from the crossbar were generated using MATLAB software.

References:

1. L.O.Chua, "Memristor - the missign circuit element," *IEEE Trans. Circuit Theory*, Vols. CT-18, no. 5, pp. 507-519, September 1971.
2. S. S, K. K and K. M. S, "Analysis of Passive Memristive Devices Array: Data-Dependent Statistical Model and Self-Adaptable Sense Resistance for RRAMs," in *Proceedings of the IEEE*, 2012.
3. C.Yakopcic and T. M. Taha, "Hybrid Crossbar architecture for a Memristor based memory," *Proceedings of IEEE NAECON*, 2014

Minimization of resistance of gravure printed electrodes with silver nano ink by controlling printing conditions

C. H. Kim,^{1,*} S. Y. Lee,¹

¹Chungnam National University, Daejeon, KOREA

Abstract:

The silver nano ink is commonly used for printing the conductive patterns in printed electronics applications because of its low drying temperature under the value that affects physical structure of polymer substrate. To be effective as conductor, the printed patterns should have low resistance as possible. The resistance of printed patterns for electrodes fabricated using printing technology should be minimized. This parameter depends on the pattern width and thickness; however, from the viewpoint of printability, the printed patterns should be printed at the designed width. The resistance of the printed patterns as well as printability is affected by various printing conditions. In this paper, the printing condition is optimized to minimize the resistance and spread ratio of electrode printed by the roll-to-roll gravure method. To minimize resistance and spread ratio of the printed electrode, the drying temperature, wind speed, ink viscosity, and linear velocity of printing are selected as effective factors in this study. The experimental design method is used to minimize the number of experiments and to obtain optimum conditions. The test samples were fabricated to a line pattern having a width of 500 μm and a length of 80 mm by roll-to-roll gravure method using silver nano ink on PET film. The resistance was measured by a multimeter, and line width and height were measured by 3D surface profiler. The experimental results were analyzed using ANOVA. It was found that the main factors that affect the resistance and spread ratio among the conditions were ink viscosity and printing speed. The printing conditions were also optimized: drying temperature 160 $^{\circ}\text{C}$, wind speed 40 Hz, printing velocity 15 mm/s, ink viscosity 30,000 cPs. From the results, it was predicted that we would have the resistance of 42.09 Ω and spread ratio of 100.15 % at the optimized conditions. The result of reproducibility test for verifying the prediction value from the optimum conditions, the resistance and spread ratio were measured as 41.35 Ω and 103.79%, respectively. Therefore, the difference between prediction and actual

values of resistance and spread ratio are 2.6 % and 6.75%, respectively.

In conclusion, in order to make the patterns of precise line width and of low resistance, ink viscosity and printing speed must be co-considered to achieve the goal. In case of drying condition, it must be high but avoid producing the strain of substrate.

Keywords: nano silver ink, printed electronics, printed electrodes, resistance.

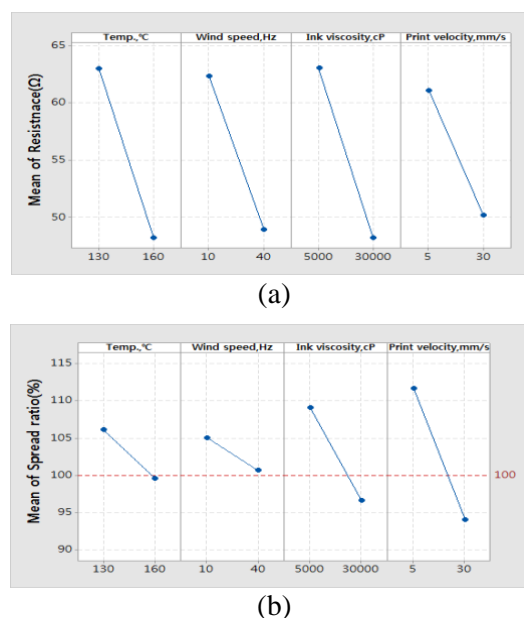


Figure 1: Main effect plots of factors on (a) resistance, (b) spread ratio

References:

1. Sung, D., de la Fuente Vornbrock, A., Subramanian, V. (2010), Scaling and Optimization of Gravure-printed Silver Nanoparticle Lines for Printed Electronics, *IEEE Trans. Compon. Packag. Technol.*, 33, 105-114.
2. Yang, M. et al. (2014) Mechanical and environmental durability of roll-to-roll printed silver nanoparticle film using a rapid laser annealing process for flexible electronics, *Microelectronics reliability*, 54, 2871-2880.

Nickel oxide nanoparticle incorporated polypyrrole nanocomposite for supercapacitor application

Vijeth H, Ashokkumar S P, Yesappa L, Vandana M, Devendrappa H*

Department of physics, Mangalore University, Mangalagangothri, 574199, India

*Corresponding Author: dehu2010@gmail.com

Abstract:

In present work, polypyrrole (PPy) and polypyrrole-nickel oxide (PPy-NiO) was synthesised using in situ chemical polymerisation method. The incorporation on nanoparticle into the polypyrrole is confirmed by using FTIR and EDAX analysis. The supercapacitor electrodes were fabricated and characterised using three electrodes configuration using 1M KOH aqueous electrolyte. The highest specific capacitance found to be 421.48 F/g at 10 mVs⁻¹ PPy-NiO nanocomposite. Electrochemical impedance analysis shows very low series resistance of 5.69 Ω and 1.12 Ω for PPy and PPy-NiO nanocomposite respectively.

Keywords: Supercapacitor, Polypyrrole, Nickel oxide, Nanocomposites, Cyclic voltammetry, Specific capacitance.

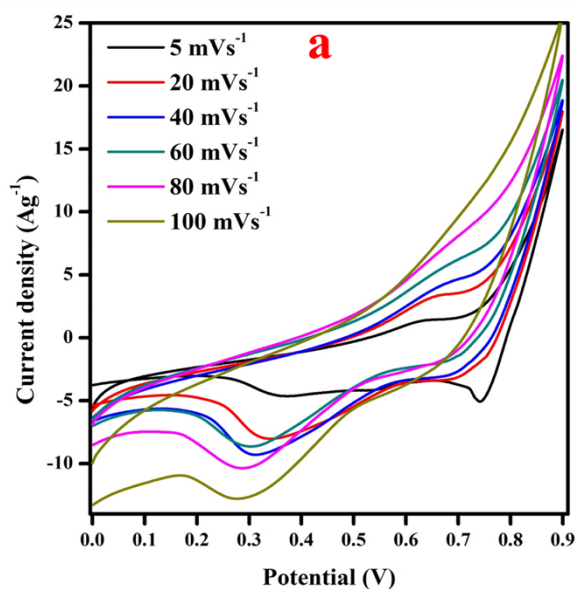


Figure 1: . Cyclic voltammetry curve of Pure PPy at different scan rate using 1M KOH aqueous electrolyte solution.

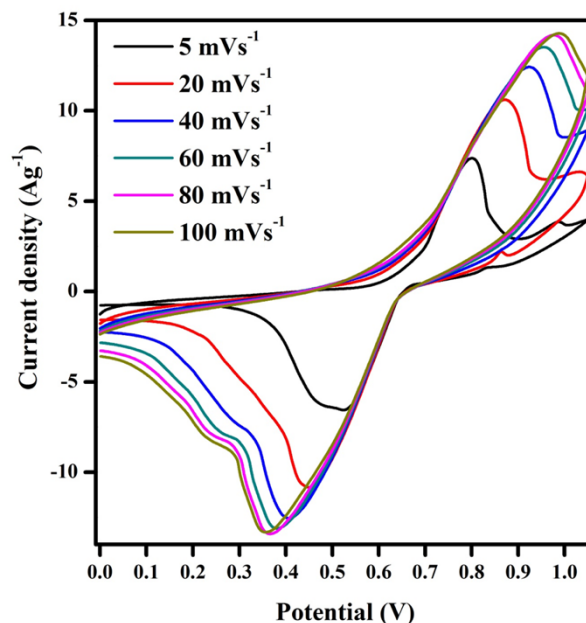


Figure 2: Cyclic voltammetry curve of PPy-NiO nanocomposite at different scan rate using 1M KOH aqueous electrolyte solution.

References:

1. Ji, J., Zhang, L. L., Ji, H., Li, Y., Zhao, X., Bai, X., Ruoff, R. S. (2013), Nanoporous Ni (OH) 2 thin film on 3D ultrathin-graphite foam for asymmetric supercapacitor. *ACS nano*, 7, 6237-6243.
2. Sk, M. M., Yue, C. Y., Ghosh, K., & Jena, R. K. (2016), Review on advances in porous nanostructured nickel oxides and their composite electrodes for high-performance supercapacitors. *J. Power Sources*, 308, 121-140.

Si nano-polycrystalline body with ferromagnetic property and vanishing of electrical resistance at local high frequencies

T. Saiki,^{1*} Y. Iida,¹ M. Inada,¹

¹Kansai University, Faculty of Engineering Science, Suita, Japan

Abstract:

Improvement on reduction of skin effect for metals as an electricity conductor at high frequencies is important problem and future objects to reduce consumption energy. We now investigate for the resistances of nano-structured metals as electricity conductors at high frequencies.

Singular vanishing of electrical resistances near a local high magnetic harmonic frequency of a few MHz was observed. This phenomenon has not been observed for conventional ferromagnetic metals. The measured electrical resistances changed to almost 0 mΩ at room temperature. At the same time, negative resistance of the sintered Si nano-polycrystalline body was observed. Numerical calculation was also performed on the electrical resistance with frequency dependency. The calculation could explain the variation of the relative permittivity of the Si nano-polycrystalline and the phenomenon for vanishing the resistivity at frequency of MHz theoretically.

A Si nano-polycrystalline body made of the reduced Si nanoparticles from Si oxide powder was fabricated. It was found by measuring the magnetization property of the body that the sintered Si nano-polycrystalline body has ferromagnetism.

Dangling bonds (unpaired electrons) have long been known to occur due to defects in Si crystals. Si nanoparticles have many dangling bonds. High-density dangling bonds cause the sintered Si nano-polycrystalline to have ferromagnetism. The density of the unpaired electrons in the sintered Si nano-polycrystalline was observed using ESR. It has been clarified that the Si nanopowder and the sintered Si nano-polycrystalline have numerous dangling bonds. Both densities of the dangling bonds were evaluated.

The Si nano-polycrystalline body will be applicable to electronic transmittance lines or semiconductors.

Keywords: Si, nano-polycrystalline, ferromagnetic, magnetic resonance, negative permittivity, skin effect, ESR.

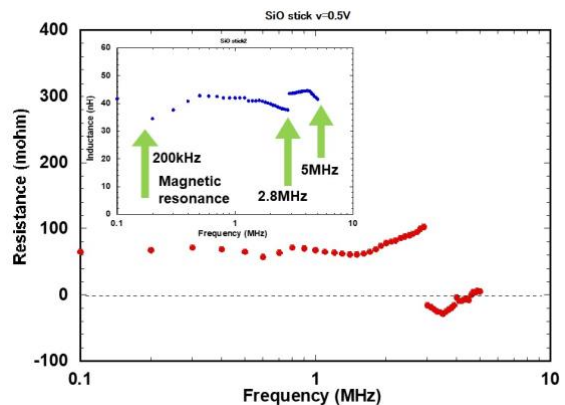


Figure 1: Figure shows measured resistances of sintered Si nanopolycrystalline body at high frequencies of a few MHz with decreasing frequency of sine wave signal. The current was 10mA at 5MHz. Measured self-inductances of nano-structured metal are also shown in inset figure. Magnetic resonances at local frequencies of such as 200kHz, 2.8MHz and 5MHz were observed, and the resistivities changed to near zero at the magnetic resonance frequencies of 2.8MHz and 5MHz in experiments.

References:

1. Masuda, S., Saiki, T., Iida, Y., and Inada, M., "High Frequency Core Inductor Using Sintered Aluminum Nano-paste with Aluminum Nano-polycrystalline Structure", Conference on the Lasers and Electro-Optics (CLEO) (2017), San Jose, CA, USA, May 18, STh1J.
2. Saiki, T., Iida, Y., and Inada, M., (2018), Appearance of ferro-magnetic property for Si nano-polycrystalline body and vanishing of electrical resistances at local high frequencies, *J. of Nanomaterials*, **2018**, ID 9260280, 1-12.

Quantum Dots as QLED devices for automotive lighting systems

J.J.Santaella,^{†,‡} K.Critchley,^{*} S.Rodríguez-Bolívar,[‡] F.M.Gómez-Campos,[‡]

[†] VALEO Lighting Systems, Department of Electronics, Martos, Spain

^{*} University of Leeds, School of Physics and Astronomy, Leeds, UK

[‡] Universidad de Granada, Dpto de Electrónica y Tecnología de Computadores, Granada, Spain

Abstract:

Lighting in the automotive world has undergone a radical change in recent years thanks to LED devices^{1,2}. The use of halogen lamps is being replaced by these light emitting diodes. One of the main advantages, apart from the consumption and the long useful life, is the style that these devices offer. The current and future trend in the automotive world is to achieve ever greater lighting surfaces with flexible features and shapes in three dimensions (3D). However, the current LED technology formed by discrete devices of point light sources makes this task very complex and expensive. A new nanometric technology called quantum dots (QDs) can end the issues described above effectively. Thus QDs are nanocrystals semiconductors where electrons are confined in a region of space of nanometric dimensions. Specifically, LED lighting devices based on QDs (quantum dot LEDs), known by their acronym QLED, offer a promising future as a new generation of lighting devices due mainly to three factors: purity of color, processibility and stability³. We report the design and manufacturing of a 6-pixel (4.5mm²/pixel) electroluminescent QLED (Figure 1) based on CuInS₂/ZnS Quantum Dots as active layer. The multilayer QLED device was fabricated with a conventional structure as follows^{4,5}: ITO as anode, PEDOT:PSS as hole injection layer (HIL), TFB as hole transport layer (HTL), CIS/ZnS QDs as active or emission layer, ZnO NPs as electron transport layer (ETL) and Al layer as cathode. In addition the electrical curve I-V (Figure 2) was measured for each pixel independently observing how the fabrication process and layer thickness have an influence in the shape of the plot. This study will also permit us to discuss the creation of a computational model of the QLED device. This is vital to thoroughly understand the influence of transport layers structure in the electrical behavior which is critical when designing the automotive electronics to control the lighting device in the future.

Keywords: quantum dots, QLED, automotive applications, lighting systems, electroluminescence, transport layers, nanoparticles.

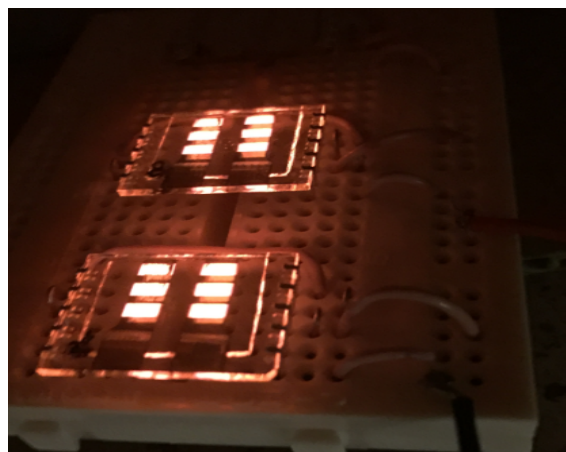


Figure 1: Figure illustrating the QLED fabricated following the structure: Anode/HIL/HTL/EL/ETL/Cathode.

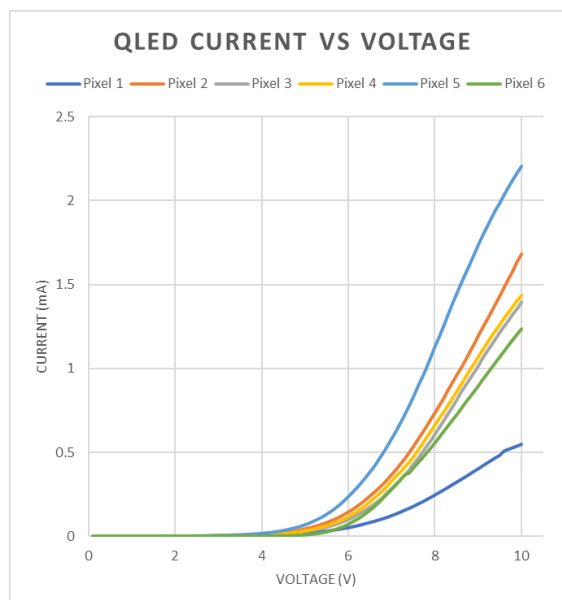


Figure 2: Figure illustrating the fundamental I-V curve that we are tempting to simulate: modelling the QLED device to understand the transport mechanism behind the device physics.

Acknowledgements

This work was supported by VALEO, multinational automotive company.

F.M.G.C and S.R.B were supported by Project ENE2016_80944_R, funded by the Spanish Ministerio de Economía, Industria y Competitividad.

References:

1. Technology and applications of light emitting diodes, *LEDs Magazine*, August 2013.
2. Boulay, P. (2017) Automotive lighting: technology, industry and market trends
3. V. Wood and V. Bulović, "Colloidal quantum dot light-emitting devices," *Nano Rev.*, vol. 1, no. 0, pp. 1–7, 2010.
4. Jong-Hoon Kim and Heesun Yang, "All-solution-processed, multilayered CuInS₂/ZnS colloidal quantum-dot-based electroluminescent device," *Opt. Lett.* 39, 5002-5005 (2014)
5. Zelong Bai, Wenyu Ji, Dengbao Han, Liangliang Chen, Bingkun Chen, Huaibin Shen, Bingsuo Zou, and Haizheng Zhong, Hydroxyl-Terminated CuInS₂ Based Quantum Dots: Toward Efficient and Bright Light Emitting Diodes *Chemistry of Materials* 2016 28 (4), 1085-1091

Handling ligands on PbS nanoparticle surface for optimization of photovoltaic devices

F. Rodríguez-Mas¹, S. Fernández de Ávila¹, J.C. Ferrer¹, J.L. Alonso¹

¹ University Miguel Hernández, Department of Communications Engineering, Elche, Alicante, Spain.

Abstract:

It is well known the essential role that ligands on the surface of nanoparticles (NPs) have. Ligands can control the size and solubility of the NPs in addition to influence charge transport between the NPs and their surrounding media.

The combination of several ligands on the surface of the nanoparticle would allow to tailor some of these properties in order to optimize different NPs for potential applications.

Mixed monolayer lead sulfide nanoparticles (NPs) have been synthesized following a new synthesis route. Thiophenol and 1-decanethiol have been used as ligands for the PbS NPs as shown in Figure 1. This route starts from the synthesis of PbS coated in thiophenol. Subsequently, by chemical baths, 1-decanethiol was incorporated into the nanoparticles. Thereby, nanocrystals with a combination of two ligands were synthesized (figure 1).

In this contribution we study the incorporation of mixed monolayer PbS NPs into bulk heterojunction photovoltaic devices to compare their performance with that found for hybrid devices with only thiophenol capped PbS NPs. Solar cells with structure ITO / PEDOT:PSS / PCBM:P3HT:PbS NPs / Al have been fabricated and characterized under dark and 1 sun of illumination.

Hybrid photovoltaic devices with PbS nanoparticles coated only with thiophenol are used as reference.

The incorporation of mixed monolayer PbS nanoparticles in the active layer (poly (3-hexylthiophene) : phenyl -C61- butyric acid methyl ester) was favoured by 1-decanethiol, because this helps to the solubility of the nanoparticles in toluene. Thereby, the nanoparticles with two ligands were correctly embedded into the P3HT:PCBM layer. An improvement of the electrical parameters for these solar cells, in comparison with the results obtained from the reference cells is observed (Figure 2).

Thus, this contribution reports the observed effects of the integration of mixed monolayer

PbS NPs in bulk heterojunction photovoltaic devices.

Keywords: hybrid solar cells, nanoparticles, lead sulfide, mixed monolayer, synthesis, quantum dot.

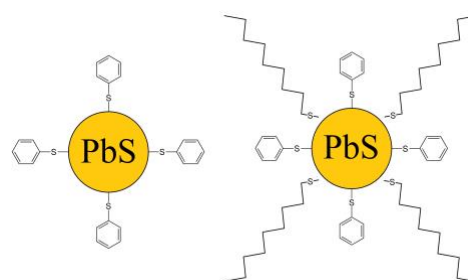


Figure 1: Lead sulfide nanoparticle coated by thiophenol and lead sulfide nanoparticle coated by thiophenol and 1-decanethiol.

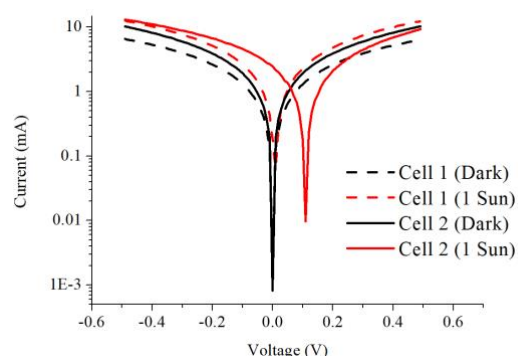


Figure 2: Comparative I-V curves for hybrid solar cell 1 (with thiophenol only ligands PbS NPs) and cell 2 (with mixed thiophenol and 1-decanethiol ligands PbS NPs).

References:

1. Taylor, R., Coulombe, S., Otanicar, T., Phelan, P., Gunawan, A. (2013), Small particles, big impacts: A review of the diverse applications of nanofluids, *J. Appl. Phys.*, 113, 011301.
2. Kim, Y. J., Yang, Y. S., Ha, S., Cho, S. M., Kim, Y. S., Kim, H. Y., Yang, H., Kim Y. T. (2005), Mixed-ligand nanoparticles of chlorobenzenemethanethiol and n-octanethiol as chemical sensors, *Sens. Actuator B*. 106, 189-198.

Effect of Electrode Surface Treatment Through Electrical Discharge Machining on Microbial Fuel Cells

H.-Y. Tsai,¹ W.-H. Hsu,^{2,*} M.-Z. You,²

¹ National Tsing Hua University, Department of Power Mechanical Engineering, Hsinchu, Taiwan

² National United University, Department of Mechanical Engineering, Miaoli, Taiwan

Abstract:

Microbial fuel cells (MFCs) generate low-pollution power by feeding organic matter to bacteria. Thus, MFCs have become a crucial technology for applications in energy recovery and environmental protection. In an MFC system, the electrode materials have a critical impact on the capacity for power generation, and high-surface-area materials and different surface treatments have been used to increase electrode performance [1-3].

In this paper, a novel surface treatment method for electrodes involving electrical discharge machining (EDM) is proposed. In the EDM process, the recast layer is formed on the machined surface, and defects such as micro/nano scale cracks and notches are often detected. The recast layer and micro/nano scale cracks increase the surface area and surface roughness of the machined surface. Thus, the reaction area and electronic conversion efficiency of the electrodes can be improved by using the EDM surface treatment method.

In this study, the base material of the electrodes is 304 stainless steel mesh. To understand the practicality of the method, the effects of applied pulse current of EDM surface treatment on the MFCs' performance levels are investigated. The results of EDM surface treatment of stainless steel are shown in Fig.1. Fig. 1(a) shows the surface of a unmodified stainless steel. The surface morphology in Fig. 1(b), 1(c) and 1(d) result from EDM surface treatment using a pulse current of 0.5, 1.0 and 1.5 A, respectively. The average surface roughness R_a in Fig. 1(a), 1(b), 1(c) and 1(d) are 0.188, 0.711, 0.844 and 0.944 μm , respectively. An increase in the pulse current of EDM surface treatment results in an increase in the surface roughness and surface area of the modified surface.

The maximum power density of MFCs equipped with a unmodified anode and EDM modified anode using a pulse current of 1.5A are 101.37 and 205.94 mW/m^2 , respectively, with mutual difference about 2 times. The reason can be attributed to that the the micro/nano scale cracks

and notches caused by EDM surface treatment increase the surface area of anode. The results demonstrated that the proposed novel EDM surface treatment is feasible and has potential for development.

Keywords: Microbial fuel cells, MFC, electrical discharge machining, surface treatment, nano-crack

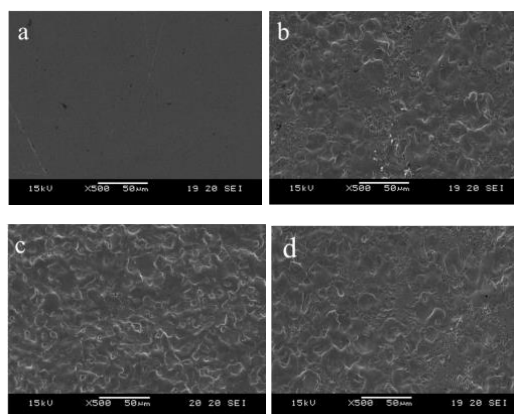


Figure 1: Surface of (a) unmodified stainless steel and EDM modified stainless steel at applied pulse current of (b)0.5 A, (c)1.0 A and (d) 1.5 A.

References:

1. Feng, Y., Yang, Q., Wang, X., Logan, B.E. (2010), Treatment of carbon fiber brush anodes for improving power generation in air-cathode microbial fuel cells, *J. Power Sources*, 195, 1841-1844.
2. Lamp, J.L., Guest, J.S., Naha, S., Radavich, K.A., Love, N.G., Ellis, M.W. Puri, I.K. (2011), Flame synthesis of carbon nanostructures on stainless steel anodes for use in microbial fuel cells, *J. Power Sources*, 196, 5829-5834.
3. Zheng, S., Yang, F., Chen, S., Liu, L., Xiong, Q., Yu, T., Zhao, F., Schröder, U., Hou, H. (2015), Binder-free carbon black/stainless steel mesh composite electrode for high-performance anode in microbial fuel cells, *J. Power Sources*, 284, 252-257.

Thermal and Mechanical Reinforced Montmorillonite Polyurethane-Nanocomposites and its commercial application for shoe adhesive

Kai Zhao¹, Zijiang Yang², Yiheng Zhang², Wolfgang Bremser^{*1}

¹ Universität Paderborn, Technische Chemie, Coatings, Materials and Polymers (CMP)
Warburger Str. 100, D-33098 Paderborn, Germany

² College of Chemistry and Molecular Engineering, Qingdao University
of Science & Technology, Qingdao, China

Abstract:

Significant improved mechanical (shear, tensile, impact and flexural strength), thermal (distortion, decomposition and glass temperature) and electrical (dielectrical breakdown strength) properties of polymer-layered silicate nanocomposites was observed compare with matrix polymer and hence can be used to replace some metal applications. Another Improvements can include a decreased gas permeability and flammability, controllable viscosity and reduced curing temperature and speed. Our research focuses on the modification of layered silicate (e.g. Laponite, Montmorillonite and Vermiculite) with different organic and anorganic modifier, innovative production of polymer-layered silicate nanocomposite with enhanced properties for various coating applications, and to obtain designed organized colloidal structure, e.g. two-dimensional arrangement of laminar particle. In this Poster we report synthesis and characterization of a thermal and mechanical enhanced commercial Polyurethane (PUR) adhesive for shoes with modified Montmorillonite (MMT). The influence of different parameters, e.g. modifier species for MMT, concentration of modified MMT, dispersion technics of MMT into PUR are researched in order to obtain the best enhancement of PUR adhesive.

(3-Aminopropyl)dimethylethoxysilane (APDMES, S2) modified MMT is better dispersed into PUR marix than other modified MMT under limited concentration and therefor significantly improved thermal (Figure 1) and mechanical (Figure 2) properties are obtained.

Keywords: polymer-layered silicate nanocomposite, montmorillonite, thermal and mechanical enhanced polyurethane adhesive, scanning electron microscope (SEM), focused

ion beam (FIB), shear stress, decomposition temperature.

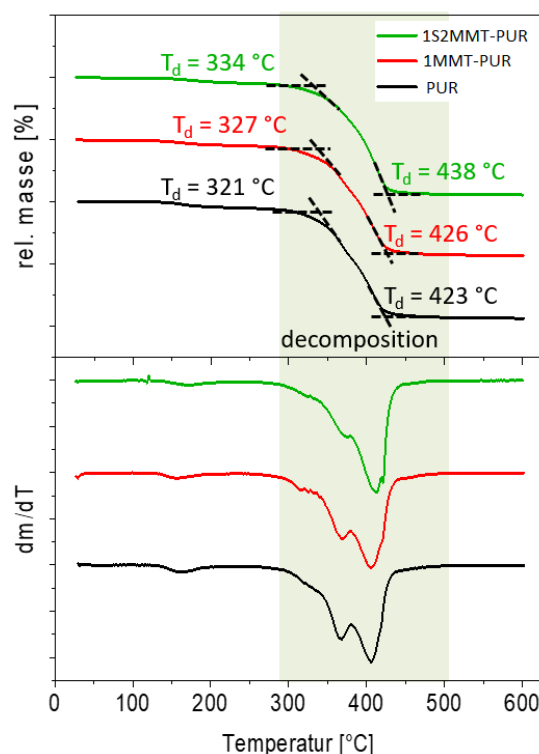


Figure 1: Enhanced decomposition temperature (15 °C) of PUR with (green) APDMES modified MMT compared to (black) pure PUR and (red) PUR with unmodified MMT.

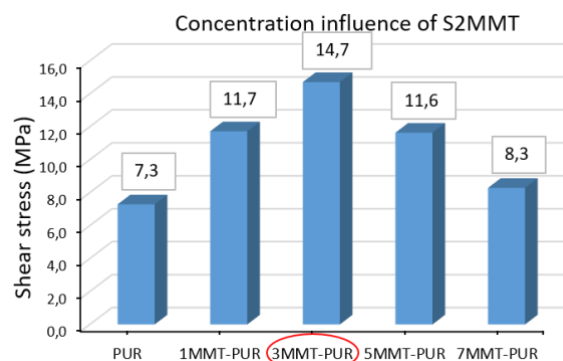


Figure 2: Concentration influence of APDMES-MMT on shear stress of enhanced PUR adhesive

References:

1. Cooperation project with BASF Coating GmbH: “Synthesis and Characterization of Mechanical and Thermal Reinforced PVA-MMT and Epoxiharze-MMT Nanocomposite.

Joint project: LHybS, EFRE 2014-2020
“Development of Mechanical and Thermal Reinforced Polyurethane (PUR)-MMT Adhesive.

Determination of antibacterial and antioxidant activities of electrospun water rich angiosperms wastes nanofibers

W. Soliman,^{1,2,*} W. Mamdouh,^{1,2}

American University in Cairo, Department of Chemistry, Cairo, Egypt
Avenue, P.O. Box 74 New Cairo 11835- Egypt

*Correspondence: Wafaa.soliman@aucegypt.edu, phone +202 01022065550

Abstract:

Food waste has become a huge problem globally since thousands of different food items are wasted all over the world which affects our environment severely due to the emissions of greenhouse gas due to anaerobic decomposition and leakage at the garbage. Fruit wastes like the peels and seeds are a major contribution to the waste products thrown everyday especially in juice industries (1).

The antioxidant and antimicrobial activities of food wastes have been of great interest nowadays due to oxidative stress and antibiotic resistance problems (2, 3). However the stability of the fruits or vegetables wastes was a challenge to perform these activities under controlled release and remains stable for long period of time. Therefore, the purpose of this research it is to determine the antimicrobial and antioxidant activity of angiosperm wastes and the enhancement of these activities in its electrospun nanofibers form activity.

The nanoformulation like electrospun nanofibers is to increase the stability and bioavailability and investigate its effect on the antimicrobial and antioxidant activity.

Characterization of the waste content like phenolics, saponins, flavonoids etc after extraction and then characterization of the nanofibers was carried out using different techniques such as scanning electron microscope (SEM) for diameter determination and Fourier Transform Infrared (FT-IR) spectroscopy for functional groups investigation (9).

The antimicrobial agents discovered in plants are of great interest since antibiotic resistance is becoming a worldwide public health concern (4). Moreover, there is a high demand to use antimicrobials in food packaging to kill and avoid microbial growth in food which will cause a decrease in the shelf life and food spoilage. Usually the bioactive constituents in plants that make them possess antimicrobial activities are phenol, tannin, saponin, alkaloid,

flavonoid, steroids, carotenoids, and cyanogenic glycosides (5).

Most of antioxidants perform their activities due to their phenolic or polyphenolic contents (7, 8). There are many water rich angiosperms wastes that have been reported and studied have shown that they have antioxidant activities like orange peel (6), tomato skin, watermelon rinds etc.

Nanofibers increase the surface area of the formulated material which results in increasing its activity and bioavailability.

This idea would change the whole perspective of throwing angiosperms remaining's like peels, rinds, seeds and use them as cheap, safe and natural source for pharmaceutical industries or even as food preservatives (2). The expected results would increase the awareness of the people in Egypt and worldwide to the importance of benefiting from food waste. More importantly, the cost effectiveness of the extraction, preparation and characterization processes will attract industrial firms to be part of these activities.

Keywords: Antioxidant, Antibacterial, water rich, nanofibers and PVA

References:

1. Melikoglu, M.; Lin, C.; Webb, C. Analysing Global Food Waste Problem: Pinpointing the Facts and Estimating the Energy Content. *Open Engineering* 2013, 3 (2), 157–164. <https://doi.org/10.2478/s13531-012-0058-5>.
2. Bremer, B., Bremer, K., Chase, M., Fay, M., Reveal, J., Soltis, D. & Stevens, P. (2009). An update of the Angiosperm Phylogeny Group classification for the orders and families of flowering plants: APG III. *Botanical Journal of the Linnean Society*.
3. IU, O. (2014). Phytochemical Analysis and Antibacterial Activities of Citrullus Lanatus Seed against some Pathogenic

- Microorganisms. *Global Journal of Medical Research*, 14(4).
4. Thirunavukkarasu, P., Ramanathan, T., Ravichandran, N., & Ramkumar, L. (2010). Screening of anti-microbial effect in watermelon (*Citrullus* sp.). *Journal of Biological Sciences*.
 5. Valgas, C., Souza, S. M. D., Smânia, E. F., & Smânia Jr, A. (2007). Screening methods to determine antibacterial activity of natural products. *Brazilian Journal of Microbiology*, 38(2), 369-380.
 6. Bremer, B., Bremer, K., Chase, M., Fay, M., Reveal, J., Soltis, D. & Stevens, P. (2009). An update of the Angiosperm Phylogeny Group classification for the orders and families of flowering plants: APG III. *Botanical Journal of the Linnean Society*.
 7. Pisoschi, A. M. (2011). Methods for total antioxidant activity determination: a review. *Biochemistry & Analytical Biochemistry*.
 8. Antolovich, M., Prenzler, P. D., Patsalides, E., McDonald, S., & Robards, K. (2002). Methods for testing antioxidant activity. *Analyst*, 127(1), 183-198.
 9. Pathak, P.; Mandavgane, S.; Kulkarni, B. Fruit Peel Waste as a Novel Low-Cost Bio Adsorbent. *Reviews in Chemical Engineering* 2015, 31, 361–381.

Oxidation controlled WS₂/Black phosphorus nanocomposit catalyst for water treatment

Rak Hyun Jeong,^{1,2} Dong In Kim,¹ Ji Won Lee,^{1,2} Jung-Hoon Yu,¹ Yang Ju Won,¹
and Jin-Hyo Boo,^{1,2,*}

¹Department of Chemistry, Sungkyunkwan University, 16419 Suwon, Republic of Korea,

²Institute of Basic Science, Sungkyunkwan University, 16419 Suwon, Republic of Korea

Abstract:

The discovery of graphene, a hot issue in the field of materials science, has clearly attracted great interest worldwide and has had tremendous impact in many areas. Over the past few years, research on 2D materials has actually been very advanced. Research on layered 2D materials is at the forefront of material science. In addition to graphene, there are many other two-dimensional materials, but the transition metal chalcogenide is a typical two-dimensional material. It is characterized by a variety of series and easy to control, but with a slightly slower charge mobility. Black phosphorus is an intermediate between graphene and Transition metal dichalcogenide(TMDC) and is studied as a next-generation two-dimensional material due to the anisotropy caused by the curved honeycomb structure. Since the 2D material basically has many plate shapes, there is a great deal of research on the layer-by-layer type junction structure.[1]

This composite catalyst is designed to have a lower dimension than two dimensions and to be combined with each other, so that the band structure can be designed to suit the application and complement each other's disadvantages. Among the TMDCs, WS₂ can be a promising catalytic material due to its unique electrical properties, and black phosphorus with properly controlled oxidation can act as a redox functional group.[2] We synthesized black phosphorus that was oxidized properly and easily at a low cost and made a catalyst for water quality improvement through composite with WS₂ (figure 1). Through these composites, we studied nanocatalysts that satisfy bandgap changes and disadvantages of each other. This material was measured by TEM, SEM, XRD, XPS, UV-VIS spectrophotometer, FT-IR and RAMAN spectroscopy. Such catalyst materials are used in various fields such as hydrogen

generation, atmospheric purification, and water purification.

Keywords: Two dimensional material, nanocomposit, Transition metal chalcogenide, black phosphorus, water treatment, nano catalyst

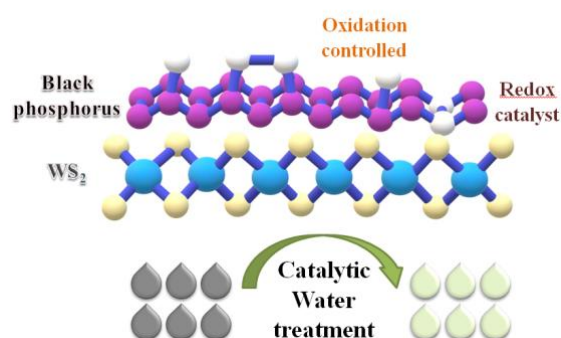


Figure 1: Proposed schematic diagram for the catalytic water treatment of oxidation controlled BP/WS₂ nano composite material

References:

1. Bin Luo, Lianzhou Wang (2016) Recent advances in 2D materials for photocatalysis. *Nanoscale* 8,6904
2. Puritut Nakhnivej, Manish Chhowalla, Ho Seok Park (2019) Revealing molecular-level surface redox sites of controllably oxidized black phosphorus nanosheets. *Nature Materials* 18, 156–162

Evaluation of novel composite material based on Nanoscale ZeroValent Iron for nanobioremediation of chlorinated ethenes: Degradation efficiency, microbial populations and material changes during ageing process

J. Semerád,^{1,2,*} A. Ševců,³ N. A. H. Nguyen,³ K. Pospišková,⁴ J. Filip,⁴ T. Cajthaml,^{1,2}

¹ Institute of Microbiology, Czech Academy of Sciences, v.v.i., Vídeňská 1083, CZ-142 20, Prague 4, Czech Republic

² Institute for Environmental Studies, Faculty of Science, Charles University, Benátská 2, CZ-128 01, Prague 2, Czech Republic

³ Technical University of Liberec, Studentská 2, CZ-461 17, Liberec, Czech Republic

⁴ Regional Centre of Advanced Technologies and Materials, Palacký University, Šlechtitelů 27, CZ-783 71, Olomouc, Czech Republic

Abstract:

Nowadays, nanoscale Zero-Valent Iron (nZVI) is one of the most used materials in the remediation industry. Its high degradation efficiency is well described for many pollutants (1). Despite its high effectivity and due to its nonspecific reactivity, nZVI is usually applied in high doses (up to 50 g/L) (2). New modifications of zero-valent iron nanoparticles, by coating or combining with other materials, could improve its properties, decrease the doses and thus improve the cost-effectiveness of nZVI applications. Biochar, a material well known by high sorption ability, could serve as a potential matrix for the new nZVI composite material. The matrix of biochar could adsorb chlorinated solvents which will be consequently degraded by nZVI. In the presented study, the potential of Biochar-nZVI composite material for nanobioremediation of chlorinated ethenes is discovered. Moreover, the potential effect of biochar on biostimulation was also discovered. During the 2-month experiment, the material structural changes were monitored via several physicochemical parameters and X-ray diffraction. Additionally, to discover the effect of composite material on resident microbes, microbial biomass was estimated and the changes in microbial populations were detected via molecular genetics methods.

Combining the results of the material analysis, physicochemical parameters, degradation efficiency, and microbial analysis, we provide detailed information about the ageing process of nZVI inside of composite material, degradation efficiency and about its effect on resident microbial species.

Keywords: Nanoscale Zero-Valent Iron, nZVI, Biochar, Chlorinated ethenes, Toxicity

References:

1. Mueller, N. C., Braun, J., Bruns, J., Cernik, M., Rissing, P., Rickerby, D., Nowack, B., (2012), Application of nanoscale zero valent iron (NZVI) for groundwater remediation in Europe, *Environ. Sci. Pollut. R.*, 19, 550-558.
2. Grieger, K. D., Fjordboge, A., Hartmann, N. B., Eriksson, E., Bjerg, P. L., Baun, A., (2010), Environmental benefits and risks of zero-valent iron nanoparticles (nZVI) for in situ remediation: Risk mitigation or trade-off? *J. Contam. Hydrol.*, 118, 165-183.

Natural Sunlight Photocatalysis Efficiency of ZnO Nanowires for Water Purification

M. Le Pivert,^{1,*} M. Capochichi-Gnambodoe,¹ N. Martin,¹ Y. Leprince-Wang,¹

¹ Université Paris-Est, ESYCOM, UPEM, 5 Bd Descartes, 77454 Marne-la-Vallée Cedex 2 France
*corresponding author, e-mail : marie.lepivert@u-pem.fr

Abstract:

For some years now, photocatalysis process for water depollution has been studied intensively due to its efficiency for organic contaminant degradation and mineralization to harmless compounds. Zinc Oxide (ZnO) is a very promising photocatalyst due to its direct band gap at room temperature (3.37 eV) and its large exciton binding energy (~60 meV). Moreover, this material is abundant in nature, inexpensive and nontoxic. The main obstacles for using ZnO as a photocatalyst are the high recombination rate of photo-generated electron/hole pairs; and its wide band-gap, which only allows the use of photons from UV spectrum in photocatalytic process. In literature, carbon doped in ZnO nanowires (ZnO NWs) can be obtained by a simple traditional hydrothermal growth followed by a post-annealing ^[1]. Carbon may come from formaldehyde, a by-product generated by HMTA decomposition in the solution during the nanowire growth, which will be adsorbed in ZnO NWs. The post-annealing conducts to integrate carbon in ZnO and also conducts to improve ZnO NWs crystallinity. ZnO NWs with a band gap of 3.23 eV was obtained by a simple hydrothermal method following by an annealing at 350°C during 30 minutes against 3.28 eV for NWs as grown. Methyl Orange (MO), an organic dye widely found in textile industry wastewater, reputed as one of the most difficult to degrade compared to the other dyes such as Methylene Blue (MB). We report the ZnO NWs annealed at 350°C photocatalytic efficiency for MO degradation under natural sunlight in an open atmosphere. Experiments were realized at room temperature (~33°C) in July as applied in the literature ^[2]. The photocatalytic degradation of MO with initial concentration of 10 µM, was carried out under natural sunlight (~75 µW/cm² of UV light) in the presence/absence of ZnO NWs and monitored by UV-Vis spectroscopy. Adsorption test was also conducted in the dark in order to prove that the ZnO activity is due to natural

sunlight. After 4h under natural sunlights a degradation rate of 48% was obtained for ZnO NWs against no degradation without ZnO NWs and/or with ZnO NWs in the dark.

Keywords: ZnO, Nanowires, Hydrothermal synthesis, Photocatalysis, Sunlight, water purification, carbon doping.

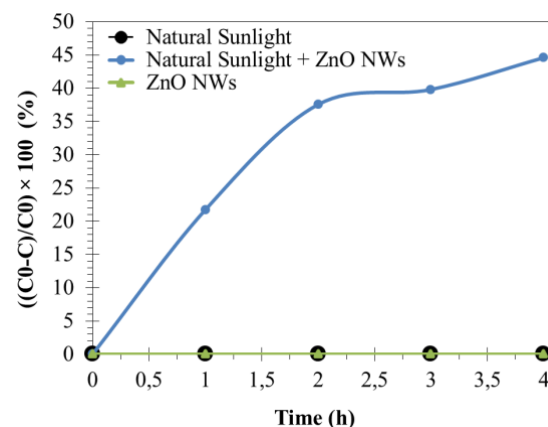


Figure 1: MO degradation rate evolution by photocatalysis process in the presence/absence of ZnO NWs under Natural Sunlight and MO adsorption rate evolution (MO : 10 µM, V = 4 mL, sample surface = 1.8 cm², no agitation, 33°C, ~75 µW/cm² of UV light or dark).

References:

1. Duan, X., Chen, G., Gao, P., Jin, W., Ma, X., Yin, Y., Guo, L., Ye, H., Zhu, Y., Wy, Y. (2017), Crystallography facet tailoring of carbon doped ZnO nanorods via selective etching, *Appl. Surf. Sci.*, 406, 186-191.
2. Eskizeybek, V., Sari, F., Gülce, H., Gülce, A., Avci, A. (2012), Preparation of the new polyaniline/ZnO nanocomposite and its photocatalytic activity for degradation of methylene blue and malachite green dyes under UV and natural sun lights irradiations, *Appl. Cata. B.*, 119-120, 197-209.

Relationship between size of acicular ferrite needles and mechanical properties of weld beads with Mn₂O₃- or TiO₂-NPs.

A. Jiménez-Jiménez ^{1,*}, A. M. Paniagua-Mercado ¹, V. M. López-Hirata ², A. García-Bórquez ¹, A. S. De Ita-De la Torre ³, M. L. Saucedo-Muñoz ², E. Miguel-Díaz ⁴, C. Mejía-García ¹.

¹ Instituto Politécnico Nacional, Escuela Superior de Física y Matemáticas, Sección de Estudios de Posgrado e Investigación, CDMX, México.

² Instituto Politécnico Nacional, Escuela Superior de Ingeniería Química e Industrias Extractivas, Depto. Ingeniería en Metalurgia y Materiales, CDMX, México.

³ Universidad Autónoma Metropolitana-Azcapotzalco, Depto. Materiales, CDMX, México.

⁴ Instituto Tecnológico Superior de la Sierra Norte de Puebla, Div. Ingeniería Industrial y Forestal, Puebla, México.

*e-mail: abel237jimenez@gmail.com

Abstract:

This work was aimed to relate the mechanical properties with the presence of acicular ferrite in weld beads with Mn₂O₃- or TiO₂-nanoparticles (NPs) added before the Submerged Arc Welding process. Such NPs were applied on the bevel surface formed between two AISI 1025 steel plates to be welded. The mechanical properties of the weld beads were determined through Tensile, Vickers hardness and Charpy V-Notch impact tests, meanwhile, the microstructural features formed in the welding zones were analyzed by scanning electron microscopy (SEM). Tensile strength (TS), yield strength (YS) and Vickers microhardness (HV) were lower for weld beads with Mn₂O₃- or TiO₂-NPs in comparison to those without NPs. On the other hand, the Charpy V-notch toughness (T) was bigger respect to a weld bead without NPs (Control), 60% by adding Mn₂O₃-NPs and 30% TiO₂-NPs. SEM micrographs show a clear increase of surface density (SD) of acicular ferrite, which is more related to the length due to the morphology of formed needles; all this in comparison with a weld bead Control. It was determined that the length (L) of the acicular ferrite needles increases in 131 and 155 % when adding Mn₂O₃- or TiO₂-NPs, respectively. Moreover there is a decrease tendency of the TS, YS and HV determined values with an increase of the surface density (or length) of acicular ferrite, see table 1. As conclusion, that the type of added oxide NPs directly influences the dimensions of the acicular ferrite needles, and this on turn the mechanical properties of the weld bead.

Keywords: Acicular Ferrite, Mechanical properties, Mn₂O₃- and TiO₂-NPs, Submerged Arc Welding.

Table 1: Acicular ferrite phase features and mechanical properties of weld beads.

Weld bead	L [μm]	SD [%]	TS [MPa]	YS [MPa]	HV	T [J]
Control	10.5	25.6	600	456	201.7	80
Mn ₂ O ₃	24.3	36.4	519	376	178	128
TiO ₂	26.8	41.3	505	344	177	105

References:

1. Paniagua-Mercado, A. M., Lopez-Hirata, V. M., Dorantes-Rosales, H. J., Estrada Diaz, P., and Diaz-Valdez, E. (2009) Effect of TiO₂-containing fluxes on the mechanical properties and microstructure in submerged-arc weld steels, *Mater. Charact.*, vol. 60, 36-39.
2. Paniagua-Mercado A. M., López-Hirata V. M. and Saucedo-Muñoz M. (2005) Influence of the chemical composition of flux on the microstructure and tensile properties of submerged-arc welds, *J. Mater. Process. Technol.* vol. 169, 346-351.

Electrical and piezoresistive sensing capacities of concrete with carbon nanomaterials

T. F. Yuan,¹ S.H. Hong,¹ J.Y. Lee,² Y.S. Yoon^{1,*}

¹ Korea University, School of Civil, Environment and Architectural Engineering, Seoul, Korea

² McGill University, Department of Civil Engineering and Applied Mechanics, Montreal, Canada

Abstract:

Most of our infrastructures have been widely constructing by concrete. However, common causes of the deterioration of concrete reduced integrity of concrete structures with time. Hence, structural health monitoring (SHM) has attracted much attention from researchers, which can monitor and evaluate the full scale structural behavior and provided real time data using various types of sensors. Due to the less cost effectiveness of operation under current system, SHM technologies are difficult to applying to the large scale concrete structures. Many researchers have suggested the structure with self-sensing elements of infrastructures, which allows to save maintenance cost for a structural diagnosis. With several advantages compared to the conventional strain sensors embedded or attached to the element, conductive cement-based composites for self-sensing have been developed. For the functional purposes, the conductive materials should measure its own strain due to an electromechanical property called piezoresistivity (Fig. 1). Therefore, in this study, the electrical and piezoresistive sensing properties of concrete with two different nanomaterials (graphene and carbon black) and electric arc furnace slag were evaluated. More specifically, the effect of different conductive materials on the electrical resistivity with various ages, piezoresistive sensing capacity in terms of correlation between fractional change in resistivity (FCR) and cyclic compressive stress, and gauge factor were also assessed. Based on the data analysis, the feasibility of each conductive materials for developing concrete sensors was discussed as well.

Keywords: graphene, carbon black, electrical resistivity, gauge factor, piezoresistive sensor.

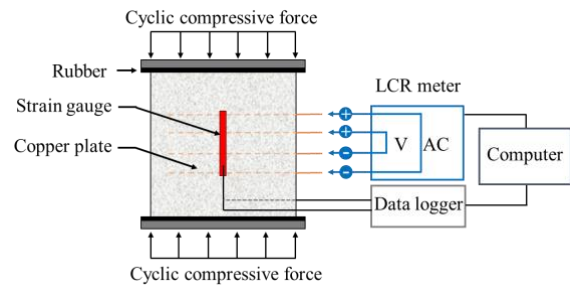


Figure 1: Figure illustrating the experimental setup for compressive sensing.

References:

1. D'Alessandro, A., Rallini, M. Ubertini, F. (2016) Investigations on scalable fabrication procedures for self-sensing carbon nanotube cement-matrix composites for SHM applications, *Cem. Concr. Compos.*, 65, 200-213
2. Yoo, D.Y., You, I., Lee, S.J. (2018) Electrical and piezoresistive sensing capacities of cement paste with multi-walled carbon nanotubes, *Arch. Civil Mech. Eng.* 18, 371-382

Nanoporous Carbonaceous Adsorbents for Enrichment of Ventilation Air Methane (VAM) with Methane

E. Brodawka,^{1,*} M. Bałys,¹ J. Szczurowski,¹ L. Czepirski,¹ K. Zarębska,¹ P. Da Costa²

¹ AGH University of Science and Technology, Faculty of Energy and Fuels, Krakow, Poland

² Sorbonne Université, Institut Jean le Rond D'Alembert, Paris, FRANCE

Abstract:

Currently, the special interest is a separation of gaseous mixtures containing a low concentration of methane (biogas, ventilation air methane, landfill gases) which could be separated using carbonaceous adsorbents (activated carbons, carbon molecular sieves, activated carbon fibres). It is well known that methane is an anthropogenic greenhouse gas (more than 20 times as potent as CO₂), which imposes the most significant influence on the global warming issue. Ventilation air methane (VAM) is the largest source of coal mine methane (CMM) emissions. Most coal mines around the world discharge ventilation air methane (VAM) into the air directly. In Poland, around 600 mln m³ CH₄ was emitted to the atmosphere with mine ventilation air. Methane emitted from coal mines ventilation systems into the air is the most difficult to use as an energy source, because of the low methane concentration (typically 0.3 to 0.5 vol% in the Polish mine workings), large airflows and variable, both flow and concentration. Adsorption - based processes including Pressure Swing Adsorption (PSA) are potential technologies that could be used to recover methane from vent streams and enrich the methane to a concentration level that could be practically used in a thermal or catalytic flow-reversal oxidizers lean-gas turbine or methane fuel cell.

In this paper new concept for the realization of the PSA cycle to enrich the mixture streams with methane was analyzed. The removal of methane from VAM is the separation between methane and nitrogen and properly selected adsorbent is a key to the separation by means of the PSA process. The separation effect is based on each component's selectivity for the adsorbent material. The most promising adsorbents for VAM enrichment with methane seems to be nanoporous carbonaceous adsorbents thanks to its unique porous texture with narrow micropores, large specific surface

area and porosity, hydrophobic surface, various surface functional groups. The new concept of the PSA process was verified in the experimental unit. The gas mixture was fed into the column packed with the adsorbent. When the separation between components of the mixture is realized, the enriched stream on the top of the column is collected as the product. The column is regenerated by reducing the pressure to vacuum. Desorbed gas is recovered on the bottom of the column. A mathematical model was developed to optimize process variables (cycle time, pressure ratio) for the individual steps. The results of the experiment confirmed the correctness of calculations undertaken. The concentration of methane in the product (desorbed gas) increases during depressurization step from 0.3 vol.% (methane concentration in the feed gas) to 2.0 vol.% at the end of this step. The results indicated that selected activated carbon can be successfully applied in N₂/CH₄ separation for ventilation air methane and there is still a chance for improvement in the performance of these systems and further experiments should be continued to, optimize of process variables, as well as search new types of carbonaceous adsorbents.

Keywords: Pressure Swing Adsorption, nanoporous carbonaceous adsorbent, ventilation air methane, gas mixture separation

References:

1. Bałys, M., Szczurowski, J., Czepirski L., (2016), Adsorption technology for Ventilation Air Methane enrichment, *Selected issues related to mining and clean coal technology*, Monograph, 253-257
2. Brodawka, E., (2018), Separation of biogas components by adsorption on activated carbon, „Zrozumieć naukę”: II edition national scientific conference, The book of articles, 46-51.

A study of equivalent circuit models of lithium-ion battery under irregular electrical discharge

Se-Hun Kim*

Faculty of Science Education and Educational Science Research Institute,
Jeju National University, Jeju 63243, Republic of Korea

Abstract:

We investigated the electrical performance for the lithium-ion battery discharge under the constant current. The simulations to evaluate the operation of the battery were carried out by the equivalent circuit models which are consisted of the resistance, capacitance and power source. During the discharge of Li-ion battery, the voltage and resistor were measured under the condition of maintaining 2A constant current. The output results for the electrical elements of the resistor and capacitor corresponding to the equivalent circuits are calculated by the simulation based on the experimental results obtained from the time dependence of the current and the voltage. The triple RC circuit model showed more the reduced error between the experimental results and the simulated data than that of the single RC circuit model. This study suggests that the discharge of dc Li-ion battery is well operated by obeying the equivalent circuit model composed of the multiple RC elements.

Keywords: Lithium-ion battery, Equivalent circuit model, Discharge, State of charge (SOC), Equivalent circuit models

References:

1. V. Ramadesigan, P. W. C. Northrop, S. De, S. Santhanagopalan, R. D. Braatz, V. R. Subramanian, *J. Electrochem. Soc.* 159, R31 (2012).
2. M. Chen and G. A. Rincon-Mora, Energy Conversion, *IEEE Transactions on* 21, 504 (2006).
3. M. A. Roscher, J. Assfalg, O. S. Bohlen, Vehicular Technology, *IEEE Transactions on* 60, 98 (2011).